Ludwig-Maximilians-Universität München

Department Biologie I

Bereich Genetik

Evolutionary divergent ligand activation of PKA-like kinase from *Trypanosoma brucei*

Dissertation der Fakultät für Biologie
der Ludwig-Maximilians-Universität München

vorgelegt von

George B. Githure

München, im September 2014

Erklärung

Ich versichere hiermit an Eides statt, dass die vorliegende Arbeit, angefertigt am Institut für Genetik des Departments Biologie I der LMU München bei Herrn Professor Dr. Boshart, selbständig durchgeführt und keine anderen als die angegebenen Hilfsmittel und Quellen benutzt habe.

München, am 09.09.2014   _____

George B. Githure

Erklärung

Ich versichere, dass ich keine Dissertation anderweitig eingereicht habe und mich auch noch keiner Doktorprüfung unterzogen habe.

München, am 09.09.2014   _____

George B. Githure

Erklärung

Ich versichere, dass ich diese Dissertation oder Teile dieser Dissertation nicht bereits bei einer anderen Prüfungskommission vorgelegt habe.

München, am 09.09.2014   _____

George B. Githure

Abstract

Protein kinase A (PKA) is the main effector protein of the ubiquitous second messenger cAMP and is involved in a multitude of cell signaling. This kinase has been identified in several human pathogens including *Trypanosoma brucei*, the causative agent of African trypanosomiasis, and shown to play a role in response to key environmental triggers that govern the parasite's life cycle progression.

In *T. brucei,* one regulatory subunit (TbPKAR) and three catalytic subunit isoforms (TbPKAC1-3) form a R_1/C_1 heterodimer and the R subunit possesses an unusually long N-terminal domain. General interest was raised by the discovery that the kinase is not activated by cAMP, despite the seemingly high conservation of the cyclic-nucleotide binding domains (CNBs).

In silico analysis of TbPKAR, in comparison to its mammalian homologue, confirmed the high conservation of the CNB modules except for the phosphate-binding cassette (PBC), which is the hub for cAMP's molecular interaction. It appeared that while interactions of cAMP's nucleoside moiety were conserved, those of the phosphate group were not. The key phosphate interaction residues in the mammalian PKA were transferred into TbPKAs' PBCs by site-directed mutagenesis. This mutant was shown to not only bind cAMP but also undergo the conformational changes required for the release of the catalytic subunit. This indicated that TbPKA has conserved the capacity for ligand interaction and activation.

Further analyses of the kinase's activation mechanism prompted the establishment of an in vitro kinase assay system, using heterologously expressed TbPKA holoenzyme. Initial attempts to reconstitute the holoenzyme from *E. coli* and Sf9/Baculovirus expression systems failed. Co-purification, after co-expression, of the recombinant subunits in the two expression systems was also unsuccessful. Investigation of the biochemical co-factors required for holoenzyme formation led to the discovery that the aforementioned recombinant subunits could form a stable holoenzyme after incubation with trypanosome cell lysate. This indicated that, contrary to other PKA kinases, TbPKA holoenzyme formation requires some species-specific co-factors. The kinase complex was successfully purified from the closely related *Leishmania tarentolae's* expression system (LEXSY). Although the holoenzyme formation factors are yet to be fully characterized, it appears that PTMs and mainly phosphorylations are important in this aspect.

Membrane permeable adenosine analogues have been shown to influence the onset of trypanosome differentiation (Laxman et al., 2006). TbPKA has been suggested to be involved in the differentiation signaling cascades. The in vivo influence of these analogues on TbPKA was tested using a transgenic reporter protein. Most of the compounds were shown to activate TbPKA but a few inhibited the well-established cold shock activation mechanism, hence acting as antagonists (S. Bachmaier, this lab). In vitro kinase assays using the recombinant TbPKA holoenzyme could reveal that the agonistic effect was by direct interaction with the kinase. The most potent analogues

were derived at the N7 position of the adenine ring and had physiologically relevant half activation constants (~200 nM).

Further studies were hence focused on characterizing the biochemical and molecular nature of TbPKA nucleoside activation. The structure of TbPKA was modeled using the mammalian PKA crystal structures as template. Structure model predictions were supported by biochemical evidence in showing that TbPKA's PBC has lost the capacity to interact with the phosphate group of cyclic nucleotides but gained unique features for nucleoside interaction. The importance of the ribose-sugar's hydroxyl groups was highlighted by the fact that deoxy-adenosine analogues could not activate the kinase. Structure model analysis could predict that specific hydrogen interactions are established between the hydroxyl groups and residues of the PBC. The half activation constants of the naturally occurring purine base nucleosides were; ~30 nM for inosine, ~200 nM for guanosine and ~1 μM for adenosine. Both inosine and guanosine were in the range of cAMP activation potency in mammalian PKA (~100 nM for the RI holoenzyme). The keto group at position 6 of inosine/guanosine's purine base was predicted to be more influential than adenosine's amine group in the activation, by establishing specific hydrogen bond interactions. Most of these features were predicted to be conserved in all kinetoplastid members, suggesting a common evolutionary path in this mode of activation.

Purine nucleosides have a real potential of been the physiological activators of TbPKA. Although most protozoa including *T. brucei* lack a de novo purine base synthesis mechanism they have developed an elaborate purine salvage pathway that could be the source of the physiological activator.

Abbreviations

AC	Adenylate cyclase
AKAP	A kinase anchoring protein
BSA	Bovines Serum Albumin
BSF	Blood Stream Form
BEVS	Baculovirus Expression Vector System
cAMP	3'-5'-cyclic adenosine monophosphate
cGMP	3'-5'-cyclic guanosine monophosphate
cNMP	Cyclic nucleotide monophosphate
cpm	Counts per minute
DEAE	Diethylaminoethyl cellulose
DMSO	Dimethyl sulfoxide
DOC	Deoxycholic acid
FCS	Fetal Calf Serum
GST	Gluthathion-S-Transferase
HMM	Hidden Markov Model
IPTG	Isopropyl thio-b-D-galactoside
LS	Long Slender
LB	Luria Bertani
LEXSY	Leishmania Expression System
MW	Molecular Weight
M/V	mass per volume
OD	Optical Density
ORF	Open Reading Frame
PCF	Procyclic form
PDE	Phosphodiesterase
PBC	Phosphate Binding Cassette
PFR	Paraflagellar rod
PKA	Protein kinase A
PVDF	polyvinylidene fluoride
RT	Room Temperature
SIF	Stumpy Induction Factor
SDS	Sodium dodecyl sulfate
SDM	Semi-defined medium
SOB	Super optimal broth
SS	Short Stumpy
T7Pol	T7polymerase
TAE	Tris-acetate-EDTA buffer
TCA	Trichloroacetic acid
TE	Tris-EDTA buffer

TetR	Tetracyclin Repressor
TEV	Tobacco Etch Virus
UTR	Untranslated region
VASP	Vasidolator-stimulated phosphoprotein
VSG	Variant surface glycoprotein
V/V	Volume per volume
WT	Wild type
WHO	World Health Organization

1 Introduction

1.1 *Trypanosoma brucei* as the causative agent of Human African Trypanosomiasis (HAT) or 'sleeping sickness'

1.1.1 *T. brucei's* phylogeny and morphology

Trypanosomes are parasitic protozoa that belong to the order Kinetoplastida and the family of Trypanosomastidae. The order and family comprises of members that have a single flagellum, and a self-replicating dense granule of DNA known as a kinetoplast. In *Trypanosoma brucei*, the large kinetoplast lies at the base of the flagellum (in the basal body) and is at one end of a long and unique mitochondrion (Fig. 1.1). The flagellum emerges from the flagellar pocket, and extends laterally down along the undulating membrane of the organism. Trypanosomes range in length from 12-40 µm, depending on the life cycle stage (Vickerman, 1985).
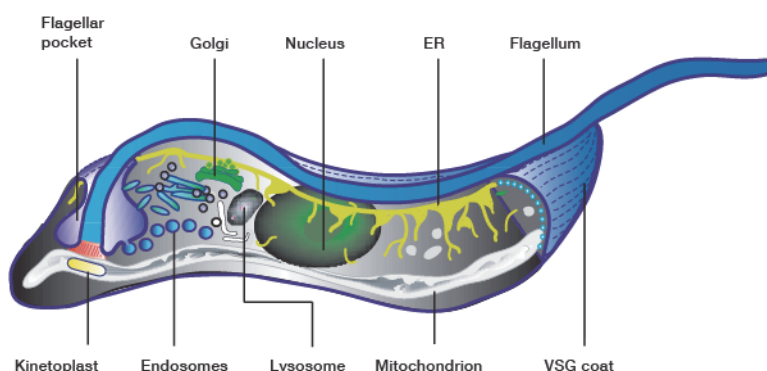
Fig. 1.1. A schematic representation of *Trypanosoma brucei's* ultrastructure: the main organelles are shown at their relative positions. The picture was adapted from Engstler and Overath, 2004.

1.1.2 *T. brucei's* epidemiology

T. brucei is an obligate and digenetic parasite, transmitted by an insect vector to mammalian hosts. There are three subspecies of *T. brucei*: *T. b. gambiense and T. b. rhodesiense* – responsible for Human African Trypanosomiasis (HAT), also known as 'sleeping sickness' – as well as *T. b. brucei,* causative agent of Animal African Trypanosomiasis (AAT or 'Nagana'). The disease is transmitted by tsetse flies of the genus *Glossina* and the geographic distribution of the parasite is restricted to that of the tsetse fly. Consequently, the diseases are found exclusively in sub-Saharan Africa, between the latitudes of 14°N and 20°S of the equator (Simarro et al., 2009), see Fig. 1.2. *T. b. gambiense* gives rise to the chronic form of the disease and is endemic in west and central Africa, being responsible for more than 90% of the reported HAT cases. *T. b. rhodesiense*, on the other hand, causes the acute form of HAT and is found in eastern and southern Africa, causing less than 5% of the reported cases (WHO, 2013). The *T. b.*

gambiense infection is progressive over an average three-year duration, while that of *T. b*. *rhodesiense* is characterized by epidemic outbursts leading to death within months. Importantly, the two human-infective species can also be hosted by both domestic and wild animals, acting as reservoirs of the disease even after eradication from the local human population.
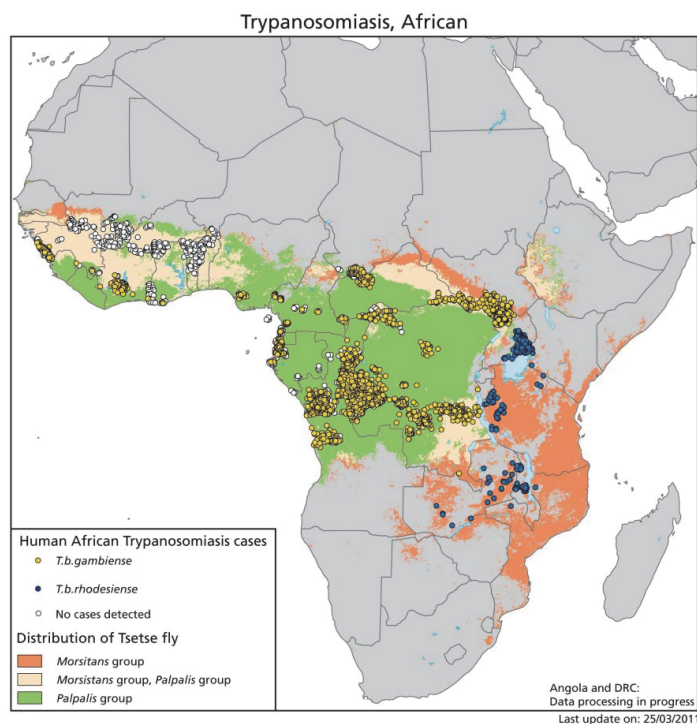
Fig. 1.2. Distribution of Human African Trypanosomiasis (HAT): The two human infectious *T. brucei* sub-species, *T. b. gambiense* (west Africa) and *T. b*. Simarro et al. (2009) *rhodesiense* (east and southern Africa) and their respective tsetse fly vector groups. Image obtained from the Atlas of human infectious diseases (published by Wiley-Blackwell, 2012).

The diseases (both in humans and animals) are fatal if untreated, leading to the loss of many human lives and great economic loss due to the challenge of rearing livestock. Trypanosomiasis was almost eradicated in the 1960s by the colonial powers, after a series of epidemics in the early 1900s that led to the loss of hundreds of thousands lives. A resurgence occurred after the colonial era, where about 70 000 annual cases were reported in the 1990s. In recent years, control efforts have reduced the number of cases to less that 10 000 per year (WHO, 2013). However, the treatments available have had little to no improvement for more than 60 years and are highly toxic and cumbersome to administer. Complete eradication of this disease requires more effective and safe medicine, coupled with better diagnostic and vector control tools.

1.2 *Trypanosoma brucei* as a model organism for molecular biology

Research in trypanosomes is facilitated by the fact that *T. b. brucei* is not pathogenic to humans. Humans and related primates possess innate immunity, known as the trypanosome lytic factor (Vanhollebeke et al., 2008), however, *T. b. gambiense and T. b. rhodesiense* are resistant to the lytic factor and are therefore more challenging to work with safely in the laboratory. In order to understand the intricate mechanisms that govern an organism's survival, a good knowledge of the genome as well as good molecular tools are essential. The genomes of key pathogenic trypanomastids have been sequenced, assembled, annotated: *Trypanosoma brucei* (Berriman et al., 2005), *Leishmania major* (Ivens et al., 2005) and *Trypanosoma cruzi* (El-Sayed et al., 2005). This resource has been made publicly available through TriTrypDB (Aslett et al., 2010). Over 9000 genes were identified in the *T. brucei* genome of which only 50% have functional annotation.

Reverse genetic approaches are mainly by gene knock out strategies and RNAi knock down. Gene recombination in kinetoplastids is mainly by homologous recombination (Asbroek et al., 1993). This has been harnessed to knock out non-essential single copy genes, using 5' and 3' UTRs of the targeted gene, flanked by a drug resistance selectable marker (Gaud et al., 1997). Gene silencing by RNAi is only possible in *T. brucei*, as the other trypanosomastid members appear to lack some components of the RNAi pathway (Ullu et al., 2004). Functional analysis of the genome has therefore made more progress in *T. brucei*, as RNAi greatly complements the gene knock out strategy by allowing multiple gene copy silencing. In some cases, essential genes can also be silenced and analyzed before cell viability is adversely affected.

A forward genetic approach has been developed using RNAi libraries generated from randomly sheared genomic fragments (Morris et al., 2002). An inducible library in bloodstream form *T. brucei* has recently been used for global-phenotyping for genes involved in various key features for survival of the parasite such as differentiation, metabolism and motility (Alsford et al., 2011). This system has also enabled characterization of the efficacy and resistance of the available HAT drugs (Alsford et al., 2012). Whole genome microarrays analysis has also been used to study the parasite's transcriptome (Kabani et al., 2009).

The last decade has also seen great advancements in proteomics where very sensitive mass spectrometers are coupled with sample enrichment techniques such as subcellular fractionation and affinity chromatography. Quantitative proteomic approaches such as Isobaric Tag for Relative and Absolute Quantitation (ITRAQ) and Stable Isotope Labeling of Amino acids in Cell culture (SILAC) have been adopted for trypanosome research (Butter et al., 2013; Gunasekera et al., 2012; Portman and Gull, 2012; Urbaniak et al., 2012).

Both the genomic and proteomic approaches are providing the research community with a high amount of new data that is not only important in trypanomastid research aimed at

new drug discovery, but also in the better understanding of fundamental principles of biology.

1.3 *Trypanosoma brucei* differentiation

In the mammalian host, *T. brucei* is found in the haemolymphatic system during the first stage of the disease and later in the central nervous system, after penetrating the blood brain barrier. In the insect vector the parasites transit from the proboscis to the midgut and onward to the salivary glands via the proventriculus (Hoare, 1972). Some of the challenges faced by the parasite exposed to these very different environments include: the host immune response, drastic change in nutrient availability and oxidative stress (Bringaud et al., 2012; Fenn and Matthews, 2007). Consequently, the parasite has to quickly adapt to these sudden changes through tightly regulated and coordinated, stage-specific gene expression.

1.3.1 *Trypanosoma brucei's* life cycle

The parasite requires 20-30 days in the tsetse fly for full maturation to the infective cell cycle arrested metacyclic form (Aksoy et al., 2003). This infective form is covered by a variable surface glycoprotein (VSG) coat, which protects it from lytic factors in the human plasma (Pays, 2006). Transmission of *T. brucei* to the mammalian host occurs during a blood meal by the insect vector (Fig. 1.3). Once in the haemolymphatic system, the parasite rapidly undergoes cell cycle re-entry accompanied by a series of morphological and biochemical changes. These include mitochondrial repression since glycolysis alone suffices to produce energy from the readily available blood glucose (Vickerman, 1965) and a switch to a more elaborate antigenic variation system, allowing the parasite to evade the host immune system (Barry and McCulloch, 2001; Pays, 2005).

The parasite exists in the haemolymphatic system as a heterogeneous population comprising of proliferating long slender form (LS) and cell cycle arrested short stumpy form (SS) (Vickerman, 1985). The LS form proliferates by binary fusion roughly every six hours (Seed, 1978) and as the parasitaemia increases, a soluble trypanosome derived factor known as Stumpy Induction Factor (SIF) accumulates in the blood, triggering growth arrest of the parasite in the G1/G0 cell cycle stage at the peak of parasitaemia. This is accompanied by a series of biochemical and morphological changes to produce the SS form, pre-adapting the parasite for life in the tsetse fly (Reuner et al., 1997; Rico et al., 2013; Vassella et al., 1997a).

This commitment for uptake by the tsetse fly is irreversible, as the SS form cannot revert to LS proliferation. Furthermore, as its host immune system-evading antigenic variation is deregulated, the SS form is eliminated by the host within a few days. However, a new population of LS form, expressing a different VSG due to random antigenic variation, assures the parasite's survival. This creates a cycle of parasitaemia that prolongs the survival of the host as well as increasing the chance of transmission of the parasite to complete the life cycle (Matthews and Gull, 1994).

Infected blood, ingested during a tsetse fly bite, makes its way to the lumen of the fly's midgut where the SS form differentiates to the procyclic form (PCF). The main changes include full activation of mitochondrial activity, also noted by the increase in size of the organelle. This happens very quickly since the glucose in the blood meal is rapidly depleted. The parasite is hence obliged to develop the ability to oxidize alternative substrates, mainly proline, in a complete respiratory chain (Haston, 1972; Priest and Hajduk, 1994; van Weelden et al., 2003).

In the procyclic form, the VSG coat is quickly lost by proteolytic cleavage and replaced by a procyclin coat, which is more suited to protect the parasite against proteolysis in the midgut of the fly (Gruszynski et al., 2006; Roditi et al., 1989). Procyclics penetrate the ectoperitrophic space where they proliferate and acquire a longer cell body. They then move to the proventriculus before finding their way to the salivary glands where they attach by the flagellum to the microvilli of the epithelial cells. The parasite then undergoes maturation to the infective metacyclic form, pre-adapted to life in the blood of a mammalian host (Vickerman, 1985).
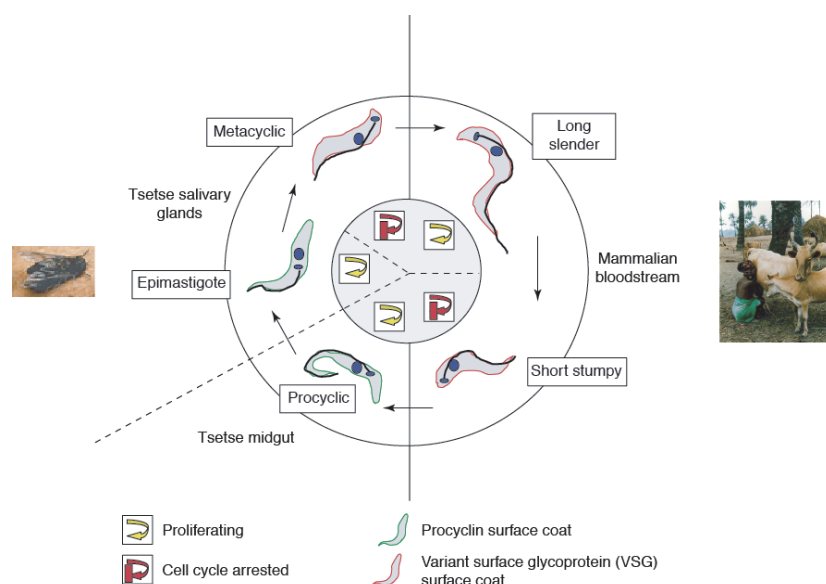
Fig. 1.3. *T. brucei* life cycle: In both the mammalian host and insect vector, the parasite undergoes many morphological changes in alternating proliferative and non-proliferative stages. Picture modified from (McKean, 2003).

1.3.2 *T. brucei* strains in the laboratory

Most of the research in trypanosomes is carried out with the *T. b. brucei* sub-species, owing to the fact that it is non-infective to humans, as discussed earlier. This sub-species can be cultured in two forms: the blood stream form (BSF) at 37°C and the procyclic insect form (PCF) at 27°C. The culture medium for these two life cycle stages has been optimized for rapid and sustainable growth (Brun et al., 1979; Hirumi and Hirumi, 1989). After long-term passaging in animals, *T. b. brucei* lines developed the capacity to proliferate in the host without differentiating to the short stumpy stage. These

cell lines have a very low rate of antigenic (VSG) switching (Barry and McCulloch, 2001) hence termed monomorphic. They grow readily in culture and are used for most of the molecular and biochemical research. Differentiation studies are more often carried out with cell lines that readily differentiate from BSF to PCF, known as pleomorphic cell lines. They require more demanding culture conditions and are often passaged in immuno-compromised mice or rats (Vassella and Boshart, 1996).

1.4 Signal transduction mechanisms that govern differentiation in *T. brucei*

The survival of *T. brucei* throughout the life cycle stages is largely dependent on its capacity to perceive changes in its surrounding environment and use them as a trigger for the required biochemical and morphological changes. A quorum sensing mechanism that induces cell cycle arrest and nutrient availability has been discussed in the previous section. Other differentiation triggers identified so far include: millimolar concentrations of citrate/cis-aconitate (CCA) (Brun and Schonenberger, 1981); cold shock (Engstler and Boshart, 2004); exposure of the parasite's cell surface to limited proteolysis (Sbicego et al., 1999) and pH stress (Rolin et al., 1998). The signal transductions that govern the response to these triggers are still poorly understood. Whole genome microarray analyses of the BSF and PCF forms' transcriptome have shown that a high percentage of genes are differentially expressed in the life cycle stages (Jensen et al., 2009; Kabani et al., 2009). Proteomic analyses using SILAC and mass spectrometry have also shown major protein expression changes in the life cycle stages (Butter et al., 2013; Gunasekera et al., 2012; Urbaniak et al., 2012)

Reversible protein phosphorylation is a key posttranslational modification for any signaling pathway and would be expected to play a major role in trypanosomes. Analysis of the *T. brucei* genome has revealed 170 conventional protein kinases (ePKs) and 12 atypical protein kinases (aPKs) (Jones et al., 2014; Parsons et al., 2005) Some members of this kinome have been characterized by reverse genetics and shown to be essential and involved in cell-cycle regulation, (Hammarton, 2007). SILAC has also been used to study the phospho-proteome of the BSF and PCF lifecycle stages revealing a significant differential phosphorylation pattern involving more than a third of the proteome and most of the kinome (Urbaniak et al., 2013). A significant intra-protein differential phosphorylation pattern between the two life cycle stages was also noted. This suggests that the phosphorylation profiles of a given protein may have a distinct function in each stage. These global approaches have revealed life cycle dependent upregulation and downregulation of key players in many signaling cascades without assembling complete pathways.

The CCA induced differentiation from short stumpy (SS) to procyclic form is however relatively well understood. In the SS form, differentiation is inhibited by a tyrosine phosphatase known as TbPTP1B. Inhibition of TbPTP1B by RNAi or chemical inhibitor (BZ3) results in spontaneous differentiation of SS to PCFs, in the absence of any external

trigger (Szoor et al., 2006). The TbPTP1 is involved in a phosphorylation-dephosphorylation self-repressive loop with its substrate TbPIP39 (Szoor et al., 2010). CCA is transported into the cell by a family of carboxylate transporters named PAD (proteins associated with differentiation), whose expression is upregulated in the SS stage (Dean et al., 2009). Once in the cell, CCA interrupts the TbPTP1-TbPIP39 cross talk by reducing the TbPIP39 mediated activation of TbPTP1 hence initiating differentiation (Rico et al., 2013).

Signaling cascades involving cAMP as a second messenger have been suggested to be involved in the parasite's differentiation process. As discussed previously, loss of sensitivity to SIF by LS bloodstream form trypanosomes has been credited for the generation of monomorphic cell lines (Matthews et al., 2004). SIF has to date not been identified, but cell-permeable hydrolysable cAMP analogues have been shown to mimic the LS to SS differentiation-inducing effect caused by SIF (Laxman et al., 2006; Vassella et al., 1997b). Further evidence that cAMP may be involved in differentiation signaling came with the observation that its levels increased during differentiation (Mancini and Patton, 1981) and upon treatment of trypanosomes with culture medium containing SIF (Vassella et al., 1997a)

One hypothesis suggests that cAMP conveys the SIF signal as a second messenger; however, increase of intracellular cAMP by RNAi down regulation of phosphodiesterases (PDEs) was not sufficient to induce differentiation (Oberholzer et al., 2007). Moreover, a comparative analysis of PDE hydrolysable vs. non-hydrolysable cAMP analogues showed that the latter could not induce cell-cycle arrest (a prerequisite for differentiation). Cell permeable degradation products of cAMP namely, pCPT-AMP and pCPT-adenosine were shown to be more potent than the hydrolysable cAMP analogues, indicating that these molecules could be the actual effectors in the differentiation process (Laxman et al., 2006). More recent studies have shown that hydrolysable cAMP analogues decreased the levels of TbTOR4, whose loss of function is attributed to stumpy formation; hydrolysis resistant cAMP analogues had no effect on this kinase (Barquilla et al., 2012).

It would therefore appear that cAMP is not directly involved in the differentiation process.

1.5 Elements of cAMP signaling in kinetoplastids

The textbook knowledge of cAMP/PKA signaling includes binding of exogenous cell effectors, such as hormones or neurotransmitters, to G-protein-coupled receptors (GPCR) triggering the release of the $G\alpha$ subunit from the $G\beta\gamma$ dimer. The $G\alpha$ then activates adenylyl cyclase (AC) for production of cAMP from ATP (Levitzki, 1988). cAMP-dependent protein kinase (PKA) is the main effector protein and has been credited with regulating most of the cAMP mediated events, including: metabolism (Krebs and Beavo, 1979); ion channel conductivity (Cantrell et al., 2002; Li et al., 1993); gene regulation (Montminy, 1997); cell growth and division (Boynton and Whitfield, 1983); cell differentiation (Liu, 1982; Schwartz and Rubin, 1985); and flagellar motility (Tash and

Means, 1983). Other intracellular cAMP effectors include cyclic-nucleotide gated channels (Kaupp and Seifert, 2002) and Epac, a guanine nucleotide exchange factor (Bos, 2006). The termination and modulation of the cAMP signal is largely controlled by the hydrolysis of cAMP to 5'-AMP by the phosphodiesterase family of proteins (PDEs), (Lugnier, 2006). The counterbalancing activity of the ACs and PDEs plays an important role in regulating the signaling.

In trypanosomes, AC activating GPCRs have not been identified in any of the sequenced kinetoplastid genomes. This is exceptional to kinetoplastids, since GPCRs are present in other protozoans and fungi. In *D. discoideum*, for example, four GPCR subtypes (cAR1-4) have been characterized as receptors for extracellular cAMP (Saran et al., 2002).

Adenylyl cyclases have been identified in kinetoplastids, but differ both in structure and relative abundance. While only 9 transmembrane ACs have been identified in the mammalian system, *T. brucei* counts up to 60 putative AC coding genes while those of the *Leishmania* and *T. cruzi* species range from 5-10 (http://www.tritrypdb.org). All kinetoplastid ACs are characterized by a large extracellular N-terminal domain and a single membrane-spanning region that connects to the intracellular catalytic domain (Bieger and Essen, 2001). In contrast, mammalian ACs consist of a variable extracellular N-terminus and two large cytoplasmic domains separated by two membrane-spanning domains (Sadana and Dessauer, 2009). In kinetoplastids, the N-terminal domain of the ACs has been suggested to be the receptor for extracellular ligands, owing to its structure and variability (Paindavoine et al., 1992; Seebeck et al., 2004).

Four families of PDEs (PDE A-D) have been identified in kinetoplastids, all of which are homologous to the class 1 family of human PDEs. PDE A, B and C from *T. brucei*, *T. cruzi* and *Leishmania sp*. have been cloned and biochemically characterized. They are all specific for cAMP but show a variable affinity for the ligand depending on the family and/or the species, with Km values for cAMP ranging from lower micromolar to sub-millimolar concentrations (Gould and de Koning, 2011).

1.6 The PKA kinase

The PKA kinase has been identified in all kinetoplastid genomes analysed. This kinase has been the subject of study in this laboratory, initially under the hypothesis that it is the main effector for cAMP signaling in trypanosomes. Several independent lines of evidence in this lab have however shown that this kinase does not respond to cAMP. As this thesis is aiming at understanding this unconventional property and alternative modes of activation, the current knowledge for activation of the conventional PKA will be discussed in greater detail.

PKA kinase belongs to the AGC group of protein kinase superfamily. The higher eukaryotic PKA kinase is a heterotetrameric holoenzyme complex comprised of a regulatory subunit dimer and two catalytic subunits (R_2C_2). Two molecules of cAMP bind to each regulatory subunit (R) resulting in a series of conformational changes that

culminate in the release of the catalytic subunits (C) and hence the activation of the kinase (Ogreid and Doskeland, 1981), see Fig. 1.4.
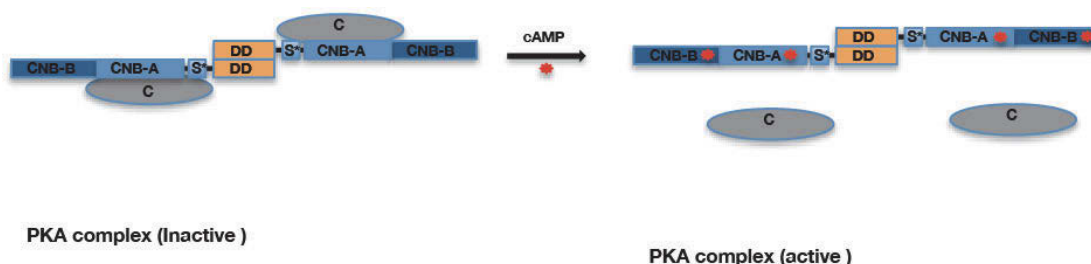
Fig. 1.4. A schematic representation the mammalian PKA heterotetrameric (R$_2$C$_2$) holoenzyme: Two cAMP molecules bind in the CNB domains inducing conformational changes that lead to the release of the catalytic subunits.

The mammalian PKA is comprised of several isoforms of both the R and C subunits that give rise to tissue specific holoenzyme complexes. Although the mode of cAMP binding is highly conserved, the various isoform complexes respond to different concentrations of cAMP owing to specificities in complex assembly (Cadd et al., 1990; Hofmann et al., 1975; Ventra et al., 1996). In most protozoans studied so far, the isoform diversity is, in most cases, limited to only a single copy of the regulatory subunit for one or more copies of the catalytic subunits (Gould and de Koning, 2011).

1.6.1   PKA kinase regulatory subunit (R subunit)

The role of the regulatory subunit is not only limited to inhibiting the catalytic subunit but also protecting it from protease degradation i.e. proteolytic inactivation (Hemmings, 1986). It also interacts with other macromolecules, limiting the kinase complex to distinct cellular localization (Scott and McCartney, 1994). In higher eukaryotes, there are two main types of R subunit: type I (R1) and type II (RII). These two types have a similar domain organization but differ in several aspects including the molecular weights (43 kDA for RI and 45 kDA for RII), amino acid sequences and auto-inhibition site (Corbin et al., 1975). The RI is mostly localized in the cytoplasm while the RII is exclusively particulate (Corbin et al., 1977). The two types are further subdivided into α and β isoforms, increasing both tissue and cellular specificity. For example, the RIIβ is predominantly expressed in the adipose tissue (Cummings et al., 1996). However, despite the aforementioned differences, the higher eukaryotic R subunit possesses a conserved and well-defined domain structure (Fig. 1.5). The N-terminal domain (amino acids 1-90) is comprised of the dimerization and docking domain (D/D domain), responsible for the homo-dimer formation and interaction with A-kinase anchor proteins (AKAPS) whose role is to confer tissue and subcellular specific anchoring of the kinase complex (Banky et al., 1998; Esseltine and Scott, 2013; Newlon et al., 1999). The N-terminus is followed by a variable linker region (amino acids 90-100) containing a substrate like inhibitor sequence, which directly interacts with the C subunit. The RI type contains a pseudosubstrate motif

(RRXA or RRXG) while the RII type contain an actual substrate site (RRXS/T) where the serine or threonine can be phosphorylated by the C subunit upon docking (Hofmann et al., 1975). The phosphorylation of the RII type reduces its affinity for the C subunit, hence dissociation occurs at lower cAMP concentrations (Rangel-Aldao and Rosen, 1976). The RI type is not phosphorylated but instead has a high affinity for Mg/ATP, which enhances its re-associations (Ogreid and Doskeland, 1983).

The C-terminal region of this protein is comprised of two tandem cyclic nucleotide binding domains termed CNB:A and CNB:B, respectively. The CNBs are highly conserved amongst all species and are likely a result of a gene duplication event (Takio et al., 1984; Titani et al., 1984). The R/C interface is extended from the linker region into the CNB:A, but CNB:B is much less involved in the interaction with the C subunit. cAMP binds first to CNB:B inducing a conformational change that allows a second cAMP molecule to access CNB:A, resulting in the disruption of the R/C interface and the release of the C subunit (Herberg et al., 1996).

Attempts to isolate and characterize cAMP effector proteins in kinetoplastids spans for more than three decades. It is, however, only at the dawn of the genomic era that the R subunit of *T. brucei* amongst other kinetoplastids' was cloned, mostly aided by the conservation of the CNB domains across species. The R subunit from three species of the kinetoplastid group have so far been cloned and characterized: *T. brucei* (T. Klöckner, Ph.D. thesis 1996; (Shalaby et al., 2001), *T. cruzi* (Huang et al., 2006) and *L. donovani* (Bhattacharya et al., 2012). Messenger RNA and protein quantification by northern blot and western blot, respectively, showed that the TbPKAR is regulated in the life cycle with a five-fold higher expression in BSFs (Shalaby et al., 2001). A lifecycle-stage differential expression was also noted in *T. cruzi* with the highest expression in trypomastigote and least in amastigote (Huang et al., 2006). In *L. donovani*, expression of the R subunit was shown to be maximally expressed in the stationary phase of promastigotes (Biswas et al., 2011). This indicates that this kinase could indeed be involved in the differentiation process of kinetoplastids.

Sequence comparison of kinetoplastid R subunits with the mammalian counterpart has revealed a few differences in domain architecture. The C-terminal CNB domains and the linker region containing the substrate site are conserved in kinetoplastids. However, the N-terminal domain is unrelated and longer by about 120 amino acids. The residues required for the dimerization and docking (Leon et al., 1997) appear to be missing (C. Krumbholz, Ph.D. thesis 2006). This domain is conserved in all kinetoplastid R subunits characterized, so far. A depiction of the domains in comparison to the mammalian R subunit is shown below.
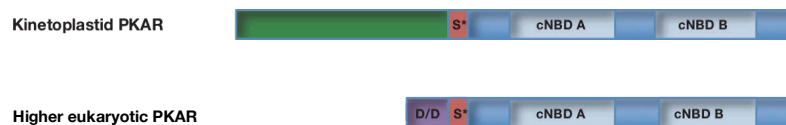
Fig. 1.5. TbPKAR has a conserved C-terminal CNB domains but a distinct kinetoplastid specific N-terminal domain: a scheme of kinetoplastid PKAR in comparison to the higher eukaryotic PKAR where the key domains are highlighted. The cyclic nucleotide binding domains (cNBDs) are highly conserved. Kinetoplastid PKARs lack the dimerization and docking (D/D) domain and have in place an unrelated longer N-terminal domain.

1.6.2 PKA kinase catalytic subunit

All members of the AGC family of kinases have a conserved catalytic core about 250 amino acids long, stretching from residue 40 to 285 (Hanks et al., 1988). This core adopts a bilobal topology comprising of a small N-terminal lobe mainly composed of β strands and a predominantly helical, large C-terminal lobe (Knighton et al., 1991a; Knighton et al., 1991b), see Fig. 1.6. The N-terminal lobe binds Mg/ATP leaving the γ phosphate poised for transfer to the substrate. The C-terminal lobe binds the substrate peptide, orients the γ phosphate for phosphotransfer and directs catalysis (Taylor et al., 1993). The catalytic loop lies in the cleft between the N and C lobes.

In PKA, the catalytic core is flanked by an N-terminal tail (N-tail) and C-terminal tail (C-tail). These tails are anchored to both lobes acting as cis regulatory elements (Taylor et al., 2008). Full functionality of the PKA kinase in any physiological system i.e. activity, localization and capacity to interact with other proteins, is governed by a series of co- and posttranslational modifications (PTM). One key PTM is the phosphorylation of a Threonine, in the heart of the activation loop (Thr197, in mammalian Cα). Full activity of the kinase is conferred by this phosphorylation (Steinberg et al., 1993). Other PTMs are usually either on the C-terminal or the N-terminal tails of the kinase, which wrap around the N and C lobes providing for both cis (kinase activity) and trans (protein interaction) regulatory elements (Taylor et al., 2012). Hence, these tails are specificity defining elements, an example of which is the N-tail of the mammalian Cα subunit. This kinase contains a myristoylation on the N-terminal glycine (Gly1), a deamidation (Asn2) and a phosphorylation (Ser10), influencing kinase interactions, activity and localization (Tholey et al., 2001).

The PKA kinase has many cellular targets and is involved in almost every area of cellular function. All the substrates, including physiological inhibitors, share a common recognition site mainly consisting of the phosphorylation/pseudophosphorylation site (P site) and a few crucial Arginines at P-6 and P-3 or P-3 and P-2 positions (Zetterqvist et al., 1976). A hydrophobic residue often occupies the P+1 position (Kemp et al., 1975).
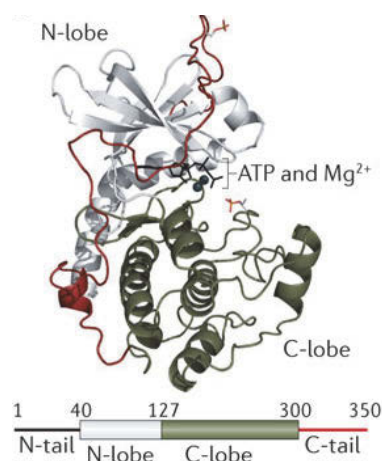
Fig 1.6. Structure of The cyclic AMP-dependent protein kinase (PKA): The catalytic core comprising of the N and C lobe is conserved in all eukaryotic kinases. Catalysis takes place in the cleft between the two lobes. The N and C tails wrap around the core and provide a template for kinase specific cis and trans elements, image from Taylor at al 2012.

In the mammalian system, there are five different subunit isoforms of relative abundance and tissue/cellular distribution, namely the Cα, Cβ, Cγ, PrKX and PrKY. The Cα is the most abundant form and appears to be constitutively expressed in most cells (Uhler et al., 1986). The human Cα and Cβ isoforms share 93% homology while that between Cα:Cγ and Cα:PrKX is 82 and 54%, respectively (Soberg et al., 2013). The Cα, Cβ and Cγ form a clade within the AGC family that excludes PrKX and PrKY. The PrKX exibit a distinct characteristic in holoenzyme formation. This kinase can only be inhibited by the RI type of regulatory subunits but not by the RII type (Diskar et al., 2010).

Three isoforms (TbPKAC1, TbPKAC2, TbPKAC3) have been cloned from *T. brucei's* genomic DNA (Kramer et al., 2007). TbPKAC1 and TbPKAC2 share a 93% homolgy while TbPKAC3 shares 55% homology with the TbPKAC1 and TbPKAC2 isoforms (S. Kramer, Ph.D. thesis 2006). Three isoforms of the catalytic subunits have also been cloned and characterized in *Leishmania major* (Siman-Tov et al., 1996; Siman-Tov et al., 2002) and in *T. cruzi* (Huang et al., 2002) portraying a similar homology profile to that of *T. brucei*. Analysis of both the mRNA and protein levels in LS and SS of the bloodstream stage, as well as in procyclic life stages, showed a life cycle dependent expression profile for TbPKAC1 and TbPKAC2 subunits while TbPKAC3 remained relatively unchanged throughout. More precisely TbPKAC1 had its peak expression in the bloodstream stages contrary to PKAC2, which was predominantly expressed in the procyclic form (S. Kramer, Ph.D. thesis 2006; C. Schulte zu Sodingen, Ph.D. thesis 2000).

1.7 PKA activation mechanism in higher eukaryotes

Decades of structural and biochemical studies of the mammalian PKA have a led to a comprehensive understanding of the activation mechanism of this kinase. The CNB domains are at the heart of this mechanism; given that they not only bind cAMP, but also provide a substantial interaction interface with the catalytic subunit in addition to the linker region (containing the inhibitor sequence). Each CNB is a small module of about 120 amino acids consisting of an 8-stranded β barrel, sandwiched between two helical elements (see Fig. 1.7). At the N-terminal end of the β barrel are the N-terminal helical

bundle consisting of α:N and α:A helices while the C-terminal helical bundle consist of α:B and α:C helices. Within the β barrel is a highly conserved sequence motif known as the phosphate-binding cassette (PBC), which provides the molecular basis for cAMP interaction. The PBC consists of a short helix (α-P) and a loop inserted between β-strand 6 and 7 (Diller et al., 2001; Rinaldi et al., 2010; Su et al., 1995).
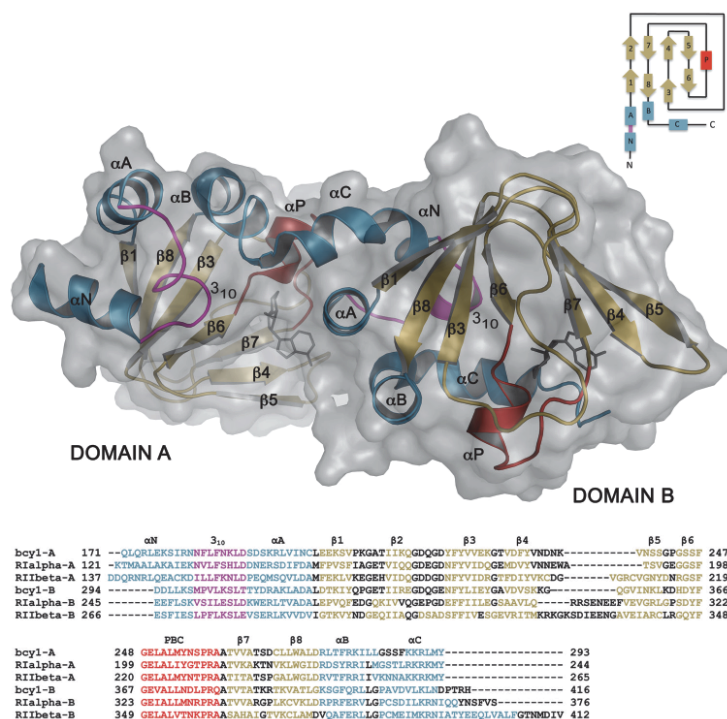
Fig. 1.7. The crystal structure of yeast bcy-1: The C-terminal of all regulatory subunits is comprised of two CNB domains that respect a general α-helix/β-sheet fold. Sequence alignment of three crystal structures from different organisms showed that the domains can be superimposed, image from Rinaldi et al., 2010.

1.7.1 The molecular basis for cAMP binding in the PBC

The high conservation of the PBC extends to all cyclic nucleotide-binding proteins (Rehmann et al., 2007). Analysis of several R subunits from different species generated the following consensus signature, F-G-E-[LIV]-A-L-[LIMV]-x(3)-[PV]-R-[ANQV]-A where x is any amino acid (Canaves and Taylor, 2002). Specific hydrogen bonds are formed between Glu (in blue) and the 2'-OH of the ribose sugar while Arg (in red) interacts with the equatorial O1 of the phosphate group. A few unspecific hydrogen bonds are also formed, mainly involving Gly and Ala residues. The Glu and Arg are hence the key interaction residues (Su et al., 1995; Diller et al., 2005). The Arg is especially important as it not only interacts with the phosphate of cAMP but also interacts with distal residues ensuring a cAMP-bound specific protein fold. In addition to the hydrogen bonds, a series of hydrophobic interactions involving other residues of the PBC and distal residues form a hydrophobic cap, protecting the hydrogen bonds (Diller et al., 2001). Fig. 1.8 depicts the PBC:A pocket of mammalian RIIβ where the residues of the PBC are in purple and

the distal residues recruited to the PBC upon cAMP binding are in blue. The adenine ring is also involved in the interaction but mainly by recruiting aromatic residues from the helical domains to form a hydrophobic stacking interaction, stabilizing cAMP in the PBC pocket (Berman et al., 2005).
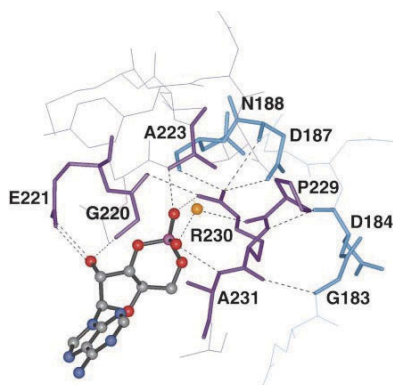
Fig. 1.8. cAMP interaction with the Phosphate Binding Cassette of RIIβ CNB:A: A depiction of the interaction network established between the sugar-phosphate moiety of cAMP and the PBC. Cyclic AMP is portrayed in a ball-and-stick model. Violet depicts the side chains of the conserved PBC structural motif. Dashed lines represent hydrogen bonds. The gold sphere represents a conserved solvent molecule. Image from Diller et al., 2001

1.7.2 Conformational rearrangement upon cAMP binding leading to the release of the C subunit

In the inactive holoenzyme state, the PBC in CNB:B is more accessible owing to the fact that the PBC in CNB:A is buried in the R/C interface and is partially occluded by the C subunit (Kim et al., 2007; Ogreid and Doskeland, 1981) see Fig. 1.9. Upon interaction of cAMP with PBC:B, the hydrogen bond network formed, tightens the PBC pocket. This induces a movement of the C-terminal bundle of CNB:B towards the PBC. In the process, a kink is formed between the α:B and α:C helices with the latter covering the cAMP molecule by establishing a hydrophobic interaction with the purine base. This shields the ligand from the surrounding solvent and also stabilizes the cyclic nucleotide in the bound conformation (Su et al., 1995; Diller et al., 2001; Berman et al., 2005). The α:B/α:C helices provide a large interaction interface with the C subunit in the extended conformation as shown in Fig. 1.9. The rearrangement of the C-terminal helical bundle results in the breakage of a salt bridge established between it and the N-terminal helical bundle, in the C subunit bound state. Once the salt bridge is broken, the N-terminal helical bundle retracts and in so doing reduces the R/C interaction interface. This enables the second cAMP molecule to access and interact with PBC:A. The same series of conformational rearrangement ensues in CNB:A module. The N-terminal bundle of CNB:A finally retracts and with it the undocking of the inhibitor sequence from the active site cleft of the C subunit, hence releasing the active kinase (Kim et al., 2007; Kim et al., 2005; Rehmann et al., 2007).
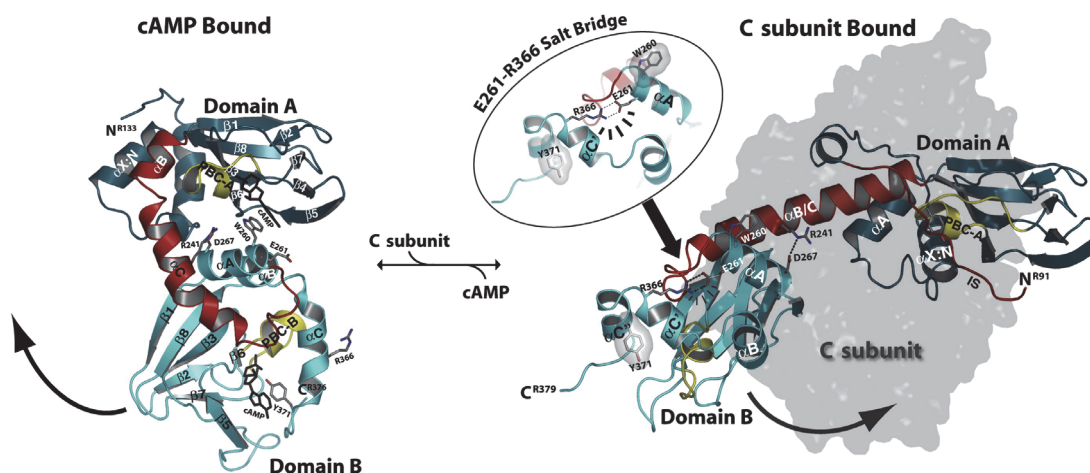
Fig. 1.9. Conformational rearrangement of RIα subunit upon cAMP or C subunit binding: Binding of cAMP results in a series of structural rearrangement, notably the breakage of a salt bridge that locks the C subunit bound state and the kinking of the α:B / α:C helix (in red) from its extended C bound state, resulting in the disruption of the R/C interaction interface. Image from Kim et al., 2007.

1.8 Biochemical strategies for studying PKA kinases

The specificity of the phosphotransfer to a well-determined motif on the target protein, as discussed in section 1.6.2, has been exploited in designing antibodies that can recognize the phosphorylated substrate motif and therefore aid in monitoring the kinase activity. Artificial substrate peptides, based on the general consensus of the substrate motif such as kemptide (Kemp et al., 1976), are also routinely used for in vitro analysis.

There are also kinase specific inhibitors, amongst which is the only other known physiological PKA inhibitor, apart from the regulatory subunit. The heat stable protein kinase inhibitor PKI has a pseudo substrates site (similar to RI type regulatory subunit) and was initially isolated as a contaminant of PKA kinase purification (Demaille et al., 1978). Although the physiological role of this protein still remains unknown, peptide inhibitors (containing the recognition and inhibitory sites) have been developed and commonly used for probing PKA kinase specific activity (Glass et al., 1986). The ATP binding on the catalytic subunit for phosphoryl- transfer has also been exploited to develop competitive ATP analogues whose γ phosphate cannot be transfered. These ATP analogues include H89 (Hidaka et al., 1984) and KT5720 (Kase et al., 1987). The specificity of these competitive antagonists is however much less than that of PKI (Murray, 2008).

Increasing intracellular cAMP concentrations is a common strategy for in vivo characterization of this kinase. In mammalian cells, ACs can be targeted to increase cAMP production with agonists such as forskolin and cholera toxin; however, these compounds are inactive in trypanosomes (Rolin et al., 1996). The degradation of cAMP by PDEs can be blocked with by specific antagonists. Two mammalian PDE inhibitors, dipyridamole and etazolate, have been used in *T. brucei* (Kunz et al., 2004). Membrane

permeable cAMP analogues such as 8-Br-cAMP or pCPT-cAMP are also commonly used.

1.9 Background of the Ph.D. thesis: previous research on *T. brucei* PKA in this laboratory

1.9.1 Features of *T. brucei* PKA: structure and composition

After the successful cloning of the regulatory subunit and the three isoforms of the catalytic subunit, rabbit polyclonal antibodies were generated against recombinant full-length TbPKAR and TbPKAC subunit fragments, expressed in *E. coli*. TbPKAC1 and TbPKAC2 are very related and thus only a common antibody could be produced (T. Klöckner, Ph.D. thesis 1996; C. Schulte zu Sodingen, Ph.D. thesis 2000).

Co-immunoprecipitation studies showed that the regulatory subunits could interact with each of the three subunits but, more interestingly, it was shown that the holoenzyme exists as a heterodimer in contrast to the higher eukaryotic heterotetramer (S. Kramer, Ph.D. thesis 2006). Analysis of the kinase using the immunoprecipitated material showed that it has all the features of a canonical PKA, as pertains to substrate specificity and inhibition by PKI and ATP analogues (H89 and KT5720) (T. Klöckner, Ph.D. thesis 1996; S. Kramer, Ph.D. thesis 2006).

In vitro characterization using heterologously expressed, enzymatically active, TbPKA necessitated a eukaryotic expression system. Full-length TbPKAC1 and TbPKAC3 subunits were expressed in the baculovirus expression vector system (BEVS). TbPKAC3 was characterized in this way (N. Wild, unpublished; D. Sohmen, Diploma thesis 2008) but the in vitro activity of TbPKAC1 could not be determined. An even greater challenge was the in vitro reconstitution of the holoenzyme complex. The full-length TbPKAR, expressed in *E. coli*, could not inhibit the BEVS expressed TbPKACs (D. Sohmen, Diploma thesis 2008).

Several genetic manipulation approaches have been carried out, highly suggesting that this kinase is crucial for the survival of the parasite. Down regulation of the three catalytic isoforms by RNAi resulted in reduced growth and impairment in cytokinesis (S. Kramer, Ph.D. thesis 2006). The regulatory subunit was successfully knocked out, but the resulting cell line had a severe growth and motility phenotype (C. Krumbholz, this lab). It was also noted that the depletion of the R subunit resulted in down regulation of TbPKAC1/2 while TbPKAC3 levels were barely affected (C. Krumbholz, this lab). TbPKAC3 was also successfully knocked out in a PCF cell line, showing no severe phenotype (C. Schulte zu Sodingen, Ph.D. thesis 2000).

Localization studies have shown that this kinase is predominantly localized in the flagellar rod (C. Krumbholz, Ph.D. thesis 2006). The TbPKAR N-terminal domain is involved in the localization as well as in the interaction with the catalytic subunits (C. Krumbholz, Ph.D. thesis 2006). It was shown that truncating at least the first ten residues of this domain was sufficient to loose both of these functions.

1.9.2 Features of *T. brucei* PKA: Activation by cyclic nucleotides

cAMP affinity chromatography has for a long time been used to isolate the mammalian PKA from its native source. The failure to precipitate TbPKA using agarose immobilized cAMP analogues provided the first indications that TbPKA does not bind to cAMP (C. Schulte zu Sodingen, Ph.D. thesis 2000; S. Kramer, Ph.D. thesis 2006). Both in vivo and in vitro experimental approaches were designed to test for the holoenzyme activation by cAMP.

In vitro assays using co-immunoprecipitated holoenzyme showed that cAMP could not activate the holoenzyme, even at millimolar concentrations. On the other hand, a five-fold increase of the catalytic activity from the basal level could be observed in the presence of 1 mM cGMP (S. Kramer, Ph.D. thesis 2006). This was in accordance to similar findings by Shalaby et al (2000), where they performed cyclic nucleotide binding studies with TbPKAR and showed that cGMP, but not cAMP, binds to this kinase. In both studies however, the activation and dissociations constants obtained were deemed to be too high to have any physiological relevance. Other cyclic nucleotides were tested in the same set up including cyclic Inosine monophosphate (cIMP) and cyclic Xanthosine monophosphate (cXMP), but none could activate the kinase (S. Kramer, Ph.D. thesis 2006).

In vivo kinase assays were carried out using the mammalian Vasodilator-Stimulated Phosphoprotein (VASP) as a transgenic PKA reporter substrate in *T. brucei*. This assay was validated as PKA specific by using PKA specific inhibitors such as PKI and KT5720 to down regulate the reporter phosphorylation. Concentrations of up to 250 μM cell-permeant pCPT-cAMP or pCPT-cGMP did not increase in vivo VASP phosphorylation. It required a cGMP concentration of 5 mM to reproduce the in vitro activation (S. Kramer, Ph.D. thesis 2006). Concentrations of ≥ 1 mM pCPT-cAMP had an inhibitory effect by competing with the cGMP-mediated activation. Down regulation of PDEs by RNAi resulting in an intracellular increase of cAMP also showed no increase in kinase activity (S. Bachmaier, unpublished). This was however not the case with the PDE inhibitors dipyridamole and etazolate, which contrary to expectations showed an increase in kinase activity (S. Kramer, Ph.D. thesis 2006). However, more recent data using tetrahydrophthalazinone (also known as Compound A), which is a much more potent PDE inhibitor (de Koning et al., 2012) could not activate the kinase (S. Bachmaier, unpublished). The mechanism underlying dipyridamole and etazolate activation of this kinase is not understood.

1.9.3 Features of *T. brucei* PKA: Activation by stress response

In many organisms, PKA plays an important role in response to stress conditions, leading to protein activation and gene expression regulation. The in vivo kinase assay was also used to test whether the known environmental triggers were capable of stimulating the kinase. BSF cells grown at ideal conditions were subjected to different environmental cues. Increase in cell density has been shown to be able to initiate differentiation as

discussed earlier. It was however shown that a short-term increase in cell density (cell concentrated to 1×10^7/ml for 30 min) resulted in no increase in VASP reporter phosphorylation. Osmolarity was tested in hypotonic (20-60 mM NaCl) and hypertonic conditions (100-160 mM NaCl); these led to an increase and decrease of the reporter phosphorylation, respectively. The influence of pH (pH 5.5, 6.5, 8.5 and 9.5) on TbPKA activation was also tested, demonstrating that acidic conditions activated the kinase (S. Kramer, Ph.D. thesis 2006).

The perception of a decrease in temperature during transition from the mammalian (homoeothermic) to the insect host (poikilothermic) has previously been shown to influence differentiation, as discussed earlier (Engstler and Boshart, 2004). BSF cells were subjected to a range of temperatures (30°C, 20°C, 12°C, 4°C) lower than the mammalian host's body temperature (37°C). It was shown that, indeed, TbPKA's activity increases with decreasing temperature conditions (S. Kramer, Ph.D. thesis, 2006). Reverse genetic experiments by knock out and knock down of the PKA subunits confirmed the specificity of these responses (S. Bachmaier, unpublished).

1.10 Objectives of this thesis: understanding the activation mechanism of TbPKA

A key property of TbPKA is its non-responsiveness to cAMP activation, despite the seemingly high conservation of the CNB domains. Stress responses, dipyridamole and unphysiological concentrations of cGMP remain the only known activators. It would hence appear that subtle differences do exist, making this kinase and possibly all kinetoplastid PKAs unique in their activation mechanism. The mammalian PKA kinase has for many decades been studied both for its structure and biochemical features and therefore provides the ideal template for comparison with TbPKA. An in silico based approach was adapted in order to understand the molecular bases of altered properties with respect to cAMP activation.

The in vivo kinase assay has been instrumental in characterizing the activation of TbPKA, while in vitro analyses have been limited to native co-immunoprecipitated holoenzyme due to earlier faced difficulties in the heterologous expression of the holoenzyme. Establishing a robust in vitro kinase assay system was therefore a key objective of this thesis. This meant exploiting several expression systems for their capacity to express fully functional kinase subunits that can be used to form a holoenzyme complex of high yield and purity. This would then enable analysis of PKA activation in *T. brucei*

2 Materials and Methods

2.1 Materials

2.1.1 Oligonucleotides and vector constructs

2.1.1.1 Mutagenesis of TbPKAR PBC domains

❖ **Oligos**

Name	Sequence	Annealing target	Purpose
LowerPBC1mut	CACCGTGGCAgCAcgTGGTGTCTGATACATA AGTgCAAGCTCTCC	TbPKAR	Mutagenesis of TbPKAR PBC:A
UpperPBC1mut	GGAGAGCTTGcACTTATGTATCAGACACCAc gTGcTGCCACGGTG	TbPKAR	Mutagenesis of TbPKAR PBC:A
LowerPBC2mut	AACATCTGCTgCAcgGGCGTGATTGTTAAGG AATgCCAGCTCACC	TbPKAR	Mutagenesis of TbPKAR PBC:B
UpperPBC2mut	GGTGAGCTGGcATTCCTTAACAATCACGCC cgTGcAGCAGATGTT	TbPKAR	Mutagenesis of TbPKAR PBC:B

Swopped nucleotides are in lower case

2.1.1.2 In situ rescue of TbPKAR KO in *T. brucei*

❖ **Vector constructs**

	pBSK.PKAR
Origin	J. Pepperl, Diploma thesis, 2007
Short description	In situ single allele rescue of PKAR KO in MITat1.2 cell line
Plasmid linearization	PvuII
Selection marker	Phleomycin 2.5 µg/ml in BSF MITat1.2

	pBSK.PKAR-Ty1
Cloning	pBSK.PKAR was digested with BamHI and HindIII to remove the N-terminal fragment, which was then replaced by a Ty1 tag containing fragment from pLew82.PKARty1_corr (C. Krumbholz, this lab)
Short description	In situ single allele rescue of PKAR KO in MITat1.2 cell line with PKAR-Ty1
Plasmid linearization	PvuII
Selection marker	Phleomycin 2.5 µg/ml in BSF MITat1.2

	pBSK. PKAR PBCmut
Cloning	pBSK.PKAR was digested with HindIII and BglII and the fragment removed was replaced with one containing the PBC mutants from pETDuet-PKAR PBCmut (see section 2.1.1.4) digested with the same enzymes.
Short description	In situ single allele rescue of PKAR KO in MITat1.2 cell line with PKAR PBCmut
Plasmid linearization	PvuII
Selection marker	Phleomycin 2.5 µg/ml in BSF MITat1.2

pBSK.PKAR-Ty1 PBCmut	
Cloning	pBSK.PKAR-Ty1was digested with HindIII and BglII and the fragment removed was replaced with one containing the PBC mutants from pETDuet-PKAR6x-His PBCmut digested with the same enzymes.
Short description	In situ single allele rescue of TbPKAR KO in MITat1.2 cell line with PKAR-Ty1 PBCmut
Plasmid linearization	PvuII
Selection marker	Phleomycin 2.5 µg/ml in BSF MITat1.2

2.1.1.3 TbPKAC3 knockout

❖ Oligos

Name	Sequence	Annealing target	Purpose
5' C3 upp	CAGTAAGCTTTCCTCGCCATCCACTTCAA	TbPKAC3	Verifying correct integration 5' of the TbPKAC3 locus
3' C3 low	CCT TTT CCA GCT CCT CCA TTA T	TbPKAC3	Verifying correct integration 3' of the TbPKAC3 locus
T7	AATACGACTCACTATA	pBluescript vector	Sequencing from pBluescript vector backbones
T3	ATTAACCCTCACTAAA	pBluescript vector	Sequencing from pBluescript vector backbones
Neo upp	CGGTCTTGTCGATCAGGATG	Neomycin	Sequencing and verifying correct integration 3' of the TbPKAC3 locus
Neo lower	GCCGGATCAAGCGTATGCAG	Neomycin	Sequencing and verifying correct integration 5' of the TbPKAC3 locus
Hygro upp	CTGGACCGATGGCTGTGTAG	Hygromycin	Sequencing and verifying correct integration 3' of the TbPKAC3 locus
Hygro lower	GCCGGATCAAGCGTATGCAG	Hygromycin	Sequencing and verifying correct integration 5' of the TbPKAC3 locus

❖ Vector constructs

pBΔpkac3.NEO	
Origin	C. Schulte zu Sodingen, Ph.D. thesis 2000
Short description	Knock out of TbPKAC3 in Antat1.1 strain
Plasmid linearization	DraIII and PvuI
Selection marker	2 µg/ml in BSF MITat1.2
Remark	The Antat 1.1 PKAC3 intergenic targeting regions were re-sequenced in this thesis and compared to those of the MITat 427lister sequence (GeneDB) showing no difference.

pBΔpkac3.HYGRO	
Origin	C. Schulte zu Sodingen, Ph.D. thesis 2000
Short description	Knock out of TbPKAC3 in Antat1.1 strain
Plasmid linearization	HindIII
Selection marker	2.5 µg/ml in BSF MITat1.2
Remark	The Antat 1.1 PKAC3 intergenic targeting regions were re-sequenced in this thesis and compared to those of MITat 427lister sequence (GeneDB) showing no difference.

2.1.1.4 TbPKA expression in *E. coli* with the pET vector system (Novagen)

❖ **Oligos**

Name	Sequence	Annealing target	Purpose
5' PKARhis pETDuet	TTAGGTCTCACATGTCTGAA AAGGGAACA	TbPKAR	Cloning of PKAR-6xHis into pETDuet vector
3' PKARhis pETDuet	CGCGGATCCTCAGTGGTGG TGGTGGTGGTG	TbPKAR	Cloning of PKAR-6xHis into pETDuet vector
5' Strep-C1&C3 pETDuet	TTGGAATTCCATATGGCTTC GGCTTGGAGCCAC	TbPKAC1 and TbPKAC3	Cloning of strep-PKAC1 and PKAC3 into pETDuet vector (anneals to the strep tag)
3'strep-C1 pETDuet	TTCTGCCTAGGCTAAAAACC ACGGAATGCAAC	TbPKAC1	Cloning of TbPKAC1 into pETDuet vector
3'strep-C3 pETDuet	TTCTGCCTAGGCTAGATCCT CGTGTATTCACC	TbPKAC3	Cloning of TbPKAC3 into pETDuet vector
pETUpstream Primer	ATGCGTCCGGCGTAGA	pETDuet MCS1 insert	Forward primer for Sequencing of the ORF inserted in pETDuet vector MCS1
DuetDOWN1 Primer	GATTATGCGGCCGTGTACAA	pETDuet MCS1 insert	Reverse primer for Sequencing of the ORF inserted in pETDuet vector MCS1
DuetUP2 Primer	TTGTACACGGCCGCATAATC	pETDuet MCS2 insert	Forward primer for Sequencing of the ORF inserted in pETDuet vector MCS2
T7 terminator	AATACGACTCACTATA	pETDuet MCS2 insert	Reverse primer for Sequencing of the ORF inserted in pETDuet vector MCS2

❖ **Vector constructs**

	pET32a.PKAR-6xHis
Origin	Andreas Binder, this lab
Short description	Expression of C-terminal 6xHis-tagged TbPKAR in *E. coli*
Selection marker	Ampicillin 100 µg/ml

	pETDuet.PKAR-6xHis
Cloning	PKARHis-6xHis ORF was cloned from pET32a.PKAR-6xHis by amplification with 5' PKARhis pETDuet and 3' PKARhis pETDuet primer pair containing BsaI and BamH1 overhangs respectively. The BsaI digestion generated NcoI compatible ends. The target vector (pETDuet, Novagen) was digested with NcoI and BamHI.
Short description	Expression of 6xHis C-terminal tagged PKAR in *E. coli*
Selection marker	Ampicillin 100 µg/ml

	pETDuet.PKAR-6xHis PBCmut
Cloning	PCR directed mutagenesis was performed using the following primers LowerPBC1mut, LowerPBC2mut, UpperPBC1mut, UpperPBC2mut, 5' PKARhis pETDuet and 3' PKARhis pETDuet, using pET32a.PKAR-6xHis as template to generate PKAR-6xHis PBCmut ORF (see section 2.2.6). Ligation into the pETDuet vector was as described for pETDuet.PKAR-6xHis
Short description	Expression of C-terminal 6xHis-tagged PKAR PBCmut in *E. coli*
Selection marker	Ampicillin 100 µg/ml

	pETDuet.strep-PKAC1
Cloning	The TbPKAC1 ORF was amplified from pFASTBAC-strep-PKAC1 (D. Sohmen, Diploma thesis, 2008) using 5' Strep-C1/C3 and 3'strep-C1 pETDuet primers containing NdeI and AvrII overhangs respectively. pETDuet was digested with the same enzymes
Short description	Expression of N-terminal strep-tagged TbPKAC1 in *E. coli*
Selection marker	Ampicillin 100 µg/ml

	pETDuet.strep-PKAC1-dead
Cloning	Mutation to render recombinant TbPKAC1 catalytically inactive was designed by S. Kramer as described in S. Kramer Ph.D. thesis, 2006. The fragment containing the mutation was cut from pTy1-PKAC1-dead vector (S. Kramer, Ph.D. thesis, 2006) using XbaI and AatII restriction enzymes. pETDuet.strep-PKAC1 was also cut with the same enzymes, generating three fragments. A three component ligation approach was then used to obtain pETDuet.strep-PKAC1-dead. This approach necessitated laborious screening by test digest in order to obtain a correctly integrated vector.
Short description	Expression of catalytically inactive strep-PKAC1 in *E. coli*
Selection marker	Ampicillin 100 µg/ml

	pETDuet.strep-PKAC3
Cloning	The TbPKAC3 ORF was amplified from pFASTBAC-strep-PKAC3 (D. Sohmen, Diploma thesis, 2008) using 5' Strep-C1/C3 and 3'strep-C3 pETDuet primers containing NdeI and AvrII respectively. pETDuet was digested with the same enzymes
Short description	Expression of N-terminal strep-tagged TbPKAC3 in *E. coli*
Selection marker	Ampicillin 100 µg/ml

	pETDuet.PKAR-6xHis/strep-PKAC1
Cloning	Strep-PKAC1 ORF was integrated into the second MCS of pETDuet.PKAR-6xHis with the same cloning strategy as for pETDuet.strep-PKAC1 vector.
Short description	Co-expression PKAR-6xHis and strep-PKAC1 in *E. coli*
Selection marker	Ampicillin 100 µg/ml

	pETDuet.strep-PKAC1-dead
Cloning	Mutation to render recombinant TbPKAC1 catalytically inactive was designed by S. Kramer as described in S. Kramer Ph.D. thesis, 2006. The fragment containing the mutation was cut from pTy1-PKAC1-dead vector (S. Kramer, Ph.D. thesis, 2006) using XbaI and AatII restriction enzymes. pETDuet.strep-PKAC1 was also cut with the same enzymes, generating three fragments. A three component ligation approach was then used to obtain pETDuet.strep-PKAC1-dead. This approach necessitated laborious screening by test digest in order to obtain a correctly integrated vector.
Short description	Co-expression PKAR-6xHis and catalytically inactive strep-PKAC1 in *E. coli*
Selection marker	Ampicillin 100 µg/ml

	pETDuet.PKAR-6xHis/strep-PKAC3
Cloning	Strep-PKAC3 ORF was integrated into the second MCS of pETDuet.PKAR-6xHis with the same cloning strategy as for pETDuet.strep-PKAC3 vector.
Short description	Co-expression PKAR-6xHis and strep-PKAC3 in *E. coli*
Selection marker	Ampicillin 100 µg/ml

2.1.1.5 TbPKA expression in the Baculovirus expression vector system (BEVS) from Invitrogen

❖ Oligos

Name	Sequence	Annealing target	Purpose
5' PKAR	GCTCTAGAATGTCTGAAAAGGGAAC	TbPKAR	Cloning of TbPKAR wild type into pFastBac1 vector
3'PKARwt	TACATGCATGCTCACTTCCTCCCCTCTGC	TbPKAR	Cloning of TbPKAR wild type into pFastBac1 vector
3' PKAR-PTP	GACATGCATGCTCAGGTTGACTTCCCC	TbPKAR	Cloning of TbPKAR-PTP into pFastBac1 vector
PKAC1 wt 5'	GCTCTAGAATGACGACAACTCCCACT	TbPKAC1	Cloning of TbPKAC1 wild type into pFastBac1 vector
PKAC1 wt 3'	TACATGCATGCCTAAAAACCACGGAA	TbPKAC1	Cloning of TbPKAC1 wild type into pFastBac1 vector
PKAC3 wt 5'	GCTCTAGAATGAAGTCGGATGGGTGC	TbPKAC3	Cloning of TbPKAC3 wild type into pFastBac1 vector
PKAC3 wt 3'	TACATGCATGCTCAGATCCTCGTGTA	TbPKAC3	Cloning of TbPKAC3 wild type into pFastBac1 vector
pFB1_sequ_f	CCGTCCCACCATCGGGCG	pFASTBAC vector	Forward primer for Sequencing of the ORF inserted in pFASTBAC vector
pFB1_sequ_r	GCAAGTAAAACCTCTACA	pFASTBAC vector	Reverse primer for Sequencing of the ORF inserted in pFASTBAC vector
M13 forward	TGTAAAACGACGGCC AGT	Bacmid	Verifying correct integration of insert into the bacmid
M13 reverse	CAGGAAACAGCTATGACC	Bacmid	Verifying correct integration of insert into the bacmid

❖ Vector constructs

	pFastBac1 (Invitrogen)
Short description	Shuttle vector for bacmid integration
Selection markers	Ampicillin 100 μg/ml, Gentamicin 7 μg/ml (only in DH10 Bac *E. coli* strain).

	pFastBac1.PKARwt
Construction	PKAR ORF was amplified from pC-PTP-NEO-PKAR (F. Böttger, Diploma thesis 2006) with 5' PKAR (XbaI overhang) and 3'PKARwt (SphI overhang) primers and ligated into pFastBac1 vector, digested with the same enzymes.
Short description	Expression of TbPKAR in Sf9 cells.
Selection marker	Ampicillin 100 μg/ml, Gentamycin7 μg/ml (only in DH10 Bac *E. coli* strain).

	pFastBac1.PKAR-PTP
Cloning	PKAR-PTP ORF was amplified from pC-PTP-NEO-PKAR with 5' PKAR (XbaI overhang) and 3'PKAR-PTP (SphI overhang) (the 3' primer anneals to the PTP tag) primers and ligated into pFastBac1 vector, digested with the same enzymes.
Short description	Expression of PKAR-PTP in Sf9 cells.
Selection marker	Ampicillin 100 μg/ml, Gentamycin7 μg/ml (only in DH10 Bac *E. coli* strain).

	pFastBac1.PKAC1wt
Cloning	TbPKAC1 wild type was amplified from MITat1.2 genomic DNA with PKAC1 wt 5' (XbaI overhang) and PKAC1 wt 3' (SphI overhang) primers and ligated into pFastBac1 vector, digested with the same enzymes.
Short description	Expression of PKAC1wt in Sf9 cells.
Selection marker	Ampicillin 100 µg/ml, Gentamycin 7 µg/ml (only in DH10 Bac).

	pFastBac1.PKAC3wt
Cloning	TbPKAC3 wild type was amplified from MITat1.2 genomic DNA with PKAC3 wt 5' (XbaI overhang) and PKAC3 wt 3' (SphI overhang) primers and ligated into pFastBac1 vector, digested with the same enzymes.
Short description	Expression of PKAC3wt in Sf9 cells.
Selection marker	Ampicillin 100 µg/ml, Gentamycin7 µg/ml (only in DH10 Bac).

	pFastBac1.strep-PKAC1
Origin	(D. Sohmen, Diploma thesis 2008)
Short description:	Expression of strep-PKAC1 in Sf9 cells.
Selection marker:	Ampicillin 100 µg/ml, Gentamycin7 µg/ml (only in DH10 Bac).

	pFastBac1.strep-PKAC3
Origin	(D. Sohmen, Diploma thesis 2008)
Short description:	Expression of strep-PKAC3 in Sf9 cells.
Selection marker:	Ampicillin 100 µg/ml, Gentamycin7 µg/ml (only in DH10 Bac).

❖ Bacmid DNA

	pFastBac1.PKAR-Bacmid
Cloning	pFastBac1.PKAR vector was transformed into DH10Bac *E. coli* for transposition of TbPKAR (untagged) into the bacmid.
Short description	Expression of TbPKAR wild type in Sf9 cells.
Selection marker	Kanamycin 50 µg/ml, Gentamycin7 µg/ml, Tetracycline 10 µg/ml.

	pFastBac1.PKAR-PTP-Bacmid
Cloning	pFastBac1.PKAR-PTP vector was transformed into DH10Bac *E. coli* for transposition of PKAR-PTP into the bacmid.
Short description	Expression of PKAR-PTP in Sf9 cells.
Selection marker	Kanamycin 50 µg/ml, Gentamycin 7 µg/ml, Tetracycline 10 µg/ml.

	pFastBac1.PKAC1-Bacmid
Cloning	pFastBac1.PKAC1 vector was transformed into DH10Bac *E. coli* for transposition of TbPKAC1 (untagged) into the bacmid.
Short description	Expression of PKAC1wt in Sf9 cells.
Selection marker	Kanamycin 50 µg/ml, Gentamycin 7 µg/ml, Tetracycline 10 µg/ml.

	pFastBac1.PKAC3-Bacmid
Cloning	pFastBac1.PKAC3 vector was transformed into DH10Bac *E. coli* for transposition of TbPKAC3 (untagged) into the bacmid.
Short description	Expression of PKAC3wt in Sf9 cells.
Selection marker	Kanamycin 50 µg/ml, Gentamycin7 µg/ml, Tetracycline 10 µg/ml.

pFastBac1.strep-PKAC1-Bacmid	
Origin	D. Sohmen, Diploma thesis 2008
Cloning	pFastBac1.strep-PKAC1 vector was transformed into DH10Bac *E. coli* for transposition of strep-PKAC1 into the bacmid.
Short description	Expression of strep-PKAC1 in Sf9 cells.
Selection marker	Kanamycin 50 µg/ml, Gentamycin 7 µg/ml, Tetracycline 10 µg/ml.

pFastBac1.strep-PKAC3-Bacmid	
Origin	D. Sohmen, Diploma thesis 2008
Cloning	pFastBac1.strep-PKAC3 vector was transformed into DH10Bac *E. coli* for transposition of strep-PKAC3 into the bacmid.
Short description	Expression of strep-PKAC3 in Sf9 cells.
Selection marker	Kanamycin 50 µg/ml, Gentamycin 7 µg/ml, Tetracycline 10 µg/ml.

The bacmid DNA was transfected into Sf9 cells to generate viral stocks of transgenic *Autographa californica.*

2.1.1.6 TbPKA expression in *Leishmania* expression system (LEXSY) from Jena Bioscience

❖ Oligos

Name	Sequence	Annealing target	Purpose
5' PKAR SlaI	ATGCATCTCGAGATGTCTGAAAAGGGAACATCG	TbPKAR	Cloning of PKAR-10xHis into pLEXSY-I-Ble3 vector
3' PKAR Not1	TATATAATAGTTTAGCGGCCGCTCAGTGGTGGTGATGGTGGTGGTGGTGGTGATGGCTACCGCCCTTCCTCCCCTCTGCCCTTAA2525	TbPKAR	Cloning of PKAR-10xHis into pLEXSY-I-Ble3 vector
5' Strep BamH1	CGCGGATCCATGGCTTCGGCTTGGAGCCAC	TbPKAC	Cloning of strep-PKAC into pLEXSY-I-Neo3 vector
PKAC1 Rev not1	ACTATGCAATAGTTTAGCGGCCGCCTAAAAACCACG GAATGCAAC	TbPKAC1	Cloning of strep-PKAC1 into pLEXSY-I-Neo3 vector
PKAC3 Rev not1	ACTATGCAATAGTTTAGCGGCCGCCTAGATCCTCGTG TATTCACC	TbPKAC3	Cloning of strep-PKAC3 into pLEXSY-I-Neo3 vector
5' Ble BamHI	GCCGGATCCACCATGGCCAAGTTGACCAGT	Phleomycin	Converting pLEXSY-I-Neo3 to pLEXSY-I-Ble3
3' Ble SpeI	CTAGAACTAGTTCAGTCCTGCTCCTCGGCCA	Phleomycin	Converting pLEXSY-I-Neo3 to pLEXSY-I-Ble3
p2x-c2x Primer2	CAAGCACAAGAAAAGGAG	TbPKAR	Sequencing of TbPKAR
p2x-c2x Primer3	CTCGATCGCGACACGTAT	TbPKAR	Sequencing of TbPKAR
L_CI_III_sequ	GTCCACCAATCCACAGC	TbPKAC	Sequencing of both TbPKAC1 and TbPKAC3
U_CI_III_sequ	TACCGTGACTTGAA	TbPKAC	Sequencing of both TbPKAC1 and TbPKAC3

❖ Vector constructs

pLEXSY_I-neo3	
Origin	Jena Bioscience (Donated by F. Bringaud, Bordeaux university)
Short description	Inducible protein overexpression in *L. tarentolae*
Selection marker	Ampicillin 100 µg/ml

	pLEXSY_I-ble3
Cloning	The phleomycin resistance cassette was amplified from pBSK.PKAR-Ty1 (see section 2.1.1.2) using primer pairs 5' Ble BamHI and 3' Ble SpeI. The ORF was ligated into pLEXSY_I-neo3 (replacing the Neo resistance cassette) after digestion with BamHI and SpeI.
Short description:	Inducible expression of recombinant PKA in *L. tarentolae*
Selection marker:	Ampicillin 100 µg/ml

	pLEXSY_I-ble3.PKAR-10xHis
Cloning	PKAR-10xHis ORF was amplified from pBSK.PKAR-Ty1 using 5' PKARhis (pETDuet) (generates an NcoI compatible end) and 3' PKAR Not1 primer. The ORF was ligated into pLEXSY_I-ble3 after digestion with NcoI and NotI.
Short description	Expression of PKAR-10xHis in *L. tarentolae* inducible system
Selection marker	Ampicillin 100 µg/ml

	pLEXSY_I-ble3.PKAR PBC mut-10xHis
Cloning	PKAR-10xHis ORF was amplified from pBSK.PKAR PBC mut-Ty1(see section 2.1.1.2) using 5' PKARhis (generates an NcoI compatible end) and 3' PKAR Not1 primer. The ORF was ligated into pLEXSY_I-ble3 after digestion with NcoI and NotI.
Short description	Expression of PKAR-10xHis PBCmut in *L. tarentolae* inducible system
Selection marker	Ampicillin 100 µg/ml

	pLEXSY_I-neo3.strep-PKAC1
Cloning	Strep-PKAC1 ORF was amplified from pFASTBac.strep-PKAC1 (D. Sohmen, Diploma thesis 2008) using 5' Strep BamH1 (the BamHI overhang can also be digested with NcoI) and TbPKAC1 Rev not1 primer. The ORF was ligated into pLEXSY_I-neo3 after digestion with NcoI and NotI.
Short description	Expression of strep-PKAC1 in *L. tarentolae* inducible system
Selection marker	Ampicillin 100 µg/ml

	pLEXSY_I-neo3.strep-PKAC3
Cloning	Strep-PKAC3 ORF was amplified from pFASTBac.strep-PKAC3 (D. Sohmen) using 5' Strep BamH1 (the BamHI overhang can also be digested with NcoI) and TbPKAC3 Rev not1 primer. The ORF was ligated into pLEXSY_I-neo3 after digestion with NcoI and NotI.
Short description	Expression of strep-PKAC3 in *L. tarentolae* inducible system
Selection marker	Ampicillin 100 µg/ml

2.1.1.7 TbPKAR expression for tandem purification in *T. brucei*

	pC-Neo.PKAR-PTP
Origin	F. Böttger, Diploma thesis 2006
Short description	C-terminally PTP-tagged PKAR for in situ cloning in *T. brucei*
Plasmid linearization	XCMI (cuts in the PKAR ORF)
Selection markers	G418 2 µg/ml for BSFs and 20 µg/ml for PCFs

2.1.2 Cell lines

2.1.2.1 *Trypanosoma brucei* wild type cell lines

MITat1.2 (NY subclone) monomorphic BSF	(Cross, 1975; Cross and Manning, 1973)
AnTat 1.1 PCF	(Delauw et al., 1985; Geigy et al., 1975)

2.1.2.2 *Trypanosoma brucei* transgenic cell lines

2.1.2.2.1 MITat 1.2 PKAR Knock out and rescue cell lines

	MITat1.2 *Δpkar::PURO / Δpkar::HYGRO*
Common Name	MITat1.2 PKAR KO
Origin	C. Krumbholtz, this lab
Clonality	Pool
Constructs	pBSK[HYG]Rko, pBSK[Puro]Rko,
Selection markers:	Hygromycin 2.5 µg/ml, Puromycin 1µg/ml.

	MITat1.2 *Δpkar::PURO / Δpkar::HYGRO. VASP [BSD]*
Common Name	MITat1.2 PKAR KO VASP
Origin	J. Pepperl, Diploma thesis 2007
Clonality	Pool
Constructs	pBSK[HYG]Rko, pBSK[Puro]Rko, pTSARib[BSD]VASP
Selection markers	Hygromycin 2.5 µg/ml, Puromycin 1µg/ml, Blasticidin 4 µg/ml

	MITat1.2 *Δpkar::HYGRO / PKAR [BLE]*
Common Name	MITat1.2 PKAR KO / PKARwt rescue
Clonality	Clones
Constructs	pBSK[HYG]Rko, pBSK.PKAR (J. Pepperl, Diploma thesis 2007)
Selection markers	Hygromycin 2.5 µg/ml, Phleomycin 2 µg/ml.

	MITat1.2 *Δpkar::HYGRO / PKAR-Ty1 [BLE]*
Common Name	MITat1.2 PKAR KO / PKAR-Ty1 rescue
Clonality	Clones
Constructs	pBSK[HYG]Rko, pBSK.PKAR-ty1
Selection markers	Hygromycin 2.5 µg/ml, Phleomycin 2 µg/ml.

	MITat1.2 *Δpkar::HYGRO / PKAR PBCmut [BLE]*
Common Name	MITat1.2 PKAR KO / PKAR PBCmut rescue
Clonality	Clones
Constructs	pBSK[HYG]Rko, pBSK.PKAR PBCmut
Selection markers	Hygromycin 2.5 µg/ml, Phleomycin 2 µg/ml.

MITat1.2 *Δpkar::HYGRO / PKAR-Ty1 PBCmut [BLE]*	
Common Name	MITat1.2 PKAR KO - PKAR PBCmut-Ty1 rescue
Clonality	Clones
Constructs	pBSK[HYG]Rko, pBSK.PKAR Ty1 PBCmut
Selection markers	Hygromycin 2.5 µg/ml, Phleomycin 2 µg/ml.

MITat1.2 *Δpkar::HYGRO / PKAR [BLE]. VASP [BSD]*	
Common Name	MITat1.2 PKAR KO / PKARwt rescue VASP
Clonality	Clones
Constructs	pBSK[HYG]Rko, , pTSARib[BSD]VASP, pBSK.PKAR
Selection markers	Hygromycin 2.5 µg/ml, Blasticidin 4 µg/ml, Phleomycin 2 µg/ml.

MITat1.2 *Δpkar::HYGRO / PKAR-Ty1 [BLE]. VASP [BSD]*	
Common Name	MITat1.2 PKAR KO / PKAR-Ty1 rescue VASP
Clonality	Clones
Constructs	pBSK[HYG]Rko, pTSARib[BSD]VASP, pBSK.PKAR-Ty1
Selection markers	Hygromycin 2.5 µg/ml, Blasticidin 4 µg/ml, Phleomycin 2 µg/ml.

MITat1.2 *Δpkar::HYGRO/ PKAR PBCmut [BLE]. VASP [BSD]*	
Common Name	MITat1.2 PKAR KO / PKAR PBCmut rescue VASP
Clonality	Clones
Constructs	pBSK[HYG]Rko, , pTSARib[BSD]VASP, pBSK.PKAR PBCmut
Selection markers	Hygromycin 2.5 µg/ml, Blasticidin 4 µg/ml, Phleomycin 2 µg/ml.

MITat1.*2 Δpkar::HYGRO/ PKAR-Ty1 PBCmut [BLE]. VASP [BSD]*	
Common Name	MITat1.2 PKAR KO / PKAR PBCmut-Ty1 rescue VASP
Clonality	Clones
Constructs	pBSK[HYG]Rko, pTSARib[BSD]VASP, pBSK.PKAR-Ty1 PBCmut
Selection markers	Hygromycin 2.5 µg/ml, Blasticidin 4 µg/ml, Phleomycin 2 µg/ml.

2.1.2.2.2 PKAR-PTP expression cell lines

MITat1.2 *PKAR:: pkar-PTP [Neo]*	
Common Name	MITat1.2 pN-PTP-Neo-PKAR
Origin and Date	F. Böttger, Diploma thesis 2006
Clonality	Pool
Constructs	pN-PTP-Puro-PKAR
Selection markers:	Neomycin 2 µg/ml

Antat1.1 *PKAR:: pkar-PTP [Neo]*	
Common Name	Antat1.1 pN-PTP-Puro-PKAR
Origin	F. Böttger, Diploma thesis 2006
Clonality	Pool
Constructs	pC-PTP-Neo-PKAR
Selection marker	Neomycin 15-20 µg/ml

2.1.2.2.3 MITat 1.2 PKAC3 Knock out cell lines

MITat1.2 *Δpkac3::NEO* / *pkac3*	
Common Name	MITat1.2 PKAC3Neo Hemizygous KO
Clonality	clone 1 & 2, pool 2 & 3
Constructs	pB*Δpkac3*NEO
Selection marker	Neomycin 2 µg/ml
Remark	Correct integration was verified by PCR

MITat1.2 *Δpkac3::HYGRO* / *pkac3*	
Common Name	MITat1.2 PKAC3 Hygro Hemizygous KO
Clonality	Pool 1-3
Constructs	pB*Δpkac3.*HYGRO
Selection marker	Hygromycin 2.5 µg/ml
Remark	Correct integration was verified by PCR

MITat1.2 *Δpkac3::NEO* / *Δpkac3::HYGRO*	
Common Name	MITat1.2 PKAC3 Neo/Hygro KO
Clonality	Clone 1 & 2
Constructs	pB*Δpkac3.*NEO, pB*Δpkac3.*HYGRO
Selection markers	Hygromycin 2.5 µg/ml, Neomycin 2 µg/ml
Remark	Correct integration was verified by PCR

MITat1.2 *Δpkac3::HYGRO* / *Δpkac3::NEO*	
Common Name	MITat1.2 PKAC3 Hygro/Neo KO
Clonality	Clone 1, 2 & 3
Constructs	pB*Δpkac3*NEO, pB*Δpkac3*HYGRO
Selection markers	Hygromycin 2.5 µg/ml, Neomycin 2 µg/ml
Remark	Correct integration was verified by PCR

2.1.2.3 Bacteria strains

Name	Genotype	Purpose
***E. coli* SURE** (Stratagene)	e14-(McrA-) Δ(mcrCB-hsdSMR-mrr) 171 endA1 supE44 thi-1 gyrA96 relA1 lac recB recJ sbcC umuC::Tn5 (Kanr) uvrC [F′ proAB lacIq ZΔM15 Tn10 (Tetr)])]	Plasmid Amplification
***E. coli* XL10-Gold** (Stratagene)	endA1 glnV44 recA1 thi-1 gyrA96 relA1 lac Hte Δ(mcrA)183 Δ(mcrCBhsdSMR-mrr)173 tetR F'[proAB lacIqZΔM15 Tn10(TetR Amy CmR)]	Plasmid Amplification
DH10Bac (Invitrogen)	F-mcrA Δ(mrr-hsdRMS-mcrBC) 80lacZΔM15 ΔlacX74 recA1 endA1 araD139 Δ(ara, leu)7697 galU galK - rpsL nupG/bMON14272/pMON7124	Generation of a recombinant bacmid after transposition of the pFastBac vector expression constructs.
BL 21 (DE3) (Novagen)	F – ompT hsdSB(rB– mB–) gal dcm	General Recombinant protein expression
BL21 (DE3) pLysS (Novagen)	F – ompT hsdSB(rB– mB–) gal dcm (DE3)pLysS (CamR)	High-stringency recombinant protein expression
Rosetta (DE3) (Novagen)	F – ompT hsdSB(rB– mB–) gal dcm (DE3) pRARE27 (CamR)	General recombinant protein expression plus complementation of rare eukaryotic tRNAs
Rosetta (DE3) pLysS	F – ompT hsdSB(rB– mB–) gal dcm (DE3) pLysSRARE6	High-stringency recombinant protein

(Novagen)	(CamR)	expression plus complementation of rare eukaryotic tRNAs
Origami (DE3) pLysS (Novagen)	*Δara–leu7697 ΔlacX74 ΔphoA PvuII phoR araD139 ahpC galE galK rpsL* F '[lac+ lacIq pro] (DE3) gor522 ::Tn10 trxB pLysS (CamR, KanR, StrR, TetR)	High-stringency recombinant protein expression plus enhancement of disulfide bond formation
C41 (DE3) Walker strain (Miroux and Walker, 1996)	[*E. coli* F⁻ *ompT hsdS*ᵦ (rᵦ⁻ mᵦ⁻) *gal dcm* (DE3)]	High-stringency recombinant protein expression
C43 (DE3) Walker strain (Miroux and Walker, 1996)	[*E. coli* F⁻ *ompT hsdS*ᵦ (rᵦ⁻ mᵦ⁻) *gal dcm* (DE3)]	High-stringency recombinant protein expression
Lemo 21 (DE3) **(NEB)**	*fhuA2 [lon] ompT gal (λ DE3) [dcm] ΔhsdS/ p*Lemo(Camᴿ) λ DE3 = λ sBamHIo ΔEcoRI-B int::(lacI::PlacUV5::T7 gene1) i21 Δnin5 pLemo = pACYC184-*PrhaBAD-lysY*	High-stringency recombinant protein expression
Arctic expression RIL (Agilent technologies)	*E. coli* B F⁻*ompT hsdS*(rᵦ⁻mᵦ⁻) *dcm*+Tetʳ*gal endA* Hte [*cpn10 cpn60* Gentʳ][*arg*U *ile*Y *leu*W Strʳ]	High-stringency recombinant protein expression

2.1.2.4 Insect cell lines

Spodoptera frugiperda **(Sf9)**	Isolated from ovarian tissue of the fall army worm (Vaughn et al., 1977).

2.1.2.5 *Leishmania tarentolae* cell lines

	L. tarentolae T7-TR
Origin	Jena Bioscience (Donated by F. Bringaud, Bordeaux university)
Short description	Tetracycline inducible overexpression of recombinant protein
Selection marker	Nourseothricin (NTC) 10 µg/ml, Hygromycin 10 µg/ml,
Remark (s)	T7 polymerase and Tet repressor are constitutively expressed under RNA polymerase I

	L. tarentolae T7-TR:: PKAR-10xHis
Construct	pLEXSY_I-ble3.PKAR-10xHis
Short description	Inducible expression of PKAR-10xHis in *L. tarentolae*
Plasmid linearization	SwaI
Selection markers	NTC 10 µg/ml, Hygromycin 10 µg/ml, Phleomycin 10 µg/ml.

	L. tarentolae T7-TR:: PKAR-10xHis PBCmut
Construct	pLEXSY_I-ble3.PKAR-10xHis PBCmut
Short description	Inducible expression of PKAR-10xHis PBCmut in *L. tarentolae*
Plasmid linearization	SwaI
Selection markers	NTC 10 µg/ml, Hygromycin 10 µg/ml, Phleomycin 10 µg/ml.

	L. tarentolae T7-TR:: strep-PKAC1
Construct	pLEXSY_I-neo3.strep-PKAC1
Short description	Inducible expression of strep-PKAC1 in *L. tarentolae*
Plasmid linearization	SwaI
Selection markers	NTC 10 µg/ml, Hygromycin 10 µg/ml, Neomycin 5 µg/ml.

	L. tarentolae T7-TR:: strep-PKAC3
Construct	pLEXSY_I-neo3.strep-PKAC3
Short description	Inducible expression of strep-PKAC3 in *L. tarentolae*
Plasmid linearization	SwaI
Selection markers	NTC 10 µg/ml, Hygromycin 10 µg/ml, Neomycin 5 µg/ml.

	L. tarentolae T7-TR:: PKAR-10xHis/strep-PKAC1
Construct	pLEXSY_I-ble3.PKAR-10xHis & pLEXSY_I-neo3.strep-PKAC1
Short description	Inducible co-expression of TbPKAR & TbPKAC1 in *L. tarentolae*
Plasmid linearization	SwaI
Selection markers	NTC 10 µg/ml, Hygromycin 10 µg/ml, Phleomycin 10 µg/ml, Neomycin 5 µg/ml.

	L. tarentolae T7-TR:: PKAR-10xHis/strep-PKAC3
Construct	pLEXSY_I-ble3.PKAR-10xHis & pLEXSY_I-neo3.strep-PKAC3
Short description	Inducible co-expression of TbPKAR & TbPKAC3 in *L. tarentolae*
Plasmid linearization	SwaI
Selection markers	NTC 10 µg/ml, Hygromycin 10 µg/ml, Phleomycin 10 µg/ml, Neomycin 5 µg/ml.

	L. tarentolae T7-TR:: PKAR PBC mut-10xHis/strep-PKAC1
Construct	pLEXSY_I-ble3.PKAR-10xHis PBC mut& pLEXSY_I-neo3.strep-PKAC1
Short description:	Inducible co-expression of TbPKAR PBCmut & TbPKAC1 in *L. tarentolae*
Plasmid linearization	SwaI
Selection markers	NTC 10 µg/ml, Hygromycin 10 µg/ml, Phleomycin 10 µg/ml, Neomycin 5 µg/ml.

2.1.3 Enzymes

T4 DNA Ligase	M0202S	NEB, Frankfurt
Phusion DNA-Polymerase	M0530S	NEB, Frankfurt
Taq DNA-Polymerase	M0273S	NEB, Frankfurt
Restriction endonucleases	See NEB catalogue	NEB, Frankfurt
DNase (RNase frei)	A3778,0010	Applichem, Darmstadt
AcTEV protease	12575-015	Invitrogen, Karlsruhe
TEV protease		In house (see section 2.2.12.6)

2.1.4 Special chemicals and purification resins

Protease Inhibitor Complete Mini EDTA-free	Cat n°: 04693159001	Roche, Mannheim
Insta-Fluor Plus liquid scintillation cocktail	Cat n°: 6013167	PerkinElmer, Rodgau
L-rhamnose	Cat n°: A4336,0010	Applichem, Darmstadt
Ni-NTA	Cat n°: 88221	Thermo Scientific Pierce, Schwerte
Anti-Protein C affinity matrix	Cat n°: 1181502400	Roche, Mannheim
IgG sepharose 6 Fast flow	Cat n°: 17-0969-01	GE Healthcare, Munich
Strep-Tactin sepharose	Cat n°: 2-1201-010	IBA, Goettingen
Protein G sepharose	F. Schwede*	Gene Center, LMU
8-pCPT-adenosine agarose	Custom synthesis*	Biolog, Bremen
6-AH-cAMP agarose	Cat n°: A 036-06*	Biolog, Bremen
8-AET-cGMP agarose	A 019-06*	Biolog, Bremen

* Acquired through a collaboration partnership

2.1.5 Antibiotics

Ampicillin	10 mg/ml in H2O	Boehringer, Mannheim
G418	10 mg/ml / 50mg/ml in H2O	Sigma, Taufkirchen
Hygromycin	10 mg/ml / 100mg/ml in H2O	Calbiochem, Darmstadt
Kanamycin	10 mg/ml in H2O	Merck, Darmstadt
Phleomycin	10 mg/ml H2O	Cayla, Toulouse
Puromycin	10 mg/ml in H2O	Sigma, Taufkirchen
Tetracyclin	10 mg/ml in EtOH	Sigma, Taufkirchen
NTS Nourseothricin	100 mg/ml H_2O	Jena bioscience, Jena

2.1.6 Equipment

Amaxa Nucleofector II	Lonza, Köln
Bioruptor	Diagenode, Lüttich
CASY I Cell Analyzer (Modell TTC)	Schärfe System, Reutlingen
Liquid scintillations counter LS 5000 TD	Beckman Instruments, Munich
Tri-Carb 2910TR liquid scintillation analyzer	PerkinElmer, Rodgau
Geldoc 2000	Bio-Rad, Munich
Nano Drop-1000 Spectrophotometer	Peqlab, Erlangen
French® pressure cell press	Glen Mills Inc, USA
Electro Cell Manipulator 630	BTX, Genetronics, Inc., San Diego,
Spectrophotometer DU 640	Beckman Instruments, Munich

2.1.7 Kits

NucleoBond PC100 & 500	Macherey-Nagel, Düren
NucleoSpin Extract II	Macherey-Nagel, Düren
NucleoSpin Plasmid	Macherey-Nagel, Düren
NucleoBond BAC 100	Macherey-Nagel, Düren
NucleoSpin Tissue	Macherey-Nagel, Düren
Bradford Protein Assay	Bio-Rad, Munich
Bac-to-Bac® BEVS	Invitrogen, Karlsruhe

2.1.8 Software

Graph pad prism 6.0	GraphPad Software, Inc	
Jalview 14.0	Waterhouse et al., 2009	www.jalview.org/Web_Installers/install.htm
UCSF Chimera 1.7	University of California, USA	http://www.cgl.ucsf.edu/chimera/docs/relnotes/1.7.html
Modeller 9.12	Sali et al., 1993	https://salilab.org/modeller/download_installation.html
Gene Construction Kit	Textco, New Hampshire, USA	
ImageJ	National institute of health, USA	rsbweb.nih.gov/ij/download.html
4Peaks	Mekentosj, Netherland	http://nucleobytes.com/index.php/4peaks
Odyssey 2.1	LI-COR, Bad Homburg	
EnzymeX	Mekentosj, Amsterdam	http://nucleobytes.com/index.php/enzymex
EndNote X7	Thomson Reuters, Carlsbad	

2.2 Methods

2.2.1 *Trypanasoma brucei* cell culture

2.2.1.1 Cultivation of monomorphic BSF

BSF culture medium for 1 liter (HMI9)	Media supplements
Iscoves modified medium (IMDM), + L-Glutamine, - NaHCO$_3$	3.024 g NaHCO$_3$; 136 mg hypoxanthine; 28.2 mg bathocuproine sulfonate; 20 mM 2-mercaptoethanol; 39 mg thymidine; 100000 u penicillin; 100 mg streptomycin; 182 mg cysteine; 10% FCS

(Hirumi and Hirumi, 1989) with modifications from (Vassella and Boshart, 1996)

Monomorphic BSF cells were cultured in complete HMI9 medium (supplemented) in vented cell culture flasks at 37°C in a humidified incubator (98% humidity) containing 5% CO$_2$. The cells were maintained at logarithmic growth by microscopic monitoring and regular counting with the Neubauer cell chamber. The highest cell density allowed was 8x10^5 cell/ml.

2.2.1.2 Cultivation of PCF cells

PCF culture medium for 1 liter	Media supplements
SDM79-CGGPPT (PAA) pH 7.3	2.6 mM NaHCO3; 10 mg hemin; 0.1M D-Glucose; 0.091 M Sodium pyruvate; 50 mM L-threonine; 0.265 mM L-proline; 200 mM L-glutamine; 50000 U penicillin; 50 mg streptomycin; 10% FCS

PCF cells were maintained in complete SDM79 medium in sealed-cap cell culture flasks at 27°C in non-humidified incubator. The cells were maintained at logarithmic growth i.e. 2×10^6 to 1×10^7, by microscopic monitoring and regular counting with the CASY cell counter.

> ➤ **PCF suspension culture**

The cells were also grown in large volumes of up to two litres in aluminium-foil sealed Erlenmeyer flasks under constant shaking at around 100 rpm. Vigorous shaking was avoided to prevent cell shearing.

2.2.1.3 Freezing and thawing of monomorphic BSF cells

BSF freezing medium	HMI9 medium + 10% glycerol (sterilized by passage through a 0.2 μM filter)

▪ **Freezing:** BSF cells were harvested by centrifugation at 1400 g for 10 minutes at 4°C. The cells were then resuspended in freezing medium (precooled to 4°C) to give an end concentration of 4×10^6/ml and then aliquoted into cryovials. The vials were put into a Stratacooler and allowed to slowly freeze overnight at -80°C, before been transferred to the -150°C freezer for long-term storage.

▪ **Thawing:** The cells were quickly thawed in a 37°C water bath and added to 9 ml of complete HMI9 medium. They were then harvested by centrifugation and resuspended in 10 ml HMI9 medium. After at least 1 hour of recovery in the incubator, the cells were counted and diluted before addition of the required selection drugs.

2.2.1.4 Freezing and thawing of PCF cells

PCF freezing medium	SDM79 medium + 10% glycerol (sterilized by passage through a 0.2 µM filter)

▪ **Freezing:** PCF cells were harvested by centrifugation at 900 g for 10 minutes at 4°C. The cells were then resuspended in precooled freezing medium to a density of 4 x 10^7/ml and transferred into cryovials. The vials were put into a Stratacooler and allowed to slowly freeze overnight at -80°C, before been transferred to the -150°C freezer for long-term storage.

▪ **Thawing:** The cells were quickly thawed in a 27°C water bath and added to 9 ml of complete SDM79 medium. They were then harvested by centrifugation and resuspended in 10 ml complete SDM79 medium. After at least 1 hour of recovery in the incubator, the cells were counted and diluted before addition of the required selection drugs.

2.2.1.5 Stable transfection of BSF cells (Burkard et al., 2007)

Parasite transfection buffer	AMAXA proprietary recipe
Tb-BSF (Schumann et al., 2011)	90 mM NaH_2PO_4; 5 mM KCl; 0.15 mM $CaCl_2$; 50 mM HEPES, pH 7.3

0.5-1 x 10^7 BSF cells at mid-log phase (5-8 x 10^5 cells/ml) were harvested and resuspended in 100 µl of the AMAXA parasite transfection buffer or the Tb-BSF buffer. 10 µg of linearized plasmid DNA (ideally in 10 µl H_2O) was added to the cells. Electroporation was performed in 2 mm gap cuvettes with the AMAXA Nucleofector® II using program X-001 (mouse T cell). The cells were immediately transferred into 50 ml HMI9 (37 °C). The appropriate selection drugs were added at least 6 but not later than 18 hours after transfection.

For clonal selection, the electroporation mix was transferred into 30 ml HMI9 medium followed by a 1:10 and 1:100 dilutions in 30 ml HMI9 medium. The dilutions were then distributed into 24-well cell culture plates (1 ml per well). An additional 1 ml complete HMI9 medium containing 2x the concentration the appropriate selection drugs was added 6–18 hours post transfection. Transfectants were in general, visible 4 - 6 days later.

2.2.1.6 Stable transfection of PCF cells (McCulloch et al., 2004)

Cytomix	10 mM K_2HPO_4/KH_2PO_4 pH 7.6; 2 mM EGTA; 120 mM KCl; 150 µM $CaCl_2$; 25 mM HEPES; 5 mM $MgCl_2$; 0.5% glucose; 1 mM hypoxanthine; 100 µg/ml BSA
SDM79-Conditioned medium	PCF cells at late-log growth phase (1 x 10^7 and 2 x 10^7 cells/ml) were harvested and the supernatant (conditioned SDM79) was sterilized by filtration.

PCF cells at mid-log growth phase were harvested and resuspended in cytomix. 1 x 10^7 cells in 400 µl cytomix per transfection. 10 µg of linearized DNA was added and the transfection mix was transferred into a sterile 2 mm gap cuvette. Electroporation was performed with the electro cell manipulator 630 (BTX, San Diego, California) at 1.5 kV, 175 Ω and 25 µF. The transfection mix was immediately transferred into 10 ml 30% conditioned SDM79 medium i.e. 7 ml complete SDM79 medium plus 3 ml of the conditioned medium .

For clonal selection, 10 ml of a 1:1, 1:10 and 1:100 dilution of the transfected cells were plated on 96 well cell culture plates (100 µl per well). 2x the concentration of the selection drugs in 100 µL complete SDM79 medium was added 18 hours after transfection. The plates were sealed with para-film to avoid desiccation. Transfectants were visible after 12 to 14 days.

2.2.1.7 Evaluation of target protein expression in *T. brucei*

At least 5 x 10^6 cells were harvested by centrifugation at 1400g (BSFs) or 900g (PCFs) for 10 min at 4°C. The cells were washed twice in pre-cooled PBS buffer and resuspended in the same buffer to give an end concentration of 2 x 10^6 cells per µl. The same volume of 2x SDS sample loading buffer (see section 2.2.13.3.1) was added to give a final concentration of 1 x 10^6 cells per µl. The samples were boiled for 5 minutes at 95°C followed by a 30 sec sonication pulse (300 Hz) with the Bioruptor®. 5 x 10^6 cells were loaded per lane of an SDS-PAGE gel.

2.2.1.8 Extraction of genomic DNA

In general, between 6 x 10^6 and 10 x 10^6 cells were harvested by centrifugation at 4°C followed by one wash with cold PBS. The extraction was carried out using the genomic DNA extraction kit, Macherey Nagel® following the manufacturers instructions. DNA quantification was by A_{280}/A_{260} measurement using the Nanodrop® spectrometer.

2.2.2 *Spodoptera frugiperda*: Sf9 cell culture

2.2.2.1 Cultivation of Sf9 cells

Sf9 culture medium for 1 liter	Media supplements (To be added shortly before use)
TNM-FH medium (Hink, 1970) , + L-Glutamine, - NaHCO₃ (Applichem): 52.01 g/l was completely dissolved in 900 ml culture grade water. 0.35g of NaHCO₃ was added per litre of medium. The pH was adjusted to 6.1 and the media sterile filtered with 0.2 µM filters. (Storage of the media was at 4°C, away from light)	• 100000 U penicillin; 100 mg streptomycin • 10% FCS • 0.1% pluronic acid (only for shaker cultures to prevent cell shearing)

Sf9 cells were cultured at 27°C ± 0.5 °C in a dark incubator either as a monolayer culture in vented cell culture flasks or in culture Erlenmeyer flasks with loosened cap under constant shaking (120-150 rpm). The cells were maintained at logarithmic growth

between 0.5 x 10^6 and 2 x 10^6/ml. A healthy growing culture could be monitored by microscopy as described in the Growth and Maintenance of Insect Cell Lines manual (Invitrogen). The cells doubled at least once every 24 hours and were regularly counted with the Neubauer chamber. Cell viability was analyzed by premixing the cells with 0.1 % Trypan blue (diluted in PBS) where at least 90% of cells with dye exclusion was expected in a healthy cell culture.

2.2.2.1.1 Sf9 cells monolayer culture

1.0 x 10^6 cells in 5 ml complete TNM-FH medium were inoculated into a 25-cm^2 cell culture flask. This could be scaled up for bigger flasks in the same ratio. The flask's cap was loosened and laid flat in the incubator for 4-6 days until the cells reached confluency. The flask was then tilted at an angle to aspirate the medium and floating cells from the confluent culture by use of a Pasteur pipette. 5 ml of fresh complete TNM-FH medium was added before vigorously rapping of the flask against the palm of the hand and pipetting the medium across the monolayer to resuspend the cells. After complete detachment of cells (analyzed by inverted light microscope), a viable cell count was performed with Trypan blue. The cells were then freshly inoculated and the medium replaced regularly without detaching the cells, until confluency was reached.

2.2.2.1.2 Suspension Sf9 cell culture

5x10^5/ml viable Sf9 cells were inoculated into 250 ml Erlenmeyer flask (with loose cap) with 100 ml of complete TNM-FH medium. The cells were cultured in a 27°C incubator on an orbital shaker (120-150 rpm). 0.1% pluronic acid was added to protect the cells from shearing. Sub-culturing of the cells, to 5 x 10^5/ml, was performed twice a week (preferably on Monday and Thursday). If slower growth was noted, the cultures were gently centrifuged at 800 g for 5 minutes, and the pellet was resuspended in fresh medium.

2.2.2.2 Freezing and thawing Sf9 cells

Sf9 cells Freezing medium	Fresh TNM-FH medium plus 10% FCS and 7.5% DMSO

▪ **Freezing:** Sf9 cells were harvested by centrifugation at 800 g for 5 minutes and resuspended in the freezing medium to give an end concentration of 1 x 10^7/ml. The cells were then transferred into cryovials (1 ml per vial) and kept at 4°C for 30 minutes. They were then transferred into a Stratacooler and kept overnight in the -80°C freezer before transfer to the -150°C freezer for indefinite storage.

▪ **Thawing:** The cells were quickly thawed in a 37°C water bath with gentle agitation. A 25-cm^2 flask was pre-wet with 4 ml TMN-FH medium and the one ml cell volume transferred into the medium. The cells were allowed to attach in the incubator for 30-45 minutes. The DMSO containing medium was then removed and replaced with 5 ml of fresh TMN-FH medium. The medium was again changed after 24 hours, after which the

cells were grown to confluency. Direct inoculation of the cells into suspension culture was possible where by the DMSO containing medium was removed by centrifugation (500 g, 5 min) and the cells resuspended in fresh TMN-FH medium. The cells however took much longer to reach regular doubling time.

2.2.3 *Leishmania tarentolae* cell culture

2.2.3.1 *Leishmania tarentolae* static culture

L. tarentolae BHI medium for 1 litre	Media supplements (To be added shortly before use)
37g of Brain-Heart infusion medium (BHI): completely dissolved in culture grade water and autoclaved at 121°C for exactly 15 minutes. (Prolonged exposure to high temperatures was avoided). The media was left to cool down before storage at 4°C away from light	• 10 µg/ml Hemin • 100000 U penicillin; 100 mg streptomycin • 10 µg/ml NTC (only for maintenance of the T7 polymerase) • 10 µg/ml Hygromycin (only for maintenance of Tet repressor)

L. tarentolae cells were cultured in BHI medium at 26.5 °C in a dark incubator. Strain maintenance was in 10 ml vented cell culture flasks positioned upright. The cells were diluted twice a week at early stationary phase 6-8x10^7 cell/ml by 1:50 dilution on Monday and 1:20 dilution on Friday. Lower dilutions and prolonged cultures (more than 3 months) affected growth and protein expression. The T7-TR *L. tarentolae* strain required 10 µg/ml NTC and 10 µg/ml Hygromycin for the maintenance of T7 polymerase and the Tet repressor system, respectively. 10 µg/ml of Neomycin and/or Phleomycin were added, depending on the recombinant protein expressed.

2.2.3.2 *Leishmania tarentolae* suspension culture

L. tarentolae suspension culture was performed in Erlenmeyer flasks sealed with aluminium –foil in volumes of up to 500 ml under slow constant agitation at 50 - 100 rpm. Higher agitation speeds were avoided since the cells grew slower and their morphology changed to more rounded aflagellated cells. Freshly thawed cells were first grown in stationary culture for a few days before transfer to suspension culture.

2.2.3.3 Freezing and thawing *L. tarentolae* cells

L. t. freezing medium (10 ml) (Should be prepared shortly before use)	0.37g BHI medium was completely dissolved in 7 ml culture grade water. 3 ml Glycerol and 10 µg/ml Hemin was added followed by sterile filtration with 0.2 µM filter.

▪ **Freezing:** logarithmically growing cells (around 5 x1 0^7/ml) were mixed with an equal volume of the freezing medium and aliquoted into cryovials (1 - 1.5 ml per vial). The cells were then cooled step-wise in a Stratacooler by overnight storage at -80°C and then transferred to the -150°C freezer for long-term storage.

▪ **Thawing:** The cells were quickly thawed in a 27°C water bath and then transferred into a 15 ml falcon tube containing 8-10 ml complete BHI medium. The cells

were then centrifuged for 5 minutes at 2000g. The glycerol containing media was discarded and the cell pellet resuspended in 10 ml complete BHI medium. The cells were transferred in to 25-cm^2 TC-flask and the required selection drugs added within 12-20 hours.

2.2.3.4 Stable transfection of *L. tarentolae* cells (Jena Bioscience, LEXSY manual)

The *L. tarentolae* cells were thawed and adapted to cell culture by a few passages (for not more than a one month). The cells were then harvested at a density of around 5×10^7/ml by centrifugation at 2000 g for 3 minutes. Half of the culture volume was then discarded and the cells resuspended in the remaining medium to attain 1×10^8 cells/ml and put on ice for 10 minutes. 5-10 µg of transforming linearized DNA in ≤50 µl sterile water was added to 350 µl of the pre-chilled cells and transferred into the electroporation cuvettes (d=2 mm). Electroporation was performed with the electro cell manipulator 630 (BTX, San Diego, California) at 1.5 kV, 175 Ω and 25 µF. The cuvettes were then put back on ice for 10 minutes followed by transfer of the cells into ventilated cell culture flasks containing 10 ml of complete BHI medium.

Selection drugs were added 20-24 hours after transfection. Recombinant cells grew as a cloudy suspension after about 5 days. At least one passage was necessary in order to completely get rid of non- transfected cells.

2.2.3.5 Evaluation of recombinant protein expression in *L. tarentolae*

Tetracycline (10 µg/ml) was added to the cell culture cells expressing the inducible recombinant protein after sub-culturing to $1\text{-}2 \times 10^7$ cells/ml. Samples were taken every 24 hours until the cells reached stationary growth phase. The cells were then washed twice with pre-chilled PBS (2000 g for 5 min). The cell pellets were then resuspended in PBS plus an appropriate amount of 2x or 6x SDS sample loading buffer, to give an end concentration of 1×10^7 cell/µl. 2-5 µl were loaded per lane of SDS-PAGE gel.

2.2.4 *E. coli* cell culture

1x LB liquid medium for 1 litre	10 g tryptone; 5 g yeast extract; 10 g NaCl; dissolved in culture grade water, pH 7
2x LB liquid medium	20 g tryptone; 10 g yeast extract; 20 g NaCl; dissolved in culture grade water. pH 7
2x agar	32 g agar was dissolved in culture grade water
SOB medium	20 g/l tryptone; 5 g/l yeast extract; 10 mM NaCl; 2.5 mM KCl; 10 mM MgCl$_2$; 10 mM MgSO$_4$; pH 7

(After completely dissolving the media components, and adjusting the pH with NaOH where necessary, the medium was autoclaved for 20 min at 121°C)

2.2.4.1 *E. coli* solid media culture

2x LB liquid medium was added to an equal volume of liquid 2x agar (heated to melting point in the microwave). The required selection antibiotics were added at a 1:1000 dilution, once the LB agar mix had cooled down to around 50°C. The LB-agar was then poured into petri dishes, which were then left with the lid open to allow escape of vapor

during cooling. Freshly transformed *E. coli* strains were plated on the solid media plates and incubated at 37°C until formation of colonies.

2.2.4.2 *E. coli* liquid media culture

Liquid cell cultures were inoculated from fresh colonies, especially for the overexpression of recombinant protein. 10–500 ml cell cultures could be inoculated in 50-2000 ml baffled Erlenmeyer flasks. The cultures were kept under constant shaking at 200 rpm and at temperatures varying from 18°C – 37°C depending on the experiment.

2.2.4.3 Freezing and thawing *E. coli* cells

E. coli storage buffer	25 mM Tris-HCl pH 8.0; 65% glycerin; 0.1 M MgSO$_4$

0.5 -1 ml of an overnight saturated culture was added to the storage buffer in a 1:1 ratio and stored at -80°C. The *E. coli* strain was reactivated by streaking the glycerol stock on a fresh LB-plate containing the required antibiotics followed by overnight incubation at 37°C.

2.2.4.4 Making chemical competent *E. coli* cells (Chung and Miller, 1988)

TSB buffer	Polyethylenglycol 10%, DMSO 5%, MgCl$_2$ 10 mM and MgSO$_4$ mM were dissolved in LB medium. The pH was adjusted to 6.5 with NaOH followed by sterile filtration.

An overnight culture of the *E. coli* strain was inoculated into fresh LB medium in a 1:100 dilution. The new culture was incubated at 37°C until OD$_{600}$ 0.6. The cells were harvested by centrifugation at 2000 g for 15 min at 4°C. The supernatant was carefully discarded and the pellet carefully resuspended in pre-cooled TSB buffer (1/10th of the culture volume). 100 µl aliquots were made in Eppendorf tubes, pre-cooled to -80°C with dry ice and ethanol.

2.2.4.5 Making electrocompetent *E. coli* cells (Dower et al., 1988)

An overnight culture of an *E. coli* strain grown at 37°C shaking at 200 rpm, was re-inoculated into fresh LB medium in a 1:100 dilution. After reaching OD$_{600}$ 0.6, the cells were cooled down on ice for 20 minutes and harvested by centrifugation (4000 g, 15 min, 4 °C). The cell pellet was then carefully resuspended in an equal volume, to the LB culture, of sterile pre-cooled deionized water and incubated on ice for 30 minutes. Cells were centrifuged and washed once more in deionized water and once in 1/10 volume of pre-cooled 10% glycerin. The bacteria pellet was finally resuspended in 1/100 volume of 10% glycerin and aliquoted in – 80°C pre-cooled Eppendorf tubes and stored in the –80 °C freezer.

2.2.4.6 Transformation of *E. coli*

❖ **Electroporation**

50 µl of electrocompetent cells were thawed on ice and gently mixed with 1-3 µl of DNA (at least 10 pg). The cell-DNA mix was incubated on ice for one minute and then transferred into a pre-cooled Gene Pulser 2 mm Cuvettes (Bio-Rad). Electroporation was performed with the Gene Pulser (Bio-Rad) at 25 µF, 2.5 kV and 200 Ω. Cells were immediately transferred into 1 ml pre-warmed SOB-medium. After incubation for 45 min at 37 °C on a shaker at 200 rpm, 100 µl of the cells were plated on LB agar plates containing the appropriate antibiotics until the formation of colonies. A few 1:10 dilutions, before plating, were often necessary in order to obtain lesser colony populations.

❖ **Chemical**

50 µl of competent cells were thawed on ice and gently mixed with 1-3 µl of DNA (at least 10 pg). The cell-DNA mix was incubated on ice for 30 min during which a heating block was heated to 42°C and SOB medium warmed to 37°C. After the incubation on ice, the mix was transferred to the heating block for 90 sec and quickly put back on ice for two min. Cells were then transferred into 1 ml pre-warmed SOB-medium and incubated for 45 min at 37 °C on shaker at 200 rpm. The Cells were centrifuged at 5000 g for 2 min and resuspended in $1/10^{th}$ of the SOB medium, which was then plated on LB agar plates containing the appropriate antibiotics until the formation of colonies. A few 1:10 dilutions, before plating, were often necessary in order to obtain lesser colony populations.

2.2.4.7 Isolation of plasmid DNA from *E. coli*

Plasmid DNA was isolated using the DNA purification kits from Machery Nagel® as described by the manufacturers. Small amounts of plasmid DNA, required for testing the integrity of the plasmid with restriction enzyme test digest, were isolated using the standard alkaline lysis protocol (Sambrook, 1989).

2.2.4.8 Recombinant protein test expression

Recombinant protein expressing cell cultures were harvested at specific time points and diluted to 1:10 with cold LB medium before OD_{600} measurements were taken. The samples were then centrifuged at 5000g for 2 min and the cell pellet resuspended in PBS buffer containing 1 mM PMSF protease inhibitor, to have an end concentration equivalent to $OD_{600} = 0.01$. The samples were then lysed with the Bioruptor sonifier at 300 Hz for 2 min with 15 sec cooling intervals. The lysates were centrifuged at maximum benchtop centrifuge speed (15 000 – 20 000 g) for 10 min. The soluble fraction (s) was separated from the insoluble fraction (P) and the latter resuspended in an equal volume of PBS buffer. The pellet was often sonified once in order to ensure complete homogenization.

5 µl or 20 µl of both the soluble (S) and insoluble fractions (P) were loaded on an SDS-PAGE gel for Western blotting and coomassie blue staining, respectively.

2.2.5 Nucleic acid methods

2.2.5.1 Agarose gel electrophoresis

TAE buffer	40 mM Tris-HCl pH 8.0, 40 mM NaOAc, 1 mM EDTA
6x DNA loading buffer	40% saccharose, 0.25% xylene cyanol

DNA samples were mixed with 6x DNA loading buffer and run on a 1% agarose gel containing 1µg/ml ethidium bromide (in TAE buffer) at 10 V/cm. 1 kb DNA ladder (NEB) was used for size determination and amount estimation. DNA was visualized with the GelDoc 2000 (Biorad). A UV illuminator table (360 nM) was used when cutting DNA bands from the gel.

2.2.5.2 DNA isolation from agarose gels

DNA was extracted from agarose gel with the Machery Nagel Gel Extraction Kit according to the instructions of the manufacturer.

2.2.5.3 Modification of DNA using New England Biolabs (NEB) enzymes

The following methods were performed as described by the manufacturers of the enzymes used (NEB): DNA cleavage with restriction endonucleases, Ligation of DNA fragments, dephosphorylation of DNA with Antarctic phosphatase.

2.2.5.4 DNA amplification by polymerase chain reaction (PCR)

Phusion polymerase High Fidelity PCR System (NEB) was used for error free DNA amplification. Taq DNA Polymerase (NEB) was used to check for correct DNA integration in the genomic DNA. PCR was performed according to the manufacturers instructions. PCR products were purified with the PCR Purification Kit (Machery Nagel).

2.2.5.5 DNA Precipitation and clean up

TE buffer	10 mM Tris-Cl, pH 7.5. 1 mM EDTA

DNA was precipitated by addition of one volumes isopropanol and 1/10 volume of 3 M sodium acetate (pH 7.4) and then centrifuged at 20000 g for 20 minutes at 4 °C. The DNA pellet was washed once with 70% ethanol and centrifuged at 20000 g for 20 minutes at RT. The ethanol was carefully discarded, under the sterile bench for transfection DNA, and then left to dry. The DNA was resuspended in either ddH$_2$O or TE buffer.

2.2.5.6 Quantification of DNA

DNA was quantified using the Nano Drop-1000 spectrophotometer (Peqlab).

2.2.5.7 Sequencing of DNA

DNA was sequenced with the ABI 3730 sequencing machine (in house). The sequencing

PCR was performed with BigDye v3.1 as specified by the service provider. The evaluation of the chromatograms was performed using the 4Peaks software.

2.2.6 PCR site-directed mutagenesis of TbPKAR's phosphate binding cassettes (PBC)

The mutations discussed in section 3.3.2.1 were introduced into the PBC domains of TbPKAR by PCR site directed mutagenesis of overlap extensions as described by (Ho et al., 1989). Briefly, complementary primer pairs containing the mutations of both PBC domains (see section 2.1.1.1) and two other primers (5'PKARHispETDuet and 3'PKARHispETDuet, section 2.1.1.4) annealing at both the 5' and 3' ends for integration into the pETDuet *E. coli* expression vector, were used to generate the PKAR PBCmut ORF. The first PCRs were with primer pairs 5'PKARHispETDuet/LowerPBC1mut and 3'PKARHispETDuet / UpperPBC1mut, generating two PCR products with overlapping ends. In the second PCR, only the 5'PKARHispETDuet and 3'PKARHispETDuet primers were used with equimolar concentrations of the PCR products from the first PCR reaction. In the first cycle of the reaction, the overlapping ends of the PCR products annealed and acted as primers for the extension to obtain the entire ORF which could then be amplified with the aforementioned primer pair. The process was repeated for mutation of the second PBC domain, using the second complimentary primer pairs (LowerPBC2mut and UpperPBC2mut) and the previous PCR product (containing the first set of mutations) as template. The final PCR product, containing mutations at both PBCs, was ligated into the MCS1 of pETDuet vector to generate pETDuet.PKAR-6xHis PBCmut as described in section 2.1.1.4. The ligation was transformed into *E. coli* SURE chemical competent cells. The plasmid DNA extraction and purification was performed as described 2.2.4.7. The pETUpstream and DuetDOWN1 Primers were used to verify the integrity of the PKAR PBCmut ORF by sequencing. This vector was then used as template for swapping mutations into the pBSK.PKAR and pBSK.PKAR-Ty1 vectors to generate the corresponding mutant versions as described in section 2.1.1.2.

2.2.7 Cloning of TbPKA in pETDuet expression vectors

The PKA subunits were either expressed individually or co-expressed in TbPKAR/TbPKAC1 or TbPKAR/TbPKAC3 combinations, for holoenzyme reconstitution. The PKAR-6xHis subunit was amplified by PCR and cloned into the first multiple cloning site (MCS) of the pETDuet vector to form the pETDuet.PKAR-6xHis vector. TbPKAC1 and TbPKAC3 subunits were N-terminally strep-tagged by PCR and cloned into the second MCS of pETDuet vector to form pETDuet.strep-PKAC1 and pETDuet.strep-PKAC3, for individual expression or added into the pETDuet.PKAR-6xHis, forming pETDuet.PKAR-6xHis/strep-PKAC1/3 dual expression vectors. Details for individual vector construction can be found in section 2.1.1.4. Sequencing of the PKA ORFs was done using the pETDuet sequencing primers also described in section 2.1.1.4.

2.2.8 Cloning TbPKA for Baculovirus expression vector system (BEVS)

2.2.8.1 Generating PKA recombinant pFASTBAC1 vector

The PKA subunits were cloned into the pFASTBAC 1 shuttle vector as described for each subunit in section 2.1.1.5. After plasmid amplification and purification, the PKA subunits sequences were verified using the pFB1_sequ_f and pFB1_sequ_r primers (D. Sohmen, Diploma thesis 2008).

2.2.8.2 Generating PKA recombinant Bacmids

10 ng of each pFASTBAC1 vector was diluted in TE buffer and transformed into 100 µl of the bacmid containing DH10Bac *E. coli* cells by electroporation as described in section 2.2.4.6. 900 µl of pre-warmed SOB medium was added and the cells incubated at 37°C with shaking at 200 rpm for 5 hours, time required for the site-specific transposition of the foreign gene into the baculovirus genome. 100 µl of the cells were plated on an LB-agar plate containing, 50 µg/ml kanamycin, 7 µg/ml gentamycin, 10 µg/ml tetracycline for selection of DH10Bac transformants as well as 500 µg/ml X-gal and 120 µg/ml IPTG for blue/white selection of colonies containing recombinant bacmid. The blue and white colonies appeared 36 hours after incubation at 37°C. 10 white colonies were picked and plated again on LB-agar plate containing the same antibiotics as well as X-gal and IPTG and incubated overnight at 37°C. Having confirmed that the colonies remained white, one of them was inoculated in 200 ml LB culture medium containing the antibiotic selection mentioned above. The recombinant bacmids were isolated using the BAC purification kit (Machery Nagel). Correct transposition of the PKA subunits into the bacmid was verified by PCR using the M13 forward and reverse primers. The bacmids were then used to generate viral stocks in Sf9 cells as described in section 2.2.11.2.

2.2.9 Cloning TbPKA for LEXSY protein expression

Leishmania tarentolae has been engineered for inducible protein overexpression by introducing the T7 polymerase-Tet repressor system (Jena Bioscience). The T7-TR cell line and the pLEXSY_I-neo3 vector were donated by F. Bringaud, Bordeaux University. The pLEXSY_I-neo3 neomycin cassette was swapped with that of phleomycin to generate pLEXSY_I-ble3, as described in section 2.1.1.6. It was hence possible to co-express TbPKAR with one of the TbPKAC subunits in the same cell line. PKAR-10xHis, strep-PKAC1 and strep-PKAC3 were generated by PCR and cloned into either of the two vector backbones as described in section 2.1.1.6. Sequencing of PKAR-10xHis was performed using p2x-c2x Primer2 and p2x-c2x Primer3 both of which anneal to the ORF (p2x-c2x Primer1 primer was used in case of poor coverage from the other two primers). Likewise, L_CI_III_sequ and U_CI_III_sequ primers were used to sequence both TbPKAC1 and TbPKAC3, annealing at highly conserved sections. The sequencing primers were designed by D. Sohmen (Diploma thesis 2008). Linearization of the plasmids was performed with SwaI. Transfection in *L. tarentolae* T7::TR is described in section 2.2.3.4.

2.2.10 Knock out of TbPKAC3 in MITat 1.2 monomorphic cell line

pBΔpkac3.NEO and pBΔpkac3.HYGRO had previously been used to knock out PKAC3 in the Antat 1.1 strain (C. Schulte zu Sodingen, Ph.D. thesis 2000). The PKAC3 UTRs, flanking the resistance cassettes, had hence been amplified from the Antat 1.1 strain. The homology of the UTRs with those of the MITat 1.2 strain was first verified by sequencing using the T7, Hygro lower or Neo lower primers for the 5' UTR and T3, Hygro upper or Neo upper primers for the 3' UTR (see section 2.1.1.3). The sequences were compared with the TbPKAC3 UTRs of MITat 427 strain (TritrypDB). There was no difference between the two strains and hence the vectors were linearized and transfected into the MITat 1.2 cell line using the AMAXA nucleofector electroporator as described in section 2.2.1.5. Correct integration of the resistance cassettes into the TbPKAC3 loci was verified by PCR after extraction of genomic DNA (2.2.1.8), using the 5' C3 upper and Neo lower for the Neomycin integration and 5' C3 upper and Hygro lower for hygromycin integration. The 5' C3 upper primer was designed to anneal upstream of the 5' UTR.

2.2.11 Recombinant protein expression

2.2.11.1 Expression of TbPKA in *E. coli* expression system

2.2.11.1.1 PKAR-6xHis in Rosetta *E. coli* strain

pETDuet-PKAR-6xHis was transformed into the *E .coli* Rosetta strain and plated on LB-agar plates containing 100µg/ml ampicillin and 34µg/ml chloramphenicol. A clone was picked from an overnight solid media culture and immediately inoculated into the LB medium required for expression, usually between 200 and 500 ml. The culture was incubated at 37°C shaking at 200 rpm until the OD_{600} was between 0.2 and 0.3. The culture was then transferred to 20°C and further incubated under constant shaking until the OD_{600} reached 0.5-0.6. 400 µM IPTG was then added followed by a further incubation for 4 hours to overnight. The cells were harvested by centrifugation at 5000 g for 15 min at 4°C and after completely discarding the supernatant, the cell pellets were stored at -80°C until purification of the protein.

2.2.11.1.2 TbPKA expression in Lemo21 *E. coli* strain

Lemo21 *E. coli* strain was shown to express the TbPKAC subunits relatively better than other strains (see section 3.2.2.2). After transformation of pETDuet.strep-PKAC1 and pETDuet.strep-PKAC3 vectors into lemo21, the cells were plated on LB-Agar plates containing 100 µg/ml ampicillin, 34µg/ml chloramphenicol and 500 µM L-rhamnose which inhibits any T7 polymerase leakiness. A single clone from the overnight culture was inoculated into LB culture medium containing 100 µg/ml ampicillin and cultured at 37°C with constant shaking at 200 rpm. At OD_{600} 0.2-0.3, the culture was cooled down to 20°C and at OD_{600} 0.4-0.5, the cells were induced for expression with 400 µM IPTG. After 4 hours in culture, the cells were harvested as described in the previous section.

pETDuet.PKAR-6xHis/strep-PKAC1 and pETDuet.PKAR-6xHis/strep-PKAC3 vectors were transformed into lemo21 and the expressed as described for the PKAC individual subunits.

2.2.11.2 Expression of TbPKA in the Baculovirus expression vector system (BEVS)

2.2.11.2.1 Transfection of Sf9 Cells with recombinant bacmid DNA

9×10^5 cells in 2 ml of TMN-FH medium with neither FCS nor selection drugs, from a 3-4 day suspension culture (cell viability ≥97%), were seeded in 6-well flat bottom culture plates. Cells were allowed to attach for 1 hour. In the mean time, the following solutions were prepared:

Solution A	1 µg of bacmid DNA in 5 µl sterile water into 100 µl TMN-FH medium without FCS or selection drugs
Solution B	~6 µl CellFECTIN® Reagent into 100 µl TMN-FH medium without FCS or selection drugs

Solution A and B were mixed gently and incubated for 15-45 at room temperature. The attached cells were washed once with TMN-FH medium (lacking FCS and selection drugs). 0.8 ml of the unsupplemented TMN-FH medium was added to the lipid-DNA mixture (solution A+B) and mixed gently. The 1 ml solution was then added to the cells and incubated at 27°C for 5 hours. The lipid-DNA complex was then removed and 2 ml of complete TMN-FH medium was added to the cells followed by a further 72 hours incubation or until signs of viral infection could be seen (see Invitrogen Bac-Bac manual). The P0 viral stock (2 ml) was then collected for further boosting to obtain higher titer viral stocks.

2.2.11.2.2 Baculovirus titer amplification (Fitzgerald et al., 2006)

1 ml of the P0 viral stock was inoculated into 50 ml of freshly diluted cells from a suspension culture at a density of 0.5×10^6 cells/ml, in a 500 ml Erlenmeyer flask.

The culture was incubated at 27°C under constant shaking at 80 rpm. Neubauer chamber cell counting was done every 24 hours to monitor growth and the cells and when necessary split back to 0.5×10^6 cell/ml, until proliferation arrest. About a two fold swelling of the cells was also observed at this point. The P1 viral stock was collected 48 hours after the proliferation arrest, by harvesting the cells and storing the supernatant at 4°C away from light. In order to generate the P2 viral stock, 15 ml of P1 viral stock was added to 400 ml of freshly diluted cell culture (0.5×10^6 cell/ml) where growth was monitored as described above until proliferation arrest. The P2 viral stock was harvested and stored at 4°C. The P2 viral stock was often sufficient to obtain high expression of recombinant protein.

2.2.11.2.3 Evaluation of recombinant protein expression in Sf9 cells

Cells infected with P2 viral stocks at a density of $0.5–1 \times 10^6$ cell/ml were harvested every 24 hours by centrifugation at 800 g for 5 minutes followed by two washes in cold PBS.

The cells were then resuspended in Laemmli sample loading buffer to have an end concentration of between 0.5 - 1 x 10^4/µl. 2-5 µl gave sufficient PKA signal on a Western blot while 10 µl were sufficient for coomassie staining. The ideal amount of the P2 viral stock used, resulted in only one cell division before proliferation arrest.

2.2.12 Affinity purification of recombinant fusion protein

2.2.12.1 Co-immunoprecipitation with anti-Ty1 tag coupled Protein G sepharose

2.2.12.1.1 Covalent coupling of anti-Ty1 to protein G-sepharose

"Borate buffer low"	50 mM boric acid; 3 M NaCl, pH 9.0
"Borate buffer high"	200 mM boric acid; 3 M NaCl, pH 9.0

2 ml of protein G-sepharose beads (50% slurry) were pre-equilibrated with 5 ml of deionized water by 5 min overhead rotation followed by centrifugation (1400 g, 3 min). The beads were then washed twice with PBS and once with borate buffer low. The equilibrated beads were incubated with 2 ml anti-Ty1 hybridoma (BB2) supernatant (Keith Gull, Manchester) for 3 hours to overnight at RT. The supernatant was removed by centrifugation the antibody containing protein G-sepharose beads were washed twice in 10 ml borate buffer low and resuspended in 10 ml borate buffer high. After discarding the borate high buffer, 20 mM dimethylpimelimidate (cross-linker) was then added to the beads and incubated for 30 min at RT on an overhead shaker. The beads were washed once in 10 ml 0.2 M ethanolamine and incubated with another 10 ml for 2 hours at RT. This was followed by two washes with 10 ml PBS/ 0.02% NaN_3 and resuspension in 1000 µl PBS / 0.02% NaN_3 (50% slurry) and storage at 4 °C.

2.2.12.1.2 Co-immunoprecipitation of TbPKA from *T. brucei* cell extract

IP lysis buffer	50 mM Tris-HCl pH 7.5; 2 mM EGTA; 150 mM NaCl, + 0.2% Nonidet P40; 1x complete Mini EDTA-free protease inhibitor cocktail (Roche)
IP wash buffer	50 mM Tris-HCl pH 7.5; 2 mM EGTA; 150 mM NaCl

Mitat 1.2 cells expressing Ty1 tagged PKA were harvested as described in section 2.2.1.7. 5 x 10^7 cells were resuspended in 200 µl IP lysis buffer (this could be scaled up in the same ratio cell/lysis buffer) and incubated on ice for 20 minutes with regular vortexing. The crude lysate was then centrifuged at 20 000 g for 20 min in a precooled benchtop centrifuge. The soluble fraction (input material) was then separated from the insoluble fraction. 40 µl of protein G-Ty1 sepharose beads (50% slurry)) were centrifuged at 1000 g for 3 min to remove the storage buffer then washed twice in IP buffer. The soluble fraction was incubated with the beads for at least an hour on an overhead rotor but could also be left overnight in the cold room. The supernatant (unbound fraction) was separated from the beads by centrifugation (1000 g, 3 min). The beads were washed

twice with 1 ml of IP lysis buffer and once with IP wash buffer. The beads were then suspended in an equal volume of 2x Laemmli loading buffer. The input material and unbound fraction were also mixed with equal amount of 2x Laemmli loading buffer. All samples were boiled at 95°C for 5 minutes and left to cool down before loading on an SDS-PAGE gel or storage at -20°C. The beads containing samples homogenized by pipetting up and down before loading.

2.2.12.2 PTP-tag purification of TbPKA from *T. brucei*

PA-150 buffer	150 mM KCl, 20 mM Tris-HCl, pH 7.7, 3 mM MgCl$_2$, 0.1 % Tween20
TEV buffer	150 mM KCl, 20 mM Tris-HCl, pH 7.7, 3 mM MgCl$_2$, 0.5 mM EDTA, 1 mM DTT, 0.1 % Tween20
PC-150 buffer	150 mM KCl, 20 mM Tris-HCl, pH 7.7, 3 mM MgCl$_2$, 1 mM CaCl$_2$, 0.1 % Tween20
EDTA/EGTA elution buffer	5 mM Tris-HCl pH7.7, 10 mM EGTA, and 5 mM EDTA

2.2.12.2.1 PKAR-PTP purification from BSF (MITat 1.2 cell line)

At least 1×10^9 MITat 1.2 cells expressing PKAR-PTP were harvested from a litre of cell culture and washed twice with cold PBS buffer. The cell pellet was resuspended in 5 ml PA-150 buffer supplemented with 1x complete Mini EDTA-free protease inhibitor cocktail (Roche). Cell lysis was performed by sonication with the Bioruptor (3x 30 sec pulses at 150 Hz). The crude lysate was then centrifuged at 10 000 g for 10 min in a benchtop centrifuge after aliquoting the samples in Eppendorf tubes. A 100 µl (settled bead volume) of IgG sepharose 6 fast flow was equilibrated with PA-150 buffer by centrifugation at 1000 g for 3 min. The cytoplasmic lysate was added to the beads in a 15 ml falcon tube and incubated for 4 hours with low speed overhead rotation. The flow through was collected by centrifugation and the beads washed twice with 10 ml of PA-150 buffer. The beads were then equilibrated for TEV cleavage by another wash with 10 ml TEV buffer. 2 ml of TEV buffer and 6U of TEV protease (Invitrogen) were added to the beads and transferred into a 2 ml Eppendorf tube followed by overnight incubation with slow overhead rotation. 100 µl (settled bead volume) of anti-protein C affinity matrix was equilibrated by two washes of PC-150 buffer in a second 2 ml Eppendorf tube. The overnight TEV cleavage product was transferred into a 2 ml flow through column (Thermo Scientific Pierce) where the TEV eluate was recovered by gravity flow. 5 mM CaCl$_2$ (from 1 M stock solution) was added to the TEV eluate in order to titrate the EDTA in the TEV buffer. The mix was then transferred to the column containing the equilibrated anti-protein C beads followed by a 2-hour incubation. The flow-through was collected on a second column and the resin washed twice with 10 ml of PC-150 buffer. The elution was performed by incubation of the anti-protein C beads with 0.5 ml of the EDTA/EGTA elution buffer. The first two elutions were collected after a 30 min incubation by overhead rotation while the last three were performed similarly but only for 10 min.

2.2.12.2.2 PKAR-PTP purification from PCF (Antat 1.1 cell line)

At least $2.5\text{x}\ 10^{10}$ Antat 1.1 PCF cells expressing PKAR-PTP were harvested from a litre of suspension cell culture (see section 2.2.1.2). The purification procedure was the same as in the case of the BSFs but scaled up to accommodate the higher cell number. The cells were lysed in 10 ml PA-150 buffer. 400 μl (settled bead volume) of IgG sepharose 6 fast flow was incubated with the cytoplasmic lysate overnight. 10U of TEV protease were added to the charged beads in a 4 ml TEV buffer volume. 400 μl anti-protein C affinity matrix beads were used for the second step purification. The final elutions were collected similarly but with 0.8 ml of the EGTA/EDTA elution buffer.

2.2.12.2.3 PTP-tag purification from Sf9 cells

200 ml of freshly diluted Sf9 cells at a cell density of 1×10^6 cells/ml was infected with 5 ml of PKAR-PTP P2 viral stock and incubated for 48 hours at 27°C shaking at 140 rpm. The cells were harvested (800 g, 5 min, 4°C) and washed twice with cold PBS. The cell pellet was resuspended in 5 ml PA-150 buffer and lysed by sonication as described in the previous section. The crude lysate was centrifuged at 20 000 g for 20 min on a benchtop centrifuge. 300 μl of IgG 6 fast flow sepharose beads were equilibrated with PA-150 buffer and incubated with the lysate's soluble fraction for at least 2 hours. 50 μl of homemade TEV protease (see section 2.2.12.6) was added and incubated with the beads in TEV buffer as described in the previous section (the enzymatic activity was comparable to 10U of the commercial protease). The TEV cleavage eluate was recuperated on a 2 ml fast flow gravity column. The TEV protease (His tagged) was depleted from the eluate by Ni-NTA resin (100 μl settled bead volume) precipitation, as described in the next section.

2.2.12.3 His tag purification of TbPKAR

Lysis buffer	50 mM Tris-HCl pH-7.4, 150 mM NaCl, 0.2% Triton-X, 10 mM imidazole pH 7.4 and 1x complete Mini EDTA-free protease inhibitor cocktail (Roche)
Wash 1 buffer	50 mM Tris-HCl pH-7.4, 150 mM NaCl, 0.2% Triton-X, 10 mM imidazole pH 7.4
Wash 2 buffer	50 mM Tris-HCl pH-7.4, 150 mM NaCl, 0.2% Triton-X, 20 mM imidazole pH 7.4
His elution buffer	50 mM Tris-HCl pH-7.4, 150 mM NaCl, 250 mM imidazole pH 7.4
Storage buffer	20mM MOPS pH 7.0, 150 mM NaCl, 1 mM beta-mercaptoethanol

The purification of His tagged TbPKAR was carried out in both the *E. coli* and *L. tarentolae* expression systems. The purification steps were the same for both systems except for the differences summarized in the table below.

Expression system	Starting material	Lysis volume	Lysis method	Ni-NTA settled bead volume
E. coli	200-500 ml■	5-15 ml	French press	500 μl
L. tarentolae	500 ml◆	5 ml	Detergent lysis; douncer homogenization	200 μl

■: 200-500 ml of *E.coli* LB culture was induce with 400 μM IPTG at 20°C for 4 hours

◆: 500 ml of *L. tarentolae* (5-6 x10^7cell/ml) in BHI medium was induced with 10 μg/ml tetracycline for 24 hours.

Recombinant PKAR-6xHis expressed in *E. coli*, as described in section 2.2.11.1.1, were harvested (5000 g, 15 min, 4°C) and washed twice in cold PBS before been resuspended in lysis buffer. The cells were lysed by two passages in the French press at 10000 psi.

L. tarentolae cells were harvested (2000 g, 5 min, 4°C) and also washed twice in cold PBS. The cells were resuspended in lysis buffer and incubated on ice for 20 min, to allow detergent lysis, followed by douncer homogenization (20 strokes).

Both crude lysates were centrifuged at 20000 g for 20 min to recuperate the soluble fraction. Ni-NTA beads (see table for amount) were equilibrated by two washes in 10 column volumes (CVs) of wash buffer 1 (500 g, 3 min, 4°C) in 15 ml falcon tubes. The lysate's soluble fraction was incubated with the beads for 1 hour on an overhead rotor. After recuperating the flow through (500 g, 3 min, 4°C), the beads were washed twice with 10 CVs of wash buffer 1, by 10 min overhead rotation, and once with 10 CVs of wash buffers 2. 80% of the wash buffer was discarded; the beads were resuspended in the remaining buffer and transferred into a 2 ml gravity flow column (Thermo scientific Pierce). After the rest of the wash buffer had flowed through, the bottom of the column was sealed and 5 CV of elution buffer were added. The elution was collected in 1 CV fractions. The elution fractions were loaded on an SDS-PAGE gel and analyzed by coomassie staining. The protein containing eluates were pooled and dialyzed into the storage buffer and stored on ice in the cold room for several weeks without any loss of function.

2.2.12.4 Strep tag purification of TbPKAC subunits

Lysis buffer	50 mM Tris-HCl pH 7.4, 150 mM NaCl, 0.2% Triton-X, 1 mM beta-mercaptoethanol, and protease inhibitor cocktail
Wash buffer	50 mM Tris-HCl pH 7.4, 150 mM NaCl, 0.2% Triton-X, 1 mM beta-mercaptoethanol
Strep elution buffer	50 mM Tris-HCl pH 7.4, 150 mM NaCl, 2.5 mM desthiobiotin (desthiobiotin is directly dissolved in the buffer)

The purification of strep-tagged TbPKACs was carried out in the three expression systems namely; *E. coli,* BEVS and *L. tarentolae*. The purification steps were generally the same for all systems expect for the differences summarized in the table below.

Expression system	Starting material	Lysis volume	Lysis method	Strep-tactin settled bead volume
E. coli	200-500 ml■	5-10 ml	French press	400 μl
BEVS	200-500 ml✲	5-10 ml	Detergent lysis; douncer homogenization	400 μl
L. tarentolae	500 ml◆	5 ml	Detergent lysis; douncer homogenization	200 μl

■: 200-500 ml of *E.coli* LB culture was induce with 400 μM IPTG at 20°C for 4 hours

❖: 200-500 ml BEVS was infected with 5-10 ml P2 viral stocks and incubated for 48 hours

◆: 500 ml of *L. tarentolae* (5-6 x10^{7}cell/ml) in BHI medium was induced with 10µg/ml tetracycline for 24 hours.

The cells were harvested and washed twice with cold PBS buffer. The lysis was performed as indicated in the table above. The soluble lysate fractions were obtained by centrifugation at 20 000 g for 20 min at 4°C on a benchtop centrifuge. Strep tactin beads (see table for amount) were transferred into a 2 ml gravity flow column (Thermo scientific Pierce) and equilibrated with 2 CVs of the wash buffer. The soluble fraction of the lysate was then let to enter the column by gravity flow. The column was reloaded three times with the lysate to maximize binding. The resin was washed 3x with 10 CVs of wash buffer, where every wash was collected separately. The column was sealed at the bottom and 5 CVs of the elution buffer were loaded. The protein eluate was collected in one CV at 5 min intervals. The eluates were pooled and concentrated using micron® protein concentration columns (5000 MWCO), as described by the manufacturers.

The TbPKAC proteins were stable for several weeks in the elution buffer when stored on ice in the cold room.

2.2.12.5 Two step (His and strep) purification of TbPKA Holoenzyme expressed in LEXSY

200-500 ml of strep-PKAC1/PKAR-10xHis *L. tarentolae* cells at mid log phase (2-3x10^7 cells/ml) were induced with 10 µg/ml tetracycline for 24 hours. The cells were harvested and lysed as described section 2.2.12.3. Strep tag purification was then performed in a gravity flow column as described in the previous section. The strep tag eluate was adjusted for Ni-NTA purification by addition of 10 mM imidazole. A second gravity flow column was prepared for His tag purification by loading 200 µl of Ni-NTA beads (settled bead volume) and equilibrating the resin with His wash buffer 1 (see section 2.2.12.3). The bottom of the column was then sealed and the strep eluate was loaded. Binding to the column was either by gravity flow (2-3 more re-loadings were necessary) or overhead rotation for 30 minutes after sealing both the top and bottom of the column. The resin column was then washed twice with His wash buffer 1 and once with His wash buffer 2, followed by elution as described in see section 2.2.12.3. The holoenzyme eluates were pooled and dialyzed against the storage buffer (20mM MOPS pH 7.0, 150 mM NaCl, 1 mM β-mercaptoethanol). Concentration of the protein was performed using micron® protein concentration columns (5000 MWCO), as described by the manufacturers.

The holoenzyme was stable for several weeks in the storage buffer when stored on ice, in the cold room.

2.2.12.6 His tag purification of TEV protease from Rosetta *E.coli*

pTPSN vector, expressing HIS-tagged TEV (Tobacco Etch Virus) NIa protease with S219N mutation that removes a self cleavage site (Lucast et al., 2001), was obtained from Keogh's lab (Harvard medical school) together with the purification protocol . rTEV-6xHIS under regulation of a T7 Promoter was transformed into Rosetta *E. coli*.

Inoculation for protein expression was done in a 500 ml LB culture. Induction was done at OD_{600} 0.4 with 0.1 mM IPTG for 4 hours at room temperature. After harvesting the cell (5,000 g, 15 min, 4°C), the purification was carried out as follows.

Ni-NTA Lysis buffer	50mM Tris-HCl pH 8.0, 150mM NaCl, 10mM Imidazole, pH 8.0, 10mM βME, 150 μM PMSF
Wash buffer	50mM Tris-HCl pH 8.0, 150mM NaCl, 20mM Imidazole, pH 8.0, 10mM βME, 150μM PMSF
Elution buffer	50mM Tris-HCl pH 8.0, 150mM NaCl, 250mM Imidazole, pH 8.0, 10mM βME, 150 μM PMSF
Storage buffer	20% glycerol, 50mM Tris-HCl, pH 8.0, 1mM EDTA, pH 8.0 5mM DTT

The *E.coli* cell pellet was resuspended in 5x volumes Ni-NTA lysis buffer and passaged twice in the French press at 10000 psi. The soluble fraction was recuperated by benchtop centrifugation at 20 000g for 20 min at 4°C. After equilibrating 600 μl Ni-NTA slurry resin with lysis buffer in a 15 ml falcon tube (500 g, 3 min, 4°C), the soluble fraction was mixed with the resin and incubated for 60 min on an overhead rotor. The resin was then separated from the unbound fraction (flow through) by centrifugation and the resin transferred into a 2 ml gravity flow column. The resin was washed 3x with 10x CVs of the wash buffer where each wash was collected separately. 5x CVs of the elution buffer was then added and the eluate collected in 1 CV fractions. A 15 % SDS- PAGE gel was run and stained with coomassie to determine which fractions contained the protease. Fractions 1-4 were pooled and dialyzed against the storage buffer. The protease was tested for its capacity to cleave recombinant PKAR-PTP (see section 2.2.12.2.3) in comparison to the commercially available protease (Invitrogen). Aliquots were made and stored in the -80°C freezer.

2.2.13 Protein analysis methods

2.2.13.1 Affinity purification of antibodies

Previously made antibodies were purified from their respective immune sera as follows: PKAR sera (9430) (C. Schulte zu Sodingen, Ph.D. thesis, 1996) for the PKAR; PKAC 1/2 sera (pGEX2) and PKAC3 sera (pGEX1) (T. Klöckner, Ph.D. thesis 1996). The antisera were affinity purified according to the method of (Olmsted, 1981). Recombinant TbPKA subunits were purified as described previously: PKAR-6xHis from *E. coli*, strep-PKAC1 from *E. coli* and strep-PKAC3 from baculovirus/Sf9 expression. 200-250 μg per subunit was boiled in Laemmli loading buffer and transferred into a single (9 cm wide) well on an SDS-PAGE gel. After running the gels, the proteins were transferred onto a PVDF membrane followed by incubation for 60 sec in Ponceau S staining solution (0.1% Ponceau S in 1% acetic acid). The protein band was cut out and destained in deionized water (at least 3x 10 min washes were performed). The strip was transferred into a 15 ml falcon tube and incubated in 5% skim milk powder / PBS for 1 hour. A quick rinse with PBS and 3 x 10 min washes were done before the strip was incubated with 1 ml antiserum for 3-4 hours. Another quick rinse with PBS and 3x 10 min washes were

carried out followed by elution of the antibodies with 1 ml 0.2 M glycine/1 mM EGTA pH 2.2 for exactly 10 minutes. The eluate was transferred into an Eppendorf tube containing 200 µl 1 M Tris-HCl pH 8.0 for neutralizing the acidic elution buffer. 200 µg/ml BSA was added in order to stabilize the antibody. The eluate was then dialyzed for 12-24 hours against 1000 volumes of PBS, with 3 buffer changes at least every 3 hours. 0.02 % NaN_3 was added to the antibody solutions and stored at 0°C.

2.2.13.2 Standard protein analysis methods

2.2.13.2.1 Discontinuous SDS polyacrylamide gel electrophoresis (SDS-PAGE)

I.　Separating buffer for 2 (8.6 x 6.7; wxl) gels (Biorad)

	10%	12%	15%
Acrylamide/ bisacrylamide 37.5:1 (rotiphorese Gel 30)	4 ml	4.8	6 ml
Separating gel buffer (1.5 M Tris-HCl pH 8.8, 0.4% SDS)	3 ml	3 ml	3 ml
H_2O bidest	5 ml	4.2 ml	3 ml
10% w/v APS	40 µl	40 µl	40 µl
TEMED	8 µl	8 µl	8 µl

II.　Stacking buffer for 2 gels

Acrylamide/ bisacrylamide 37.5:1 (rotiphorese Gel 30)	0.78 ml
Stacking gel buffer (1.5 M Tris-HCl pH 6.8, 0.4% SDS)	1.5 ml
H_2O bidest	3.7 ml
10% w/v APS	30 µl
TEMED	6 µl

III. SDS sample Laemmli buffer for 10 ml

	2x	6x
4× Tris·Cl/SDS, pH 6.8*	2.5 ml	7 ml
Glycerol	2.0 ml	3.0
SDS	0.4 g	1 g
DTT	0.31 g	0.93 g
Bromphenol blue	0.1 mg	0.12 mg
H_2O	Added to 10 ml	Added to 10 ml

IV. SDS electrophoresis buffer

SDS electrophoresis buffer, 10x (1000 ml)	• 30.2 g Tris base (0.125 M final), • 144.0 g glycine (0.96 M final) • 10.0 g SDS • H_2O to 1000 ml

Protein analysis by SDS-PAGE was performed according to (Laemmli, 1970) and as described in current protocols in cell biology (Gallagher, 2001). The protein samples were mixed with the SDS Laemmli sample buffer and boiled at 95°C for 5 minutes. The gels were cast with the separating and stacking buffers in the Biorad gel electrophoresis

apparatus, following the manufacturers instructions. After loading the samples, the gels were run in 1x SDS electrophoresis buffer at 25 mA per gel. The broad range pre-stained protein marker from NEB was used to monitor the running and estimating the molecular mass of unknown proteins.

2.2.13.3 Colloidal coomassie staining of SDS-PAGE gels

Staining solution* **(1000 ml)**	• 0.02 % (w/v) CBB G-250, • 5 % (w/v) aluminum sulfate-(14-18)-hydrate. • 10 % (v/v) ethanol (96%) • 2 % (v/v) orthophosphoric acid (85 %)
Destaining solution **(1000 ml)**	• 10 % (v/v) ethanol (96 %) • 2 % (v/v) orthophosphoric acid (85 %)

* Aluminum sulfate is first dissolve in deionized water. Ethanol is then added and shortly after the CBB G-250. Phosphoric acid is added last (the incorporation of the acid to the alcoholic media lets the Coomassie molecules aggregate into their colloidal state) and finally filled up with deionized water.

The SDS-PAGE gels were transferred into a staining dish covered with deionized water and washed 3x for 10 min on a horizontal shaker. The coomassie solution was shaken, in order to evenly distribute the colloidal particles, and poured into the container to cover the gels. The gels were then incubated in the coomassie stain for 2-12 hours then followed by two quick rinses in deionized water and a further destaining for 10-60 minutes. Sticking dye particles were removed from the staining dish with a lint-free paper towel. The staining solution could be reused several times. This staining technique has very little or no background and is therefore suitable for scanning of the gels with an infrared scanner.

2.2.13.4 Western blot analysis

2.2.13.4.1 Semi-dry western blot transfer

Anode buffer	300 mM Tris pH 10.4; 20% methanol
Cathode buffer	25 mM Tris pH 9.4; 20% methanol; 40 mM 6-aminohexanoic acid

The electrophoretic transfer of proteins to PVDF membranes was done with the semi-dry technique according to (Kyhse-Andersen, 1984).
The PVDF membrane and 1 mm thick Whatman blot papers were cut to the dimensions of the gel 6x9 cm for Biorad minigels. The PVDF membrane was soaked in methanol for 30 sec and then submerged into deionized water. Two Whatman papers were soaked in the anode buffer and one Whatman in the cathode buffer. The assembly was carried out as follows: the PVDF membrane was laid on the two (anode buffer soaked) Whatman papers followed by the gel and finally the single (cathode buffer soaked) Whatman paper. Bubbles were pressed out of the assembly using a hand held roller. Blotting was done with a current to surface ratio of 0.8 mA/cm^2, for one hour.

2.2.13.4.2 Western blot antibody probing for infrared detection with Odyssey scanner (LICOR)

❖ **Primary antibodies**

Polyclonal anti-PKAR 9430 (Schulte zu Sodingen, Ph.D. thesis 2000)	Rabbit	1/500
Polyclonal anti-PKAC1/2 pGex2 (T. Klöckner, Ph.D. thesis 1996)	Rabbit	1/1000
Polyclonal anti-PKAC3 pGex1 (T. Klöckner, Ph.D. thesis 1996)	Rabbit	1/300
Polyclonal anti-RXXS/T (NEB, Cat n°: 9624 S)	Rabbit	1/1000
Monoclonal anti-strep (IBA, Cat n°: 2-1507-001)	Rabbit	1/2000
Monoclonal anti-humanRIα (Origin not clear)	Mouse	1/2000
Polyclonal anti-VASP (Immunoglobe, Cat n°: 0012-02)	Rabbit	1/5000
Mono-clonal anti-PFR A/C L13D6 (Kohl et al., 1999)	Mouse	1/2000
Polyclonal anti-Histone3 (Gassen et al., 2012)	Rabbit	1:100000
Monoclonal anti-Ty1 IgG1-Hybridoma (BB2)	Mouse	1/2000

❖ **Secondary antibodies**

IRdye 680 LT anti- rabbit IgG (LI-COR)	Goat	1:20000
IRdye 800 anti-mouse IgG (LI-COR)	Goat	1:50000

After the semi-dry protein transfer, the PVDF membranes were incubated with PBS buffer containing 5% skimmed milk powder for 1 hour at RT. The primary antibody was diluted in PBS buffer containing 0.1% Tween and 1% skimmed milk powder, as indicated above. Incubation was for one hour to overnight, depending on the antibody. The membranes were rinsed shortly and washed 3x for 10 minutes in PBS containing 0.2% Tween. The secondary antibodies were diluted (as indicated above) in PBS buffer containing 0.1% Tween, 1% skimmed milk powder and 0.02% SDS (from a 10% stock solution). The membranes were then incubated with the secondary antibody for 1 hour, protected from light, followed by another series of washes 3x for 10 minutes in PBS buffer containing 0.2% Tween. The membranes were dried between two Whatman papers and scanned with the Odyssey IR Scanner according to the manufacturer's instructions. Whenever necessary, the band intensities were quantified with the Odyssey 2.1 Software.

2.2.13.5 Protein quantification

2.2.13.5.1 Bradford protein assay

Protein quantification using Bradford protein reagent was carried out according to the initial protocol (Bradford, 1976). A protein standard containing a range of 1 to 20 µg of BSA protein was made in triplicates in 2 ml disposable cuvettes (Applichem) and the volume adjusted to 800 µl with deionized water. At least two dilutions of the protein samples were made in triplicates and also treated similarly to the BSA. 200 µl Bradford reagent (warmed to room temperature) was added, and incubated for 5-60 min at room temperature. Absorbance measurements were carried with the DU 640

spectrophotometer (Beckman Instruments, Munich) at OD_{595} nm. The standard curve was generated using the spectrometer-integrated software, which also gave a read out of the protein concentration after the OD_{595} nm measurements.

2.2.13.5.2 BSA standard curve protein quantification with the Odyssey scanner (LICOR)

A BSA protein standard was made in 1x sample loading buffer and run on SDS-PAGE gel along side the protein samples. Colloidal coomassie staining of the gel was performed as described earlier. The gel was then scanned with the Odyssey scanner and the bands intensity quantified. A standard curve was generated with the Odyssey 2.1 software and the protein concentration was estimated from the standard curve.

2.2.13.6 Concentration of protein samples

2.2.13.6.1 Trichloroacetic/Deoxycholate (TCA/DOC) protein precipitation for SDS-PAGE

To one volume protein sample solution, 1/100 volume of 2% DOC (M/V) was added and kept on ice for 15 min. 1/10 volume of 100% TCA (M/V) was added and vortexed vigorously for 30 sec. The samples were kept on ice for one hour and then centrifuged at 10 000 g for 10 min at 4°C. The protein pellets were washed with -20°C acetone to remove residual TCA. The sample was resuspended in sample loading buffer. In case the sample turned yellow, a few microlitres of 1 M Tris-HCl pH 8.8 was added to restore the blue colour.

2.2.13.6.2 Microcon® protein concentration

Concentration of protein for functional assays was carried out with centrifugal Millipore protein concentration columns (MWCO 10 kDa) according to manufacturer's instructions.

2.2.14 In vivo reporter (VASP) kinase assay

The human Vasodilator-Stimulated Phosphoprotein (VASP) is phosphorylated by cAMP dependent kinases (Harbeck et al., 2000). Transgenically expressed human VASP has been used as a reporter substrate to measure *T. brucei* PKA activity in vivo (S. Kramer, Ph.D. thesis 2006).

2.2.14.1 In vivo reporter (VASP) kinase assay: cold shock activation of TbPKA

BSF cells at a cell density of 5-8 x 10^5 were harvested (1400 g, 10 min at 37°C). The cells were then resuspended in fresh HMI9 medium to an end concentration of 1 x 10^8 cell/ml. They were then let to recover from the centrifugation by incubation at 37°C for 10 min in a gently shaking heating block. In the mean time, a 4°C water bath was prepared and the temperature was constantly monitored with a thermometer. Empty Eppendorf tubes were placed in the water bath suspended by a floating-tube rack. After the 10 min incubation,

100 µl aliquots of the cell sample were sequentially transferred into each Eppendorf tube and incubated for 10 min. 50 µl of each sample was then transferred into Eppendorf tubes containing 10 µl of 6x SDS-PAGE sample loading buffer in a 95°C heating block. The controls for each sample were lysed in SDS sample buffer at the sample time point. It was important to immediately pipette up and down to ensure rapid cell lysis. The samples were sonified once for 30 sec with the Bioruptor at 300 Hz. 20 µl of the sample was loaded on 10% SDS-PAGE gel and run until the 46 kDA marker band (broad range protein marker NEB) was about 1 cm from running out. The VASP reporter was probed by Western blot as described in section 2.2.13.4.

2.2.14.2 In vivo reporter (VASP) kinase assay; compound activation of TbPKA

100x concentrations of compounds to be tested were prepared in the appropriate solvents (see table in section 2.2.15). The cells were harvested and let to recover at 37°C as described in the previous section. 99 µl aliquots of the cells were prepared at 37°C. 1 µl of each 100x concentrated compound was sequentially added followed by rapid mixing of the reaction by gently tapping the tube. 1 µl of the respective solvent was also added in the control samples. After 5 min of incubation, the cells were lysed as described earlier

2.2.15 In vitro kinase assay with radiolabeled ATP

Radioactive PKA kinase assay was performed according to (Hastie et al., 2006), adapted from (Witt and Roskoski, 1975).

Enzyme dilution buffer	50 mM MOPS pH 7; 100 mM NaCl; 1 mM EGTA; 1 mM DTT; 10 mM MgCl$_2$,
10x kinase reaction buffer	500 mM MOPS pH 7; 1 M NaCl; 10 mM EGTA; 10 mM DTT; 1 mg/ml BSA; 100 mM MgCl$_2$,
Kemptide (Sigma Aldrich) **(LRRASLG; Kemp et al., 1976)**	1 mM stock solution (10x) in H$_2$O
ATP (NEB)	1 mM stock solution (10x) in MOPS buffer pH 7
[γ^{32}P] ATP (Hartmann Analytic Braunschweig)	111TBq (3000Ci)/mmol 370MBq (10mCi)/ml

A maximum of 40 samples could be assayed at a time. Each condition was assayed in duplicate including two controls, one lacking the substrate (kemptide) and the other one lacking the PKA kinase. A wire mesh was suspended in a beaker containing a magnetic stir bar and 75 mM phosphoric acid (at least 5 ml per sample). P81-phosphocellulose paper (Whatman, Dassel) was cut into squares of 2 x 2 cm and labeled according to each reaction tube with a pencil. The 1 mM ATP was spiked with [γ-^{32}P] ATP to give 200-400 cpm/pmol. This was quantified by loading 1 µl on the P81-phosphocellulose paper and measuring with the scintillation counter as described below for the samples.

The kinase reaction mix was prepared at 4 °C by the addition of: 5 µl of 10x reaction buffer; 5 µl 1 mM kemptide (5 µl of H$_2$O for the control reaction); 5 µl recombinant PKA

(diluted in the enzyme dilution buffer) or 5 µl of the kinase storage buffer and 30 µl of H_2O. Each reaction tube was placed on a 30°C heating block at 15 sec intervals and left for at least 2 minutes to allow temperature equilibration. The kinase reaction was started by the addition of 5 µl spiked ATP (also at 15 sec intervals), quickly homogenized by mild vortexing and placed back on the heating block. After 10 min, 40 µl of each sample was pipetted on to the p81-phosphocellulose paper and immediately immersed into the 75 mM phosphoric acid for 5 min. The phosphoric acid was replaced and the washing step repeated 3 times, followed by a final rinse in acetone. The phosphocellulose papers were dried using a hair dryer (can also be left to air dry) and put into scintillation vials containing 4 ml scintillation liquid. The phosphotransfer on kemptide was measured with the scintillation counter according to the manufacturer's instructions. Graph fitting of the data was performed with Graph pad prism 6.0.

❖ **Dose response measurements**

Compound	Solvent	Supplier
cAMP	H_2O	Biolog, Bremen
cGMP	H_2O	Biolog, Bremen
AMP	H_2O	Sigma Aldrich
Adenosine	H_2O	Sigma Aldrich
Guanosine	H_2O	Sigma Aldrich
Inosine	H_2O	Sigma Aldrich
Toyocamycin	Anhydrous DMSO	Berry & associates
Tubercidin	70% ethanol	Sigma Aldrich
5-Iodotubercidin	Anhydrous DMSO	Biolog, Bremen
5-Iodo-2'-deoxytubercidin	Methanol	Jena Bioscience
5-Bromotubercidin	Anhydrous DMSO	Biolog, Bremen
Sangivamycin	Anhydrous DMSO	Berry & associates
6-Bromotubercidin	Anhydrous DMSO	Biolog, Bremen
8-pCPT-2'-O-Me-Adenosine	Anhydrous DMSO	Biolog, Bremen
Dipyridamole	Anhydrous DMSO	Sigma Aldrich
Cis-aconitate	H_2O	Sigma Aldrich
2'-deoxyadenosine	Methanol	Sigma Aldrich
3'-deoxyadenosine (Cordycepin)	Methanol	Santa Cruz Biotechnology
2'-3'-dideoxyadenosine	Methanol	Santa Cruz Biotechnology
2'-O-methyl-adenosine	Methanol	Santa Cruz Biotechnology
3'-O-methyl-adenosine	Methanol	Jena Bioscience
Loxoribine	Anhydrous DMSO	Biolog, Bremen

Recombinant TbPKA holoenzyme was purified as described in section 2.2.12.5. Prior to testing the activation potency of new compounds, it was important to establish that the amount of kinase holoenzyme used was within the linear range of the assay, even at maximum activation. This was determined using a highly potent activator such as toyocamycin (see section 3.3.3.1). A serial dilution of the kinase holoenzyme in at least

10x the EC_{50} of toyocamycin was assayed as described above. The amount of holoenzyme used per assay point often ranged between 5 - 10 pmoles.

The compound to be tested was added to the reaction mix prior to the addition of the kinase and ATP. For the highest starting concentration, an 80 µl reaction volume was prepared in an Eppendorf tube by adding: 10 µl of the 10x reaction buffer; 10 µl of 1 mM kemptide; the amount of compound necessary to give the required concentration in a 100 µl final volume while limiting the organic solvent (see above) to 1% of the final volume. The volume was then adjusted to 80 µl with H_2O. The reaction mixes for the other assay points (40 µl volume) were prepared similarly with the only exception of adding the same amount of the compound's solvent. A 1:2 serial dilution was then performed by taking 40 µl of the 80 µl starting concentration and mixing it with the following assay point by pipetting up and down and again with the following assay point. The kinase was then added and the reaction started at 30°C by adding the spiked ATP as described earlier.

Whenever possible, the dilution series aimed at comparing two or more compounds were prepared in the same solvent.

2.2.15.1 Conversion of scintillation measurements (cpm) to enzymatic activity (U)

The kinase activity in U (nmoles of transferred phosphate min^{-1}) ml^{-1} was calculated according to the following formula:

$[(r - b/sa) \times d \times 1.25 \times 200]/10$ where:

- **r** is the average cpm measured from the kinase reaction
- **b** is the average cpm measured from the blank reactions
- **sa** is the specific radioactivity of the ATP (cpm. $nmol^{-1}$)
- **d** is the 'fold dilution' of the kinase
- **1.25** is a correction for the transfer of only 40 µl of a 50-µl assay volume
- **200** corrects for the addition of only 5 µl of diluted protein kinase preparation to each assay
- **10** is the incubation time in min

The specific activity in U mg^{-1} could be determined by incorporating the amount of kinase used.

2.2.16 Bioinformatic analyses

2.2.16.1 Multi-sequence alignment analysis and annotation using Jalview 2.0

The Jalview program provides tools for multiple sequence alignment analysis and also facilitates annotations and structure predictions (Waterhouse et al., 2009). This workbench was used to compare *T. brucei's* PKA subunits to the eukaryotic PKA subunits whose structure has been determined by crystallization studies.

❖ **Sequence analysis of TbPKAR CNB domains**

The following sequences were uploaded on Jalview in FASTA format and aligned with Clustal Omega (Sievers et al., 2011). The first three are the sequences of the N-terminal deletion mutants used to obtain the crystals structures. Kinetoplastids PKAR N-terminal domains were equally deleted to match the reference sequences.

Name	Sequence	Accession N°
Bovine RIα	91-379	PDB: 1rgs
Rat RIIβ	108-412	PDB: 1cx4
Yeast bcy-1	168-416	PDB: 3OF1
L. donovani	203-502	LdBPK_130160.1 (TritrypDB)
T. cruzi	203-503	TcCLB.506227.150 (TritrypDB)
T. brucei	202-499	Tb927.11.4610 (TritrypDB)

Colour was attributed to the multi-alignment according to the Clustal program residue similarity criteria. A representative 2D structure annotation was carried out based on the structural information of the reference sequences. A consensus conservation logo was also generated.

❖ **Sequence analysis of TbPKAR N-terminal domain**

N-terminal sequences of the three kinetoplastid representatives, were aligned in Jalview as described earlier. A 2D structure prediction and annotation was carried out using the Jnet secondary structure prediction software (Cole et al., 2008).

❖ **Sequence analysis of TbPKAC subunits**

Name	Sequence	Accession N°
Mouse Cα	1-350	PDB: 2CPK
TbPKAC1	1-334	Tb927.9.11100 (TritrypDB)
TbPKAC3	1-338	Tb927.10.13010 (TritrypDB)

The mammalian Cα was used as reference to analyze the sequences of TbPKAC1 and TbPKAC3. The alignment and 2D annotation was carried as out as described above. The key functional features and posttranslational modifications of the three kinases were also annotated based on published work.

2.2.16.2 TbPKA structure homology modeling and analysis

(Performed in collaboration with Andreas Anger, Gene center, LMU)

TbPKAR (202-499) was submitted as query sequence on HHpred where a multiple sequence alignment was built and converted into profile HMMs. This was then compared to the PDB70 database to obtain a list of the closest homolog templates (Hildebrand et al., 2009; Soding, 2005). The output, ranked by highest homology to the query sequence,

revealed that the bovine RIα crystal structures amongst which, PDB: 1rl3 (cAMP-free) and 1rgs (cAMP-bound) were the highest ranked templates. These two structures were selected as template for a comparative 3D structural modeling, based on satisfaction of spatial constraints, using Modeller 9.12 program (Eswar et al., 2008; Fiser and Sali, 2003; Sali and Blundell, 1993). A similar approach was used to model Δ201TbPKAR/TbPKAC1 heterodimer using the mammalian Δ91RIα/Cα as template. The N-terminal domain of TbPKAR was modeled based on a family of tropomodulin proteins characterized for the their α/β leucine rich domains (see section 3.1.5). The table below summarizes the templates used.

Query sequence	Modeling template (PDB N°)	Structure model
TbPKAR (202-499)	1rl3	TbPKAR cAMP-free
TbPKAR (202-499)	1rgs	TbPKAR cAMP-bound
TbPKAR (202-499)/TbPKAC1	2QCS	TbPKA heterodimer
TbPKAR (1-202)	1pgv	TbPKAR N-terminal LRR domain

The models structures were further analyzed and edited using UCSF Chimera 1.7. Ligand replacement in the bound structure was done in the same spatial co-ordinates. The nucleosides (guanosine and inosine) used to replace adenosine see section 3.4.4.2, were downloaded from http://mastersearch.chemexper.com/.

3 Results

3.1 In silico analysis of *T. brucei's* PKA kinase

Most of the features of the PKA kinase family are conserved in *T. brucei* as reported in section 1.7. There is however sufficient biochemical evidence from this lab suggesting that this kinase is not responsive to cAMP activation (section 1.9.2). The molecular bases underlying this particularity are still not understood. There is to date no structural information available for any member of the kinetoplastid PKA family. On the other hand, the mammalian PKA structure has been extensively studied and its mode of activation is well understood. This kinase was hence a suitable template for a detailed in silico comparison with TbPKA. The aim was to establish that this kinase qualifies as a member of the PKA family while establishing the reason behind the activation anomaly.

3.1.1 Conservation of TbPKAR's CNB domains

The C-terminal domain of TbPKAR was analysed in relation to other kinetoplastid members and reference sequences as described in section 2.2.16.1. The aim was to analyse the conservation of the key features that govern the binding of cAMP and the inhibition of the catalytic subunit as described in section 1.7. The key features analysed included:

- The residues or motifs implicated in cAMP binding
- The R subunit inter/intra-domain interactions that govern the co-operative binding of cAMP
- The R subunit inter/intra-domain interactions that govern the conformational changes that lead to the release of the C subunit
- The inhibition of the catalytic subunit i.e. the conservation of the R/C interaction interface

3.1.1.1 Global CNB domain conservation analysis

Before the analysis of the aforementioned features, the multi-sequence alignment (Fig. 3.1) was first checked for the global CNB domains conservation in relation to TbPKA as summarized in the table below.

Table 1. Pairwise comparison of TbPKAR's C-terminal domain (202-500), in percentage identity, to other kinetoplastids and sequences of three reference crystal structures.

Name	(%) Identity
T. brucei	100
T. cruzi	79
L. donovani	68
Bovine RIα	37
Yeast bcy-1	34
Rat RIIβ	24

T. cruzi is more related to *T.brucei* than *L. donovani* is while the bovine RIα is the closest among the reference sequences. This is an indication that kinetoplastid PKAR would be more closely related to the mammalian type I R subunit isoforms. All sequences were compared between the inhibitor sequence region and the C-terminal end, where the non-crystalized part of the reference sequences is depicted in lower case (Fig. 3.1). It could hence be shown that despite the higher homology to the type I R subunit, a key particularity is the fact that kinetoplastids R subunit possess a type II like substrate inhibitor sequence (see section 1.6.1).

The 2D annotation based on the structural information of the reference sequences depicts the general α/β organization of the tandem CNB domains as reported in section 1.7. It could be deduced that this general organization is respected in kinetoplastids, based on the relatively high conservations of residues at any structurally defined segments of the sequence (Fig. 3.1). There are however a few key areas of divergence from the reference sequences, notably the β4-β5 loop region, which is involved in the interaction with the C subunit in an isoform-specific manner (Zhang et al., 2012). This region is highly conserved in kinetoplastids but appears to differ substantially from the reference sequences, more so in the CNB:B. The helices are generally less conserved in both sequence and structure, despite a high conservation of their function. The α:C in CNB:B is particularly different in both amino acid sequence and length in the reference sequences. The conservation of this region also appears to be relatively low in kinetoplastids.
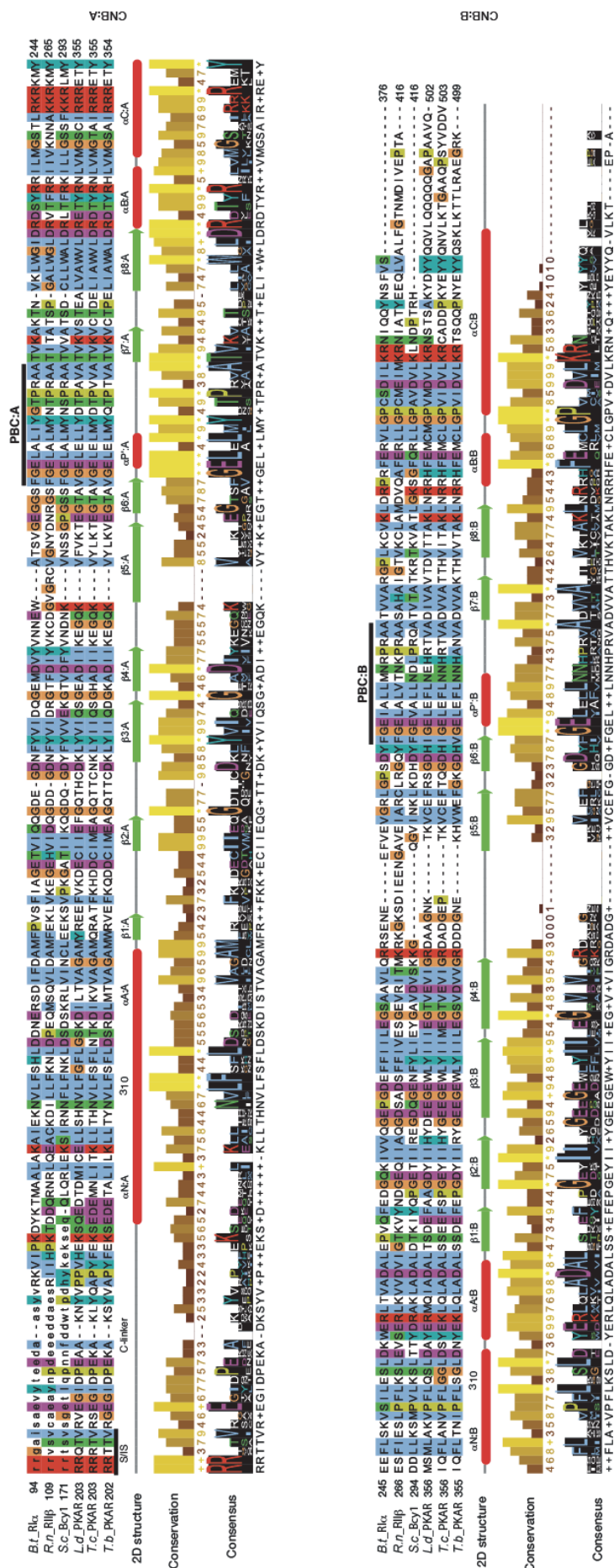
Fig. 3.1. Homology comparison of PKA cyclic nucleotide binding (CNB) domains: TbPKAR C-terminal domain was aligned with kinetoplastid PKARs and three R subunits whose structure has been determined, as described in section 2.2.16.1. All sequences begin with the isoform specific substrate or pseudosubstrate inhibitor sequence (S/IS) (underlined). The reference sequence residues in lower case were not part of the crystal structure. 2D structure annotation was based on the structural information of the three reference sequences, also compared by Rinaldi et al (2010). The beta sheets (in green) are in general more highly conserved than the alpha helices (in red). Regions of highest variability are the β4-β5 loop and the α:C helix of CNB:B. The phosphate-binding cassette (PBC), which is the hub for cAMP interaction is also highlighted.

3.1.1.2 The molecular bases of cAMP interaction in the PBC: the hydrogen bond network

As described earlier in section 1.7.1, the β barrel harbors the phosphate-binding cassette (PBC), which serves as the conserved core for the binding of cAMP's sugar-phosphate moiety. A closer look at the multi-alignment of the R subunits shows that the consensus signature motif of this domain is not fully conserved in kinetoplastids R subunits (Fig. 3.2). The Gly and Glu (in blue) are conserved, indicating that the interactions involving the PBC and the 2'-OH of the ribose-sugar moiety are conserved. However, the residues responsible for interaction with the phosphate group are not fully conserved. The main non-conserved residue is Arg (in red) since it forms a specific hydrogen bond with the O1P of the phosphate group while also playing a role in maintaining the architecture of the PBC as shown in Fig. 1.8. The residues in orange form unspecific hydrogen bonds with the phosphate group. Given that the side-chain is not involved in the interaction, it is likely that any residue at the same position would fulfill the same role. The first Ala is however replaced by a Glu (in grey), which is highly conserved in all kinetoplastids. The conservation of an electrically charged residue at this position suggests a possible gain of function in kinetoplastids.

Fig. 3.2. Kinetoplastids PBC is not conserved for phosphate binding: A close-up of the PBC from the multi-sequence alignment in section 3.1.1.1. The residues responsible for specific and unspecific hydrogen bond formation are colour coded and denoted as shown.

3.1.1.3 The molecular bases of cAMP interaction in the PBC: the hydrophobic interaction network

❖ **Protection of the PBC/cAMP hydrogen bonds network**

The hydrogen bonds formed in the PBC are protected from solvents by a hydrophobic interaction network involving residues of the PBC and distal residues recruited to the PBC by the cAMP induced conformational changes (Berman et al., 2005). The key residues of the PBC involved in this network are leu and Ala at position 201 and 211 in bovine RIα, respectively. These residues are also conserved in kinetoplastids (Fig. 3.2). The distal residues recruited to the PBC are found within the β2 to β4 loop of each CNB. The multi-alignment of this region shows that these residues are globally conserved in kinetoplastids. The only exception is a Gln in the β2 sheet (Fig. 3.3), which interacts with Ala 211 of the PBC of bovine RIα . In kinetoplastids, the Gln is replaced by either an aromatic or aliphatic residue.

Fig. 3.3. The hydrophobic residues forming a protective shield around the cAMP hydrogen bonds in the PBC, are conserved in kinetoplastids: a multi-sequence alignment of the β2-β4 fragment of both CNB domains, based on the alignment of section 3.1.1.1, highlighting the residues that protect the hydrogen-bond network in the PBC.

❖ **Hydrophobic capping of the adenine ring moiety**

In the series of conformational rearrangement induced by the binding of cAMP, the cAMP's adenine ring interacts with a distal aromatic residue, to form a hydrophobic Π-Π stacking interaction (Berman et al., 2005; Rinaldi et al., 2010). The stacking residue in PBC:A is always from the CNB:B domain (Fig. 3.4). For both RIα and bcy-1 the PBC:A capping residue is an aromatic residue from αA:B helix. However, the RIIβ stacking residue is an Arg from αB:B (residues in blue). The PBC:B stacking residue is always from αC:B helix of the same CNB domain (residues in green). These residues are in most cases neither conserved in their nature nor in the linear sequence, as shown below. In kinetoplastids, the PBC:A capping residue can be predicted to be the Tyr (in blue) also conserved in yeast's R subunit while the RIα has a Trp at that position. The PBC:B capping residues is however not easily predictable by linear sequence but three tyrosines in linear proximity to the conserved Tyr of both RIα and RIIβ, are the highest likely candidates. 3D modeling will be more informative in this aspect.

```
  B.t_RIα    260 WERLTVADAL        FERVLGPCSDILKRNIQQYNSFVS----------------376
  R.n_RIIβ   281 SERLKVVDVI        FERLLGPCMEIMKRNIATYEEQLVALFGTNMDIVEPTA---416
S.c_PKAR(Bcy1) 309 YDRAKLADAL     FQRLLGPAVDVLKLNDPTRH--------------------416
  L.d_PKAR   371 YERMQIADAL        FEMCMGPVMDVLKRNSTSAKYDYYQQVLQQQQQGAPAAVQ-503
  T.c_PKAR   371 YEKLQLADAL        FEMCLGPVIDVLKRCADDPKYEYYQNVLKTGAAQPSYVDDV 503
  T.b_PKAR   370 YEKLQLADAL        FEMCLGPVIDVLKRTSQQPNYEYYQSKLKTTLRAEGRK---500
                   αA:B               αB:B           αC:B
```

Fig. 3.4. The aromatic residues interacting with the adenine ring of cAMP are likely to be conserved in kinetoplastids: a multi-sequence alignment of the alpha helices of CNB:B domain involved in capping the PBC, by interacting with the adenine ring of cAMP. The residues in blue are involved in PBC:A cAMP capping and in green PBC:B cAMP capping. Conservation of PBC:A capping in kinetoplastids appears to be linearly predictable but that of PBC:B could involve one of the three tyrosines (green squares under the alignment).

3.1.1.4 CNBs intra/inter domain network and cooperative cAMP binding

The cooperativity of cAMP binding is assured by well defined inter domain contacts between the two CNB domains. As reported in the previous section, the stacking residue of cAMP's adenine ring in domain A is usually a residue from a helix in CNB:B. This is however not the only contact established between these two domains. A hydrogen bond network is established between residues of PBC:A and residues in the helices of CNB:B (Rinaldi et al., 2010). The network of interaction is isoform specific as shown by the graphical representation of the three R subunit crystal structures in the Fig. 3.5a. All the residues involved in the interaction network are also conserved in kinetoplastids CNB domains, as highlighted in the multi-alignment (Fig. 3.5b).

-66-

Fig. 3.5. Conservation of the interdomain interaction network between CNB:A and CNB:B, mediated by cAMP binding to the PBC: A. Graphic representation of the interdomain hydrogen bonds and hydrophobic interactions (capping residues are depicted by their electron density, as descibed in the previous section) of the cAMP-bound structures of RIα, bcy-1 and RIIβ (adapted from Rinaldi et al., 2010). B. Multi-sequence alignment showing that the same residues are also conserved in kinetoplastids. Although there is linear conservation of all the residues across the different R subunits, the interactions established are isoform/subunit specific.

The C subunit bound state is kept locked by a salt bridge in CNB:B, established between a Glu from α:A and an Arg from α:B helix, as reported in section 1.7.2. These two residues are conserved in all kinetoplastids. Glu 261 (α:A) and Arg 366 in mammalian RIα would correspond to Glu 371 and Arg 475 in TbPKAR, respectively.

3.1.1.5 The R/C interface conservation in TbPKA

cAMP mediated breakage of the salt bridge creates an extended surface along the αB/C helix of CNB:A, providing one of the key anchoring point of the R subunit to the C subunit (Fig. 1.8). There are four main sites involved in the R/C interaction: site 1 is the docking surface for the inhibitor sequence of R subunit to the active site cleft of the C subunit; site 2 involves the hydrophobic portion of the PBC and the 3_{10} loop; site 3 mainly involves the aforementioned interaction between the αB/C helix of the R and the activation loop of the C subunit and site 4 is the interaction between αB helix of CNB:B and the αH-αI loop of the C subunit (Brown et al., 2009; Kim et al., 2007; Kim et al.,

2005). All the residues involved in these interactions are conserved in kinetoplastids PKAR subunits. The site one interaction interface presents some interesting features due to the involvement of residues upstream of the inhibitor sequence in an isoform specific manner. This region was analysed for any relation of kinetoplastids PKARs to the mammalian isoforms.
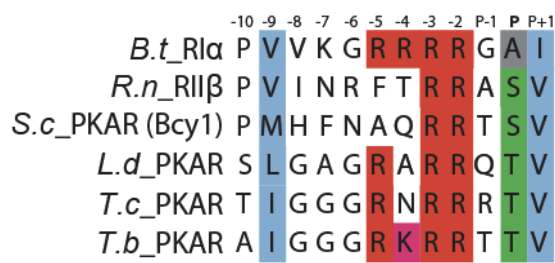
Fig. 3.6. The Isoform specificity of the inhibitor sequence: A multi-sequence alignment of the inhibitor sequence (underlined) and the upstream sequence, involved in isoform specific interactions with the C subunit. The P site defines the inhibitor sequence as a substrate (P=Thr/Ser) or pseudosubstrate (P= Ala). The P+1 residue is always hydrophobic. The colour scheme is based on the conservation of the residues and their role in the R/C interaction, hydrophobic interactions in blue and hydrogen bonds in red.

The basic mechanism of inhibition involves the P-2 and P-3 Arginines (Fig. 3.6) which bind to the (acidic) active site cleft, Glu170^c, Glu203^c and Glu 230^c (the c superscript denotes the C subunit). This is conserved in all R subunits as well as in PKI peptide inhibitors (Kim et al., 2007; Knighton et al., 1993; Wu et al., 2007). The P+1 residue binds to a hydrophobic pocket (P+1 loop) in the C subunit. In RII isoform, the P site Ser is involved in hydrogen bond interactions with Lys168^c and Asp 166^c, docking the five residues firmly onto the large lobe of the C subunit (Wu et al., 2007). This feature is likely to be conserved in kinetoplastids given that they have a Ser or Thr at the P site (type II like). The RI isoform has two additional Arginines preceding the inhibitor sequence, the P-4 Arg interacts with Glu 203^c while the P-5 Arg interacts with Asp 328^c. This additional interactions with the C-terminal tail of the C subunit result in a closed conformation around the R subunit (by bringing the C-terminal to wrap around the R), while in the RII type the C-terminal is not recruited, hence an open conformation. The P-5 Arg is conserved in all kinetoplastids while the P-4 site is functionally conserved but only in *T. brucei*. The interacting residues (Glu and Asp) on the catalytic subunit are also conserved (see section 3.1.3), indicating that this interaction could be conserved in *T. brucei*.

It would hence appear that the TbPKAR subunit has both the RI and RII type features, in this region.

3.1.2 TbPKAR N-terminal domain is a distinct kinetoplastid feature

Reverse genetic analysis of TbPKAR's much longer N-terminal R subunit domain has suggested its involvement in the flagellar localization of the kinase as well as providing an additional and crucial R/C interaction interface (see section 1.7.1). Structural analysis to

validate these findings is however still missing. An in silico approach based on multiple sequence alignment and structural modeling was adopted, in order to gain a better in sight into the role played by this kinetoplastid specific domain. The N-terminal of the three kinetoplastids R subunits analysed so far, were aligned and analysed for general conservation. A 2D and 3D structure was also predicted as described in section 2.2.16 (Fig. 3.7). The general comparison showed that this domain is well conserved in kinetoplastids but more in *T. cruzi* (72%) than in *L. donovani* (59%). The 2D structure prediction revealed an α-helix/β–sheet structure, stretching out through the entire sequence. This feature was further confirmed in the 3D structure model where the region with the highest probability lies between residues 24-166 (Fig. 3.7b). The template domain that provided the best fit for comparative structural modeling is defined as a right handed beta-alpha superhelix leucine-rich repeat (LRR) domain, from the super family of ribonuclease inhibitor like (RNI-like) proteins (scop id: c.10.1.1). An LRR fold is comprised of 20-30 residues of which, a highly conserved segment (HCS) of 11-12 residues and a variable segment (VS). The general consensus for the HCS is either LxxLxLxxNxL (11 residues) or LxxLxLxxCxxL (12 residues), where L is Leu, Ile, Val, or Phe (annotated in black in the conservation consensus (Fig. 3.7a); N is Asn, Thr, Ser, or Cys and C is Cys, Ser, or Asn. The HCS is usually a beta sheet flanked by the variable (often helical) VS. This LRR protein fold is commonly characterized as a hub for protein interaction, with the VS being more favored for interaction (Kajava, 1998; Kobe and Kajava, 2001). It is therefore plausible that this domain not only has a cis regulatory role by providing an extended R/C interface but also a trans regulatory role by its capacity to interact with other proteins, possibility influencing both the activity and localization of the kinase. The first ten residues (1-10) as well as the region between residues 165-200 (downstream of the LRR domain) appeared to be mostly disordered. In this disordered region right before the inhibitor sequence, lies a Gly repeat (GGG) conserved in all kinetoplastids (coloured in purple, Fig. 3.7a). This is probably a flexible linker region between the highly conserved C-terminal CNB domains and the kinetoplastid specific N-terminal domain. The TbPKAR phosphorylation sites have previously been mapped by phosphor-proteomics (Nett et al., 2009; Urbaniak et al., 2013). The majority of these sites are downstream of the LRR domain and upstream of the CNB domains.

Most of the phosphorylation sites would appear to be unique for *T. brucei* (in red) since in most cases the residues are not conserved in the other kinetoplastids (in green). The role played by these modifications is still unk

A
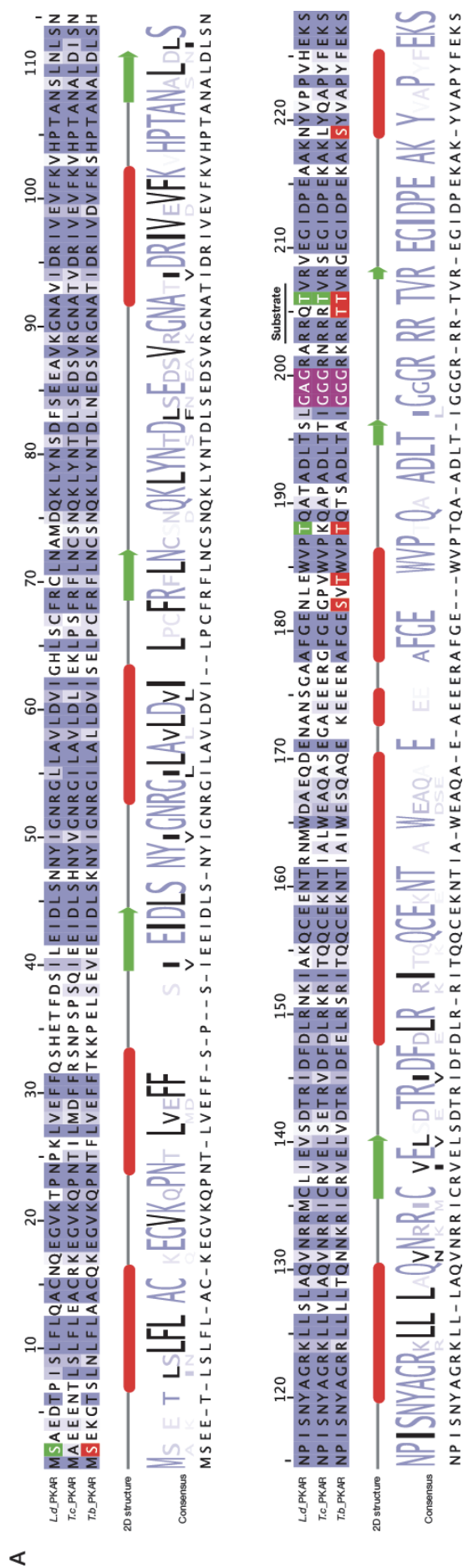
B
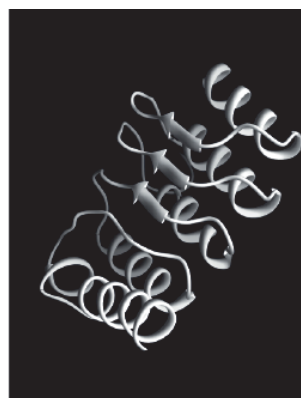
Fig. 3.7. The N-terminal domain of TbPKAR is conserved in all kinetoplastids: A. Multi-sequence alignment of kinetoplastids N-terminal domains as described in section 2.2.16.1. The 2D was predicted using Jnet predict on the Jalview workbench. The consensus sequence highlights the LxxLxLxxNxL/ LxxLxLxxCxxL motifs where L are the residues in black. These motifs define the leucin-rich repeat folds (Kobe and Kajava, 2001). A glycine rich repeat (in purple) upstream of the substrate sequence motif (underlined) is also highlighted (possibly a linker region between the N and C-terminal domains). Phosphorylated residues as revealed by Nett et al (2009) and Urbaniak et al (2013) are highlighted in red. Similar residues in the other kinetoplastids are in green. **B.** Structure model of the LRR domain (residues 24-166) modeled as described in section 2.2.16.2. The α-helix/β-sheet alteration had also been predicted by the 2D structure.

3.1.3 Conservation of TbPKA catalytic subunits as entities of the PKA holoenzyme complex

Two distinct isoforms of TbPKA catalytics subunits (TbPKAC1 and TbPKAC3) were compared to the mammalian $C\alpha$ kinase by multi-sequence alignment as described in section 2.2.16.1. The first objective was to highlight the conservation of the key fuctional features related to catalysis. Although biochemical analyses have shown that these kinases are capable of substrate specific ATP γ-phosphate transfer, no isoform specific features have so far been identified. This is especially important in (unicellular) *T. brucei*, since it has been shown that these isoforms are not redundant (C. Schulte zu Sodingen, Ph.D. thesis 2000). The second objective was to show that the catalytic subunits are also conserved in their capacity to interact with the regulatory subunit. The holoenzyme formation has experimantally been put to evidence, but the molecular conservation of the complex formation in relation to the mammalian PKA has not been established. This is important in understanding how the *T. brucei* complex relates to the activation mechanism of the mammalian PKA.

Residues and motifs that play a role in catalysis i.e. ATP binding, substrate recognition and phophoryl transfer in the catalytic core of the AGC family of kinases were shown to be highly conserved in the two isoforms of TbPKA (Fig. 3.8). However the C-terminal tail, which is usually highly conserved in the PKA kinase family, was less conserved in *T. brucei* PKA. Notably, an FDDY (F^{327}-Y^{330} of $C\alpha$) and a PXXP (P^{313}-P^{316} of $C\alpha$) motif that influence ATP and substrate binding (Kannan et al., 2007). The role of the N-terminal and C-terminal tails in confering kinase specificity by influencing the activity, localization and capacity to interact with other proteins by their series of co- and posttranslational modifications, as discussed in section 1.6.2, was also analysed. As noted earlier, the mammalian N-terminal PTMs (Myritorylation, deamidation and phosphorylation) seem to be absent in both TbPKAC1 and TbPKAC3. The only other modifications functionaly characterized on mammalian $C\alpha$ are the autophosphorylations on Thr197 and Ser338 (Cheng et al., 1998). A few other autophosphorylation sites have since been identified by MS phospho-site mapping of *E. coli* expressed kinase (Seidler et al., 2009). TbPKACs phoshorylation sites have also been mapped as previously reported for TbPKAR (Net et al., 2009; Urbaniak et al., 2013). These modifications are highlighted in red in the multi-alignment below. The phosphorylation sites on the mammalian $C\alpha$ are much fewer in comparison to those of TbPKAC1, while TbPKAC3 presents the least sites. In TbPKAC1, most sites are located on the N and C-tails indicating a role in isoform specific regulation. It was also noted that some of the phosphorylation sites in both TbPKAC1 and TbPKAC3 are in the vicinity of the highly conserved threonine phophorylation in the activation loop (Thr197 in mammalian $C\alpha$). The profile of these phosphorylations differs between TbPKAC1 and TbPKAC3, also indicative of isoform specificity.

Analysis of the conservation of the R/C interaction interface in *T. brucei* revealed that the key residues involved in the R/$C\alpha$ interaction are also conserved in both TbPKAC1 and

TbPKAC3, as shown in the multi-alignment annotation. This suggests that TbPKAC isoforms likely share a common R/C interaction features with the mammalian Cα. It is however highly likely there are additional *T. brucei* specific features.

Fig. 3.8. TbPKAC catalytic core is highly conserved as a member of the PKA kinase family: The sequences of TbPKAC1 and TbPKAC3 were compared to that of the structure-determined mammalian Cα, as described in section 2.2.16.1. The 2D structure was annotated in reference to the crystal structure of the mammalian Cα (Knighton et al., 1991). The annotations of functions were attributed based on published work as follows: ATP and Substrate binding (Knighton et al., 1991; Knighton et al., 1993; reviewed in Smith et al., 1999); R/C interaction interface (Kim et al., 2005; Kim et al., 2007). The posttranslational modifications are highlighted as follows: in red are the phosphorylation sites as mapped by MS (Seidler et al., 2009 for the mammalian Cα; Nett et al., 2009 and Urbaniak et al., 2013 for TbPKACs); in purple are the N-terminal myristolylation (Gly) and deamidation (Asn) sites (Carr et al., 1982; Jedrzejewski et al., 1998). The only PTM that is highly conserved in the PKA family members is the activation loop phosphorylation (asterisks)

3.1.4 Structural modeling of TbPKA

Most of the features required for full functionality of both the R subunit and the C subunits, are conserved in TbPKA on the linear sequence level, as reported in the previous section. An important differences was however the non-conservation of the PBC. These key features were further analysed for spatial conservation by 3D structural modeling. First, the C-terminal domain of TbPKAR was modeled in the cAMP-free and cAMP-bound states as described in section 2.2.16.2, based on the crystal structures of the bovine RIα. TbPKAC1 was modeled in its R subunit bound state using the mammalian RIα/Cα heterodimer as template. The cAMP-bound TbPKAR and TbPKAC1/TbPKAR structural models were annotated to highlight the key features as revealed by the multiple sequence alignment (Fig. 3.9b). In the cAMP bound state of TbPKAR, the spatial conservation of intra and inter domain network of interactions could be confirmed. It was also the case for the C subunit bound state with notably the conservation of the salt bridge (residues in blue circles), as reported in section 3.1.1.4. The two conformations of the B/C helix (in red) i.e. kinked in the cAMP-bound state and extended in the C subunit bound state for a larger interaction interface were also revealed in the structure model. The "cAMP-bound" structure model was also instrumental in understanding the molecular bases of TbPKA activation (see section 3.4).
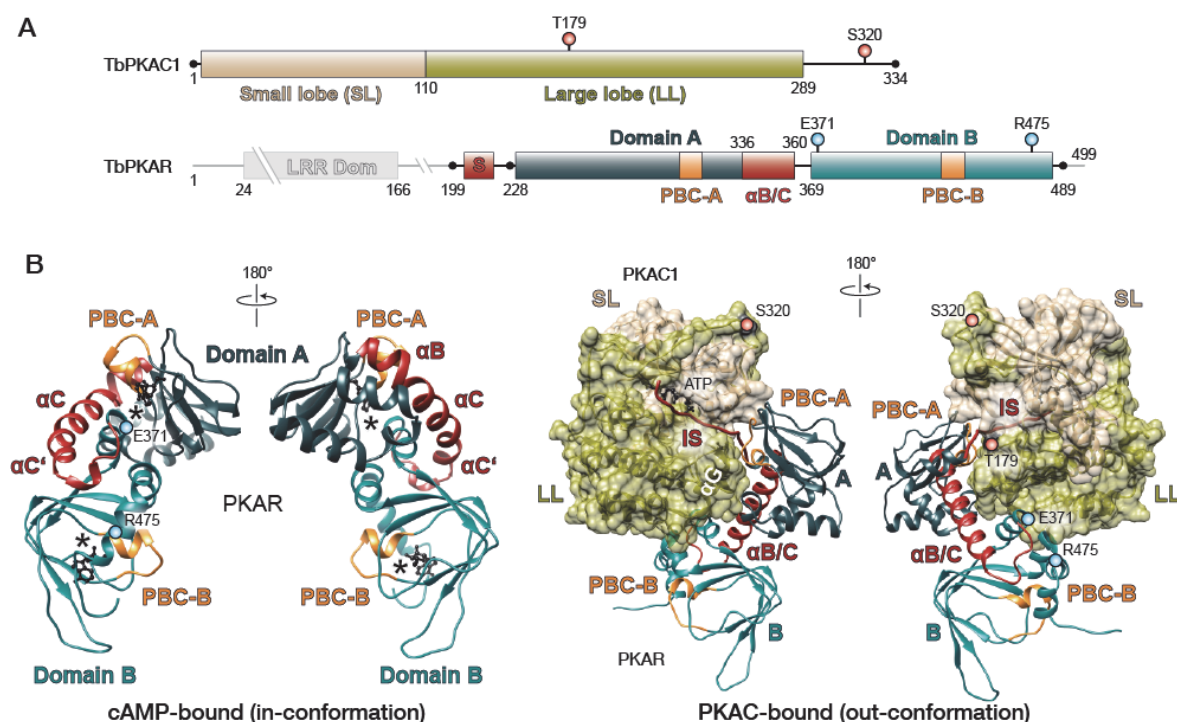
Fig. 3.9. TbPKA structure model: A. A graphic representation of TbPKAR and TbPKAC1 with annotations of the key domains as well as key regulatory elements, notably the phosphorylation sites of the mammalian Cα and the salt-bridge residues on the R subunits (in coloured circles) **B.** Structure model of TbPKAR (on the left) based on the crystal structure of *Bos taurus* RIα, bound to cAMP (cAMP is denoted by asterisks), modeled as described in section 2.2.16.2 and the holoenzyme structure model (on the right) based on the mammalian RIα/Cα holoenzyme structure.

3.2 In vitro reconstitution of a functional TbPKA holoenzyme

The current understanding of TbPKA's non-responsiveness to cAMP is mainly based on the in vivo characterization of the kinase, as discussed in section 1.7.2. In vitro characterization of this phenomenon has been limited by the lack of a robust assay system. One of the key problems is the difficulty to express the catalytic subunits in heterologous expression systems, notably in *E. coli*, contrary to the mammalian PKA as first reported by Slice and Taylor (1989). Additionally, reconstitution of TbPKA holoenzyme from heterologously expressed subunits has so far been unsuccessful. Expression of this kinase was carried out in various expression systems with the aim of obtaining fully functional kinase subunits as well as a kinase holoenzyme complex that could be used in kinase activation assays.

3.2.1   Homologous expression and purification of TbPKA

Purification of TbPKA from its native source is the safest way to ensure full functionality of the kinase as long as the isolation approach is not harmful to the protein and that high yields and purity can be guaranteed. A mild two-step purification approach was developed using the PTP-tag approach (Schimanski et al., 2005). The tag is comprised of two adjacent protein-A fragments and a protein-C epitope moiety, separated by a TEV protease cleavage site. This tag had previously been C-terminally fused to the PKAR ORF in the pC-Neo-PTP vector (Schimanski et al., 2005) as depicted below (F. Böttger, Diploma thesis 2006). pC-Neo-PKAR-PTP was transfected into both the MITat 1.2 BSF and Antat 1.1 PCF cell lines. Purification was however first optimized in the PCF cell line as this would ensure a higher yield, given the capacity of these cells to grow to a much higher density than the BSFs. Purification using this PKAR subunit as bait would enable the pull-down of the holoenzyme isoform complexes.
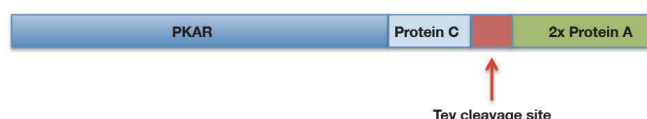
Fig. 3.10. PTP tag purification strategy: The tandem purification is achieved by binding of the tagged protein to an IgG column via a tandem protein A moiety; release of the protein by TEV protease cleavage followed by binding of the protein C epitope-tag to a anti-protein C immunoaffinity column. A buffer containing a chelating agent for divalent cations, such as EGTA, is used to elute the protein from the second column.

3.2.1.1 Optimization and purification of PKAR-PTP holoenzyme isoforms

The cell lines generated from the transfection showed no phenotype in growth or morphology. This is likely due to the fact that the fusion protein was targeted to one of the endogenous locus, hence averting the overexpression growth phenotype reported by C. Schulte zu Sodingen (Ph.D. thesis 2000). Although PTP tag purification is well established in *T. brucei*, the efficiency of some of the purification steps is dependent on

the nature of a given protein. The cleavage of the 2x-protein-A moiety and accessibility of protein-C to its binding matrix are critical steps. The purification of a 0.5 litre PCF culture was carried out as described by Schimanski et al (2005) and every step analysed by Western blot using the polyclonal anti-PKAR antibody (Fig. 3.11). The first three samples loaded, clearly show both the PKAR-PTP and PKARwt (from the second allele) at 75 kDa and 56 kDa, respectively. The intensity of these bands is not representative of the expression level since the polyclonal PKAR antibody also recognizes the protein-A moiety of the tag (IgG binds to protein A), hence increasing the intensity of PKAR-PTP. The lysis was highly efficient since up to 98% of PKAR-PTP was recovered in the soluble fraction. The protein loss after the first column was estimated by quantifying the band intensities of the input material compared to the flow through after IgG column binding. Up to 90% of the initial input material was bound to the IgG beads, this being within the documented range (Schimanski et al., 2005). TEV protease cleavage was also quite efficient as shown by the loss of the Protein-A moiety (about 13 kDa band shift) and the absence a of TbPKAR signal on the IgG column, after cleavage. There were no detectable protein losses in the second purification step. The apparent weaker signal observed after TEV protease cleavage is due to the loss of the protein-A moiety.
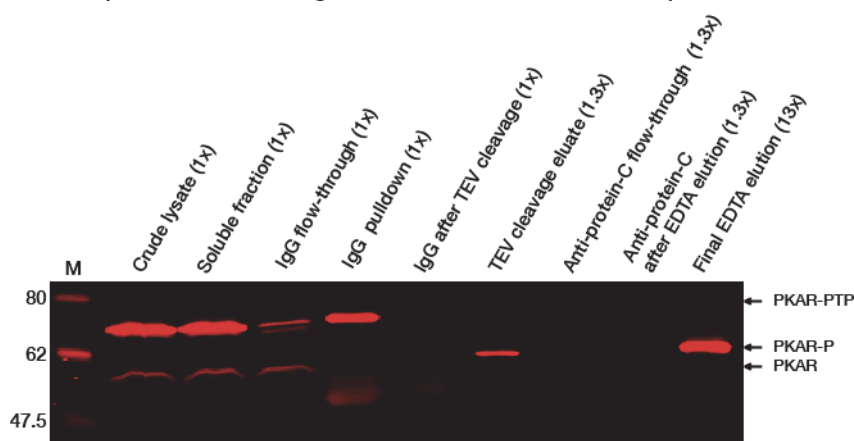
Fig. 3.11. Small scale PTP-tag purification of TbPKA: A 0.5 litre PCF cell culture expressing PKAR-PTP was harvested at logarithmic growth and processed for purification as detailed in section 2.2.12.2.2. Protein samples from the purification steps, as indicated, were resolved on a 12% SDS-PAGE gel; the Western blot was probed with anti-PKAR polyclonal antibody. Values of *x* indicate relative amounts, to the starting material. Note that the endogenous TbPKAR is also detected in the first three fractions at around 56 kDa lower band and the PTP-tagged version is present at around 75 kDa but migrates faster after TEV cleavage (58 kDa).

❖ **Large scale PTP tag purification**

PKAR-PTP holoenzyme was purified from a 1.5-litre PCF cell culture as described in section 2.2.12.2.2. Samples were taken from every purification step for Western blot analysis where in addition to TbPKAR, both TbPKAC1/2 and TbPKAC3 were probed with their respective polyclonal antibodies (Fig. 3.12a). The TbPKAC1 and TbPKAC2 isoforms are equally recognized by the same polyclonal antibody due to their high homology as

reported earlier (section 1.6.2). It could be confirmed that the catalytic subunit isoforms were co-precipitated, as expected. It should however be noted that TbPKAC2 and TbPKAC3 isoforms are predominantly expressed in PCFs (section 1.6.2). The total amount of protein from the final eluate was estimated by Bradford protein quantification to about five micrograms. Analysis of protein purity on a coomassie stained gel revealed two additional bands (Fig. 3.12b). The expected molecular weight of the kinase subunit enabled the estimation of the complex purity to about 45%, using the Odyssey infrared scanner.

The four bands were analysed by mass spectrometry, confirming the PKA subunits at their respective MW sizes, as indicated in the figure below. The two other bands were determined to be α/β tubulin, a well-known contaminant in this purification process as well as the light chain of the immobilized anti-protein C antibody (second purification column). The holoenzyme purified was hence of very low purity and yield and therefore, this approach could not be pursued any further.
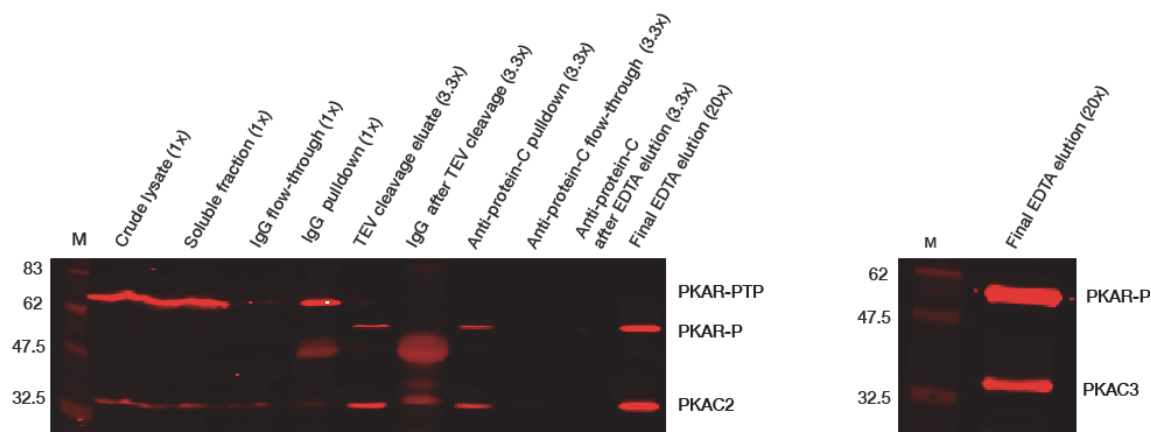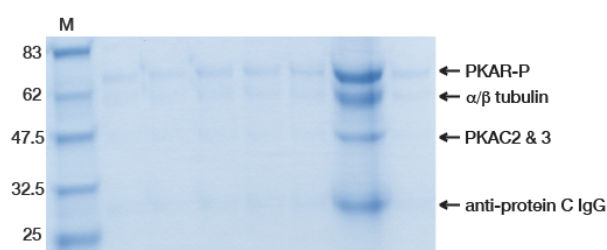
Fig. 3.12. Large scale PTP-tag purification of TbPKA: purification of a 1.5 litre PCF cell culture was carried out as described in section 2.2.12.2.2. **A.** The purification steps run on a 12% SDS-PAGE gel and analysed by Western blot using polyclonal anti-PKAR, anti-PKAC1/2 and anti-PKAC3 as indicated. Values of *x* indicate relative amounts to the starting material. **B.** The final eluate of the PTP purification also run on a 12% SDS-PAGE gel and stained with colloidal coomassie stain. The purity of PKA complex was estimated to 45% by Odyssey infrared scanner (700 nm). The identity of the bands was revealed by MS spectrometry as indicated.

3.2.2 Heterologous expression and purification of TbPKA: pET vector *E. coli* expression system

Expression of eukaryotic proteins in *E. coli* has advanced considerably in recent years with the emergence of numerous expression strains mostly catering for difficultly expressed proteins while still guaranteeing high yield and cost efficiency. TbPKA expression in this system was hence revisited with the aim of finding the conditions that would best mimic the routine expression of the mammalian PKA (Saraswat et al., 1986; Slice and Taylor, 1989). The pET-vector expression system from Novagen was chosen for its compatibility with a wide array of *E. coli* expression strains. The pET32a or pETDuet vectors were used for either single or co-expression of the subunits as tabulated below. In general, TbPKAR was C-terminally tagged with a poly-histidine tag while TbPKAC subunits were N-terminally tagged with the strep tag as summarized below.

Table 2: pETDuet TbPKA expression constructs (The cloning strategy is detailed in section 2.1.1.4)

TbPKA subunits	pET vector
PKAR-6xHis	pET32a (A. Binder, this lab)
PKAR-6xHis	pETDuet
Strep-PKAC1	pETDuet
Strep-PKAC3	pETDuet
Strep-PKAC1- PKAR-6xHis	pETDuet
Strep-PKAC3- PKAR-6xHis	pETDuet

3.2.2.1 TbPKAR expression and purification in *E. coli*

TbPKAR had previously been expressed and purified from the *E. coli* BL21 expression strain, using the pET32a-PKAR-6xHis vector (Andreas Binder, this lab). However, despite a high expression, most of the protein was found in the insoluble fraction. The expression had been performed at 30°C after IPTG induction, which is likely the reason for the high insolubility. Lower expression temperatures were tested in this new attempt. In addition, the expression strain was changed to the rosetta strain, which is a BL21 derivative that complements rare tRNA codon usage for eukaryotic protein and therefore likely to positively influence the expression. A freshly transformed rosetta/pET32a.PKAR-6xHis clone was grown to OD_{600} 0.3 at 37°C with constant agitation at 200 rpm, the culture was then split and the temperature lowered to 30°C, 24°C (RT), 20°C and 15°C. 400 µM IPTG was added at OD_{600} 0.5 followed by harvesting equal amounts at the indicated time points (Fig. 3.13a). The soluble fraction (S) was separated from the insoluble fraction (P) as described in section 2.2.4.8. Equal amount of both the S and P samples were loaded on SDS-PAGE gels and stained with colloidal coomassie for expression analysis. The expression at 30°C was much higher than at the lower temperatures. The proportion of the soluble (S) fraction was however lower than that of the insoluble (P) fractions at all time points, as discussed earlier. The protein amount at lower expression temperatures

was much less as shown in Fig. 3.13a. The soluble proportion was on the other hand higher than the insoluble proportion in the lower temperatures. Overnight expression at lower temperatures yielded more protein but did not affect the soluble/insoluble ratio. Lowering expression temperature was hence shown to improve the protein expression and thereby adopted in the large-scale purification protocol described in section 2.2.12.3. Preliminary Ni-NTA purification had shown that up to 3 mg/litre of cell culture could be obtained. This amount was surplus to requirement and enabled optimization to obtain higher purity in compromise to a lower yield by reducing the bead volume and thereby losing some protein in the flow through (Fig. 3.13b). The chances of co-precipitating contaminants were hence reduced, resulting in highly pure eluates. A yield of ≥2.0 mg/litre of cell culture was obtained in this particular purification.
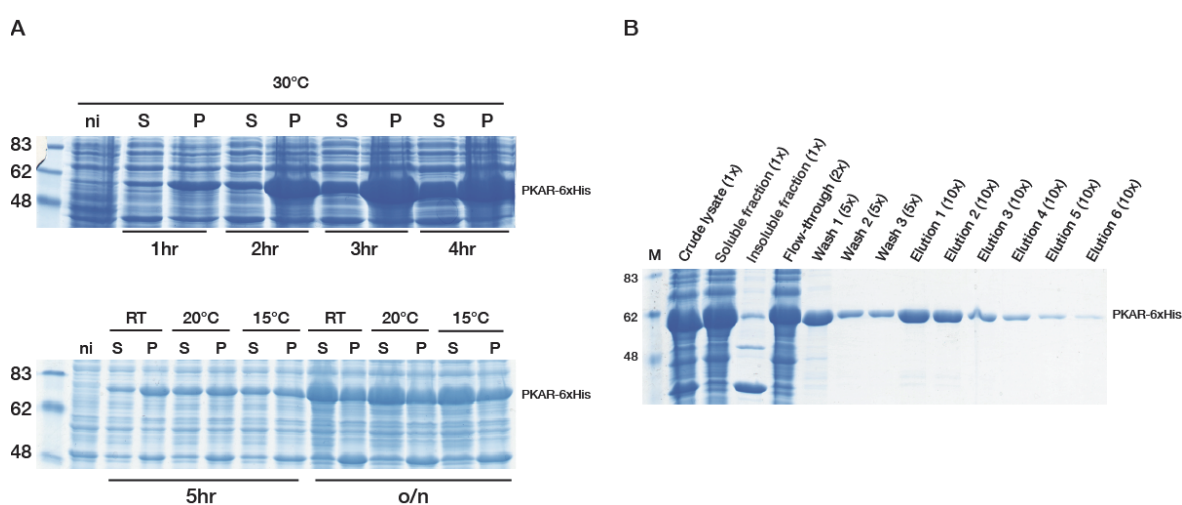
Fig. 3.13. PKAR-6xHis Purification from *E. coli* rosetta strain: A. Expression temperature optimization; PKAR-6xHis transformed rosetta cell cultures were induced with 400 µM IPTG at OD_{600} 0.5 at the indicated temperature and durations. Harvested samples were processed as described in section 2.2.4.8 where the soluble (S) and insoluble (P) fractions were analysed on coomassie stained 12% SDS-PAGE gel. **B.** 200 ml rosetta: pET32a-PKAR-6xHis culture at OD_{600} 0.5 was induced with 400 µM IPTG and cultured at 20°C overnight and purified a described in section 2.2.12.3. The samples of the purification steps were analysed on a 12% SDS-PAGE coomassie stained gel. Values of *x* indicate relative amounts to the starting material. Bradford protein quantification of the pooled final eluate estimated the yield at 2 mg/litre of cell culture.

3.2.2.2 Optimization and expression of TbPKAC1 and TbPKAC3 in *E coli*

The pETDuet-strepPKAC1 and pETDuet-strepPKAC3 constructs were transformed into various *E. coli* strains, engineered to reduce toxicity of the expressed protein. A single clone was picked and inoculated directly into the LB medium volume for final expression, thus avoiding overnight pre-cultures where auto-induction has been shown to occur in saturated cultures (Studier, 2005). The cell cultures were grown at 37°C with constant agitation at 200 rpm until OD_{600} reached 0.1-0.2 and then transferred to a 20°C incubator. Expression was induced by addition of 400 µM IPTG at OD_{600} 0.3-0.4. The samples were harvested at the indicated time points (Fig. 3.14) and processed for western blot analysis,

as described in section 2.2.4.8, and probed using TbPKA polyclonal antibodies as indicated below. Due to a relatively low expression level, it was not always possible to visualize overexpression by coomassie gel staining.
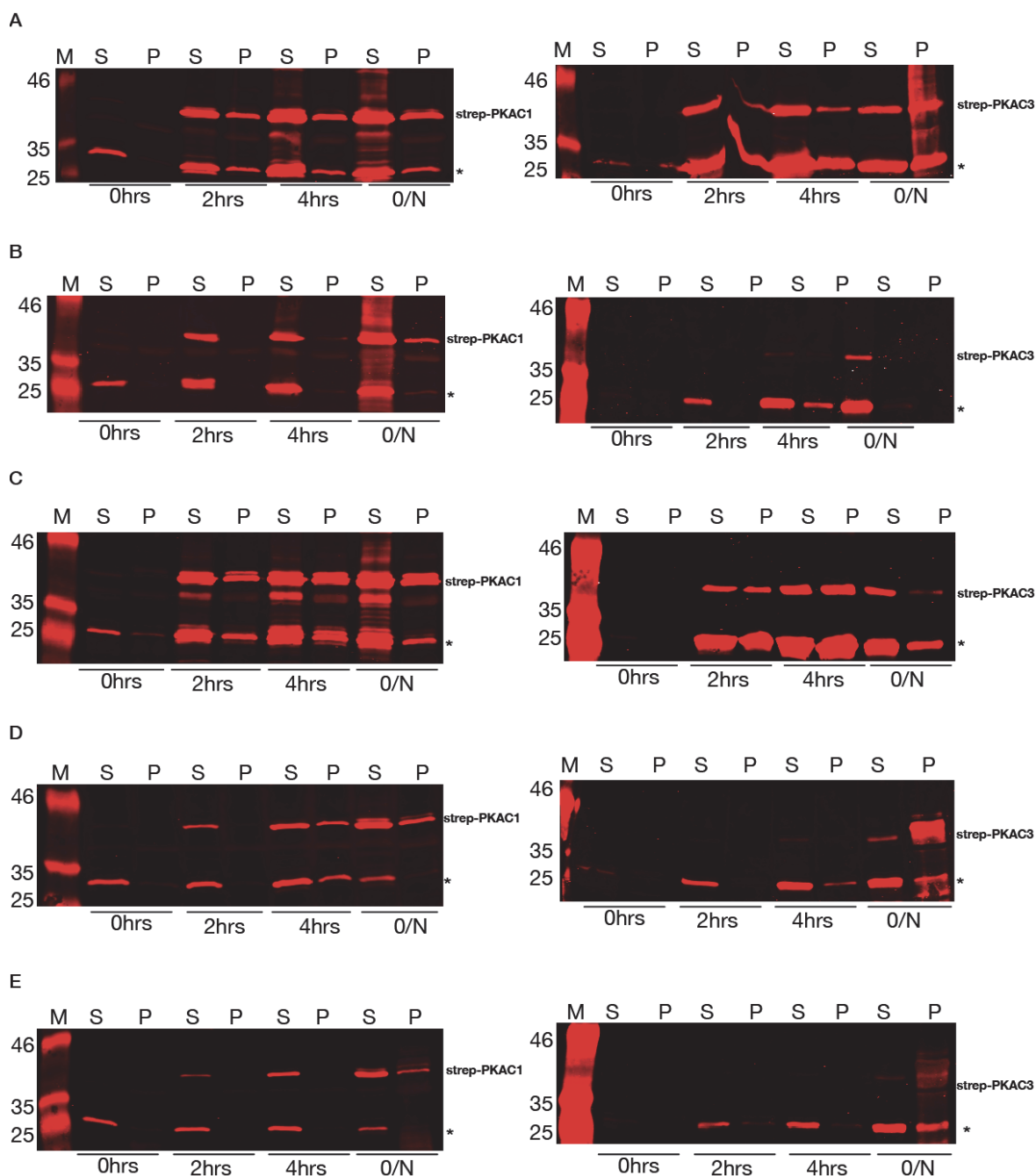
Fig. 3.14. Test expression for strep-PKACs in various expression strains: A. rosetta strain **B.** rosetta pLySs **C.** Lemo21 strain expressed without l-rhamnose **D.** Lemo21 strain expressed in 250 µM l-rhamnose **E.** Lemo21 strain expressed in 500 µM l-rhamnose. All the expression strains were induced for expression upon reaching OD_{600} 0.3-0.4 at 20°C and samples taken at the indicated time points. The samples were processed as indicated in section 2.2.4.8. The soluble (s) and insoluble fractions (s) were probed by Western blot with polyclonal anti-PKAC1 and anti-PKAC3 antibodies as indicated.

Both PKAC1 and PKAC3 expressions had a lower band at around the 25-kDa (asterisk), which is likely to be a degradation product.

The three strains are derivatives of BL21 (DE3) strain for T7 polymerase driven expression. However, the protein expression varies depending on the stringency of the T7 polymerase activity.

The rosetta strain: This strain is designed to enhance the expression of eukaryotic proteins that contain codons rarely used in *E. coli* (Fig. 3.14a). There is however no tight control over the expression i.e. the T7 polymerase is often leaky and after IPTG induction its activity is often too strong, resulting in inclusion body formation. Addition of glucose prevents auto-induction caused by nutrient deprivation (Grossman et al., 1998). 1% glucose was therefore included in LB-agar plates as well as in the LB medium. Expression of both strep-PKAC1 and strep-PKAC3 (both of around 39 kDa MW) was only visible after induction (no signal at 0 hours) and increased with time. The soluble fraction was however maximal at 4 hours post induction. Over-night expression increased protein insolubility without a significant increase in the amount of the soluble fraction.

The rosetta pLysS: This is a derivative of the rosetta strain containing the T7 lysozyme gene, which is constitutively expressed under *E. coli's* RNA polymerase. The T7 lysozyme reduces basal level expression of the gene of interest by mild inhibition of the T7 polymerase (Stano and Patel, 2004). Strep-PKAC1 was more soluble in this strain, although the expression level was lower than that of the rosetta strain. Strep-PKAC3 was very poorly expressed in comparison to the rosetta strain (Fig. 3.14b). The T7 lysozyme inhibition of the T7 polymerase slightly improved protein solubility but reduced the yield in comparison to the rosetta strain and is therefore less advantageous.

The Lemo21 strain: Designed for tunable expression, which is achieved by varying the T7 RNA Polymerase activity with increasing concentrations of l-rhamnose (Wagner et al., 2008). Concentrations of l-rhamnose ranging from 0-2000 µM are used to increase the expression of T7 lysozyme, which is under the rhaBAD promoter. Increasing amounts of l-rhamnose would therefore slow down protein expression thus favoring proper folding and also reduce the toxic effect that often leads to inclusion body formation or degradation of the protein. The strep-PKACs transformants were plated on LB-agar plates containing 500 µM l-rhamnose in order to inhibit the T7 polymerase activity, prior to induction.

The expression was carried out in LB medium containing 0 µM, 250 µM and 500 µM l-rhamnose concentrations. Expression of both catalytic subunits was noted to decrease with increasing amounts of l-rhamnose while the solubility was shown to increase (Fig. 3.14 c-e). The decrease in expression was more severe for strep-PKAC3 since there was barely any protein signal with 500 µM l-rhamnose (Fig. 3.14e). It was however noted that in the complete absence of l-rhamnose, both strep-PKACs were better expressed than in the two other strains. The migration of strep-PKAC1 on SDS-PAGE gels was also different, appearing as a double band in most cases. The *E. coli* expressed mammalian Cα auto-phosphorylates on Thr197 in the activation loop, acquiring full functionality (see

section 3.1.3). This leads to slower migration on an SDS-PAGE gel, often characterized by a double band (Steinberg et al., 1993). It is however not known whether TbPKAC1 shares the same mechanism, which would imply that the lemo21-expressed kinase would have the highest fraction of fully functional kinase. It was concluded that expression of strep-PKACs with the lemo21 strain (at 20 °C after induction with 400 µM IPTG for 4 hours) would not only result in high solubility of the kinase but also increase the likelihood of posttranslational modification occurring on the kinase.

3.2.2.3 Strep tag purification of TbPKAC1 and TbPKAC3 in lemo21 *E. coli* strain

After expression of both catalytic subunits in lemo21 under the above-described conditions, the proteins were purified following the strep purification protocol as described in section 2.2.12.4. The purification steps were analysed by Western blot and coomassie stained gel, as previously described. The yield of strep-PKAC1 (Fig. 3.15a) was about 0.3 mg/litre of cell culture, estimated by Bradford standard protein quantification. Strep-PKAC3 final elution (from an initial 200 ml culture volume) was barely visible on both the Western blot and the coomassie stained gel (Fig. 3.15b). The *E. coli* system is therefore not ideal for strep-PKAC3 purification. This system can however be exploited for the purification of strep-PKAC1.
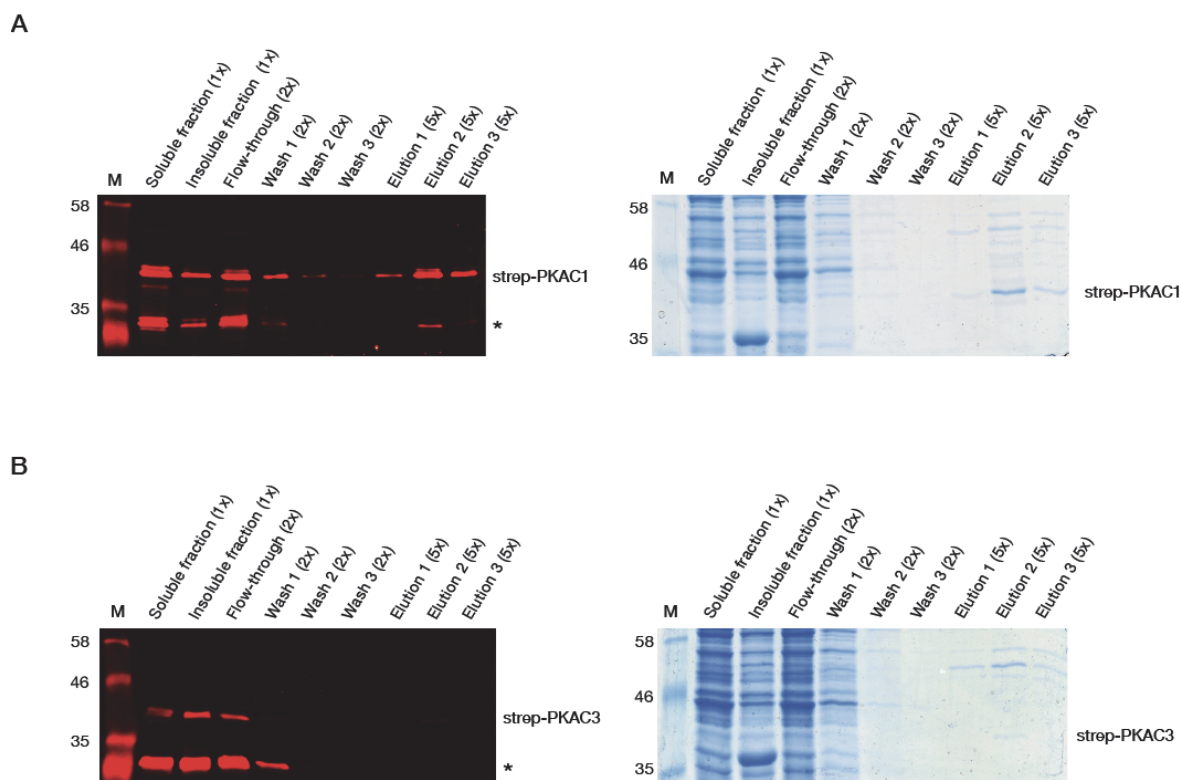
Fig. 3.15. Strep tag purification of TbPKAC1 and TbPKAC3 expressed in lemo21 *E. coli* strain: a 200 ml cell cultures of strep-PKAC1 **(A)** and strep-PKAC3 **(B)** was harvested after a 4hr induction with 400 µM IPTG at 20°C (expression conditions are detailed in section 2.2.11.1.2). The purification was carried out as described in section 2.2.12.4. The purification steps were loaded on 10% SDS-PAGE gels for Western blot

(right panel) and coomassie staining (left panel), respectively. The Western blots were probed with anti-PKAC1 and anti-PKAC3 antibodies, as indicated. Values of x indicate relative amounts to the starting material. The asterisk denotes a possible degradation product.

The final eluate was pooled and quantified by Bradford protein assay; strep-PKAC1 was estimated at 0.3 mg/litre of cell culture while step-PKAC3 was below quantifiable levels.

3.2.2.4 Co-expression and purification of TbPKA in the *E. coli* expression system

pETDuet dual expression of PKAR-6xHis/strep-PKAC1 and PKAR-6xHis/strep-PKAC3 was carried out in the lemo21 expression strain since the catalytic subunits were best expressed in this strain. The expression of PKAR was also shown to be as good as in the earlier used, rosetta strain (data not shown). The co-expression and sample processing to test for expression and solubility followed the strep-PKAC protocol as described in the previous section. Although the co-expression could not be directly compared with the expression of the individual subunits, there appeared to be little to no improvement in PKACs expression (Fig. 3.16). The PKAR-6xHis/strep-PKAC1 co-expression gradually increased with time up to 5hrs post IPTG induction. PKAR-6xHis/strep-PKAC3 co-expression also increased with time but strep-PKAC3 reached peak expression 3hrs post induction, while that of PKAR-6xHis was at 5 hrs.
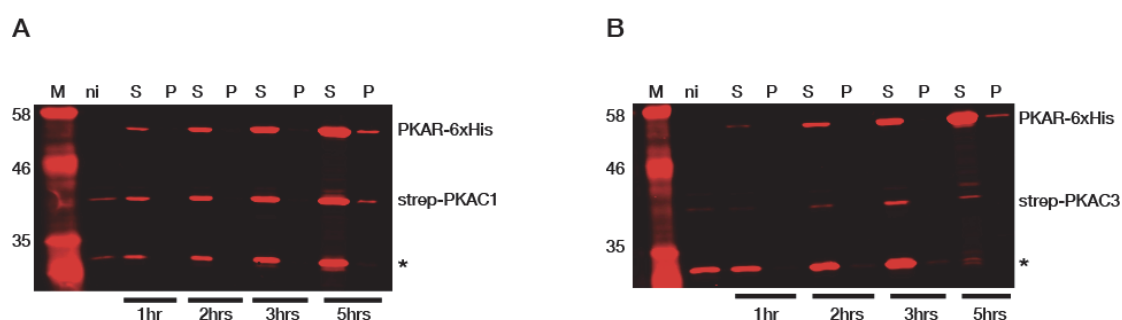
Fig. 3.16. Co-expression of TbPKA in Lemo21 *E. coli* expression strain: PKAR-6xHis was co-expressed with either strep-PKAC1 **(A)** or strep-PKAC3 **(B)** in lemo21 under the expression conditions of the catalytic subunits, as described in section 3.2.2.2. Samples were taken at the indicated time points and processed to obtain the soluble fraction (S) and insoluble fraction (P) as described in section 2.2.4.8. All samples, including the non-induced whole cell lysate (ni) were analysed by Western blot using the polyclonal TbPKA antibodies (anti-PKAR, anti-PKAC1/2 and anti-PKAC3) as indicated. The asterisk indicates a possible degradation product of the catalytic subunits, as previously observed in Fig. 3.14.

The expression of strep-PKAC3 failed to improve in the presence of the regulatory subunit, making this system also unsuitable for the purification of this isoform's holoenzyme. The PKAR-6xHis/strepPKAC1 could however be co-purified in a two-step pull down protocol using the strep tag followed by the His tag purification (Fig. 3.17a) or inversely His tag followed by strep tag purification (Fig. 3.17b). The purification steps were analysed by Western blot using both the anti-PKAR and anti-PKAC1/2 antibodies and also by coomassie stained SDS-PAGE gels. There was about a 40% loss of the expressed protein to the particulate fraction of the lysate, in both purification

approaches. A significant amount of the bait protein was captured in the first purification step for both the strep and His tag. It was however noted that upon elution from the first column, only the tagged bait subunit was still in the eluate fraction. The co-expressed subunit was lost in the unbound fraction and the first washing step, suggesting that the holoenzyme was not formed or was too unstable and dissociated during passage on the first column. The second column eluate was hence void of any protein.
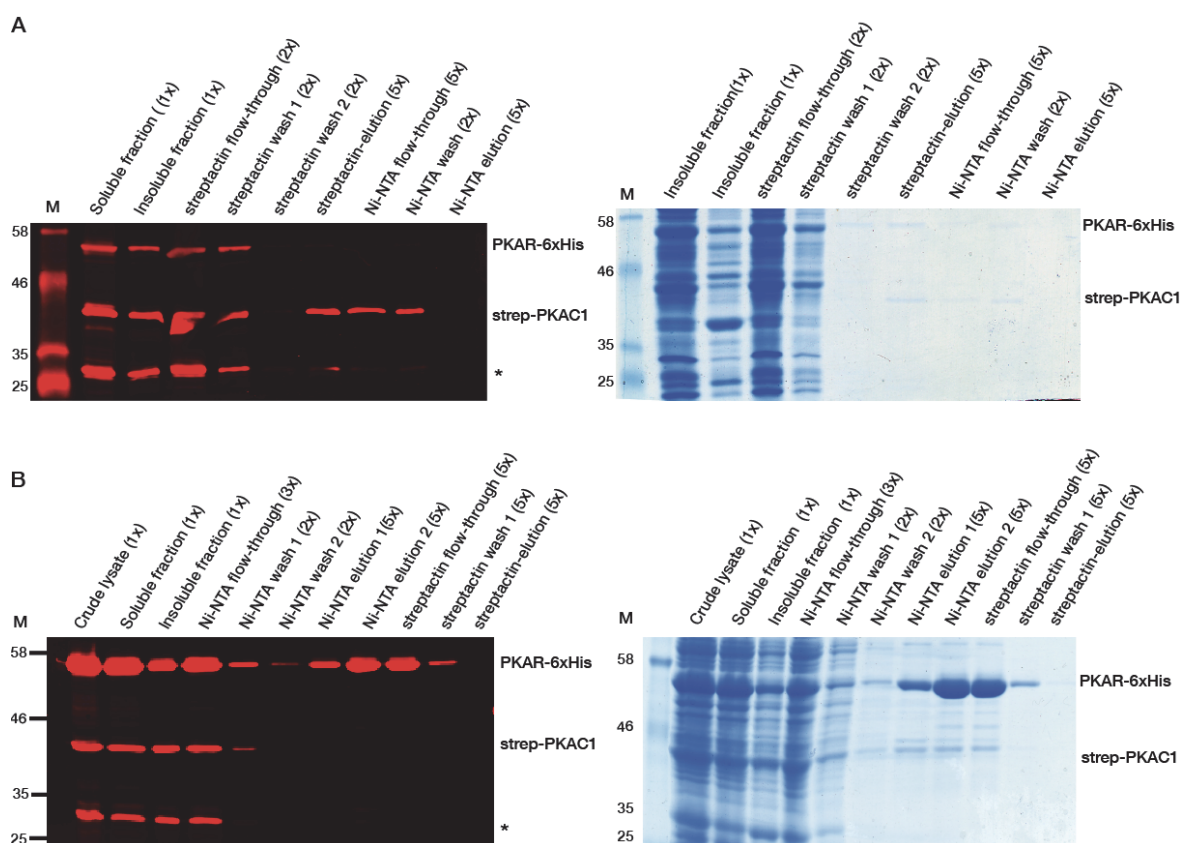
Fig. 3.17. Two step purification of PKAR-10xHis/strep-PKAC1 co-expressed in Lemo21 *E. coli* strain: a 200 ml cell culture of the PKAR-6xHis/strep-PKAC1 lemo21 dual expression was harvested after a 4 hour induction with 400 µM IPTG at 20°C and purified as described in section 2.2.12.5. **A.** Strep tag followed by His tag purification **B.** His tag followed by strep tag purification.

The purification steps were analysed by Western blot (left panel) using anti-PKAR and anti-PKAC1/2 antibodies, as indicated, and SDS-PAGE coomassie staining (right panel) where the positions of the expected proteins are indicated. Values of *x* indicate relative amounts to the starting material. The asterisk indicates a possible degradation product of the catalytic subunits.

3.2.2.4.1 In vivo analysis TbPKA holoenzyme formation in Lemo21 *E. coli*

The fact that the PKAR-6xHis/strep-PKAC1 holoenzyme could not be co-purified despite having relatively high amounts of the individual subunits in the soluble input fraction suggests that either or both of the subunits is not fully functional. This would be attributed to improper folding of the kinase or absence of crucial posttranslational modifications. Functionality of the classic regulatory subunit is often monitored by its capacity to bind cAMP (see section 1.6.1). In *T. brucei* however, this feature cannot be

exploited since the kinase is non-responsive to this ligand. The activity of the catalytic subunit is often monitored by in vitro kinase assays using artificial substrates, a feature conserved in *T. brucei*. It was however deemed to be more informative to test for the capacity of strep-PKACs to phosphorylate the regulatory subunit on its inhibitor substrate sequence (Fig. 3.6). Since there are no known serine/threonine protein kinases in *E. coli*, it was expected that the phosphorylation of PKAR-6xHis would only occur when co-expressed with strep-PKAC. This would on one hand determine whether the catalytic subunits are active and on the other whether both the R and C interact, at least transiently, in the expression system. The phosphorylation of PKAR substrate inhibitor sequence was monitored by western blot analysis of the soluble fractions of the co-expression experiment portrayed in Fig. 3.16 of the previous section. The anti-phospho-PKA substrate antibody, specific for the aforementioned motif, was used to probe the PKAR-6xHis phosphorylation.

In both the PKAR-6xHis/strep-PKAC1 and PKAR-6xHis/strep-PKAC3 co-expressions, there was no signal before induction (Fig. 3.18a). This indicates absence of any endogenous PKA activity. There was however a phosphorylation signal at the molecular weight corresponding to PKAR (56 kDa), after IPTG induction. In PKAR-6xHis/strep-PKAC1 co-expression, a faint signal could be observed at the 2hr post induction time point and was highest at the 5hr time point. The signal in the PKAR-6xHis/strep-PKAC3 co-expression was only visible at the 5hr time point. This difference was likely due to the fact that the strep-PKAC3 expression is much lower.
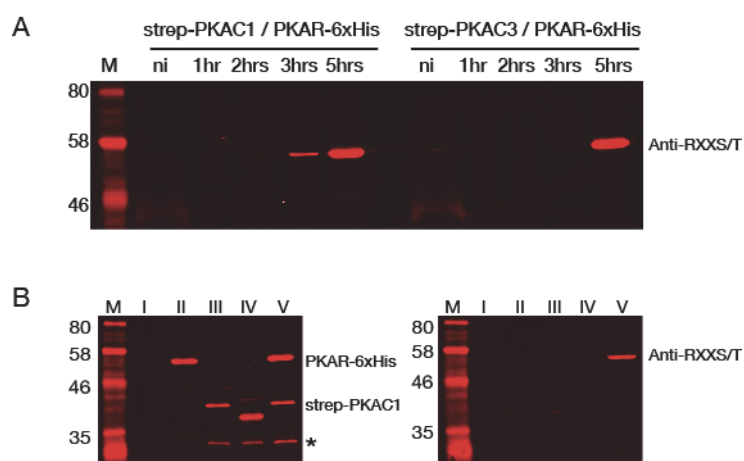
Fig. 3.18. Phosphorylation of PKAR-6xHis RRTTV motif by strep-PKACs when co-expressed in Lemo21 *E. coli*: A. The soluble fractions (S) of the PKAR-6xHis/strep-PKAC1 co-expression (Fig. 3.16), were probed on a Western blot using the anti-phospho-PKA substrate (anti-RXXS/T) antibody (NEB). **B.** The pETDuet empty vector (I), pETDuet.PKAR-6xHis (II), pETDuet.strep-PKAC1 (III), pETDuet. strep-PKAC1-dead (IV) and pETDuet.PKAR-6xHis/strep-PKAC1 (V) were expressed in Lemo21 *E. coli* for 5hrs as described in section 3.2.2.4. The soluble fractions were probed with anti-PKAR, anti-PKAC1 and anti-RXXS/T as indicated. The asterisk indicates a possible degradation product of the catalytic subunit.

This observation was further validated by also including the individual expression of; PKAR-6xHis, strep-PKAC1, a catalytically inactive strep-PKAC1 (see section 2.1.1.4) and the pETDuet empty vector (Fig. 3.18b). The RXXS/T phosphorylation was analysed 5hrs post-induction and it could be confirmed that the signal was only present when PKAR was co-expressed with the catalytic subunit. Hence the catalytic subunits appeared to be active and able to interact with the regulatory subunit, long enough to phosphorylate it but not stably enough to be purified as a complex.

The catalytically inactive strep-PKAC1 was observed to migrate faster than its active homologue (Fig. 3.18b). This is reminiscent of the slower migration of mammalian PKA as a result of autophosphorylation of its activation loop, which renders it active (see section 3.2.2.2). It is therefore likely that *E. coli* expressed TbPKACs also undergo autophosphorylation rendering them active, hence their capacity to trans phosphorylate the regulatory subunit.

3.2.3 TbPKA Expression in the Baculovirus Expression Vector System (BEVS)

In the BEVS expression system, the recombinant gene of interest is integrated by transposition into a bacmid via the pFASTBAC1 (Invitrogen) shuttle vector. The bacmid is then transfected into the insect cells to generate the viral stocks. Protein expression is achieved by infection of the insect cells with the viral stocks, where the protein of interest is expressed under a strong viral promoter (Fig. 3.19). PKA subunits were cloned into the pFASTBAC1 shuttle vector followed by generation of DNA bacmids in DH10 BAC *E. coli*. The bacmids were then used to produce high titer viral stocks (see section 2.2.11.2). Single and double expression of the PKA subunits was achieved by infection or co-infection of Sf9 cells with the viral stocks. Table 3 summarizes the various viral stocks used for expression.

Fig 3.19. The expression unit of the pFASTBAC vector: The gene of interest is expressed under the strong viral polyhedrin promoter (P_{PH}). The vector also contains the simian virus 40 (SV 40 pA) polyadenylation signal. The expression cassette is flanked by transposition recognition sites (Tn7R and Tn7L), which facilitate its integration into the bacmid vector.

Table 3. High titer viral stocks of PKA subunits, generated from TbPKA bacmids (see method section 2.2.8 and 2.2.11.2)

PKA subunit
PKAR-PTP
PKAR (untagged)
Strep-PKAC1 (D. Sohmen, Diploma thesis 2008)
PKAC1 (untagged)
Strep-PKAC3 (D. Sohmen, Diploma thesis 2008)
PKAC3 (untagged)

3.2.3.1 Expression and purification of TbPKAR in BEVS

Although the PKAR subunit could be expressed with high yield in the *E. coli* expression system, it could not form a holoenzyme complex with the PKACs, suggesting a probable lack of full functionality. Expression in a higher eukaryotic expression system would increase the chances of obtaining a functional holoenzyme. Having earlier shown that the TbPKA holoenzyme could be co-purified from trypanosomes using the PTP-tag tandem purification (see section 3.2.1), the same purification approach was used in this system for technical comparison. Sf9 cells were infected with a high titer viral stock of PKAR-PTP. Expression analysis showed that the protein is stably expressed after 24 hours. Higher expression could be achieved with longer incubation but resulted in partial degradation of the protein, very likely by proteases following virus induced cell lysis. Cells were harvested 48 hours post-infection followed by PTP-tag purification under the same conditions, previously described for PKAR-PTP in *T. brucei* (2.2.12.2.3). Analysis of the purification showed that this protein is highly expressed and that the first column elution i.e. after TEV cleavage was highly pure, making the second column passage unnecessary (Fig. 3.20). The absence of degradation products in the final eluate suggests that proteolysis would occur on the C-terminal side of the protein.

The final eluate was quantified by Bradford protein quantification giving an estimated yield of about 1 mg/litre of cell culture.
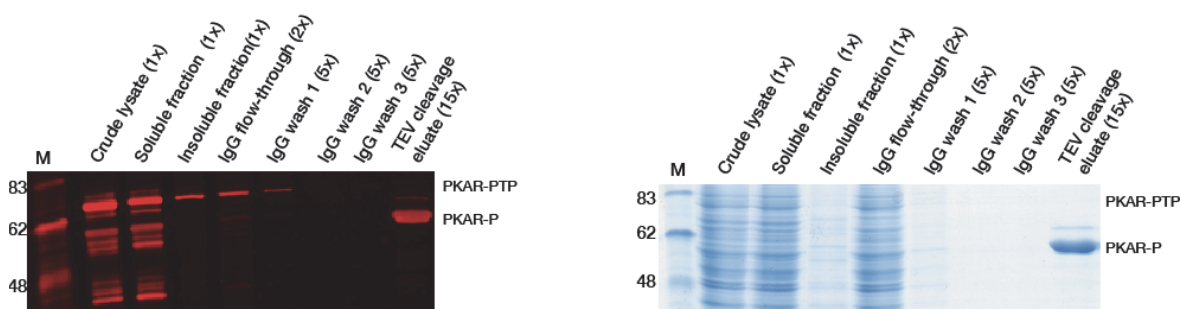
Fig. 3.20. PTP tag purification of PKAR-PTP from Sf9 cells: A 200 ml Sf9 cell culture was infected with high titer PKAR-PTP viral stock and harvested 48 hrs post-infection. The PKAR subunit was purified following the PTP-tag purification detailed in section 2.2.12.2.3. After the TEV cleavage of the PTP tag, the His-tagged TEV enzyme was depleted from the eluate with a Ni-NTA column. The purification steps were followed by Coomassie staining and Western blot probing with the polyclonal anti-PKAR antibody. Values of *x* indicate relative amounts to the starting material. The protein was partially degraded as can be seen by the numerous bands in the input fractions of the Western blot.

3.2.3.2 Expression and purification of TbPKAC1 and TbPKAC3 in BEVS

The strep-PKAC1 and strep-PKAC3 isoforms had previously been purified from this expression system in sufficiently high yields and therefore required no further optimization (D. Sohmen, Diploma thesis 2008). However, the activity of purified strep-PKAC1 protein could not be detected by in vitro kinase assays (D. Sohmen, Diploma thesis 2008), hence the necessity to reanalyse this isoform. The expression and

purification was repeated without any modifications of the initial protocol as detailed in section 2.2.12.4. The estimated yield for strep-PKAC1 and strep-PKAC3 was 0.2 and 0.6 mg/litre of cell culture, respectively. Expression of strep-PKAC3 was hence better than that of strep-PKAC1 contrary to results in the *E. coli* expression system. The absolute yield of strep-PKAC1 was comparable to that obtained from the *E. coli* expression system.
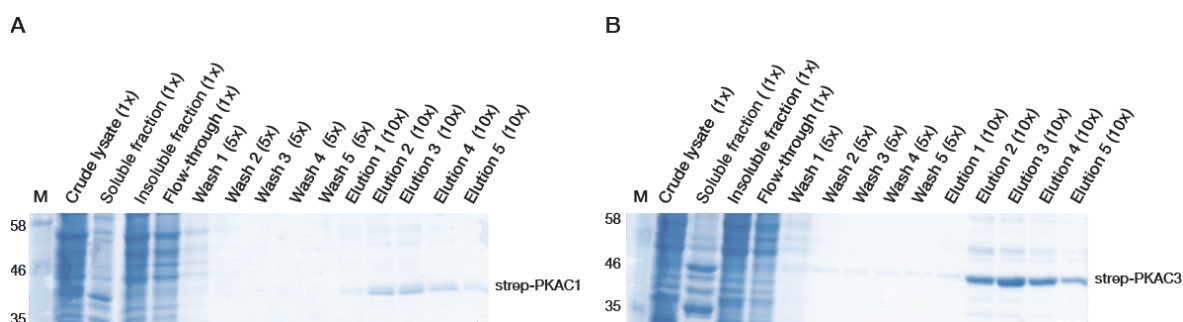
Fig. 3.21. Strep purification of TbPKAC subunits in BEVS expression system: 200 ml cell cultures of Sf9 cells were infected with high titer viral stocks of strep-PKAC1 **(A)** and strep-PKAC3 **(B)** and harvested 48hrs post-infection. The purification was carried out as described in section 2.2.12.4. The purification steps were then analysed by coomassie stained SDS-PAGE gels as indicated. Values of *x* indicate relative amounts to the starting material. All the elution steps were pooled before quantifying the final yield.

3.2.3.3 Co-expression and co-purification of TbPKA in the BEVS

The BEVS expression system is quite versatile for co-expression as any combination of viral stocks can be used for co-infection. A combination of tagged and untagged version of the TbPKA subunits would enable analysis of the tag's influence on holoenzyme formation. The co-expression of untagged PKAR and strep-tagged PKACs was followed for 72 hours and samples been taken every 24 hours (Fig. 3.22). Both holoenzyme isoforms had a peak expression at 48 hours, post-infection. Longer incubation resulted in the gradual degradation of the catalytic subunits, as portrayed by loss of signal or presence of bands of lower MW.
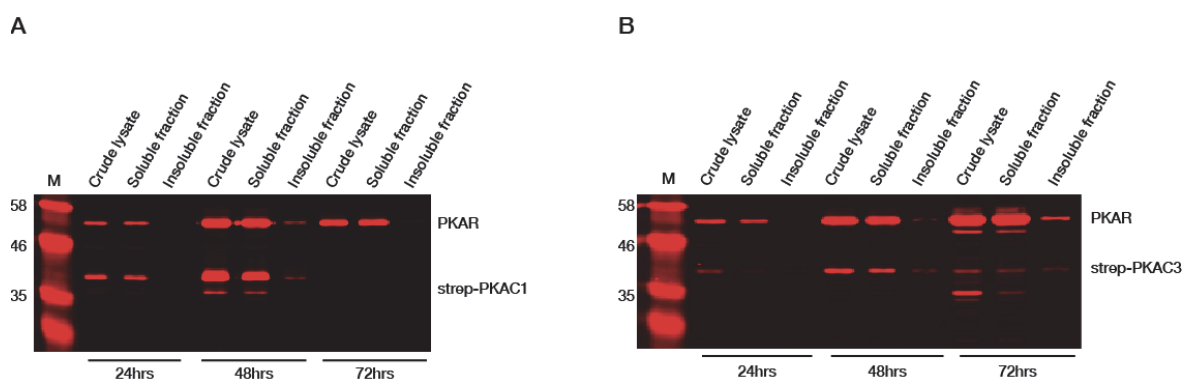
Fig. 3.22. Co-expression of TbPKA in BEVS: Sf9 cells were co-infected with TbPKAR (untagged) and either strep-PKAC1 **(A)** or strep-PKAC3 **(B)**. Samples were taken every 24 hours and processed for protein

expression analysis as detailed in section 2.2.11.2.3. The expression was analysed by Western blot using anti-PKAR, anti-PKAC1/2 and anti-PKAC3 antibodies as indicated. Peak co-expression was observed 48hrs post-infection.

Co-infection was carried out with the following subunit combinations: Strep-PKACs with untagged PKAR or PKAR-PTP with untagged PKACs. The cells were harvested at 48hrs post-infection, followed by purification of the holoenzyme as dictated by the tags. As had been observed in *E. coli* co-purification, the tagged bait protein could be precipitated but the untagged co-expressed partner was lost in the unbound fraction. A very slight signal of the untagged TbPKAR could be seen in the elution fractions (Fig. 3.23a & b) but almost negligible in comparison to the input material. Low expression of either of the co-expressed partners could be ruled out as the reason for the co-precipitation failure as shown in Fig. 3.23 b and c where both TbPKAR and TbPKAC3 were highly expressed. The influence of the tags on either of the kinase subunits could hence be ruled out. It is however plausible that a holoenzyme complex formation would only be possible in the absence of a tag on both subunits.

It was hence concluded that this system was also not suited for holoenzyme formation. The approach to test the intrinsic capacity of TbPKACs to phosphorylate the TbPKAR subunit in the expression system (see section 3.2.2.1.4) was in this case not applicable owing to the presence of many Ser/Thr kinases, including the endogenous PKA kinase in Sf9 cells.

Fig. 3.23. Purification of TbPKA holoenzyme in BEVS: Sf9 cells (200 ml culture) were co-infected with TbPKA subunits in the following combinations: **A.** Strep-PKAC1/PKAR (untagged) **B.** strep-PKAC3/PKAR (untagged) and **C**. PKAC3 (untagged)/PKAR-PTP. The cells were harvested 48 hours post infection and purified following the strep tag protocol (section 2.2.12.4) or the PTP tag purification protocol (section 2.2.12.2.3) with the sole exception being that PKAR-PTP was eluted from the column with 0.1M glycine-HCl, pH 3.0 and not cleaved off by TEV protease.

The purification steps were analysed by Western blot (left panel) using the TbPKA antibodies (anti-PKAR, anti-PKAC1/2 and anti-PKAC3) as reported previously and coomassie stained SDS-PAGE gels (right panel) here labeled according to the migration patterns of the expected proteins. Values of *x* indicate relative amounts to the starting material.

A

B

C
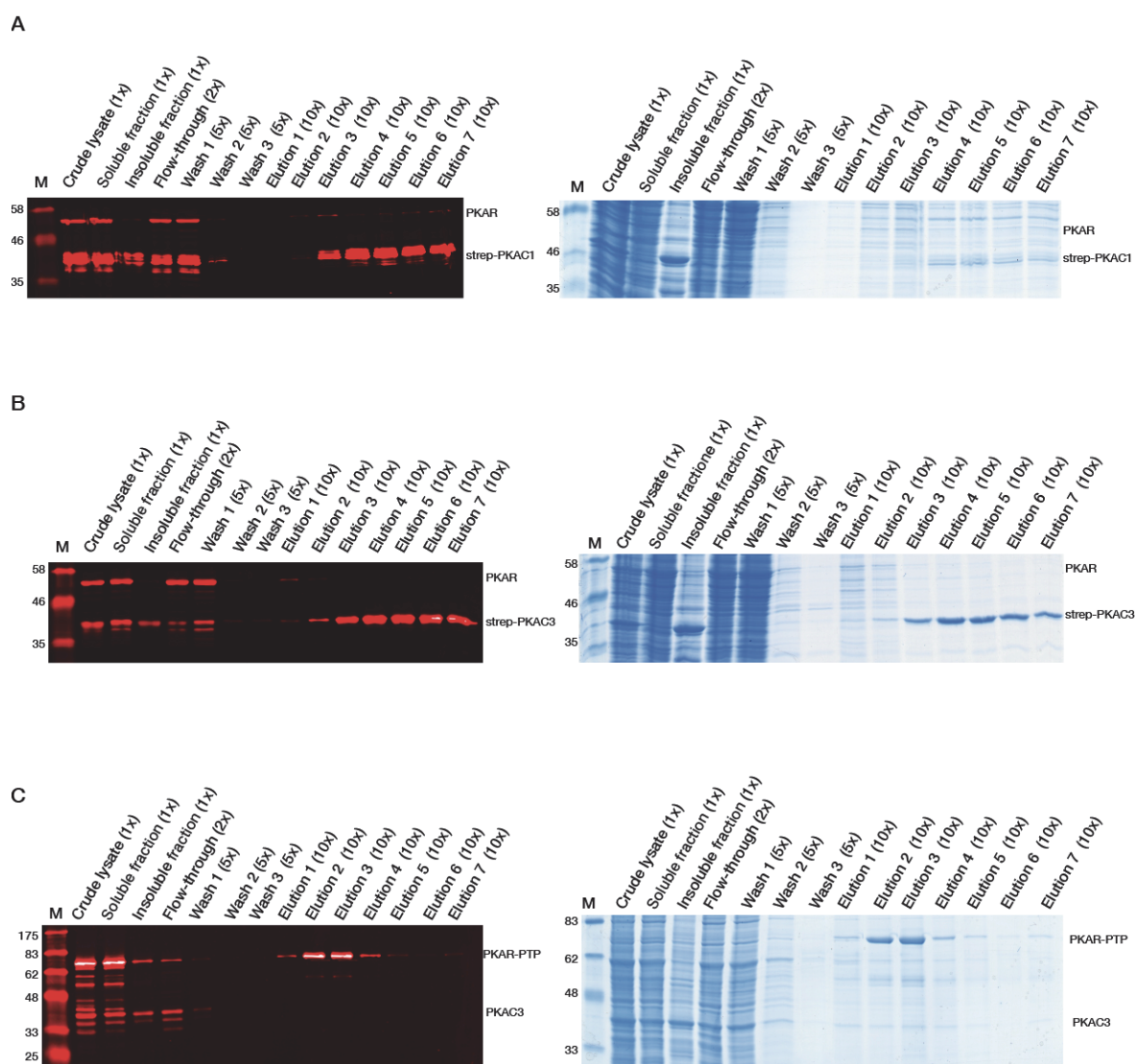
3.2.4 A trypanosome specific factor is required for holoenzyme formation

It has in many cases been shown that upon failure to express a fully functional higher eukaryotic recombinant protein in *E. coli*, switching to a higher eukaryotic expression system often resolves this problem. It was hence a surprise to realize that despite a general improvement of TbPKA expression in the higher eukaryotic (insect) system, the holoenzyme reconstitution was still unsuccessful. The holoenzyme had been successfully purified from trypanosome lysate using the PTP tag purification approach, also an additional argument for the absence of the tag's influence on holoenzyme formation. This approach was however unsuccessful in the BEVS system hence ruling out any technical contributions but rather suggesting that a trypanosome specific factor may be required for holoenzyme formation. Incubating heterologously expressed TbPKA subunits with trypanosome cell lysate was suggested to rescue or supplement the holoenzyme formation. About 150 ng (~3.8 pmoles) of BEVS purified strep-PKAC1 and strep-PKAC3 were incubated with MITat 1.2 PKAR KO cell lysate in the presence or absence of 200 ng (~3.5 pmoles) of *E. coli* expressed PKAR-6xHis. The PKAR KO cell line had previously

been made by C. Krumbholz (this lab) and also shown to have a drastically reduced expression of the PKAC1 isoform (≤10% of the wild type). The absence or reduction of endogenous TbPKA would facilitate the interpretation of the results. After two hours of incubation at room temperature, Ni-NTA resin was used to precipitate the PKAR-6xHis subunit with the aim of co-precipitating the recombinant strep-PKAC subunits. The pull-downs were analysed on a Western blot using polyclonal anti-strep antibody, hence distinguishing between the endogenous and heterologous PKAC subunits. It was shown that under these conditions, strep-PKACs interacted with PKAR-6xHis and could hence be co-precipitated.
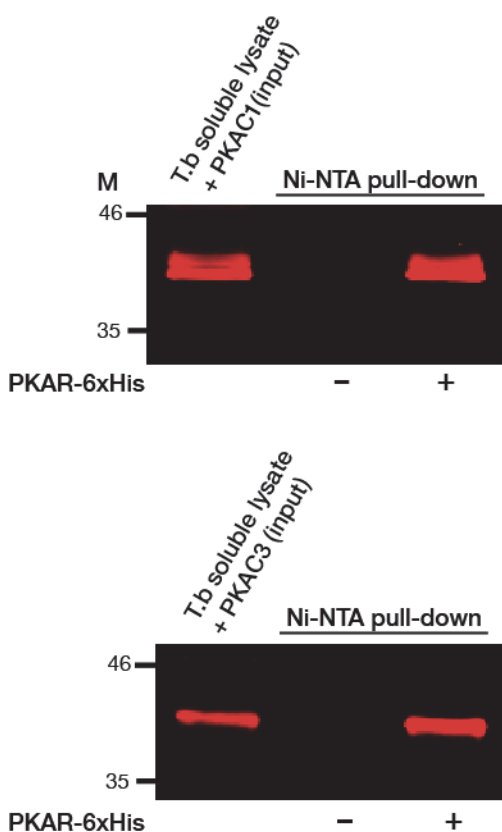
Fig.3.24. Recombinant TbPKA holoenzyme reconstitution in trypanosome cell lysate: About 3.8 pmoles of either strep-PKAC1 or strep-PKAC3 (from the BEVS expression system) was incubated with trypanosomes soluble fraction from the MITat 1.2 PKAR KO in the presence or absence of ~3.5 pmoles of PKAR-6xHis (from the *E. coli* expression system), for 2hrs at room temperature. Ni-NTA resin was then used to pull down the recombinant PKAR subunit. Co-precipitation of strep-PKAC subunits was analysed by Western blot using anti-strep antibody.

3.2.5 TbPKA expression in the *Leishmania tarentolae* expression system (LEXSY)

The findings in the previous section indicate that the holoenzyme formation necessitates trypanosome specific cofactors. The homologous expression system could however not be exploited for large-scale purification of the kinase as reported in section 3.2.1). However, an expression system from the non-pathogenic *Leishmania tarentolae* (Kushnir et al., 2005), was deemed likely to possess the factors required for holoenzyme formation, being a close relative of *T. brucei*. Stable transfections of the TbPKA subunits were made in *L. tarentolae*, using the pLEXSY vector system designed for inducible expression with the T7 polymerase-Tet repressor system. The T7 polymerase and Tet repressor genes are integrated in the genome and are constitutively expressed under the

RNA pol I polymerase (Fig. 3.25). The pLEXSY vector targets the recombinant protein's ORF to the ribosomal spacers making it possible to co-express two proteins with different selection markers. The pLEXSY constructs generated are tabulated below.

LEXSY Inducible expression
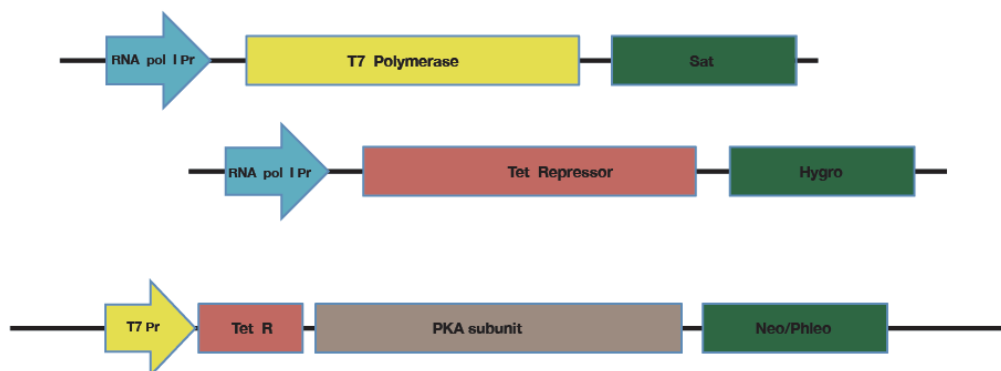
Fig. 3.25. The LEXSY inducible expression system: The T7 polymerase and the Tet repressor ORF are stably integrated in the Leishmania genome under nourseothricin (Sat) and hygromycin (Hygro) resistant markers, respectively. They are both constitutively expressed under the endogenous RNA pol I polymerase. TbPKA subunits were stably transfected using the pLEXSY vectors with either neomycin or phleomycin resistant marker selection, or both for dual expressions.

Table 4. TbPKA subunits stably transfected into *Leishmania tarentolae* and the cell lines generated with the respective selection markers (the cloning strategy is detailed in section 2.1.1.6).

TbPKA subunits in pLEXSY vector	Resistance marker
Strep-PKAC1	Neomycin
Strep-PKAC3	Neomycin
PKAR-10xHis	Phleomycin
Strep-PKAC1/ PKAR-10xHis	Neomycin and Phleomycin
Strep-PKAC3/ PKAR-10xHis	Neomycin and Phleomycin
Strep-PKAC1/ PKAR-10xHis PBC mut	Neomycin and Phleomycin

3.2.5.1 Expression and purification of TbPKA subunits in LEXSY

TbPKA expressing cell lines were generated by transfecting their respective linearized targeting constructs (above) into the leishmania T7-TR cell lines. The antibiotic resistant cell populations were then tested for protein expression after tetracycline induction (10 µg/ml). Samples were taken every 24hrs for three days and processed for Western blot analysis as described in section 2.2.3.5. The *T. brucei* paraflagellar rod antibody (anti-PFR) was used for loading control analysis and perfectly cross-reacted with the *L. tarentolae* homologue (Fig. 3.26), a further indication of the similarity between these two species. The TbPKA antibodies were also suspected to cross-react with the endogenous TbPKA subunits. However, the non-induced samples of both strep-PKAC1 and strep-PKAC3 had no signal at the expected MW of *L. tarentolae's* PKAC (around 38 kDa,

similar to TbPKACs) while an apparent *L. tarentolae* PKAR could be detected in the non-induced sample of the PKAR-10xHis expressing cell line. The cross-reaction was confirmed with a cell line devoid of recombinant TbPKAR, hence ruling out leakiness of the T7-TR repressor system (data not shown). The expression of PKAR-10xHis was stable throughout the sampling period as shown in Fig. 3.26a. Both of the strep-PKAC isoforms had the highest expression between 24-48 hours post-induction (Fig. 3.26 b & c). Strep-PKAC1 migrated in several bands whereby the migration pattern appeared to be dependent on the duration of expression (Fig. 3.26b). This is reminiscent of the life stage dependent phosphorylation of TbPKAC1 in the BSF cell line, reported by S. Kramer (Ph.D. thesis 2006). This phosphorylation slows the protein migration on the SDS-PAGE gel and increases with rising cell density from the LS to SS form. It is speculative that this could be the same phosphorylation but nonetheless indicates that this subunit could have acquired some PTMs, absent in the other expression systems.

The expression of the strep-PKAC3 appeared to be very weak and unstable given its weak signal (relative to the other expression systems under the same probing conditions) and the fact that the expression is completely lost at the 72hr time point.
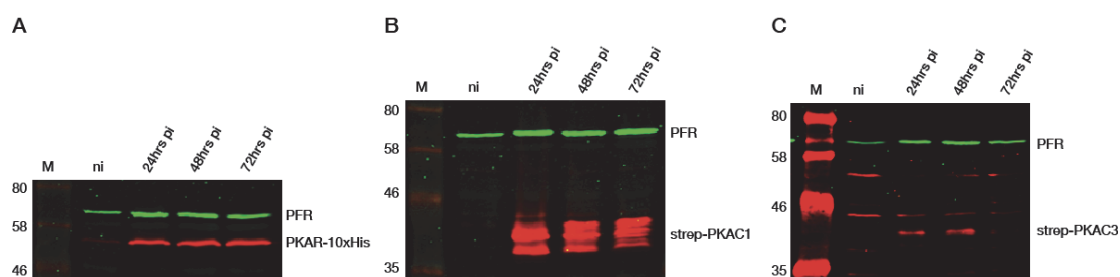
Fig. 3.26. Expression of TbPKA in LEXSY: *L. tarentolae* cells transfected with PKA subunits **A.** PKAR-10xHis **B.** strep-PKAC1 and **C.** strep-PKAC3 were induced with 10 µg/µl tetracycline. Cells samples were harvested at the indicated time points and processed for Western blot analysis of protein expression, as described in section 2.2.3.5. TbPKA antibodies were used to probe for subunits expression, as indicated. Trypanosoma anti-PFR antibody was used as a loading control and shown to perfectly cross-react with the Leishmania homologue. The TbPKAR antibody (A) slightly cross-reacted with the Leishmania PKAR as shown by the weak signal in the non-induced sample (ni).

The individual subunits were purified from a 200 ml cell culture after 24 hours of tetracycline induction, using their respective tags as previously described. Only PKAR-10xHis and strep-PKAC1 could be purified at quantifiable yields. The input (cytoplasmic fraction), the insoluble fraction and the final eluates of these two proteins were analysed by Western blot and coomassie stained gels. The yield obtained for strep-PKAC1 and PKAR-10xHis was estimated by Bradford protein standard assay to 0.02 and 0.3 mg per litre of cell culture, respectively. Expression in this system was generally lower than in both the *E. coli* and BEVS systems.
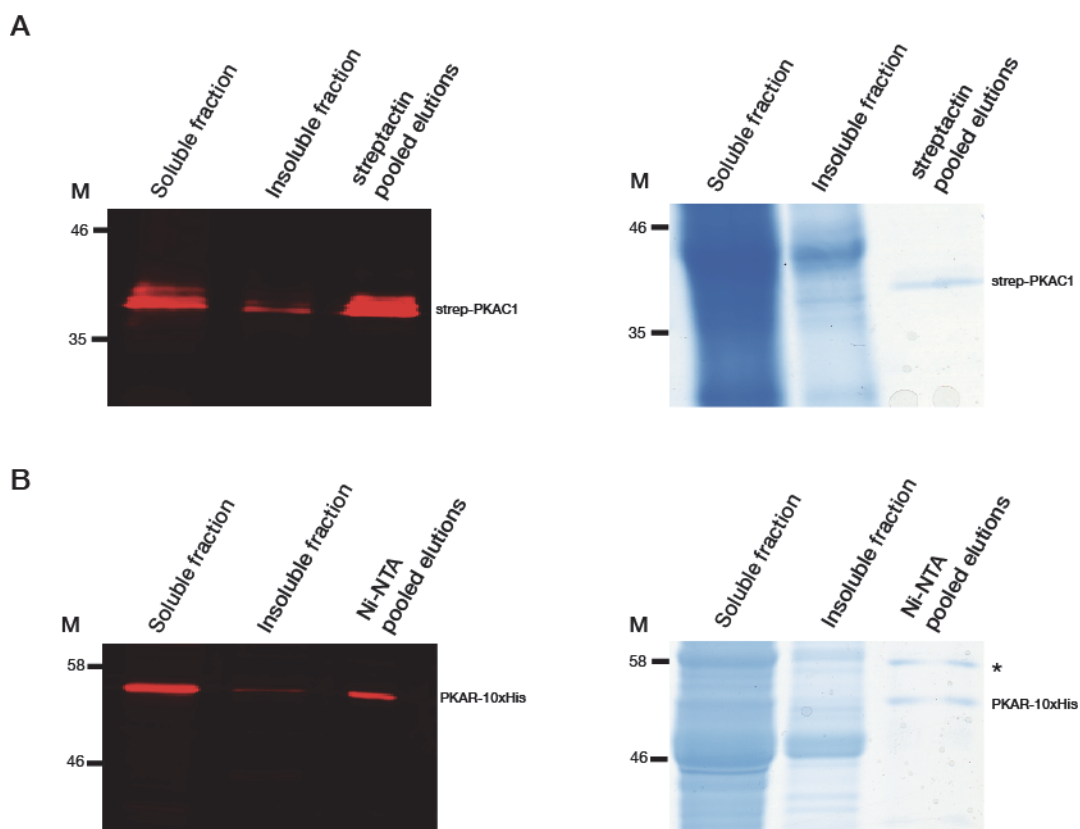
Fig. 3.27. Expression of TbPKA subunits in LEXSY: *L. tarentolae* cells expressing the PKA subunits were harvested 24 hours post-induction. The strep and His purifications were performed as described in section 2.2.12.3 and 2.2.12.4 for strep-PKAC1 (A) and PKAR-10xHis (B). Equal amounts of the soluble lysate, insoluble fraction and final pooled purification eluates were analysed by coomassie stained gels and Western blot analysis, using anti-PKAC1/2 and anti-PKAR antibodies, as indicated. A contaminating band was observed above the PKAR subunit on the coomassie stained gel (asterisk).

3.2.5.2 PKA holoenzyme co-expression and co-purification in LEXSY

The co-expression of the strep-PKAC1 or strep-PKAC3 with PKAR-10xHis was also analysed over a 72hr period after induction, as described in the previous section. The co-expression profile was similar to that of the individual subunits. The expression of strep-PKAC3 did not improve in the presence of PKAR-10xHis.
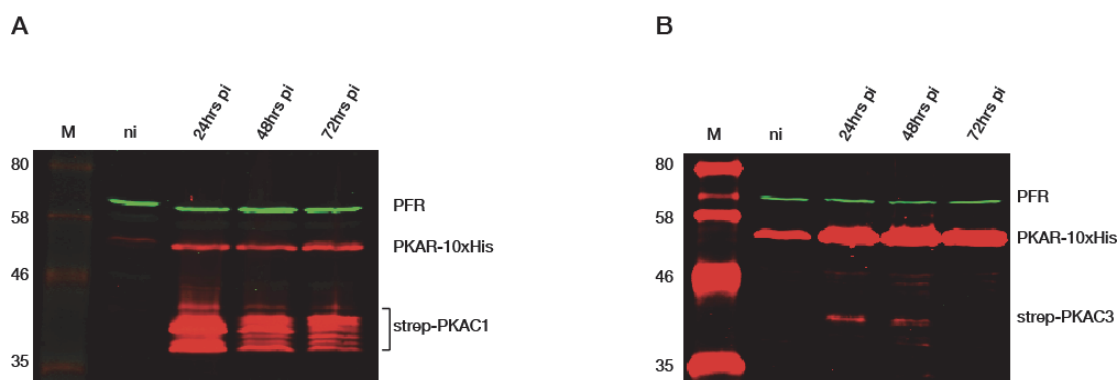
Fig. 3.28. Co-expression of TbPKA in LEXSY: The TbPKA subunits co-expressing cell lines **A.** PKAR-10xHis/strep-PKAC1 and **B.** PKAR-10xHis/strep-PKAC3 were induced with 10 µg/µl tetracycline. Sample processing and Western blot analysis was as described for Fig. 3.27. The PKAR-10xHis/strep-PKAC3 western blot was incubated overnight with the primary antibodies in a bid to enhance the signal of the weakly expressed strep-PKAC3. This explains the stronger signal for PKAR-10xHis. The cross-reaction of TbPKAR with Leishmania's homologue could also be clearly seen in the non-induced sample.

The PKAR-10xHis/strep-PKAC1 cell line was induced and cells harvested after 24 hours. The tandem strep/His purification was then performed as described in section 2.2.12.5. It was shown that contrary to the other expression systems, both kinase subunits were present in the first column eluates and more importantly in the second column eluates (Fig. 3.29a). The purity of the holoenzyme kinase obtained was very high as shown by the coomassie stained gel (Fig. 3.29b). The amount of the holoenzyme was estimated by Bradford protein assay to 0.12 mg/litre of cell culture. The molar ratio between PKAR-10xHis:strep-PKAC1 was estimated to 1:0.9, assuming that both proteins were equally stained by the Bradford reagent. The quantification was carried out using the ImageJ software (http://imagej.nih.gov/ij/). The successful purification of TbPKA holoenzyme in this system, in close to 1:1 molar ratio, confirmed that kinetoplastid specific features a required for stable complex formation. The purity of the holoenzyme on the coomassie stained SDS-PAGE gel indicates that protein cofactors are not involved but rather kinetoplastid specific PTMs are likely to confer full functionally on the holoenzyme.

A   B
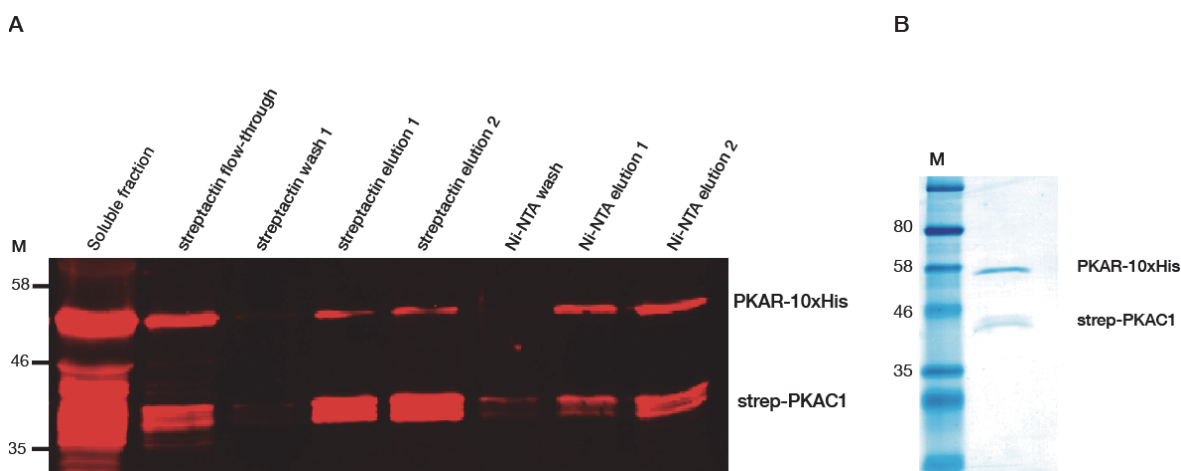
Fig. 3.29. Two step purification of TbPKAC1 holoenzyme from LEXSY: 500 ml of PKAR-10xHis/strep-PKAC1 dual expression cell line was induced with 10 µg/µl tetracycline and harvested 24hrs post-induction. The two-step purification was carried out as described in section 2.2.12.5. Purification steps were analysed by Western blot with anti-PKAR and anti-PKAC1/2 **(A)**. The final eluate was analysed for purity by coomassie stained SDS-PAGE gel **(B)**.

3.2.6 The specificity of TbPKA holoenzyme formation

The successful purification of the holoenzyme in *L. tarentolae* and its apparent high purity (Fig. 3.29b), suggests that protein cofactors are not required for the holoenzyme formation but rather posttranslational modifications on either or both subunits. A

comparative in vitro analysis of TbPKAC1 and TbPKAR subunits from the three expression systems was carried out in a bid to identify the subunit whose full functionality is dependent on the expression system. The TbPKAC3 subunit was left out mainly due to its poor expression in both *E. coli* and the LEXSY systems.

3.2.6.1 Protein purification and quantification

Strep-PKAC1 subunits were purified from the three heterologous expression systems. The subunits were quantified by BSA protein standard on a coomassie stained SDS-PAGE gel as described in section 2.2.13.6.2. The mammalian Cα (NEB) was used as reference for the determination of the specific activities. The protein yields obtained reflect the relative expression of this kinase isoform as earlier reported, where the *E. coli* and BEVS have a similar level of expression much higher than the LEXSY expressed kinase (Fig. 3.30a). The regulatory subunits were also purified from the different expression systems as reported earlier and quantified similarly to the catalytic subunits (Fig 3.30b).

PKAC1	Concentration
Strep-C1 (*E. coli*)	10 ng/µl
Strep-C1 (BEVS)	9 ng/µl
Strep-C1 (LEXSY)	1.75 ng/µl
Mammalian PKACα	250 ng/µl

Tb PKARs	Concentration
Tb PKAR (*E. coli*)	800 ng/µl
Tb PKAR (LEXSY)	25 ng/µl
Tb PKAR (BEVS)	100ng/µl
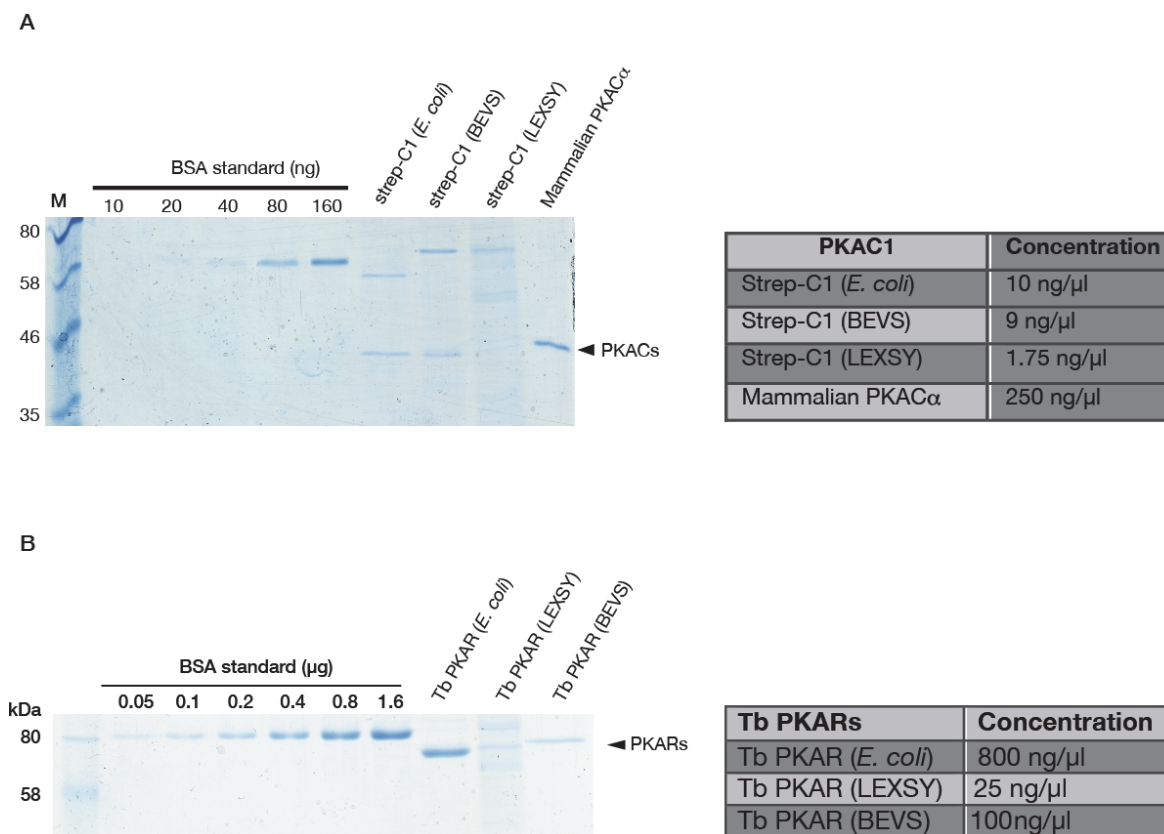
Fig. 3.30 Recombinant TbPKA quantification by SDS-PAGE BSA protein standard: A. Final eluates of strep-PKAC1 from three expression systems as indicated (purified from an initial volume of 200 ml cell culture as described in section 2.2.12.4) and the mammalian Cα (NEB) **B.** Final eluates of PKAR-6xHis (*E. coli*), PKAR-P (BEVS) and PKAR-10xHis (LEXSY). The protein concentrations were inferred from the BSA standard using the Odyssey scanner at 700 nM.

3.2.6.2 Test for cross-interaction of TbPKA subunits with the expression system's endogenous PKA

Before proceeding with the in vitro characterization, it was important to test whether the recombinant PKA subunits are contaminated by cross-interaction with the expression system's endogenous PKA. This is highly probable in eukaryotic expression, given the high interspecies conservation of the R/C interface (see section 3.1.4). The recombinant TbPKAC1 was purified from the BEVS expression system and tested with a radioactive in vitro kinase assay, as described in section 2.2.15, in the presence or absence of 10 µM cAMP. An increase in catalytic activity was expected in the plus cAMP conditions, only if the kinase was partially inhibited by the eukaryotic R subunit. There was however no significant difference in kinase activity under the two conditions, suggesting that the endogenous regulatory subunit does not interact with TbPKAC1 subunit (Fig. 3.31). The LEXSY expressed TbPKA was also suspected to interact with the Leishmania PKA. There was however no difference in plus or minus cAMP conditions (data not shown). This was however not conclusive since the close relation between Trypanosomes and Leishmania would suggest that the latter is also non-responsive to cAMP activation. The LEXSY expressed TbPKAC was retested after the discovery of suitable activators (see section 3.4.2.2)
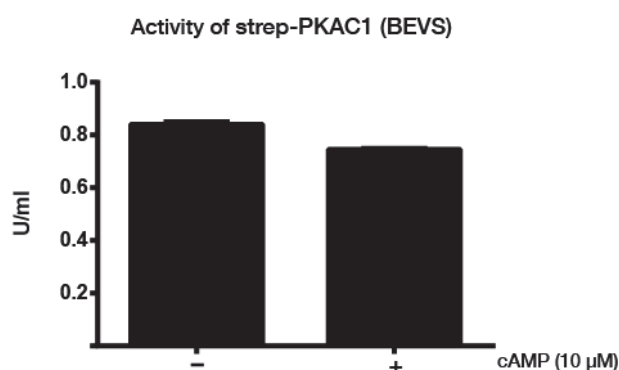
Fig. 3.31. Strep-PKAC1 expressed in Sf9 cells (BEVS) does not interact with the eukaryotic PKAR: Strep-PKAC1 was expressed and purified from Sf9 cells as described in section 3.2.3.2. In vitro kinase assay for the catalytic activity was carried out, as described in section 2.2.15, in the absence or presence cAMP, as indicated. The assay was carried out in duplicates to obtain the range, shown by the error bars.

3.2.6.3 Characterization of TbPKAC1 from the different expression systems: Determination of the specific activity

The activity of the isolated kinases was comparatively tested with the in vitro kinase assay. Equal amounts of the four kinases, whose concentration was determined in the previous section, were tested in a 1:2 dilution series in the in vitro kinase assay in order to establish the linear range of catalytic activity in the assay conditions described in section 2.2.15. Two kinase concentrations within the linear range were then used to determine the specific activity. Given the high conservation of the kinase's catalytic core within the PKA kinase family (see section 3.1.3), the in vitro activity of TbPKAC1 was

expected to be in the range of the reference kinase. It was however shown that only that of the LEXSY expressed subunit was close to the reference mammalian Cα. Kinases from the other two expression systems had a much lower specific activity (Fig. 3.32). The *E. coli* expressed kinase had the lowest activity, barely distinguishable from the background values of the measurements. The high catalytic activity of the LEXSY expressed TbPKAC1 (close to that of the mammalian Cα) coupled to the fact that it's the only one capable of forming a stable holoenzyme, suggests that full functionality of this kinase is entirely dependent on the expression system.

A

B

Kinase reaction	Mean cpm	U ml^{-1}	U mg^{-1}
Blank (no kemptide)	1229		
Blank (no PKA)	1019		
Strep-C1 E. coli	2159	0.16	16
Strep-C1 BEVS 1:2 dilution	6650	1.7	189
Strep-C1 BEVS 1:4 dilution	4470	2.1	229
Strep-C1 Lt 1:2 dilution	19293	5.6	3200
Strep-C1 Lt 1:4 dilution	11631	6.5	3714
Mammalian C α 1:160 dilution	26273	622	4800
Mammalian C α 1:320 dilution	17382	804	5500
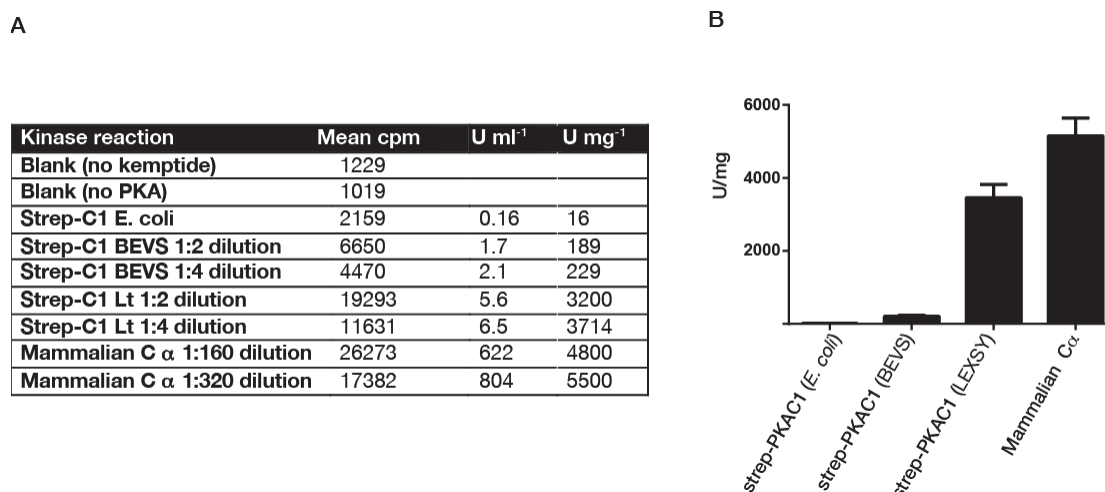
Fig. 3.32. Specific activity of recombinant TbPKAC1: A. The specific activity of TbPKAC1 subunits purified and quantified as described in section 3.2.6.1. The mammalian Cα (NEB) was used as reference. The kinase assay was performed in duplicates of a dilution series of each kinase as described in section 2.2.15. Data points within the linear range of the catalytic activity were taken to determine the activity (U/ml) and specific activity (U/mg) as described in section 2.2.15.1 **B.** The mean specific activity of two determinations as shown in A, where the error bars represent the range**.**

3.2.6.4 Characterization of TbPKAR from the different expression systems: Inhibition of TbPKAC1

The ability of TbPKAR from the three expression systems to inhibit TbPKAC1 in a reversible way would indicate full functionality of this subunit. The LEXSY expressed strep-PKAC1, having shown the highest activity, was used to test the inhibitory capacity of the different recombinant PKARs. 0.5 pmoles of strep-PKAC1 (in linear range of activity) was incubated with a 10x molar excess of the different PKAR subunits for 30 min at 4°C prior to the onset of the kinase reaction. Reversibility of the inhibition could not be tested with cAMP but with a suitable TbPKA activator, presented later in this work (see section 3.3 and 3.4). The three recombinant PKARs could inhibit the catalytic subunit in a reversible manner (Fig. 3.33), suggesting that full functionality of this subunit is not dependent on the expression system. As a future perspective, equimolar concentrations of both subunits would reveal any subtle differences between the regulatory subunits.
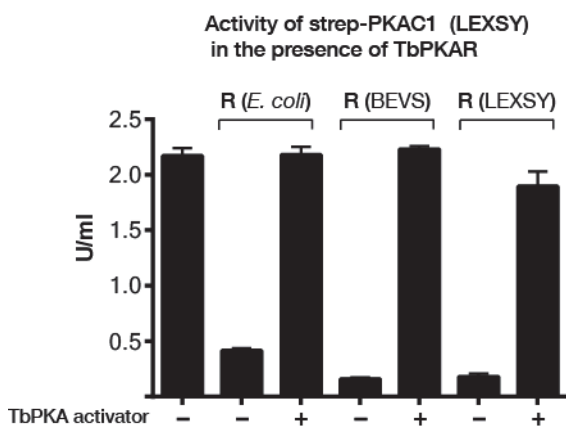
Fig. 3.33. Inhibition of TbPKAC1 by recombinant TbPKARs: Strep-PKAC1 (0.5 pmoles) expressed in LEXSY was incubated with a 10x molar excess of the three recombinant TbPKARs and in the absence or presence of 10 μM of a specific TbPKA activator described in section 3.4. The samples were run on the in vitro kinase assay in duplicates to obtain the range

3.2.6.5 Specificity of kinetoplastid PKAR/PKAC interaction

The particularity of TbPKA holoenzyme formation was further analysed by testing whether TbPKAR could inhibit the mammalian catalytic subunit and inversely, whether the mammalian R subunit could inhibit TbPKAC1.

Both the mammalian Cα (0.2 pmoles) and TbPKAC1 (0.5 pmoles) were incubated with a 10x molar excess of *E. coli* expressed mammalian RIα, RIIα (F. Herberg's lab, Kassel) or TbPKAR, as described in the previous section. The kinase reaction was then set up in the presence or absence cAMP (mammalian R subunits) or a TbPKA activator (see section 3.4 for description). The mammalian Cα was completely inhibited by its mammalian R counterpart in a cAMP reversible way, as expected, but TbPKAR had no inhibitory effect whatsoever (Fig. 3.34a). On the other hand, TbPKAC1 was completely inhibited by TbPKAR (as shown earlier) but only partially inhibited by the mammalian R subunits, both in a ligand reversible manner (Fig. 3.34b). The capacity of the mammalian R subunit to partially inhibit TbPKAC1 suggests partial conservation of the inhibitory mechanism between the two PKAs. Additional, and probably kinetoplastid specific, C subunit inhibition features might be contributed by the N-terminal domain of TbPKAR (see section 1.7.1). On the other hand, failure of TbPKAR to have any inhibitory effect on the mammalian Cα can only be explained by a possible steric hindrance of the R/C interface by the much longer TbPKAR N-terminal domain.
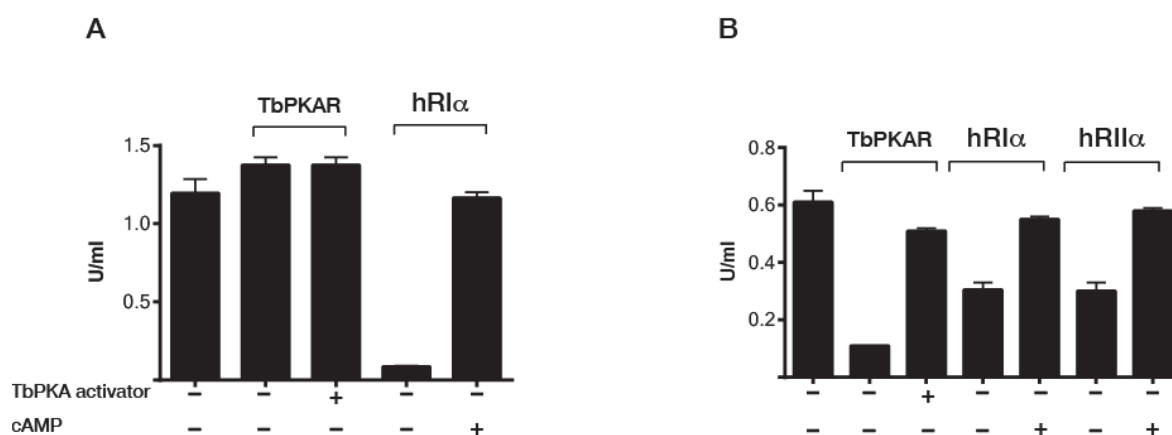
Fig. 3.34. Specificity of TbPKAR/TbPKAC interaction: A. Inhibition of mammalian Cα by TbPKAR; mammalian Cα (0.2 pmoles) was incubated with 10x molar excess of either TbPKAR (*E. coli* expressed) or human RIα in the presence or absence of cAMP (10 µM) or TbPKA activator, described in section 3.4.4, as indicated. **B.** Inhibition of TbPKAC1 by mammalian R subunits; TbPKAC1 (0.5 pmoles) was incubated in similar conditions as in A and in addition with the human RIIα. Samples were tested on the in vitro kinase assay in duplicates and the error bars indicate the range.

3.3 Characterization of the TbPKA activation mechanism

The in vivo kinase assay had prior to this work (see section 1.9) been applied to investigate how this kinase is activated. The in vitro kinase assay of purified holoenzyme established in this thesis was used to further exploit the cAMP independent activation mechanism in parallel to the in vivo assay.

3.3.1 Isoform specificity of the cold shock activation mechanism

To determine which of catalytic subunit isoform is important for cold shock mediated TbPKA activation, a reverse genetic approach was used. Previous attempt to knock out the BSF expressed TbPKAC1 had failed, suggesting that this isoform is essential. The constitutively expressed TbPKAC3 isoform had successfully been knocked out in the procyclic Antat 1.1 strain but failed in MITat 1.2 BSF cells, using the same constructs (C. Schulte zu Sodingen, Ph.D. thesis 2000). The cold shock activation is however bloodstream form specific (S. Bachmaier, this lab), meaning that the involvement of this isoform could only be determined in this lifecycle stage.

3.3.1.1 TbPKAC3 KO in BSFs by homologous recombination

The knock of PKAC3 in the Antat 1.1 cell line had been achieved by homologous recombination by transfection of linearized pΔpkac3Neo and pΔpkac3Hygro constructs. These constructs contain the Antat 1.1 PKAC3 5' and 3' UTRs, flanking the neomycin or hygromycin resistant cassettes. Failure to knock out this isoform in the MITat 1.2 cell line suggested that the UTRs between the two strains might be different. Sequence analysis, as detailed in section 2.2.10, showed no difference between the Antat 1.1 and MITat 1.2 strains. The same constructs were hence transfected into the MITat 1.2 strain using the 1000-fold more efficient Amaxa Nucleofector II (Lonza) as opposed to the previously

used ECM 630 (BTX, Genetronic) electroporator. Both constructs were transfected in parallel to obtain the hemizygous and double knock out cell lines as detailed in section 2.2.10. Gene replacement was verified by PCR (Fig. 3.35). The successful knock out of TbPKAC3 in the MITat 1.2 cell line was accredited to the use of the more recent AMAXA electroporator, this being the only varying parameter from the previous attempt.
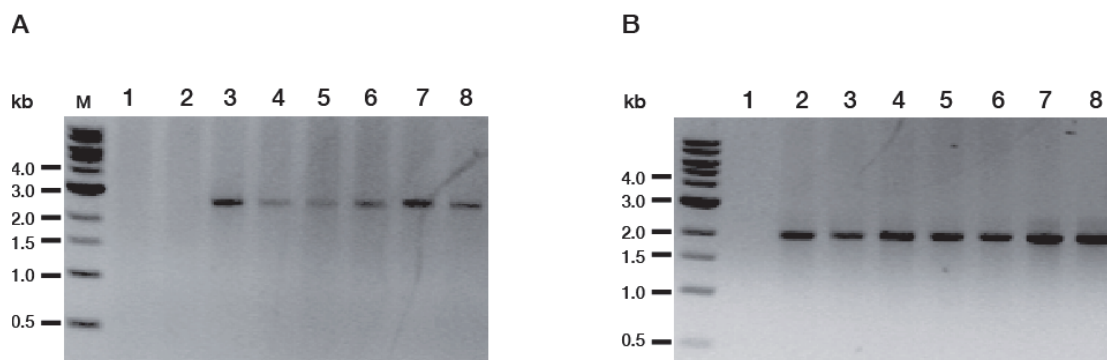
Fig. 3.35. PCR analysis of MITat 1.2 TbPKAC3 deletion: Integration of the neomycin resistant cassette in the TbPKAC3 locus by PCR (section 2.2.10) with 5' C3 upper and Neo lower primer pairs **(A)** and the hygromycin resistant cassette with 5' C3 upp and Hygro lower **(B)**, using the following genomic DNA as template: 1. MITat 1.2 wild type; 2. MITat1.2 *ΔPKAC3::HYGRO/ PKAC3*; 3, 4 & 5. Three clones of MITat1.2 *ΔPKAC3::NEO/ Δ PKAC3::HYGRO*; 6, 7 & 8. Three clones of MITat1.2 *ΔPKAC3::HYGRO/ΔPKAC3::NEO*

The protein expression levels were also checked by Western blot analysis of the cell lines, using the anti-PKAC3 antibody. The hemizygous KO cell lines showed a down regulation of protein expression of up to 40% (Fig. 3.36). There was a residual signal of about 10% in the homozygous KO cell lines, probably due to a slight cross-reaction of the anti-PKAC3 antibody with the TbPKAC1/2 subunits.
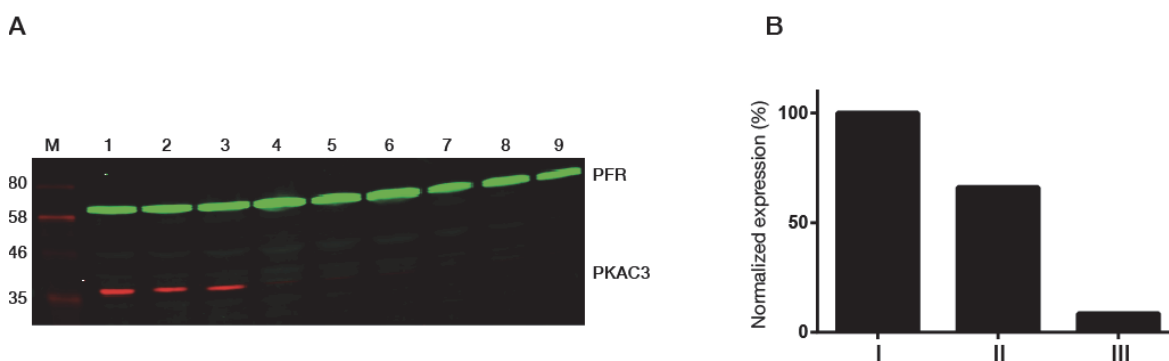
Fig. 3.36. TbPKAC3 expression test in the knock out cell lines: A. Western blot analysis of TbPKAC3 expression using the anti-PKAC3 antibody and anti-PFR as loading control: 1. MITat1.2 wild type; 2. MITat1.2 *ΔPKAC3::NEO/PKAC3*; 3. MITat1.2 *ΔPKAC3::HYGRO/PKAC3*; 4, 5 & 6. Three clones of MITat1.2 *ΔPKAC3::NEO/ΔPKAC3::HYGRO*; 7, 8 & 9. Three clones of MITat1.2 *ΔPKAC3::HYGRO/ΔPKAC3::NEO*. The Western blot samples were prepared as described in section 2.2.1.7. **B.** Percent expression of TbPKAC3 in the wild type (I) TbPKAC3 hemizygous KO (II) and TbPKAC3 homozygous KO (III) cell lines , normalized to PFR expression.

3.3.1.2 Features of the PKAC3 knock out cell line

A general microscopic analysis of the TbPKAC3 KO cell lines revealed no discernable phenotypes in morphology and motility. The population doubling time (PDT) was compared to that of the wild type cell line by maintaining the cell lines in culture with regular counting and dilution as described in section 2.2.1.1. Both hemizygous knockouts had a slightly slower growth rate, with an average PDT of 7.1 hours in comparison to 5.5 hours for the wild type. The homozygous knockout grew even slower with an average PDT of 10.5 hours.
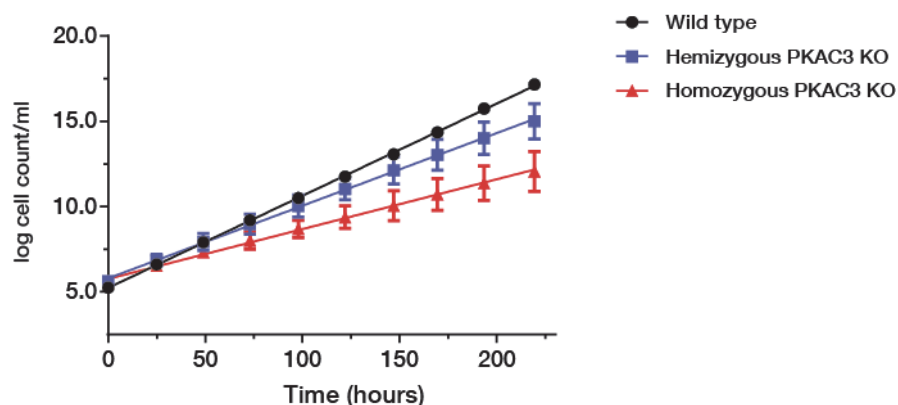
Fig. 3.37. Growth analysis of TbPKAC3 knock out cell lines: The growth of the indicated cell lines was followed by Neubauer chamber cell counting every 24hrs. The graph represents the average of two independent clones of both the hemizygous and homozygous cell lines and error bars are the range.
The average population doubling times (PDTs) are follows: MITat 1.2 wild type 5.5hrs, hemizygous KO 7.1hrs and homozygous KO 10.5hrs.

Analysis of the PKAC3 KO in the Antat 1.1 cell line had shown that other catalytic subunit isoforms are not up-regulated, suggesting lack of functional complementation (C. Schulte zu Sodingen, Ph.D. thesis 2000). The expression of TbPKAC1/2 was also tested in the KO cell line by Western blot quantification using the anti-PKAC1/2 antibody (Fig. 3.38). There was no difference in TbPKAC1/2 expression in both the hemizygous and homozygous deletion mutants, compared to the wild type cell line.
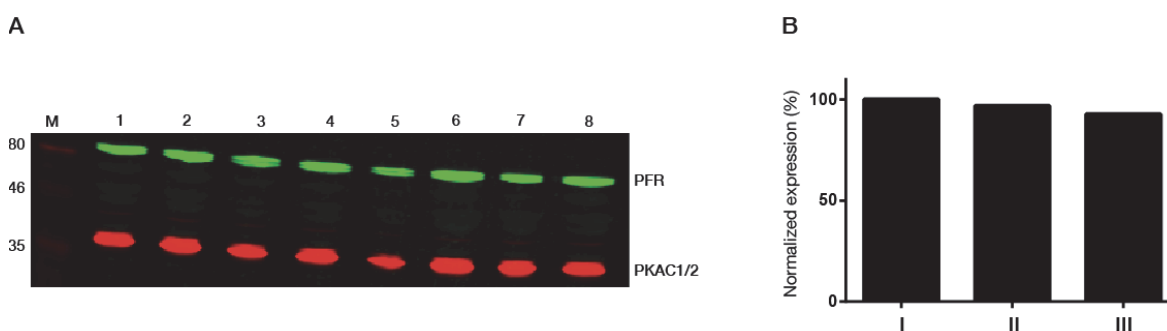
Fig. 3.38. TbPKAC1/2 expression in the TbPKAC3 KO cell lines: A. Western blot analysis of TbPKAC1 expression using anti-PKAC1/2 and anti-PFR as loading control. 1. MITat1.2 wild type; 2. MITat1.2 ΔPKAC3::NEO/PKAC3; 3, 4 & 5 Three clones of MITat1.2 *ΔPKAC3::NEO/ ΔPKAC3::HYGRO*; 6, 7 & 8 Three

clones of MITat1.2 *ΔPKAC3::HYGRO/ΔPKAC3::NEO*. The samples were prepared as described in section 2.2.1.7. **B.** Percent expression of TbPKAC1/2 in the wild type (I) PKAC3 hemizygous KO (II) and PKAC3 homozygous KO (III) cell lines normalized to PFR expression.

❖ **PKAC3 is not involved in cold shock activation (Sabine Bachmaier, this lab)**

The involvement of TbPKAC3 in cold shock activation was tested with the in vivo kinase assay after transfection of the VASP reporter into the homozygous TbPKAC3 KO cell line. It was revealed that the absence of this isoform did not affect the cold shock activation mechanism. The activation was however lost when TbPKAC1 was down regulated by RNAi. TbPKAC1 but not TbPKAC3 is important for cold shock activation, hence the focus on the former in this work.

3.3.2 The role of the Phosphate Binding cassette (PBC) in TbPKA activation

One of the main differences between TbPKAR and its mammalian counterpart lies in key residues responsible for the binding of cAMP's cyclic phosphate in the PBC (see section 3.1.1.2). Site directed mutagenesis of TbPKAR was performed on the residues occupying the same position as those responsible for cyclic phosphate interaction in the mammalian R subunit. The aim was to restore cyclic AMP binding and activation of TbPKA. This would show that this is the main non-conservation in kinetoplastid's potential to be activated by cyclic-nucleotides, as predicted by in silico analysis in section 3.1.

3.3.2.1 PCR site directed mutagenesis of TbPKAR's PBCs

The key residues identified as contributory to forming both specific and unspecific hydrogen bonds with the cyclic phosphate group (see section 3.1.1.3) were introduced into both PBCs of TbPKAR by PCR site directed mutagenesis as described in section 2.2.6.

Table 5. Mutagenesis of TbPKAR's PBCs

	PBC A	PBC B
1	E311:A	E435:A
2	T318:R	N442:R
3	V319:A	V443:A

The TbPKAR PBCmut ORF was then introduced into the pBSK.PKAR vector (J. Pepperl, Diploma thesis 2007) designed to rescue the TbPKAR KO by re-introducing the ORF into one of its loci by homologous recombination, as schematized below. Ty1 tagged and untagged rescue constructs were generated and transfected into the MITat1.2 *ΔPKAR::PURO/ΔPKAR::HYGRO* (C. Krumbholz, this lab) and MITat1.2 *ΔPKAR::PURO/ΔPKAR::HYGRO* VASP [BSD], which contains the VASP reporter for in vivo kinase assays (J. Pepperl, Diploma thesis 2007). The constructs and cell lines generated are listed below.

Δpkar::HYGRO / Δpkar::PURO

Tb PKAR rescue contructs
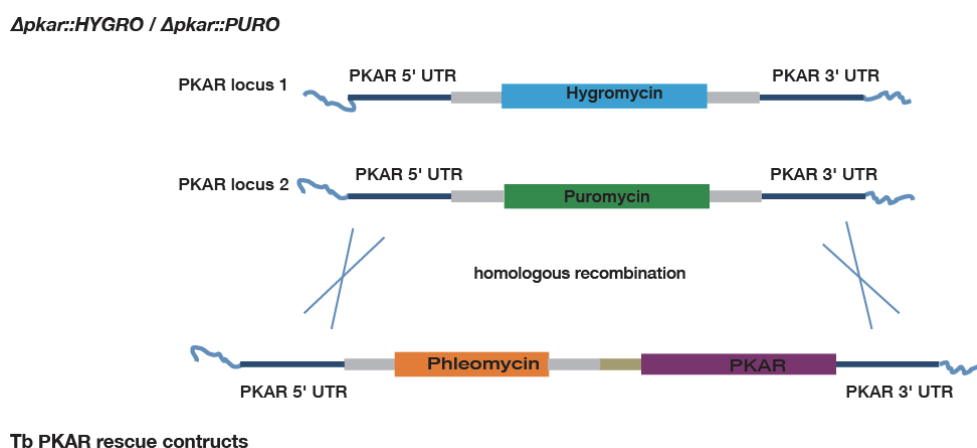
Fig. 3.39. Strategy for in situ rescue of the TbPKAR KO: single allele insertion of TbPKAR wild type and mutant ORFs by homologous recombination.

Table 6. TbPKAR KO rescue constructs and the rescue cell lines generated (The cloning strategy is detailed in section 2.2.6).

PKAR rescue constructs	PKAR rescue cell lines (common names)
pBSK.PKAR rescue (J. Pepperl, Diploma thesis 2007)	MITat 1.2 PKAR rescue
pBSK.PKAR-Ty1	MITat 1.2 PKAR-Ty1 rescue
pBSK.PKAR PBCmut	MITat 1.2 PKAR PBCmut rescue
pBSK.PKAR-Ty1 PBCmut	MITat 1.2 PKAR-Ty1 PBCmut rescue
	MITat 1.2 PKAR rescue VASP
	MITat 1.2 PKAR-Ty1 rescue VASP
	MITat 1.2 PKAR-Ty1 PBCmut rescue VASP

3.3.2.2 Analysis of PKAR PBC mutant expressing cell lines

The wild type construct rescue recovered from the growth phenotype previously observed in the KO cell line (C. Krumbholz, this lab) with a PDT of 7hrs from 9hrs in the KO cell line. However, the PBC mutant construct showed no rescue of the growth phenotype observed in KO cell line. Protein expression was confirmed for every cell line by Western blot using the anti-PKAR antibody and anti-histone3 as loading control. There was no difference in PKAR expression between the wild type and mutant rescue cell lines but only 70% of the MITat 1.2 wild type cell line (Fig. 3.40a). The expression of TbPKAC1 had been shown to be down regulated in the TbPKAR KO cell lines but concomitantly up regulated upon rescue of the knock out (J. Pepperl, Diploma thesis 2007). This was also confirmed for the TbPKAR PBC mutant and shown to be comparable to the wild type rescue, with an increase from about 30% (KO cell line) to about 70% in the rescue cell lines (Fig. 3.40b). This was an indication that the TbPKAR PBCmut could inhibit the catalytic activity by binding and forming a stable holoenzyme complex, later confirmed by co-precipitation studies. The expression of the TbPKAC3 isoform had previously been shown to be unaffected in the TbPKAR KO cell line (C. Krumbholz, this lab).

A

B
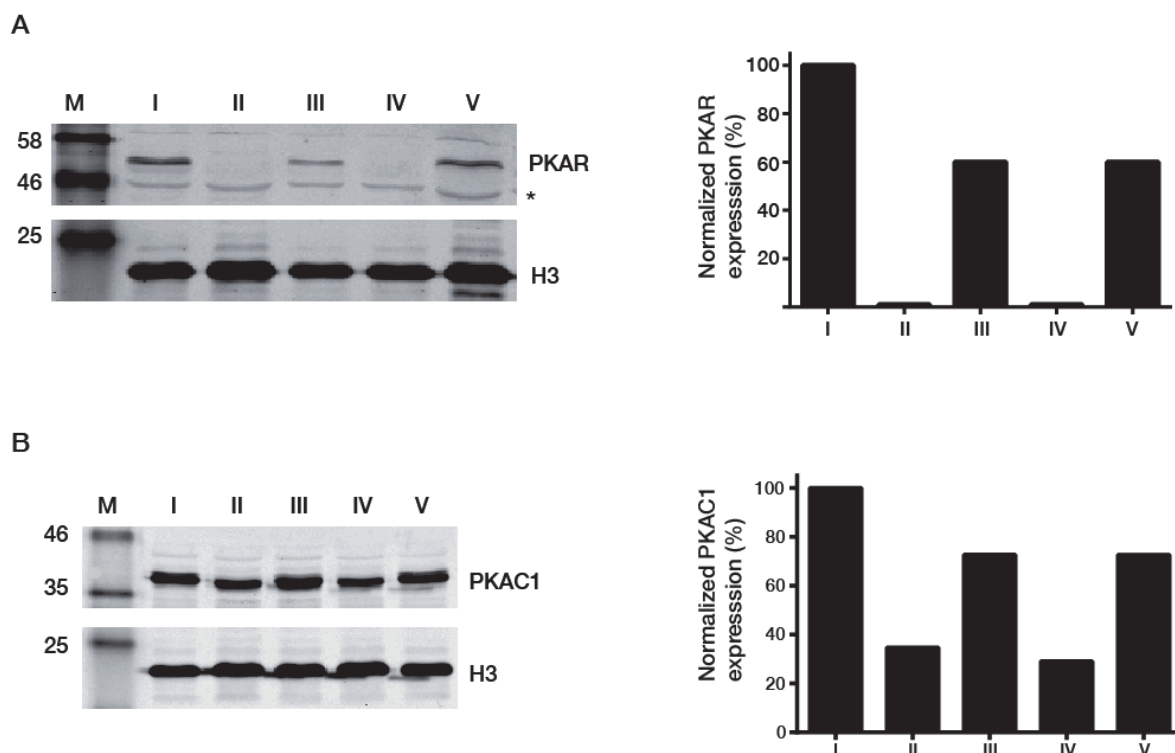
Fig. 3.40. Expression of TbPKAR PBCmut in the TbPKAR KO rescue cell line: A. Analysis of TbPKAR PBC mutant expression, as a PKAR KO single allele rescue, with the following cell lines; MITat 1.2 wild type (I), PKAR KO (II and IV), PKAR wt rescue (III) and PKAR PBCmut rescue (V). The Western blot samples were prepared as described in section 2.2.1.7 and probed with anti-PKAR, The expression was normalized with anti-histone3 and represented as a percentage of the wild type expression. The asterisk indicates an unspecific band. **B.** The expression of TbPKAC1, in the same cell lines, was analysed with anti-PKAC1/2 antibody.

3.3.2.3 cAMP/cGMP binding and activation of TbPKAR PBC mutant

❖ cAMP/cGMP affinity chromatography pull-down assay

Immobilized cAMP affinity chromatography is a widely used approach to isolate higher eukaryotic PKA. Initial attempts to pull down TbPKA from trypanosome cell lysate were not successful, hence providing (in retrospect) the first indications that this kinase could not bind to cAMP (C. Schulte zu Sodingen, Ph.D. thesis 2000; S. Kramer, Ph.D. thesis 2006). The same approach was used to test whether the mutagenesis on the PBCs was sufficient to confer cAMP binding capacity to the kinase. The capacity to bind cGMP was also tested since it has previously been shown to have some weak binding affinity for this kinase (section 1.7.2). Agarose immobilized 6-AH-cAMP and 8-AET-cGMP beads (Fig. 3.41a) were used to pull down TbPKAR and TbPKAR PBCmut from the soluble lysate of their respective rescue cell lines. As a control, soluble lysate of Hela cells was used to pull down the mammalian R subunit. The pull-downs were then analysed by Western blot using the anti-human RIα and *T. brucei* anti-PKAR antibody as indicated in Fig. 3.41b. The mammalian R subunit could be precipitated by both cAMP and cGMP beads, as

expected. More interestingly however is the fact that the cAMP beads precipitated the TbPKAR PBCmut but not TbPKAR. It could hence be shown that mutagenesis of the PBCs restored cAMP binding capacity. The cGMP beads could, contrary to expectations, neither pull down TbPKAR nor the mutant.
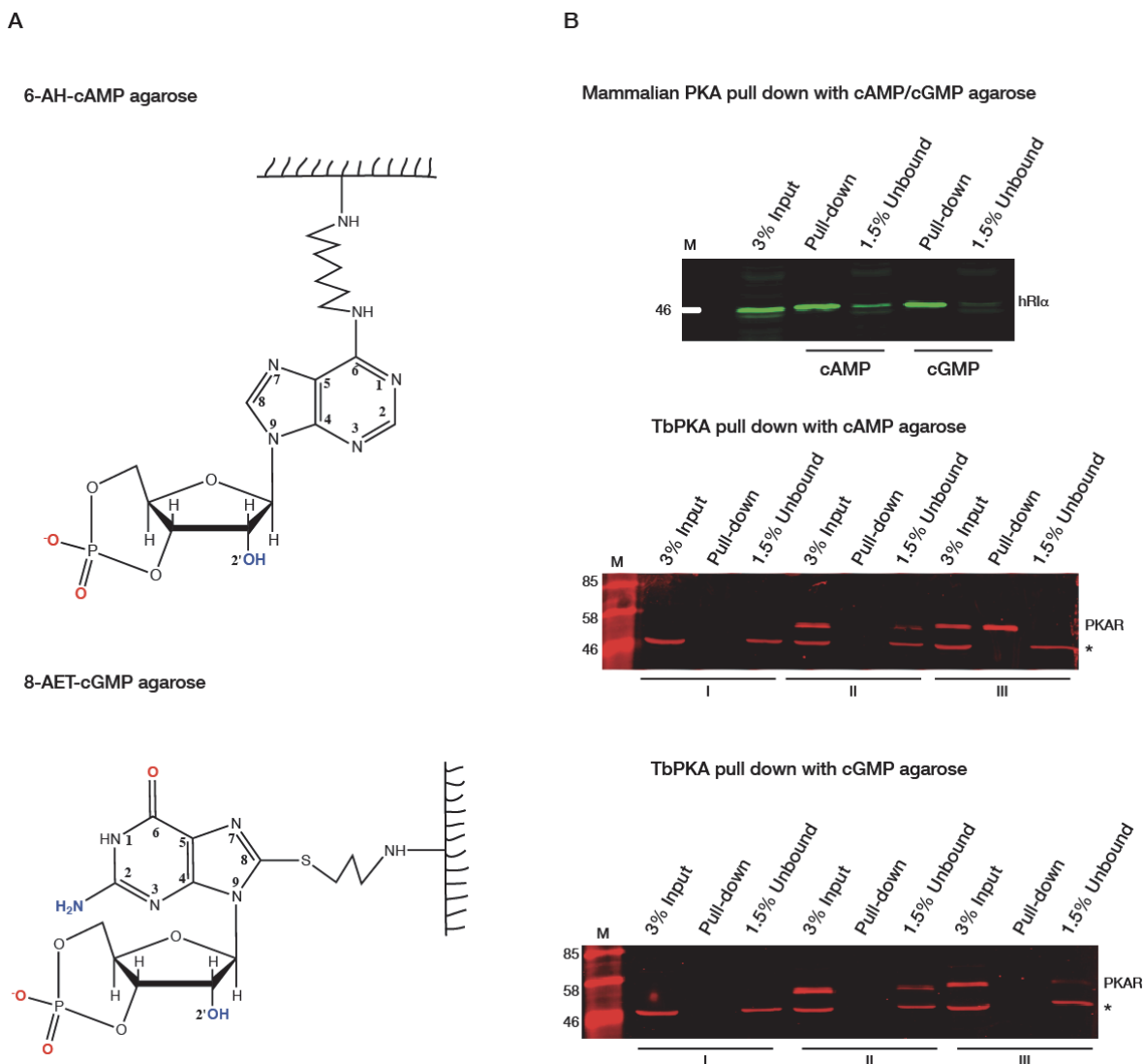
Fig. 3.41. Immobilized cAMP agarose pull down of TbPKAR PBCmut: A. Structures of agarose immobilized cAMP and cGMP; the colour coding represents the hydrogen donor (blue) and acceptor (red) capacity in hydrogen bond formation. **B.** The soluble fractions of Hela cells (half of a 50 ml confluent culture flask; obtained from Prof. Cremer, LMU), MITat 1.2 PKAR KO **(I),** PKAR wt **(II)** and PKAR PBCmut **(III)** rescue cell lines (3 x 10^7 per cell line), were incubated with 20 µl of agarose beads as described for the co-immunoprecipitation assay in section 2.2.12.1.2. The samples were analysed by western blot using the anti-RIα and anti-PKAR antibodies, as indicated. The asterisk denotes an unspecific band.

The cAMP pull-down Western blot was additionally probed with the anti-PKAC1/2 antibody in a bid to see whether the binding of cAMP to TbPKAR PBCmut was sufficient to dissociate the holoenzyme complex. This would provide an indication that TbPKA has

conserved the capacity to under go the conformational changes required to break the R/C interface upon cAMP binding, as predicted by the in silico analysis in section 3.1.

Some TbPKAC1/2 was found present in the cAMP bound fraction of the TbPKAR PBCmut pull-down, indicating that the dissociation of the holoenzyme complex was not complete. It is probable that the agarose-immobilized cAMP was impaired in its capacity to establish the interactions required to induce a full conformational change.
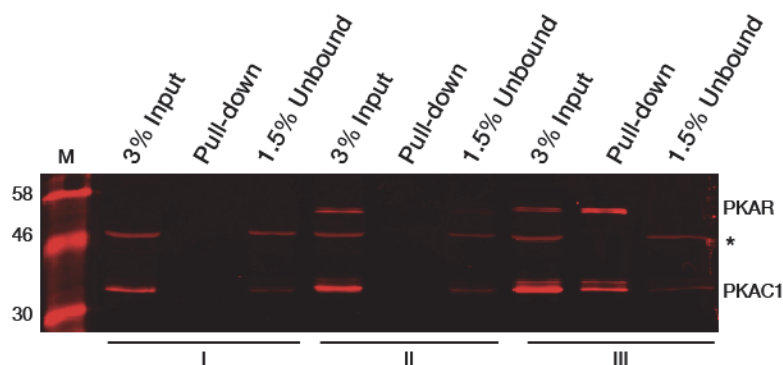
Fig. 3.42. TbPKAR PBCmut holoenzyme is not fully dissociated by agarose-immobilized cAMP: The Western blot for TbPKA cAMP pull-down in Fig. 3.41b was reprobed with anti-PKAC1/2 for cAMP induced dissociation of the holoenzyme.

❖ cAMP dissociation of co-immunoprecipitated TbPKA PBC mutant holoenzyme

The pull-down approach was changed in order to have the holoenzyme complex exposed to free cAMP. The Ty1 tagged versions of both TbPKAR and TbPKAR PBCmut rescue cell lines were used to co-immunoprecipitate the holoenzyme complexes using protein-G immobilized anti-Ty1, as described in section 2.2.12.1. The holoenzyme charged beads were then incubated with 100 µM of cAMP for 30 minutes. The beads were separated from the supernatant and both fractions analysed for the dissociation of the complex by Western blot, using anti-PKAR and anti-PKAC1/2 antibodies. The TbPKAR holoenzyme could not be dissociated by exposure to cAMP as shown by the absence of a TbPKAC1/2 signal in the supernatant fraction (Fig. 3.43a). The TbPKAR PBCmut holoenzyme was however fully dissociated upon exposure to cAMP, with the TbPKAC1/2 signal being entirely in the supernatant fraction. This provided a good indication that the TbPKA kinase has conserved the features required for cAMP-induced conformational changes.
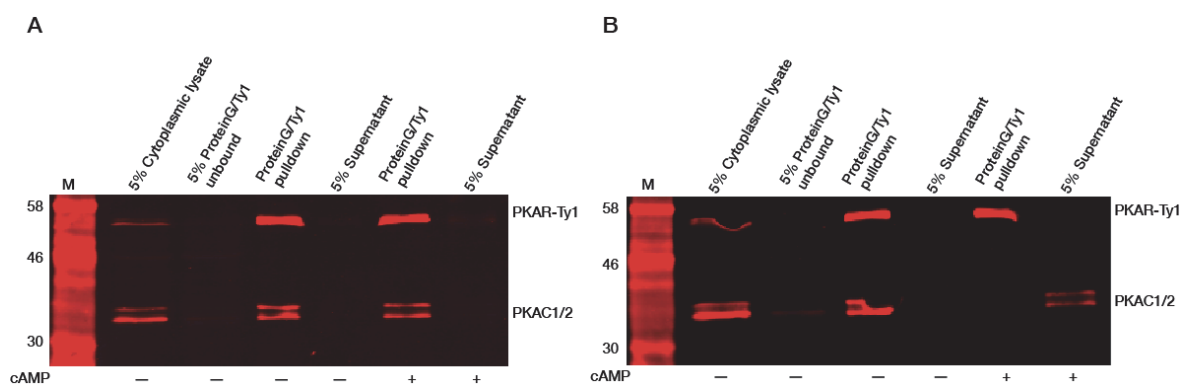
Fig. 3.43. TbPKAR PBC mutant holoenzyme is dissociated by free cAMP: Co-immunoprecipitation of the TbPKA holoenzyme from PKAR KO/PKAR-Ty1 rescue cell line **(A)** and PKAR KO/ PKAR-Ty1 PBCmut **(B)** rescue cell lines using Protein-G-Ty1 sepharose beads, as described in section 2.2.12.1.2. The matrix-bound holoenzyme was incubated in IP wash buffer containing 100 µM cAMP as indicated. The beads were separated from the buffer and both samples analysed by Western blot using anti-PKAR and anti-PKAC1/2 antibodies.

❖ **cAMP/cGMP activation of TbPKA wild type and TbPKA PBCmut**

The concept of ligand-mediated dissociation of the holoenzyme, leading to a catalytically active kinase, was further investigated using the in vitro kinase assay. Both the PKAR-10xHis/strep-PKAC1 and PKARPBCmut-10xHis/strep-PKAC1 holoenzyme complexes were purified from the LEXSY expression system as described in section 2.2.12.5 (Fig. 3.44). The PKAR-10xHis:strep-PKAC1 and PKARPBCmut-10xHis:strep-PKAC1 molar ratio were 1:1 and 1:0.75, respectively, as estimated with the ImageJ software. This suggested that the PBC mutant holoenzyme was slightly unstable during the purification process, probably owing to a lower interaction affinity.

Dose response measurements for both cAMP and cGMP were then carried out as described in section 2.2.15. Concentrations of ≥ 5 mM were shown to inhibit the catalytic activity of the kinase, hence limiting the concentration range. This was previously observed by S. Kramer (Ph.D. thesis 2006) but at the time only attributed to cAMP. Half activation constants were determined by graph fitting using the Graph pad Prism 6.0 software. It was confirmed that cAMP does not activate TbPKA but cGMP had weak activation potency (EC_{50} 0.8 mM), as earlier reported (S. Kramer, Ph.D. thesis 2006). The TbPKAR PBCmut could be activated by both cAMP and cGMP with half activation constants of 20 and 2 µM, respectively (Fig. 3.44c). This acquired capacity for cAMP activation is much lower than in the mammalian system where half activation constants, for heterodimer holoenzyme isoforms are in the lower nanomolar range. This is not surprising for TbPKA since it contains other features, such as a much longer N-terminal domain, whose functions are yet to be characterized. cGMP's activation potency was however greatly enhanced by the PBC mutagenesis by a 1000-fold from lower millimolar to lower micromolar range.
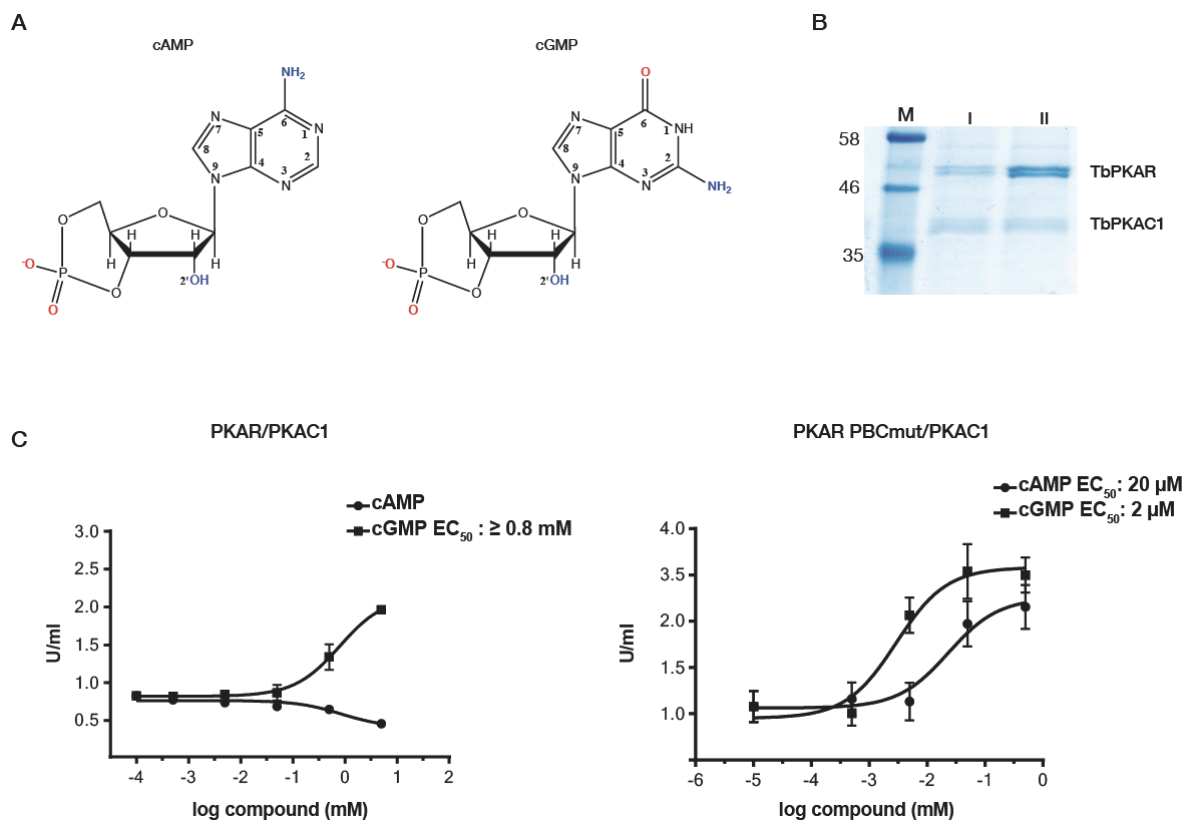
Fig. 3.44. TbPKA activation by cAMP and cGMP: A. Molecular structures of cAMP and cGMP; blue=hydrogen bond donor and red = hydrogen bond acceptor. **B.** LEXSY purified PKAR-10xHis/strep-PKAC1 with an R:C molar ratio of 1:1 (I) and PKARPBCmut-10xHis /strep-PKAC1 with an R:C ratio of 1:0.75 (II) as estimated with the ImageJ software. **C.** Dose response measurements for cAMP and cGMP activation of TbPKAC1 holoenzymes (I & II) performed by in vitro kinase assay, as described in section 2.2.15. Curve fitting was performed using Graph Pad Prism 6.0. Data points are the average of two determinations, and error bars represent the range. This data is representative of at least two independent assays.

3.3.2.4 Cold shock does not activate the TbPKA PBC mutant

The conservation of conformation changes leading to PKA activation was confirmed by cAMP dissociation of the TbPKA PBC mutant, in the previous section. Whether this mutation affects the already established in vivo cold shock activation would shed light into the importance of this domain in the physiological set up.

In vivo cold shock activation assays were performed with the PKAR KO rescue cell lines containing the VASP reporter (see section 3.3.2.1). The expression of PKAR and PKAR PBC mutant rescue was similar but only 70% of the wild type cell line, as reported in section 3.3.2.2. The in vivo kinase assay was carried out in quadruplicates, as described in section 2.2.14.1, and included the PKAR KO cell line as control.

The basal VASP phosphorylation (non-treated cells) was about 25% (Fig. 3.45). The increase in phosphorylation after cold shock treatment was a measure of the kinase activation by cold shock. The PKAR-Ty1 rescue showed a 50% increase in phosphorylation, upon cold shock treatment, while the KO cell line was non-responsive. This corresponded to the values earlier obtained for the PKARwt rescue, also compared

to the KO cell line (J. Pepperl, Diploma thesis 2007), hence no apparent influence of the Ty1 tag. There was no significant increase in phosphorylation for the PKAR PBC-Ty1 rescue cell line, indicating that the PBC might be involved in the cold shock mediated activation of TbPKA.
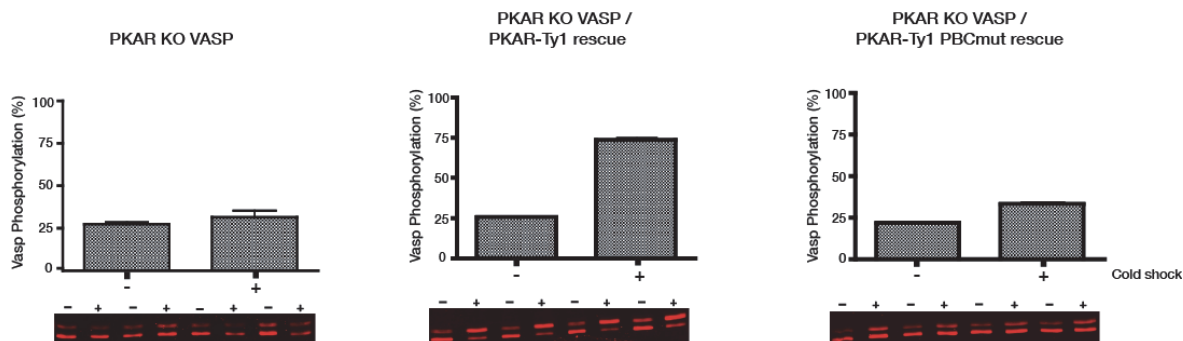
Fig. 3.45. The PKAR PBCmut does not respond to cold shock activation: In vivo reporter kinase assay as described in section 2.2.14.1. Quadruplicate samples of - or + cold shock were analysed by Western blot probing using rabbit polyclonal anti-VASP (Immunoglobe). Data analysis was performed with Graph pad Prism 6.0 and represents the percentage of phosphorylation (upper band/(upper band + lower band). The error bars are ± S.D. of the mean.

3.3.3 In vitro TbPKA activation by candidate agonists and antagonists

The in vivo kinase assay has been instrumental in identifying molecules that influence the activity of TbPKA as agonists or antagonists (S Bachmaier, this lab). The in vitro kinase activation assay was, in this work, used to determine whether these compounds acted directly or indirectly on the kinase and where possible, quantify the effect.

3.3.3.1 Agonistic effect of adenosine derivatives on TbPKA activation

Degradation products of cAMP analogues (pCPT-5'-AMP and pCPT-adenosine) have been suggested to be possible inducers of differentiation of *T. brucei* (section 1.5). Current work, in this lab, has indicated that TbPKA could be involved in the differentiation process. For example, down regulation of the TbPKAC1 isoform by RNAi has been shown to prevent differentiation from BSF to PCF (S. Bachmaier, this lab). It was hence considered likely that the aforementioned molecules would also influence the activity of TbPKA. Membrane permeable adenosine derivatives were screened with the in vivo kinase assay for TbPKA activation. A few of these compounds could indeed be shown to activate the kinase, with varying degrees of potency (S. Bachmaier, this lab).

These analogues were tested for in vitro activation of the LEXSY purified PKAR-10xHis/strep-PKAC1 holoenzyme. The majority of the analogues tested are derived at the N7 position of the purine ring. A prerequisite for this derivation is the replacement of the N7 nitrogen with a carbon, transforming adenosine to 7-deaza-adenosine also known as tubercidin (Battaglia et al., 2011). This transformation occurs naturally in some bacterial species, in the biosynthesis of nucleoside antibiotics. Tubercidin is hence an antibiotic

produced in *Streptomyces tubercidin* (Acs et al., 1964). Other nucleoside antibiotics included: toyocamycin (7-deaza-7-cyanoadenosine) from *Streptomyces toyocaemis* (Nishimura et al., 1956) and sangivamycin (7-deaza-7-carbamoyladenosine) from *Streptomyces rimolus* (Rao, 1968). Artificially derived compounds included 5-Iodotubercidin (7-Iodo-7-deazaadenosine), 5-Bromotubercidin (7-Bromo-7-deazaadenosine) and 6-Bromotubercidin (8- Bromo-7-deazaadenosine), derived at the C8 position of the purine ring. Dose response measurements of kinase activity were carried out, as described in section 2.2.15. Most of the analogues tested were shown to have an inhibitory effect on the catalytic activity, in most cases when the concentration was ≥ 10 µM. This limited the concentrations that could be used for the dose response measurements and in some cases, such as sangivamycin, the maximal activation data points could not be obtained. This is a well-documented phenomenon and most of these compounds are indeed inhibitors of a wide range of kinases (Chun et al., 1999; Massillon et al., 1994).
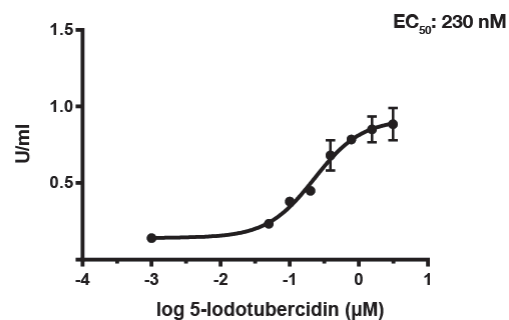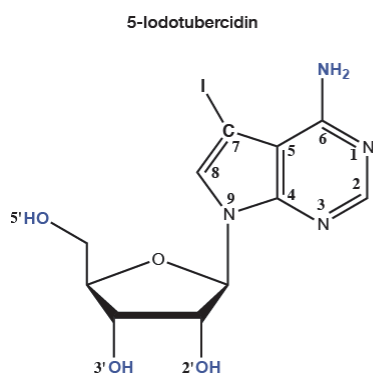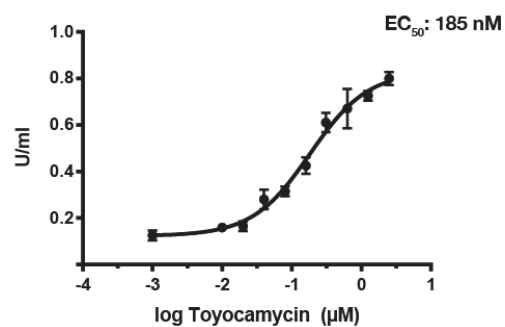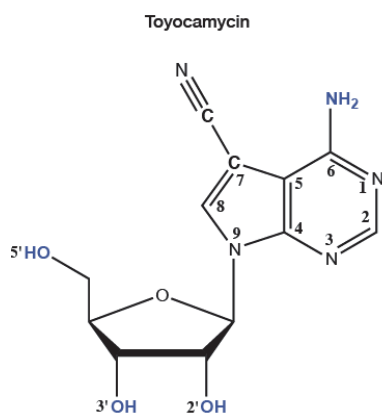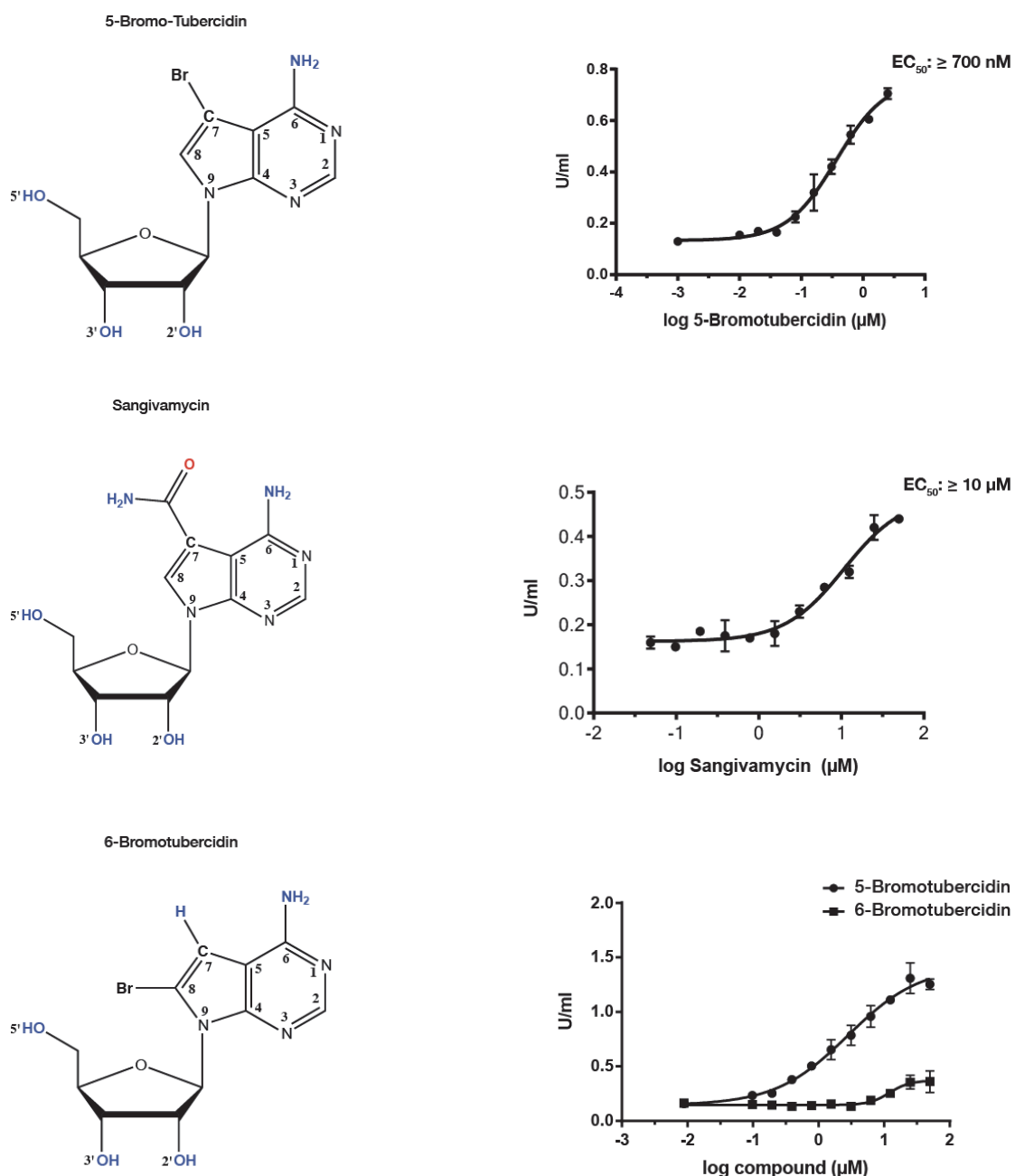
Fig. 3.45. Activation of TbPKA by adenosine derivatives: Molecular structures of adenosine derivatives (left panel) with colour decoding the capacity of the functional groups to act as hydrogen bond donors (blue) or acceptors (red). Dose response measurements of in vitro activation of recombinant TbPKA holoenzyme (right panel) as described in section 2.2.15 (solvents for each compound are also listed in this section). Curve fitting was performed with Graph Pad 6.0. Data points are the average of two determinations, and error bars represent the range. This is a representative data set of at least two independent assays. The estimated EC_{50} values are indicated; the $\geq$ sign was used when the concentration range was not sufficient to give maximal activation data points, as discussed in text.

Table 7. A comparison between the half activation constants obtained from the in vitro kinase assay and the previously carried out in vivo reporter kinase assay.

Ligand	In vitro EC_{50}	In vivo EC_{50} (S. Bachmaier, this lab)
Toyocamycin	185 nM	78 nM
5-Iodotubercidin	230 nM	392 nM
5-Bromotubercidin	≥ 700 nM	1.1 µM
Sangivamycin	≥ 10 µM	38 µM
6-Bromotubercidin	No activation	No activation

The EC_{50} values for TbPKA activation were compared to those previously obtained from the in vivo kinase assay. The in vitro assay could confirm that these compounds activate the kinase directly, possibly in a similar mechanism to the activation of classic PKA by cAMP. The half activation constant values obtained were in most cases within the range of those previously obtained from the in vivo kinase assay (see table above), with toyocamycin and 5-Iodotubercidin having the highest activation potency. The nature and position of the modification appeared to influence the activation potency. The influence of the modified position was best portrayed by a parallel analysis of 5-Bromotubercidin and 6-Bromotubercidin where despite being derived with the same molecule, only the N7 derivation could activate the kinase.

3.3.3.2 Antagonistic effect of adenosine derivatives on TbPKA activation

Contrary to the analogues studied in the previous section, a few other compounds had previously been shown to inhibit the cold shock activation mechanism. These include 8-pCPT-Adenosine and 8-pCPT-2'-O-me-Adenosine, both of which are derived by the addition of a chlorophenylthio group on the C8 position of the purine base. The 8-pCPT-2'O-me-Adenosine is additionally derived at the 2'-OH position of the ribose by its replacement with a methyl group (Fig. 3.46). Binding and competitive inhibition studies were carried out in a bid to establish whether these compounds act directly on the kinase.

The first approach was by affinity pull down using agarose immobilized 8-pCPT-adenosine in a similar approach to the cAMP pull-down (section 3.3.2.3). 2'-AHC-8-pCPT-adenosine beads (custom synthesis, Biolog Bremen) were used to pull down PKAR-Ty1 and PKAR PBCmut-Ty1 from the soluble fractions of the respective cell lines (Fig. 3.46a). Neither the PKAR-Ty1 nor PKAR-Ty1PBCmut subunits could be pulled down, suggesting that this analogue does not interact directly with TbPKA. The second approach was by the in vitro kinase assay where 8-pCPT-2'-O-me-Adenosine was tested for its capacity to inhibit toyocamycin's activation, in a competitive assay. The kinase reaction was set up with several concentrations of 8-pCPT-2'-O-me-Adenosine in the presence of toyocamycin at its EC_{50} concentration (~200 nM). There was no detectable effect of this compound on toyocamycin-mediated activation of the kinase, as shown in Fig. 3.46b. The influence of this analogue on in vivo, cold shock mediated TbPKA activation is therefore unlikely to be by direct interaction with the kinase.

A

B
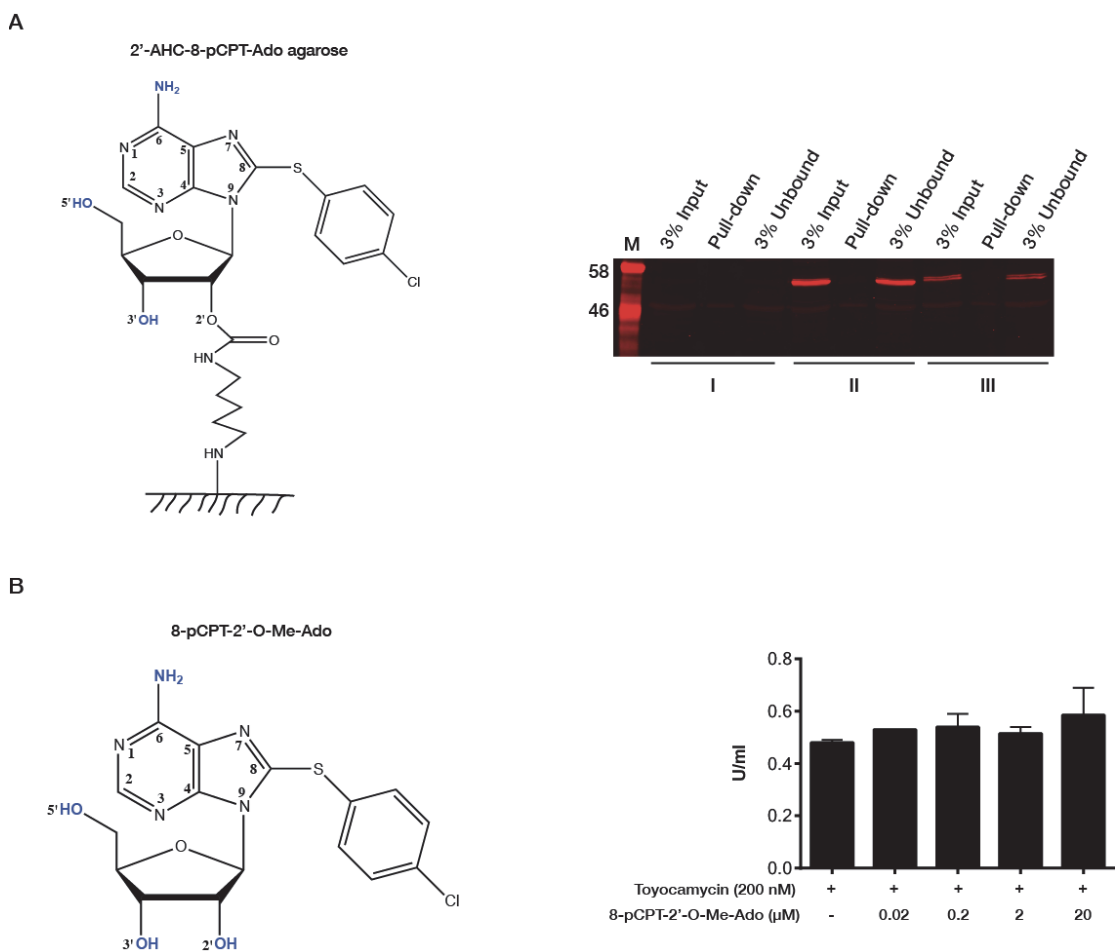
Fig. 3.46. The antagonistic effect of 8-pCPT-adenosine is not by direct interaction with TbPKA: A. Western blot analysis of agarose immobilized 8-pCPT-adenosine pull-downs from soluble lysates of MITat 1.2 PKAR KO (I), PKAR KO/PKAR-Ty1 (II) and PKAR KO/PKAR-Ty1 PBCmut rescue (III) rescue cell lines, as described in section 3.3.2.3 **B**. The antagonist effect of 8-pCPT-2'-O-Me-Adenosine on TbPKA activation: 200 nM toyocamycin was added to the kinase reaction mix containing the indicated concentrations of 8-pCPT-2'-O-Me-Adenosine and analysed by in vitro kinase assay as described in section 2.2.15. Data points are the average of two determinations, and error bars represent the range.

3.3.3.3 Effect of Dipyridamole activation of TbPKA PBC mutant

Dipyridamole is a PDE inhibitor that has been shown to activate TbPKA, in vivo. This effect has however been shown to be unrelated to the intracellular increase of cAMP, induced by this molecule (see section 1.9.2). The in vitro kinase assay was used to test whether this compound acted directly on TbPKA in a similar approach as for the adenosine analogues (section 3.3.3.1). A wide range of dipyridamole concentrations was tested and it was established that this compound does not activate the kinase by direct interaction (Fig. 3.47b).

A

B
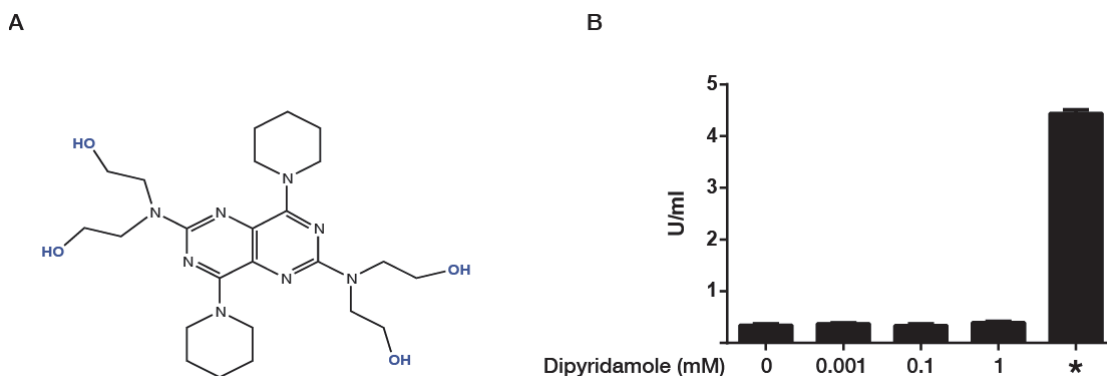
Fig. 3.47. Effect of Dipyridamole on in vitro TbPKA activation: A. Molecular structure of Dipyridamole **B.** several concentrations of dipyridamole (as indicated), were tested for in vitro activation of recombinant TbPKA holoenzyme (section 2.2.15) with 5 µM toyocamycin (*) as control. The data points are the average of two determinations, and error bars represent the range.

Testing the PKAR PBCmut for in vivo cold shock activation revealed the importance of the PBC in the kinase activation mechanism (3.3.2.4). The same approach (described in section 2.2.14.2) was used to test whether this domain is involved in dipyridamole-mediated activation of TbPKA. A similar activation profile to that of the cold shock activation was observed. More precisely, both the PKAR KO and PKAR PBCmut were non-responsive to dipyridamole, while phosphorylation increased significantly in the PKAR-Ty1 rescue. This suggests that despite the fact that dipyridamole does not act directly on the kinase; the PBC plays an important role in the perception of its effect.
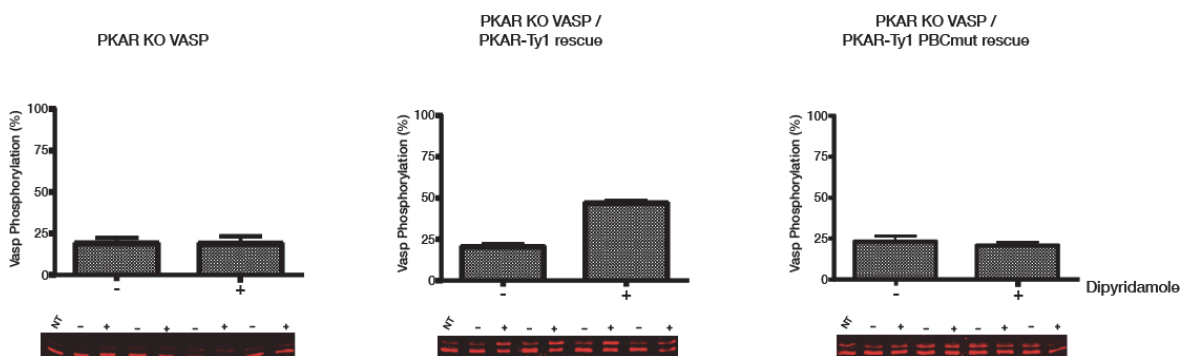
Fig. 3.48. The TbPKAR PBCmut does not respond to dipyridamole activation: In vivo TbPKA activation was carried out as described in section 2.2.14.2, using the indicated cell lines. Data analysis was performed with Graph pad Prism 6.0 and represents the percentage of phosphorylation (upper band/(upper band + lower band). The error bars are ± S.D. of the mean.

3.3.3.4 Effect of citrate/cis-aconitate on TbPKA activation

Cold shock sensitizes the parasite to CCA mediated differentiation as discussed in section 1.4. However, only a few elements of the CCA signaling pathway have so far been identified. There is increasing evidence that TbPKA is involved in the differentiation

process, making it plausible that this kinase is linked to the CCA signaling pathway. There is so far no in vivo evidence that citrate or cis-aconitate have any influence on TbPKA's activity. This compound was nonetheless tested with the in vitro kinase assay for any potency on TbPKA activation. Similarly to dipyridamole, a wide range of concentrations was shown to have no effect on TbPKA.
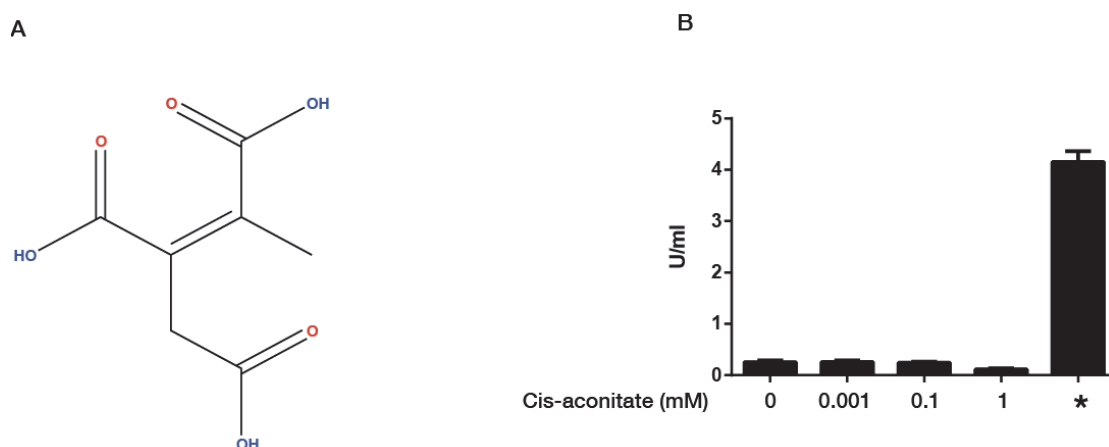
Fig. 3.49. Effect of cis-aconitate on in vitro TbPKA activation: A. Molecular structure of cis-aconitate **B.** several concentrations of cis-aconitate (as indicated), were tested for in vitro activation of recombinant TbPKAC1 holoenzyme (section 2.2.15) with 5 μM toyocamycin (*****) as control. The data points are the average of two determinations, and error bars represent the range.

3.4 TbPKA nucleoside activation and structural requirements

Work in this thesis has confirmed that cAMP does not activate TbPKA while cGMP has very low activation potency. It has also been shown that adenosine analogues can activate this kinase with varying degrees of potency, some of which are closer to half activation constants observed for cAMP activation of the mammalian PKA. In silico analysis highlighted the PBC as key to the loss of cAMP activation and this was confirmed by mutagenesis. The better activation capacity observed for adenosine analogues could be in part due to the absence of the phosphate group but also due to a specific gain of function for nucleoside binding in *T. brucei*. The molecular nature of nucleoside activation was hence further investigated.

3.4.1 Nucleotide's phosphate group hinders nucleoside interaction in TbPKA's PBC

The hypothesis that TbPKA PBC is not conserved for interaction with the phosphate group of cAMP was further investigated by analysing the activation potency of 5'-AMP in comparison to adenosine. 5'-AMP presents additional functional groups, in comparison to cAMP, both on the phosphate group and ribose sugar (Fig. 3.50a). The phosphate group is also more labile and therefore more likely to adapt a hydrogen bond forming conformation. Adenosine, also presenting more hydroxyl groups, had not previously

been tested with the in vivo kinase assay due to its poor membrane permeability. Dose response measurements were carried out for both 5'-AMP and adenosine in parallel, using the method described in section 2.2.15. 5'-AMP did not activate the kinase contrary to adenosine whose half activation constant was estimated at 0.9 µM. It was hence apparent that the presence of the phosphate group whether in 3',5'-cyclic or 5'-AMP nucleotides, hindered the interaction of adenosine with TbPKA.
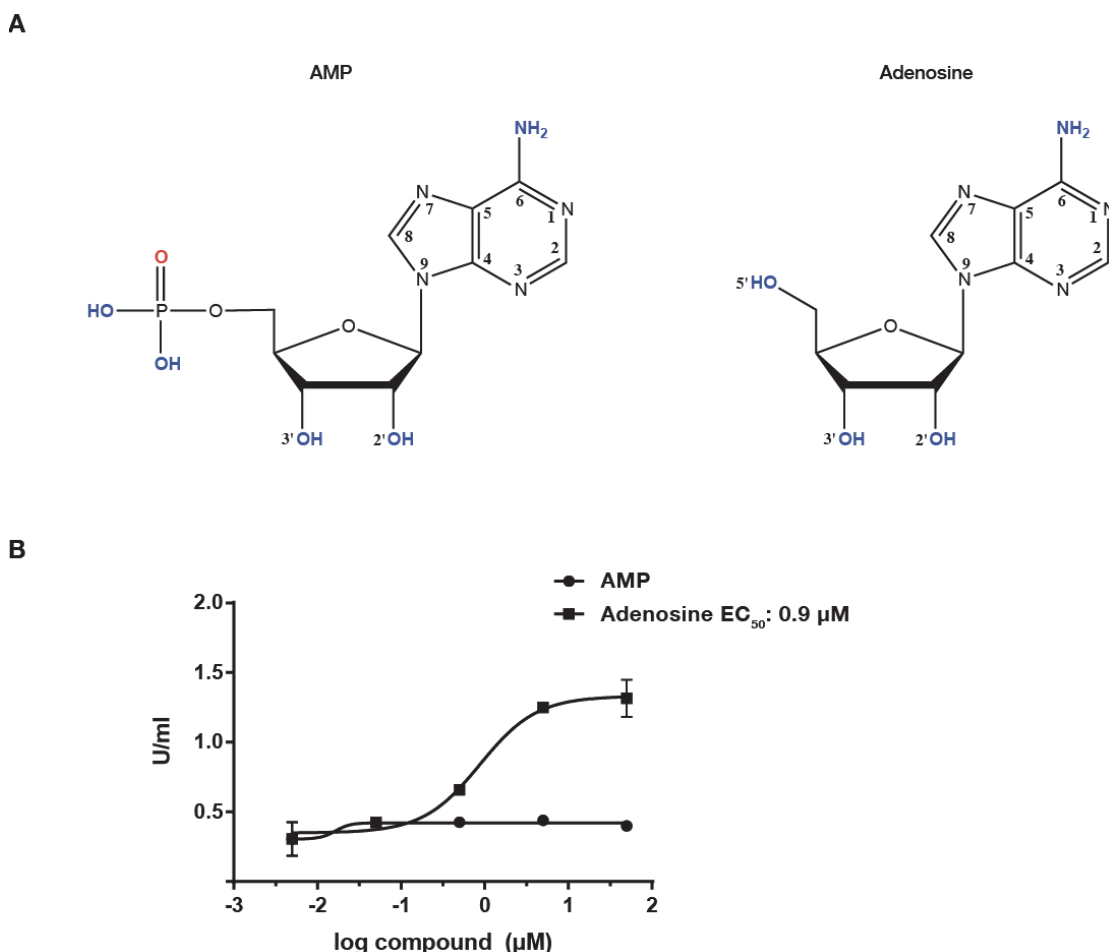
Fig. 3.50. AMP and adenosine activation of TbPKA: A. Molecular structures of AMP and adenosine with hydrogen bond donor functional groups in blue and acceptors in red **B.** Dose response measurements for the in vitro activation of recombinant TbPKAC1 holoenzyme (section 2.2.15). Data points are the average of two determinations, and error bars represent the range.

The hypothesis that the phosphate group hinders the interaction of monophosphate-nucleotides with TbPKA PBC was further investigated by structural homology modeling. The mammalian RIα was previously used to model TbPKA, highlighting the general conservation of the CNB domains and the R/C interaction interface (section 3.1.6). The same model was used to have a more detailed look at the PBC pocket in relation to its interactions with cAMP. The PBC of the mammalian R subunit and the modeled TbPKAR's were hence compared. The cAMP bound crystal structure of the mammalian RIα PDB: 1RGS is shown on the left (Fig. 3.51). A zoom in to both PBCs, adjacent to it,

highlights the key hydrogen bonds of the PBC with cAMP, as discussed in section 3.1.1.2. The spatial conservation of these interactions was analysed in the TbPKAR PBC structure model. The ribose-sugar 2'-OH group specific interaction with a Glu appeared to be conserved in TbPKA as predicted by linear sequence comparison. The phosphate interaction with Arg is not conserved since a Thr (PBC:A) and an Asn (PBC:B) occupy the same position. These residues are theoretically capable of forming specific hydrogen bonds with the phosphate but none could be predicted to do so, using the Chimera software. More interestingly however, Glu311 in PBC:A and Glu:435 in PBC:B of TbPKA, appeared to clash with the phosphate group as demonstrated by cAMP's electron density. This Glu is highly conserved in kinetoplastids, as shown in section 3.1.1.2. In the mammalian PBC, the same position is occupied by an Ala, which forms an unspecific hydrogen bond with the phosphate. Its side chain is however shorter in comparison to the Glu. The conservation of this residue in all kinetoplastids, suggests that this could be the key mechanism for monophosphate-nucleotide exclusion from the PBC pockets. It would hence appear that the PBC mutagenesis (section 3.3.2.1) key replacement was the Glu to Ala, opening the PBC pocket to phosphate interaction.
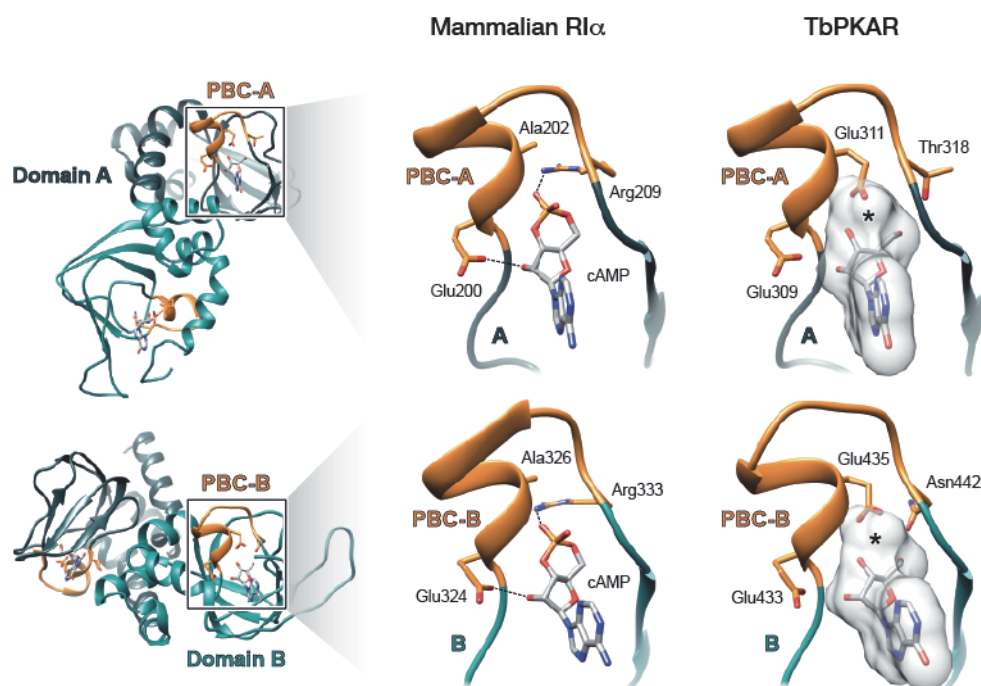
Fig. 3.51. A kinetoplastid conserved Glu would clash with the phosphate group of cAMP in the TbPKA PBC: A close up of the mammalian RIα cAMP-bound PBC (left), showing the specific hydrogen bonds (Glu-ribose and Arg-phosphate). The structure model of TbPKAR PBCs (see section 2.2.16.2 and 3.1.4), highlighting residues at similar position to the mammalian RIα. Only the Glu-ribose sugar interaction is conserved. Glu311 (PBC:A) and Glu435 (PBC:B) clash with the phosphate group as shown by the electron density of the latter.

3.4.2 Nucleoside activation is specific to kinetoplastids' PKA

The fact that kinetoplastids appear to have adopted a mechanism to seclude monophosphate-nucleotides from the PBC pocket in favor of nucleosides, suggests that they may have also developed a mechanism to enhance the nucleoside interaction. This is supported by the fact that adenosine and some of its analogues were earlier shown to activate the kinase with potencies close to that of cAMP for mammalian PKA.

3.4.2.1 The mammalian PKA is not activated by adenosine

The phosphate group in cAMP is highly indispensable in the activation of PKA. It would therefore be expected that adenosine is not potent enough to activate this kinase. Furthermore, there is no evidence in the literature that any nucleoside can activate PKA. It was however important to use the same kinase assay set up to confirm this notion while also strengthening the hypothesis that TbPKA has acquired specific nucleoside interaction features. The mammalian Cα (NEB) was assayed in the presence or absence of a 10x molar excess of the mammalian RIα (F. Herberg's lab, Kassel), as described in section 3.2.6.4. The holoenzyme was incubated in the presence of either 10 µM adenosine or 10 µM cAMP as shown in Fig. 3.52. The activity of the mammalian Cα was completely inhibited by the R subunit in a cAMP reversible way as previously shown. On the other hand, no activity was measured in the presence of adenosine, suggesting that this ligand could not sufficiently interact with the R subunit to release the catalytic activity.
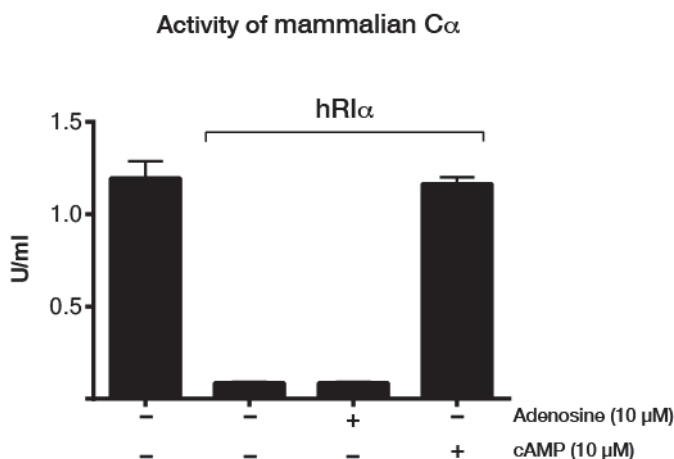
Fig 3.52. Adenosine does not activate mammalian PKA: The mammalian RIα/Cα holoenzyme was reconstituted, in vitro, by incubating 0.2 pmoles of Cα with 2 pmoles of RIα. The in vitro kinase assay (see section 2.2.15) was then run in the presence of 10 µM adenosine or 10 µM cAMP, as indicated. The data points are the average of two determinations, and error bars the range.

3.4.2.2 Leishmania PKA is activated by nucleosides

The non-responsiveness of the mammalian PKA to nucleoside activation can be generalized as a PKA feature, given the high interspecies conservation of the PBCs (see section 3.1.1). It was also deduced, by in silico analysis, that the other members of the kinetoplastid family would share the TbPKA particularities in activation. In order to validate this hypothesis, an investigative approach similar to the one adopted for TbPKA would be required for key members of the kinetoplastid family such as *Leishmania donovani* and *Trypanosoma cruzi*. This, however, lies beyond the scope of this work.

Some evidence was nonetheless obtained during the purification of TbPKA in *Leishmania tarentolae* (see section 3.2.5). The recombinant TbPKA subunits were suspected to cross-interact with those of the expression system. This would mean that an individually expressed and purified TbPKAC subunit would only attain full catalytic activity upon the release of the inhibiting *L. tarentolae* PKAR. This was tested by in vitro kinase assay in a similar approach to the one used to test for cross-interaction of TbPKA with eukaryotic PKA in Sf9 expression cells (section 3.2.6.2). *T. brucei* strep-PKAC1 was purified from *L. tarentolae*, as described in section 2.2.12.4, and tested on the in vitro kinase assay in plus or minus 10 µM adenosine. It could be shown that the catalytic activity increased by about five fold in the presence of adenosine (Fig. 3.53a)

The purification was then repeated but with a few changes after the streptactin matrix binding: the matrix bound protein was split into; one half was washed and eluted normally; the other was washed in buffer containing 100 µM adenosine, followed by normal wash buffer (to remove adenosine) and then eluted. In vitro kinase assay with the first half (normal purification) could confirm the initial finding (data not shown). The half washed with adenosine, prior to elution, had the same catalytic activity in plus or minus adenosine (Fig. 3.53b). Both eluates were analysed by Western blot, relying on the cross-reactivity of anti-TbPKAR antibody with the *L. tarentolae* PKAR (see section 3.2.5.2). It was shown that strep-PKAC1 (purified normally) had an additional signal that would correspond to *L. tarentolae's* PKAR, which was absent in the step-PKAC1 purified in the presence of adenosine (Fig. 3.53c). The second approach was adopted for further purifications and characterization of both the strep-PKAC1 and PKAR-10xHis (see section 3.2.6.3 and 3.2.6.4).

This indicates that *L. tarentolae's* PKA is also activated by nucleosides, a feature very likely shared by the other Leishmania species and all kinatoplastids, in general.
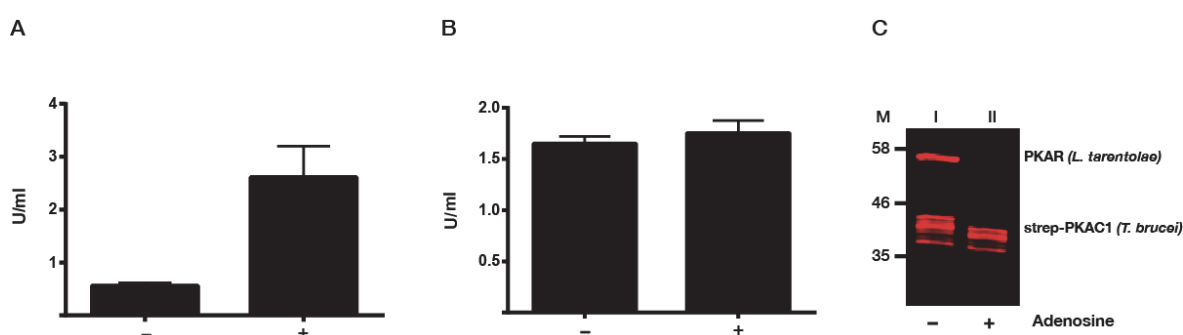
Fig. 53. *L. tarentolae* **PKAR/TbPKAC1 chimeric holoenzyme is activated by adenosine: A.** The in vitro catalytic activity of strep-PKAC1 expressed and purified from the *L. tarentolae* expression system (LEXSY) in the presence or absence of 10 µM adenosine. **B.** A similar assay performed after inclusion of 100 µM adenosine in 2/3 washes, during the purification. **C.** Western blot analysis of A and B probed with anti-TbPKAR, which cross-reacts with the *L. tarentolae* PKAR (see section 3.2.5.2) and anti-PKAC1 antibody.

3.4.3 Contribution of the hydroxyl groups of adenosine's ribose-sugar moiety in TbPKA nucleoside activation

The absence of the phosphate group frees the 5' and 3' hydroxyl groups of adenosine. These groups were deemed likely to contribute to adenosine interaction in a trypanosome specific manner. This was tested by in vitro kinase assay using deoxylated versions of adenosine: 2'-deoxyadenosine, 3'-deoxyadenosine and 2'-3'-dideoxyadenosine. It could be confirmed that the 2'-OH group interaction in the PBC pockets was conserved in *T. brucei* as its absence completely abolished adenosine activation (Fig. 3.54). The 3'-OH was also shown to be probably involved in a similar interaction as its absence also resulted to complete loss of activation. The importance of both –OH groups was further confirmed by the 2',3'-deoxyadenosine. The role of the 5'-OH group has so far not been tested.

Asymmetric substitutions on the ribose-sugar have been shown to influence nucleoside conformation (Gelbin et al., 1996), this could in turn affect the interaction capacity of the compound in the PBC pocket. The 2'-O-methyl-adenosine and 3'-O-methyl-adenosine are likely to have a similar conformation as adenosine. Absence of any activation from both compounds confirmed that the ribose-sugar hydroxyl groups are likely involved in hydrogen bond formation.

A
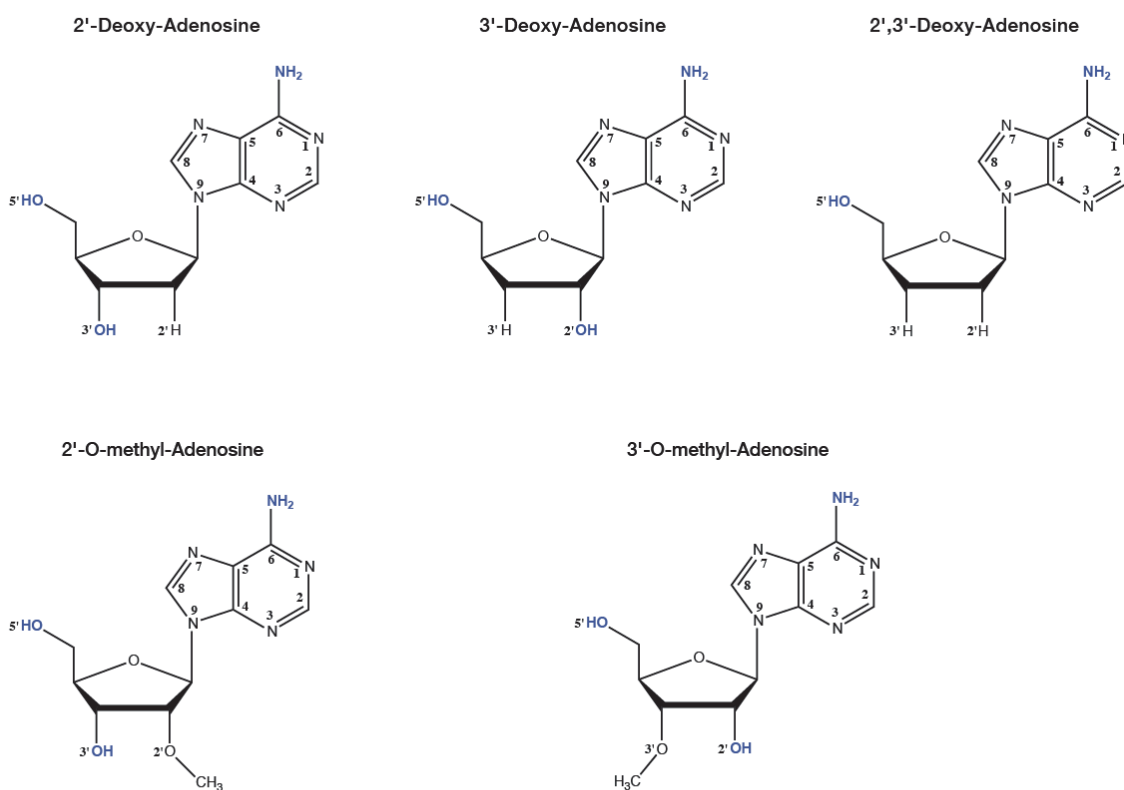
B
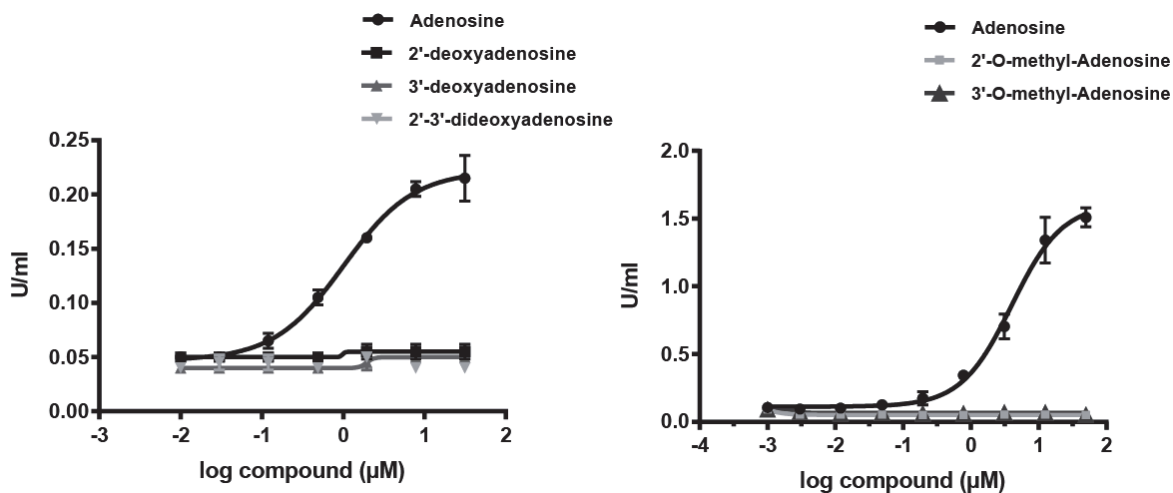
Fig. 3.54. 2' and 3' hydroxyl groups of the ribose sugar, play a role in adenosine activation of TbPKA. A. Molecular structures of 2' and/or 3' deoxylated and O-methyl adenosines, with hydrogen bond donor functional groups in blue. **B.** Dose response measurements for TbPKA activation by deoxylated adenosines (left) and O-methyl-adenosines (right), compared to adenosine (see section 2.2.15). Data points are the average of two determinations, and error bars represent the range.

Structural modeling of the PBC, as described in the previous section, was used to further analyse the contribution of the ribose-sugar moiety in nucleoside interaction. In the

structure model described in section 3.4.1, the phosphate group of cAMP was deleted to obtain adenosine, occupying the same spatial co-ordinates in the PBC. The chimera program was then used to search for any hydrogen bond formation distances between the PBC and the ribose-sugar moiety. The three hydroxyl groups were shown to be within ideal hydrogen bond formation distances as defined by the software. The 2'-OH interaction with Glu309 in PBC:A and Glu433 in PBC:B was confirmed (Fig. 3. 55). The 3'-OH was shown likely to interact with Glu311 in PBC:A and Glu435 in PBC:B, establishing two specific hydrogen bonds. This Glu was reported in the previous section as likely to play a crucial role in preventing phosphate interaction in the PBC, again suggesting its probable pivotal role in kinetoplastid's PKA activation. Although the 5'-OH group has so far not been biochemically characterized, it could be shown that this group is also favored for interaction with Thr318 in PBC:A and Asn442 in PBC:B. These two residues are in the same position as the mammalian PKA's highly conserved Arg, as discussed in the previous section. It should however be noted that adenosine interaction was analysed in the same docking co-ordinates as those of cAMP. The actual docking of nucleoside in TbPKA PBC pockets can only be revealed by structural studies.
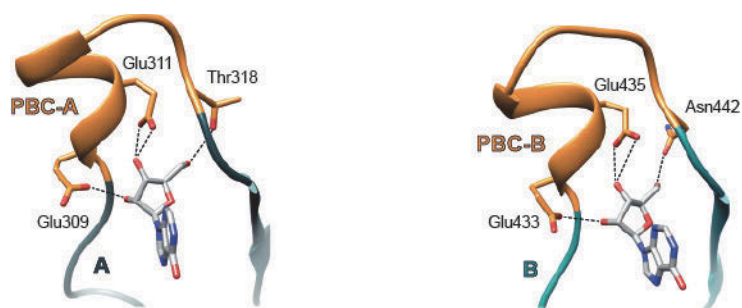
Fig. 3.55. Probable additional interactions of TbPKA PBCs with the ribose-sugar moiety: Structure model of TbPKAR PBCs (see Fig. 3.51): the phosphate group was deleted in UCSF Chimera software. The software was then used to search for ligand-protein hydrogen bond formation probabilities, confirming the conservation of Glu309 (PBC:A) and Glu433 (PBC:B) 2'-OH interaction and additionally revealing two addition interaction possibilities; Glu311 (PBC:A) and Glu435 (PBC:B) could form a double hydrogen bond with the 3'-OH while Thr318 (PBC:A) and Asn442 (PBC:B) could form a hydrogen bond with the 5'-OH group.

3.4.4 Contribution of the purine base moiety in TbPKA nucleoside activation

Adenosine analogues, derived on the purine ring, have shown that the potency for nucleoside activation can be increased or decreased depending on the position and nature of the modification. The purine base was hence further analysed in relation to its interaction with TbPKA's PBC, for additional and likely kinetoplastid-specific interaction features.

3.4.4.1 Influence of the 7-deaza modification on adenosine activation of TbPKA

The change from nitrogen to a carbon in the naturally occurring conversion of adenosine to tubercidin, as discussed in section 3.3.3.1, could influence the potency of the ligand as it transforms this position from a hydrogen bond acceptor to a donor. A significant change in TbPKA activation between adenosine and tubercidin would also signify that this position is crucial for adenosine interaction with TbPKA. The two ligands were assayed for TbPKA holoenzyme activation as previously described.

The EC_{50} values obtained indicate that tubercidin is slightly less potent than adenosine (Fig. 3.56b), suggesting that the nitrogen is more favored for interaction with the PBC. Structural modeling could however not predict any specific interactions involving this position.
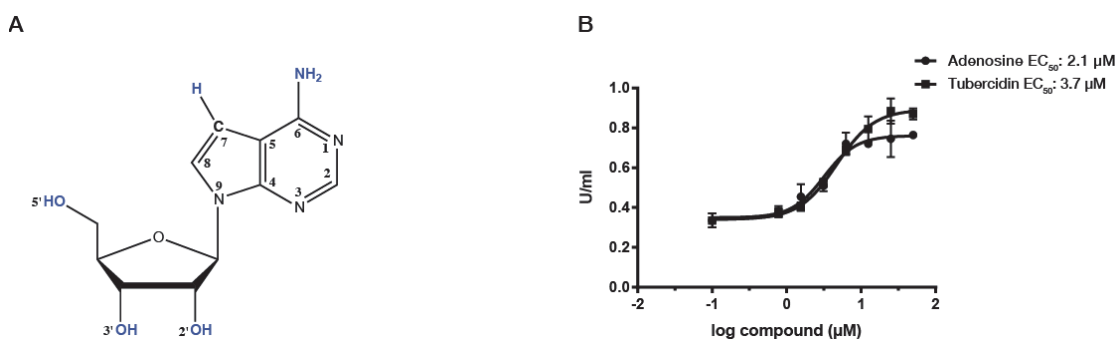
Fig 3.56. Influence of the 7-deaza modification (adenosine to tubercidin) on TbPKA activation: A. Structure of tubercidin, highlighting its hydrogen donor positions in blue **B.** Dose response measurements for TbPKA activation of tubercidin in comparison to adenosine (see method section 2.2.15). Data points are the average of two determinations, and error bars represent the range.

The contribution of the purine base modifications was compared to that of the ribose-sugar moiety by testing 5-Iodo-2'-deoxy-tubercidin. This molecule has the potency enhancing N7 iodine modification (see section 3.3.3.1) but is deprived of the 2'-OH group, on the ribose sugar, also shown to contribute to nucleoside interaction (see section 3.4.3). It could be shown that despite the presence of a potency enhancing N7 modification, the absence of the 2'-OH group could not be compensated (Fig. 3.57). This further emphasized the importance of the ribose-sugar contribution in TbPKA nucleoside binding.
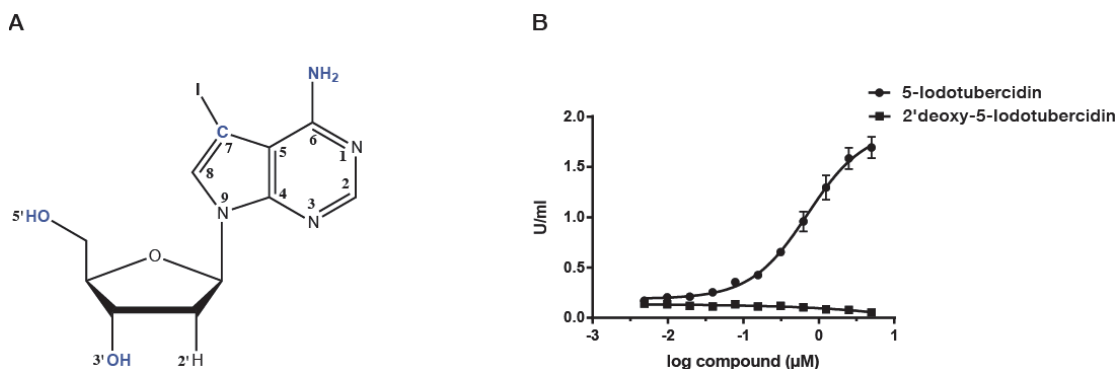
Fig 3.57. A comparison between 5-Iodotubercidin and 5-iodo-2'-deoxytubercidin activation of TbPKA: A. Molecular structure of 5-iodo-2'-deoxytubercidin, see section Fig 3.45 for 5-Iodotubercidin structure **B.** Dose response measurements for TbPKA activation by 5-iodo-2'-deoxytubercidin in comparison to 5-Iodotubercidin (see method section 2.2.15). Data points are the average of two determinations, and error bars represent the range.

3.4.4.2 Effect of other purine nucleosides on TbPKA activation

Earlier analysis of cAMP vs. cGMP's in vitro activation of TbPKA showed that cGMP harbored some capacity to activate this kinase, contrary to cAMP (see section 3.3.2.1). The only difference between the two cyclic nucleotides lies in the purine ring, where a keto group, in guanine, replaces the N6 amine group of adenine. Additionally, guanine possesses an amine group at the N2 position (Fig 3.58a). Having studied the effect of adenosine, it could be predicted that guanosine was likely to activate TbPKA and possibly with a better potency given the aforementioned differences. The influence of guanosine's N2 amine group would then be revealed by inosine, which is essentially guanosine without the N2 amine group. Both guanosine and inosine were hence assayed for TbPKA activation as previously described. Guanosine was shown to be a better activator than adenosine, as predicted, with an EC_{50} of ~250 nM. This nucleotide was in the same range as the most potent adenosine analogues (see section 3.3.3.1). However inosine was surprisingly a much better activator, with an EC_{50} of ~35 nM (Fig. 3.58b). The keto group on guanosine and inosine appears to enhance activation, in comparison to the amine group of adenosine. On the other hand, guanosine's N2 amine group would appear to lower the binding affinity of the nucleoside.
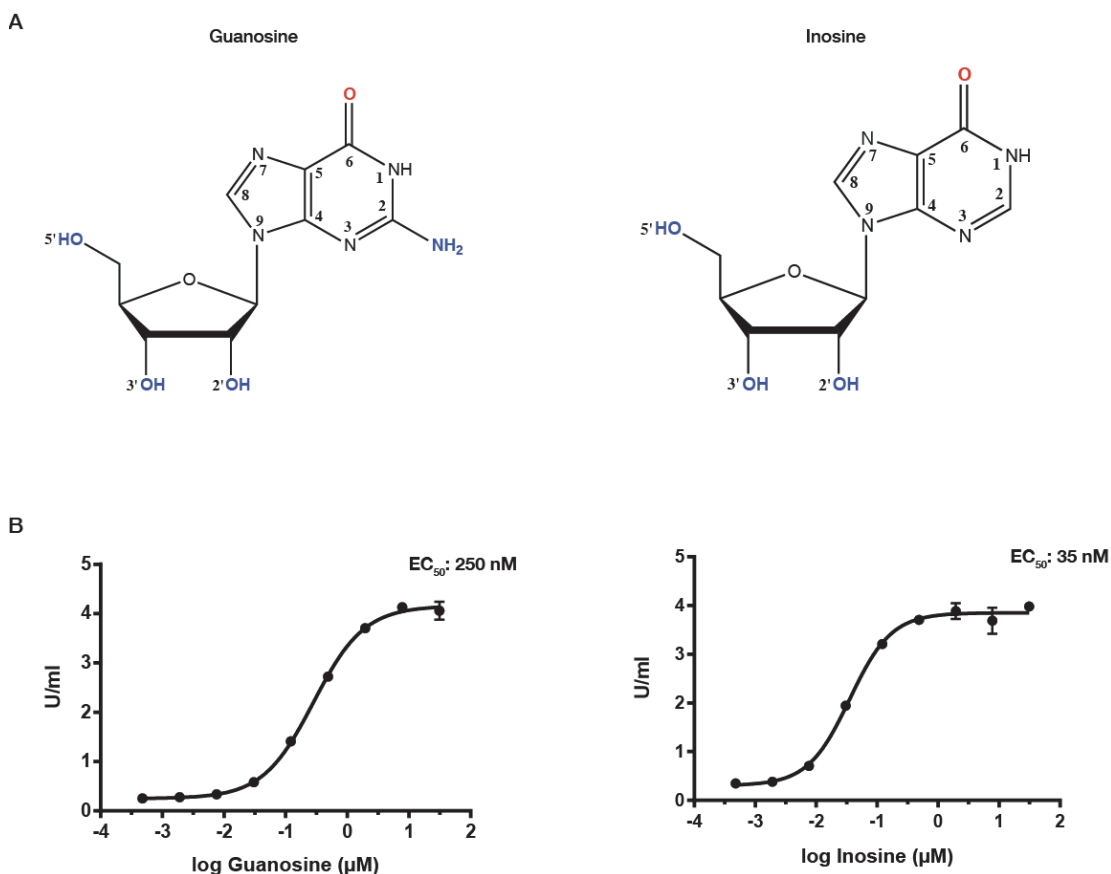
Fig. 3.58. Guanosine and inosine activation of TbPKA: A. Molecular structures of guanosine and inosine; in red hydrogen bond donors and in blue hydrogen bond acceptors (for adenosine comparison, see Fig. 3.50) **B.** Dose response measurements for TbPKA activation by guanosine and inosine (see method section 2.2.15). Data points are the average of two determinations, and error bars represent the range.

The guanine base influence on TbPKA activation was further analysed by testing the activation potency of loxoribine, which is a guanosine analogue with modifications on the N7 (allyl group) and C8 (oxo group) (Fig. 3.59a). Based on the positions of these modifications, this compound is to some extent comparable to some of the adenosine analogues analysed in section 3.3.3.1. The in vitro kinase assay showed that this molecule is devoid of any activation potency (Fig. 3.59b). The N7 modification is comparable to that of sangivamycin, which was shown to negatively influence the kinase activation. The C8 modification could also have negatively affected the purine base interaction as had been observed for 6-Bromotubercidin. Hence, despite having an intact ribose-sugar moiety, the purine base modifications rendered this analogue inactive.
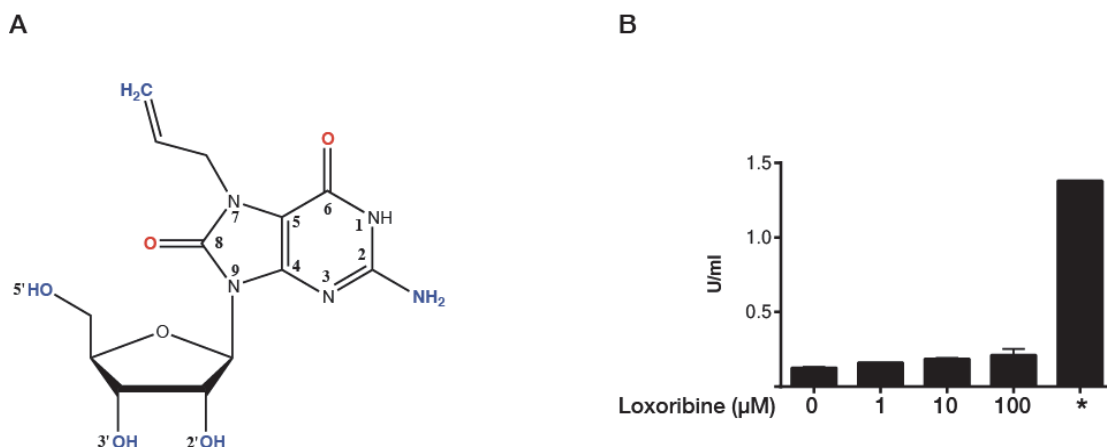
Fig. 3.59. Loxoribine activation of TbPKA: **A.** Molecular structure of loxoribine (colour coded as in the previous section) **B.** Several concentrations of loxoribine (as indicated) were tested for in vitro activation of recombinant TbPKA holoenzyme (section 2.2.15) with 5 µM toyocamycin (★) as control. The data points are the average of two determinations, and error bars represent the range.

The molecular basis of the observed differences amongst the purine nucleosides in their capacity to activate TbPKA was further investigated by structural modeling. In mammalian PKA, adenosine's purine base mainly establishes hydrophobic interactions with the PBC (section 3.1.1.3). This feature was in most part shown to be conserved in TbPKA by linear sequence analysis, except for the aromatic capping residue of PBC:B. The TbPKA structure model (Fig. 3.60a) could reveal structural conservation of these hydrophobic interactions, including the PBC:B capping residues, Tyr370 and Tyr482 in TbPKA compared to Trp260 and Tyr371 in mammalian RIα. It would therefore appear that TbPKA is capable of interacting with the adenine ring similarly to mammalian PKA. No additional interactions involving the adenine ring, especially the N6 amine group, could be predicted with the Chimera software. The adenine ring was replaced by hypoxanthine (inosine's purine base) using Chimera, occupying the same spatial co-ordinates as the former. The keto group of inosine, and guanosine, was shown to potentially form a hydrogen bond with Lys293 (PBC:A) and Asn481 (PBC:B). This feature could be responsible for the 30-fold gain of potency from adenosine to inosine. Guanosine was also placed in the PBC pocket similarly to inosine, confirming the keto group interaction. The N2 amine group was however found to be in a highly hydrophobic region with Val319 (PBC:A) and Val443 PBC:B being in very close proximity (Fig. 3.60b) . These residues are likely to oppose to the docking of guanosine in the ideal spatial orientation, hence reducing the affinity of this ligand.
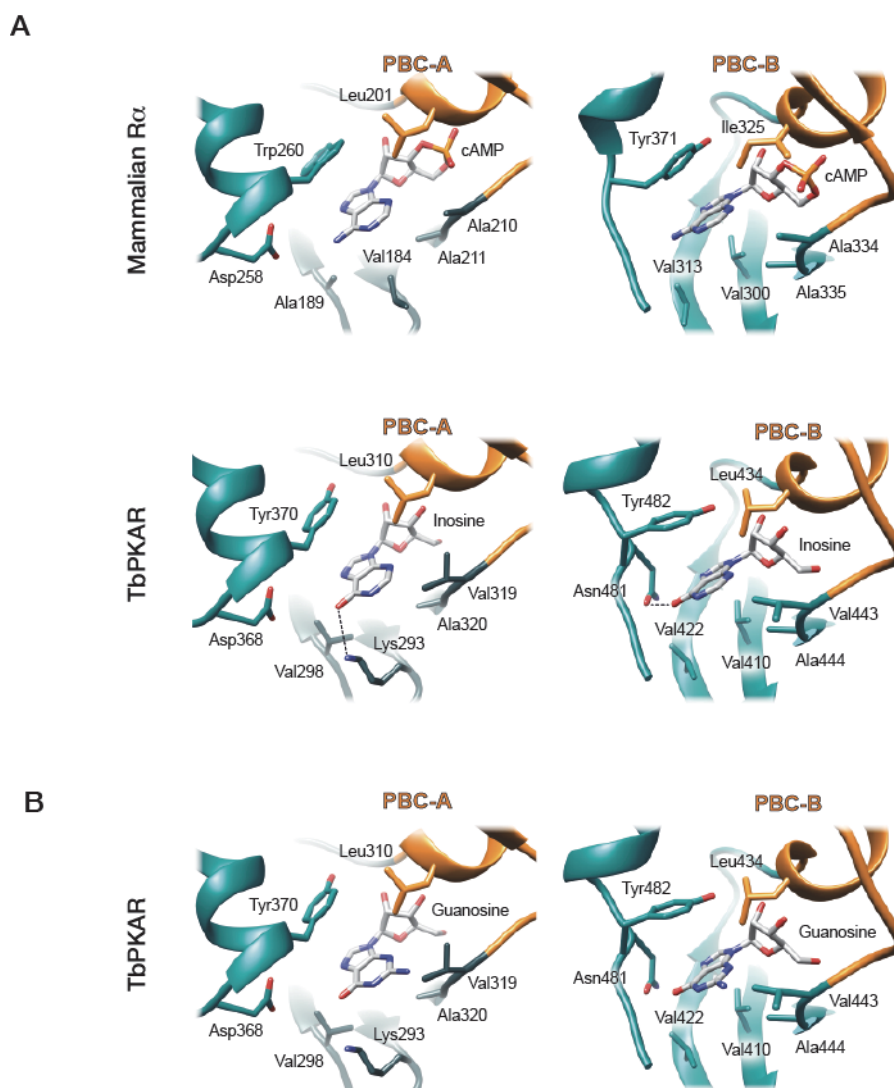
Fig. 3.60. The purine base interaction with the PBC is conserved for adenosine but guanosine and inosine would interact more favorably: A. Mammalian RIα PBC-adenine interactions (upper panel): the hydrophobic interactions on one side (mainly Valines and Alanines) and the aromatic capping residues Trp260 (PBC:A) and Tyr371 (PBC:B) on the other side. These interactions are conserved in TbPKAR as depicted by the structure model (lower panel). Replacement of adenosine with inosine in the same spatial co-ordinates, using the Chimera software, revealed that the keto group of inosine (and guanosine) can additionally form a specific hydrogen bond with Lys293 (PBC:A) and Asn481(PBC:B). **B.** The 2-NH$_2$ group of guanosine (also replacing adenosine) is in a highly hydrophobic environment, which is likely to negatively affect its binding potential.

3.5 A possible link between cold shock and ligand activation of TbPKA

The upstream machinery involved in cold shock perception, leading to activation of the kinase is still unknown. It is highly unlikely that TbPKA is directly activated by a drop in temperature, mainly owing to the fact that the recombinant holoenzyme remains intact during and after purifications, performed at 4°C. It is however plausible that the interaction of TbPKA with its putative ligand is modulated by lower temperatures. This

would conform to the predicted life cycle stage-specific cold shock activation of TbPKA, in the physiological setup.

This hypothesis was tested with the in vitro kinase assay by comparing the half activation constant of adenosine when the assay was either performed at 30°C (classic protocol, section 2.2.15) or at 20°C. It was expected that the assay kinetics would be slower at 20 °C and hence lower data point values would be obtained. This would however not affect the activation constants, unless the potency of the ligand is temperature dependent.

Temperature equilibration (20 or 30°C) was performed on all components of the kinase assay, including the TbPKA holoenzyme. Dose response measurements were then carried out at the respective temperatures.

The kinase activity at 20°C was about 2-fold lower than at 30°C, as would be expected, due to the thermodynamic differences between the two assay setups. The EC_{50} was however 3-fold lower at 20°C than at 30°C (Fig. 3.61). The half activation constant at 20°C is close to that obtained in section 3.4.1 where all the assays components were mixed at 4°C. The kinase reaction mix was however transferred to 30°C before the onset of the assay with ATP, as described in section 2.2.15. This would suggest that the holoenzyme-ligand equilibration attained at 4°C is not affected by the temperature raise.

This assay indicates that temperature could indeed directly influence the ligand-TbPKA interaction. This was however a preliminary experiment and more ligands would have to be tested in the same conditions, in order to validate this hypothesis.
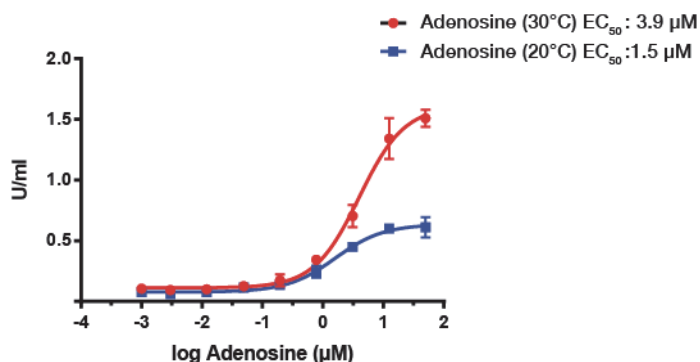

Fig. 3.61. The influence of low temperature on adenosine activation of TbPKA: Dose response measurements for adenosine activation of TbPKA were performed at 30°C or 20°C, as indicated. All the components of the assay were pre-equilibrated to the respective temperatures prior to the onset of the reaction. Data points are the average of two determinations, and error bars represent the range.

4 Discussion

4.1 TbPKA expression and holoenzyme reconstitution

Chromatographic techniques (ionic, cationic and size exclusion) have for a long time been exploited to purify the PKA kinase from its native source. The RI and RII type nomenclature of the mammalian isoforms is based on their NaCl elution profile from DEAE-cellulose (Corbin et al., 1975). The cAMP/cGMP binding capacity has also for long been exploited as an affinity chromatography approach to isolate PKA from native crude extracts, as well as from heterologous overexpression systems. Tag based affinity chromatography techniques are hence often not necessary. Attempts to isolate native TbPKA using the DEAE-cellulose purification approach was unsuccessful owing to the fact that none of the elution fractions portrayed a cAMP-dependent activity (N. Wild, this lab). Likewise, isolation of TbPKA using cAMP affinity pull-down was unsuccessful (C. Schulte zu Sodingen, Ph.D. thesis 2000). For a long time, the reason behind this failure remained unknown since the high conservation of the kinase's CNB domains highly indicated compliance of this kinase to the cAMP binding and activation mechanism. It is now evident from this and previous work that this is not the case.

In the mammalian system, the PKA subunits are easily expressed in *E. coli* at high yields where up to 20 mg of the R subunit and 5 mg of the Cα subunit per litre of cell culture can be obtained (Saraswat et al., 1986; Slice et Taylor, 1989). The holoenzyme is reconstituted by incubating the R and C subunits, usually with a slight molar excess of the R subunit, followed by size exclusion chromatography to separate the holoenzyme complex from the excess monomers (Anand et al., 2002; Canaves et al., 2000; Herberg et al., 1996).

A tag based affinity chromatography approach was adopted to isolate TbPKA, following the unsuccessful exploitation of the kinase's innate features. As discussed in section 1.9.1, the *E. coli* expression system had been used to purify the TbPKA subunits for polyclonal antibody production. The entire ORF of TbPKAR was successfully expressed but the catalytic subunits had to be rendered inactive by truncation mutagenesis. Expression of the full-length catalytic subunits was then achieved in the BEVS (higher eukaryotic) expression system. The in vitro catalytic activity of TbPKAC3 was thereby characterized but that of TbPKAC1 remained elusive. An attempt to reconstitute the holoenzyme using the *E. coli* expressed TbPKAR and BEVS expressed TbPKACs had also failed.

These pitfalls necessitated a systematic approach for TbPKA expression, with the aim of obtaining high yields of pure and fully functional kinase. Homologous purification of the holoenzyme using PTP-tagged TbPKAR subunit was successful but the yield and purity was too low for the intended in vitro characterization (section 3.2.1). Three heterologous expression systems (*E. coli*, BEVS and LEXSY) were hence tested and compared to the

homologous system. Co-expression of TbPKA subunits in the heterologous system was further aimed at facilitating the holoenzyme formation in a physiological setup.

Heterologous expression of the individual subunits had varying degrees of success.

The yield of TbPKAR expressed in *E. coli* was the highest of the three heterologous expression systems. For the first time, full-length TbPKAC1 and TbPKAC3 subunits were expressed in *E. coli* but necessitated screening for the best expression strain and conditions. However, from the three expression systems, only TbPKAC1 could be expressed and purified in sufficient quantities for further in vitro characterization. In fact, TbPKAC3 could only be expressed and purified from the BEVS expression system as previously reported (N. Wild, this lab; D. Sohmen, Diploma thesis 2008), hence no further development. The yields obtained for both TbPKAR and TbPKAC1 were, in all cases, much lower than those of the *E. coli* expressed mammalian PKA (section 3.2.2). The co-expression was also only successful for TbPKAC1/TbPKAR, in the three expression systems. However, an intact holoenzyme could only be purified from the Leishmania expression system. This success was after realizing that recombinant PKA subunits from *E. coli* and BEVS expression systems could form a stable holoenzyme, after incubation in trypanosome lysate (section 3.2.4). This raised the notion of kinetoplastid specific requirements for holoenzyme formation. The involvement of a trans element in the holoenzyme formation was deemed unlikely for two reasons: MS analysis of the endogenous holoenzyme complex purification did not reveal any candidates likely to interact with kinase complex (section 3.2.1) and also because the LEXSY purified holoenzyme had no additional bands on coomassie stained SDS-PADE gel (3.2.5.2).

It was hence deemed more likely that kinetoplastid specific PTMs are key for stable holoenzyme formation. This was further investigated by analysis of TbPKAR and TbPKAC1 subunits from the three expression systems. The central question was whether full functionality of individual or both subunits was dependent on the expression system. It could be shown that TbPKAR was fully functional irrespective of the expression system; while TbPKAC1 had the highest specific activity, close to that of the mammalian PKA, when expressed in Leishmania (section 3.2.6). This suggests that the full maturation of TbPKAC1 in Leishmania was the key element missing in the other expression systems. Functionality determination of TbPKAR was however slightly biased, since only the Leishmania-expressed TbPKAC1 was used for the inhibition studies (section 3.2.6.4). It remains plausible that the catalytic subunit could be involved in the maturation of the regulatory subunit, by trans phosphorylation. If this would then be dependent on the kinase's specific activity, *E. coli* and BEVS expressed TbPKAC1 would be less efficient. This would explain the co-purification failure despite successful co-expression in both the *E. coli* and BEVS expression systems. This would concomitantly impede the maturity of the regulatory subunit. Both TbPKAR and TbPKACs have been shown to be enriched in phosphorylations, most of which appear to be kinetoplastid specific.

4.1.1   TbPKACs involvement in kinetoplastid specific holoenzyme formation

Full activity of the mammalian catalytic subunit is dependent on posttranslational modifications (see section 1.6.2). The phosphorylation of Thr197 is highly essential for full catalytic activity. In *E. coli*, this modification is initially achieved by autophosphorylation and later by trans autophosphorylation (Steinberg et al., 1993). In higher eukaryotic expression systems, PDK1 and other activating kinases have been shown to be responsible for this phosphorylation (Cheng et al., 1998). Other mammalian Cα phosphorylation sites, so far characterized, include: Ser338 (also by trans autophosphorylation in *E. coli*), which plays a role in stabilizing the kinase by anchoring the C-terminal tail to the small lobe and Ser10, also suggested to be involved in the structural stability (Yonemoto et al., 1997). Thr197 and Ser338 phosphorylation sites are conserved in TbPKAC1 but the latter is absent in TbPKAC3 (section 3.1.3). *E. coli* expressed TbPKACs were able to phosphorylate the regulatory subunit, in vivo, but portrayed very low in vitro catalytic activity (section 3.2.2.4 & 3.2.6.3). Western blot analysis of TbPKAC1 and its catalytically inactive variant showed that the latter migrated faster on SDS-PAGE gel. This has also been observed for unphosphorylated mammalian PKA (Steinberg et al., 1993). This would suggest that at least the Thr197 equivalent is phosphorylated, probably by autophosphorylation. On the other hand, this would appear to be insufficient to render the kinase fully active. BEVS expressed TbPKAC1 was at least 10-fold more active (section 3.2.6.3) than the *E. coli* version, implying that this system could further enhance the kinase's maturity. The full extent of modifications would appear to have been attained in Leishmania, where the kinase was also at least 10 fold more active than the BEVS-expressed kinase. The specific activity of the LEXSY expressed TbPKAC1 was not compared to that of the endogenous kinase. It can therefore only be assumed that this kinase had attained full maturation in this system. This would imply that full functionality of recombinant TbPKAC1 can only be attained in an expression system closest to *T. brucei*. The Leishmania expressed TbPKAC1 was shown to have a multiple-band migration pattern on SDS-PAGE gels, which is similar to that of the endogenous kinase and probably caused by PTMs (section 3.2.5.1).

The full extent of endogenous TbPKAC1 phosphorylation was revealed by MS analysis (Nett et al., 2009; Urbaniak et al., 2013). TbPKAC1 has more phosphorylation sites than the mammalian Cα. Tyr phosphorylations sites are also present in TbPKAC1 but completely absent in mammalian PKA (see section 3.1.3). The phosphorylation pattern in TbPKAC1 is in compliance to the key regulatory regions of the AGC family of kinases, namely; the N and C-terminal tails and the activation loop (see Fig. 3.8 and Fig. 4.1). The N and C-terminal tails confer the kinase specificity by cis and trans regulation, as discussed in section 3.1.3. It is therefore not surprising that TbPKA would contain some specific features in this region. However, the large extent to which TbPKAC1 is phosphorylated in these regions has not been reported in any other member of the PKA family, so far. It is therefore highly probable that these tails are involved in the kinetoplastid specific holoenzyme formation.
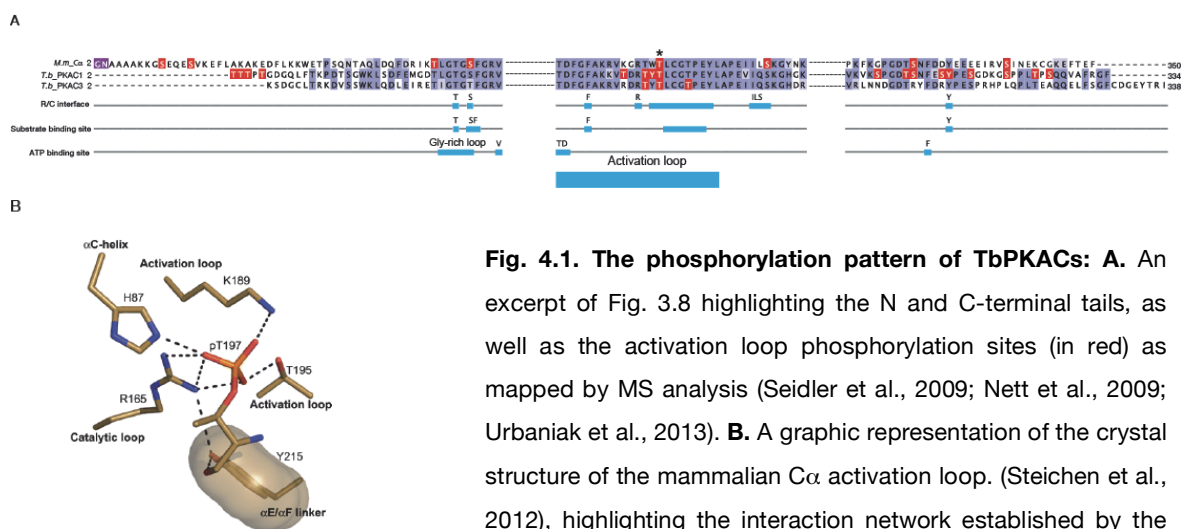
Fig. 4.1. The phosphorylation pattern of TbPKACs: A. An excerpt of Fig. 3.8 highlighting the N and C-terminal tails, as well as the activation loop phosphorylation sites (in red) as mapped by MS analysis (Seidler et al., 2009; Nett et al., 2009; Urbaniak et al., 2013). **B.** A graphic representation of the crystal structure of the mammalian Cα activation loop. (Steichen et al., 2012), highlighting the interaction network established by the phosphorylated Thr197 (highlighted by an asterisk in A).

Another interesting feature is the phosphorylation pattern of the activation loop in TbPKACs. While only one Thr (Thr197 in mammalian PKA) is phosphorylated in most AGC kinases, TbPKA has a few more adjacent phosphorylation sites, as shown above.

The phosphorylation of Thr197 in mammalian Cα enables it to establish a hydrogen bond network (Fig. 4.1b) with residues from both lobes of the kinase (Fig. 1.6), stabilizing the kinase in an active conformation (Steichen et al., 2012). The negatively charged Thr197 (in its phosphorylated state) is also involved in the R subunit interaction, as discussed in section 3.1.1.5. The architecture and role of this region is likely to differ in TbPKA, since the phosphorylation enrichment not only renders the loop highly charged but also transforms the residues from hydrogen bond donors to acceptors.

Investigating the role played by these phosphorylations may not only reveal the molecular nature of the TbPKA holoenzyme but also the specific features of TbPKAC isoforms.

4.1.2 TbPKAR involvement in kinetoplastid specific holoenzyme formation

The kinetoplastid specific N-terminal domain of TbPKAR has previously been shown to be involved in the R/C interaction, by reverse genetics (section 1.7.1 & 3.1.2). This subunit additionally contains phosphorylation sites (mapped similarly to TbPKACs) that are not only unique in kinetoplastids but some would appear to be *T. brucei* specific (Fig. 4.2).

Fig. 4.2. The phosphorylation pattern of TbPKAR: An excerpt of Fig 3.7 highlighting the TbPKAR phosphorylation sites, in red (Urbaniak et al., 2013). Residue conservation in other kinetoplastids is highlighted in green. The inhibitor substrate motif (S) in also highlighted.

While all RII type subunits are phosphorylated on the Ser/Thr (P site) of the inhibitor substrate motif, TbPKAR is additionally phosphorylated on the P-1 site (Fig. 4.2). This is highly unusual and with almost certainty a *T. brucei* specific feature, since the residue is not conserved in the other kinetoplastids. The P site phosphorylation is involved in the R/C interaction, as discussed in section 3.1.1.5. Phosphorylated RII type isoform has been shown to have a 10-fold slower R/C reassociation rate (Flockhart and Corbin, 1982). Contribution of the *T. brucei* specific P-1 phosphorylation to these and other features is not known but raises another prospect of holoenzyme specificity.

Most of the other phosphorylation sites lie between the predicted LRR domain and the inhibitor substrate motif but only a few appear to shared by other kinetoplastids since the corresponding residues are not conserved (Fig. 4.2). These phosphorylations have, so far, not been characterized. It therefore remains plausible that they contribute to the holoenzyme formation with some of the features being specific to the *T. brucei* species.

4.1.3 Heterologous PKA purification in other kinetoplastids

Heterologous expression of other kinetoplastid PKA has previously been reported. In *T. cruzi*, GST N-terminally tagged TcPKAR was purified from *E. coli* while a C-terminal HA tagged TcPKAC was purified from mammalian 293T cells (Huang et al., 2006). The group also expressed the subunit in *E. coli* but higher specific activity was obtained from the eukaryotic expressed kinase, complying to findings on TbPKAC1 in this work.

The TcPKAC subunit was shown to have a 10-fold increase in catalytic activity when incubated with cAMP. This is probably because it had been co-purified with the endogenous R subunit. Recombinant TbPKAC1 was tested similarly, in this work, showing cross-interaction in Leishmania but not in Sf9 cells (section 3.2.6.2 and 3.4.2.2). The group could nonetheless inhibit the catalytic activity of TcPKAC with *E. coli* expressed TcPKAR.

In *Leishmania donovani*, N-terminal His tagged LdPKAR, LdPKAC1 and LdPKAC2 were purified from *E. coli* (Bhattacharya et al., 2011). Both catalytic subunits were incubated with LdPKAR in 1:1 molar ratio or slight excess of the regulatory subunit (1:1.2 and 1:1.26). The catalytic activity was only partially inhibited (≤50%) and surprisingly even less in molar excess of LdPKAR.

It would therefore appear that holoenzyme reconstitution of heterologously expressed PKA subunits is possible, to some extent, in both *L. donovani* and *T. cruzi*. It nonetheless remains possible that kinetoplastids share common features for holoenzyme formation but *T. brucei* would additionally have some species-specific features.

4.2 The unique features of TbPKAC3 isoform

The TbPKAC3 isoform distinguishes itself from the other two isoforms in various ways, most of which had been established prior to this work (section 1.6.2 and 1.9.1). Despite being the only constitutively expressed isoform in the life cycle, it was successfully knocked out in both the insect (C. Schulte zu Sodingen, Ph.D. thesis 2000) and blood

stream stage (section 3.3.1.1) of the parasite. Knock out in the latter enabled to show that this isoform is not involved in the cold shock mediated activation of TbPKA (S. Bachmaier, this lab). The cold shock activation is mainly mediated by TbPKAC1, which is an essential gene and only expressed in the blood stream form.

The heterologous expression of this kinase was more challenging than that of TbPKAC1, indicating that it was perceived differently by the expression systems. TbPKAC3 has much fewer phosphorylation sites in comparison to TbPKAC1 (Fig. 3.8 & 4.1). It can hence be postulated that it maturation to full activity is less demanding, making its expression more toxic.

Although this isoform was not the main focus of this work, it remains an integral part of TbPKA and key to a better understanding of the activation mechanism. For example, the fact that TbPKAC1 and not TbPKAC3 is activated by cold shock, despite sharing the same cellular confinement, could mainly lie in the molecular nature of their respective holoenzymes. Investigating the different phosphorylation pattern between the two, would be a good starting point.

4.3 Cyclic nucleotides and *T. brucei's* PKA kinase

The activation of TbPKA by cyclic nucleotides had been investigated by several approaches both in vivo and in vitro, prior to this work (section 1.9.2). Sufficient evidence had been accumulated, showing that only cGMP could activate this kinase but with a very weak activation potency. However, an in vitro kinase assay setup that would allow quantitative dose response measurement was still lacking. This was established in this work and enabled the final confirmation of the previous findings (section 3.3.2.3). This then paved way for other key questions, mainly; why cAMP (the established PKA ligand) does not activate TbPKA and what would be the natural ligand.

In silico analysis of TbPKA (section 3.1), in comparison to its mammalian counterpart, highlighted key differences in the heart of the cyclic nucleotide-kinase molecular interaction. More precisely, the kinase's interaction with the nucleoside moiety appeared to be conserved but not that of the phosphate group. Interestingly, the entire cyclic nucleotide binding-pocket is known as the PBC for phosphate binding cassette, highlighting the importance of the phosphate interaction in PKA activation.

Site directed mutagenesis of a few residues in the PBC (section 3.3.2.1) showed that TbPKA could indeed be reengineered for cAMP activation. The half activation constant obtained with the in vitro kinase assay (~20 µM) was at least 40-fold higher than any of the mammalian PKAs: 101 nM for $RI\alpha_2/C\alpha_2$ (Herberg et al., 1996) and 584 nM for $RII\beta_2/C\alpha_2$ (Zawadzki and Taylor, 2004). This was not very surprising since many aspects of TbPKA holoenzyme are still not understood. It was mainly important to show that a few residue changes are sufficient not only to restore cAMP binding but also to enable the ensuing chain of conformational changes (section 1.7) that lead to the release of the catalytic subunit. The conservation of this response mechanism indicated that TbPKA is probably activated by an alternative ligand.

4.4 Do cyclic nucleotides activate PKA in other kinetoplastids?

cAMP has for long been associated with differentiation in kinetoplastids. Hence, early attempts to isolate protein kinase activity were aimed at identifying the cAMP-dependent activity. However, no cAMP stimulated activity could be detected in any of the kinetoplastid species (Boshart and Mottram, 1997). cAMP chromatography was also used in an attempt to isolate PKA but only unrelated proteins could be purified; in *T. brucei* (Walter, 1978; Walter and Opperdoes, 1982) and in *L. donovani* (Banerjee and Sarkar, 2001). In *T. brucei*, some cAMP effector proteins known as CARPs (cAMP Responsive Proteins) have recently been identified from an RNAi library screen (Gould et al., 2013). One of the CARP proteins (CARP1; Tb927.11.16210) has cyclic nucleotide binding domains but is completely unrelated to PKA. It is probable that this is the main cAMP effector protein in TbPKA.

Earlier work, in addition to this thesis, is sufficient to suggest that PKA is not a cAMP effector protein in kinetoplastids. There have however been claims that kinetoplastid PKA activation complies to the other PKA kinases: in *L. donovani* (Bhattacharya et al., 2012) and in *T. cruzi* (Huang et al., 2006). However, the evidence provided by both groups is, in light of this thesis, deemed insufficient.

In *L. donovani*, *E. coli* purified subunits were used to reconstitute a holoenzyme complex but only 50% of the catalytic activity could be inhibited, even in excess of the R subunit (section 4.1.3). It was then claimed that the catalytic activity increased from 50 to 90%, in the presence of cAMP. This is not conclusive, given the rather suboptimal nature of the holoenzyme used. It is likely that the R/C interface formed was very weak, hence the partial inhibition. Any slight perturbation of such a complex would likely result in further (unspecific) dissociation. cAMP dissociation of the native co-immunoprecipitated holoenzyme was also analysed but differed significantly from the approach used in this thesis. Intact cells were incubated with 400 µM of cell permeable non-hydrolysable cAMP (Sp8Br-cAMPS) for 6 hours followed by co-immunoprecipitation and analysis of the complex dissociation. In this work, the kinase complex was first co-immunoprecipitated and then exposed to cAMP (100 µM) for 30 min and then analysed for dissociation (see section 3.3.2.3). Western blot analysis of the pull-down could show that the LdPKA complex was only partially dissociated, also confirmed by in vitro kinase assay measurements of the catalytic activity. It is probable that the Sp8Br-cAMPS was partially degraded to its nucleoside version during the rather long incubation period, which then dissociated the complex. Sp8Br-cAMPS is the combined structure of 8-Br-cAMP and Sp-cAMPS. Although these compounds are operationally regarded to be non-hydrolysable, they are subject to degradation over longer periods of incubation with cell lysates or in intact cells (Rossier et al., 1979; Wood and Braun, 1973).

In *T. cruzi*, TcPKAC and TcPKAR were purified from the mammalian 293 cells and *E. coli* expression system, respectively. The catalytic subunit already portrayed cAMP induced activity, prior to the holoenzyme reconstitution as discussed in section 4.1.3. This activity

was carried on to the TcPKA holoenzyme formed, thereafter. A 100 µM cAMP was then used in an attempt to reverse the inhibition, only to obtain less catalytic activity than that of the previously tested free TcPKAC.

Work in this thesis highlighted the many pitfalls in holoenzyme reconstitution and also established the standard dose response measurements widely used to validate ligand activation.

4.5 Nucleoside activation of TbPKA kinase

Laxman and co (2006) provided the first indications that cAMP analogues are not involved in the differentiation process but rather its degradation products (5'-AMP and adenosine) as discussed in section 1.4. This prompted the testing of similar compounds for the in vivo activation of TbPKA, in line with the possible involvement of PKA in differentiation (S. Bachmaier, this lab). It could be shown that indeed adenosine analogues activated this kinase. Proof that these compounds activate the kinase by direct interaction was provided in this thesis (see section 3.3.3.1). It also became apparent that the N7 and C8 derivation of adenosine's purine base could positively or negatively influence the activation potency (see section 3.3.3.1).

The in vitro analysis enabled further testing of nucleosides that could previously not be tested due to their poor membrane permeability. The activation constant of unmodified adenosine was in the lower micromolar range, which was almost a 1000-fold gain of potency from that of cGMP (see section 3.3.2.3 and 3.4.1). It was however the activation constants of the other unmodified purine base nucleosides namely guanosine and inosine that highly indicated that nucleoside activation of TbPKA could have a physiological significance (see section 3.4.4.2). Guanosine's half activation constant was in the same range as that of the most potent adenosine analogues (~200 nM). Inosine's (~30 nM) was lower than that of heterotetrameric mammalian PKA for cAMP (section 4.3) but in the same range with heterodimeric variants: 13.5 nM for (91-379)$RI\alpha_1/C\alpha_1$ and 65 nM for (108-402)$RII\beta_1/C\alpha1$ (Zhang et al., 2012).

In silico analyses have revealed that this activation mechanism is likely to be shared by all kinetoplastids (3.1.1). The only biochemical evidence to this end was obtained from adenosine activation of a chimeric holoenzyme, comprised of TbPKAC1 and *L. tarentolae's* PKAR (section 3.4.2.2). More experimental evidence is required for the validation of nucleoside activation as a kinetoplastid specific feature.

Having used structural modeling to understand the loss of the phosphate interaction in the PBC, the same approach was used to look for any indications of gain of function as pertains to nucleoside interaction. The TbPKA nucleoside-binding pocket was considered as a combination of different structural binding motifs, corresponding to the various components of the nucleoside. Structural and bioinformatics analysis of nucleoside binding proteins have shown that the structural motifs for the different nucleoside moieties are modules shared even by non-homologous proteins (Gherardini

et al., 2010; Parca et al., 2012). In the absence of any structural studies of a nucleoside-bound kinetoplastid PKA, such knowledge may be useful in interpreting this work.

4.5.1 Contribution of the ribose sugar in nucleoside binding

The contribution of the ribose-sugar moiety in nucleoside TbPKA activation was predicted by in silico analysis and confirmed biochemically by testing the activation potency of deoxy-adenosine analogues (section 3.4.3). The involvement of the 2'-OH group was expected, since the residues involved (in other PKA kinases) are also highly conserved in kinetoplastids.

The residues predicted by structural modeling to be involved in the 3'-OH interaction (Glu311: PBC:A and Glu435: PBC:B) had also been predicted to impose steric hindrance on cAMP's phosphate group hence preventing cAMP interaction (section 3.4.1).

The involvement of the 5'-OH group in hydrogen bond interaction with the PBC was predicted by structural modeling but has not yet been biochemically tested. The residues predicted (Thr318: PBC:A and Asn442: PBC:B) occupy the position of the highly conserved Arg, involved in cAMP's phosphate interaction (section 3.4.1). These interactions are yet to be validated by reverse genetics and ultimately by resolving the kinase's crystal structure.

4.5.2 Contribution of the purine base in nucleoside binding

❖ Classic purine base nucleosides

The interactions established between the adenine ring of cAMP and the PBC domain are mainly of Π-Π stacking and hydrophobic nature. Hydrogen bonds involving the donor N6 amine group of the adenine ring have been predicted for cAMP interaction with the PBC domain but none put to evidence by structural studies (Berman et al., 2005). In silico analysis could predict the conservation of the Π-Π stacking and hydrophobic interactions in TbPKA but not the presence of any additional interaction features (section 3.1.1.3 & 3.4.4.2). Adenosine was nonetheless a relatively good activator of TbPKA with half activation constant in the lower micromolar range (~1 µM). This highlights the important contribution of the ribose-sugar moiety in compensating for the loss of the phosphate group (in cAMP) interaction.

Adenosine was however shown to be the weakest activator amongst the purine base nucleoside tested. Purine nucleobases (adenine, guanine and hypoxanthine) are very similar in size and shape and would therefore have a similar environment for all types of hydrophobic interactions. It could therefore be predicted that they would mainly vary in their hydrogen bond acceptor and donor capabilities. Almost 80% of all purine base hydrogen bonds have been shown to involve position 6 of the purine ring, with the $-NH_2$ of adenine having hydrogen bond donor capabilities and the keto group of both guanine and hypoxanthine being a hydrogen bond acceptor (Nobeli et al., 2001). As mentioned earlier, structural modeling, of TbPKA, could not predict any hydrogen formation distances for this N6 amine group of adenine. On the other hand, the keto group showed

the potential of establishing a specific hydrogen bond with a kinetoplastid-conserved Lys (see section 3.4.4.2). This possible gain in specificity would explain the observed increase in activation potency in guanosine and inosine. Inosine was however a much better activator than guanosine despite the only difference being the presence of an amine group at position 2 of guanosine's purine base. Structural modeling revealed that the 2-NH$_2$ group is likely to be docked in an unfavorable hydrophobic environment (see Fig. 3. 60b).

❖ **Influence of purine base derivation on TbPKA nucleoside activation**

Varying activation potency was observed for N7 derived adenosine analogue (section 3.3.3.1). Structural modeling suggested that the C5 carbon (N7 in non-derived purine bases) would be positioned in a hydrophobic environment in the PBC domains (see supplement in the electronic version of the thesis). This would suggest that the higher the electronegativity of the molecule bound to the C5 carbon, the better the interaction. Iodine being more electronegative than bromine was a better activator of the kinase. The cyano and carboxyamide groups of toyocamycin and sangivamycin, respectively, are electron-withdrawing groups that are also likely to have the same effect as the halogens. This worked favorably for toyocamycin having comparable potency with 5-Iodotubercidin but sangivamycin's carboxyamide group was probably too bulky to fit into the hydrophobic space thus explaining its much lower activation potency. The specificity of interaction in the hydrophobic space was confirmed by showing that while N7 derived 5-bromotubercidin could activate the kinase the C8 derived 6-Bromotubercidin had no activation potency.

4.6 How do unphysiologically high concentrations of cGMP activate TbPKA kinase?

cGMP is the only cyclic nucleotide shown to activate TbPKA but with activation potency in the millimolar range (S. Kramer, Ph.D. thesis 2006; Shalaby et al., 2001; section 3.3.2.3). Although this activation is unlikely to be physiologically relevant, the molecular nature of this activation defies the notion that TbPKA evolved to be non-responsive to phosphate-nucleotides. Two rather speculative possibilities would be the presence of cGMP-dependent protein (PKG) features in TbPKA's CNB domains or the existence of an alternative binding site.

❖ **The CNB domains could have PKG-like features**

cGMP binding proteins such as PKG (one of the best studied effector proteins) share a very high homology in their CNB domains with the cAMP binding proteins. The specificity for cGMP is mainly refined in the PBC domains where, a few amino acid differences are responsible for a 100-fold better affinity for cGMP binding in PKG (Lincoln, 1983). This is highlighted in the multi-alignment of the PBC domains below.

Fig. 4.3. The PBC specific features for cGMP binding: a multi-alignment of the PKA PBC domains as previously described (section 3.1.1.2) with those of PKG kinases: the human PRKG1α and bovine PRKG1β. Residues in blue interact with the ribose sugar, in red with the phosphate group and in green with the 2-NH2 of cGMP. In grey is the Glu, shown to clash with the phosphate group in kinetoplastids.

All PBCs form the same interactions with the ribose-sugar moiety of the nucleotide. The Gly and Glu (in blue) are hence conserved in all cases. The specific phosphate interaction with the Arg (in red) is also conserved in PKG. Two additional sites provide the PKG specificity: Thr193 in human PRKG1α (residues in green) interacts with the 2-NH$_2$ of the purine ring via both its carbonyl and hydroxyl groups. The hydroxyl group additionally interacts with the equatorial O1P of the phosphate group (Kim et al., 2011). This Thr is replaced by an Ala in most PKA kinases or a Val in kinetoplastids (Fig. 4.3), hence the absence of this interaction. It has previously been shown that replacing the Ala with Thr in RIα improves specificity for cGMP without weakening cAMP's affinity (Shabb et al., 1991). The second cGMP specific site is provided by a Leu and Cys upstream of the PBC (Leu172 and Cys173 for PRKGα, not shown in the alignment). Leu makes a nonpolar contact with the carbonyl group at the C6 position of the guanine ring while Cys interacts with the unprotonated N7 of the guanine ring through an extended hydrogen bond (Fig. 3.58; guanosine structure). These residues are neither conserved in the mammalian nor in kinetoplastid PKA.

In *T. brucei*, Thr318 and Asn442 (same position as the conserved Arg residues in red) are only one residue upstream of the conserved cGMP specific Thr and could theoretically establish similar interactions. This could however not be predicted by structural modeling. Since the precise structural nature of TbPKA's PBCs is not known, these residues remain the most probable candidates for establishing a specific interaction with the 2-NH$_2$ group of cGMP. It however doubtful that such an interaction would be capable of inducing the conformational changes required for activation. If so, it would be very weak and with a high on and off binding rate, thus requiring high concentrations of cGMP for activation.

❖ **There could be an alternative binding site**

Having earlier postulated that kinetoplastid PKA actively blocks the access to the PBC via the conserved Glu (Fig. 4.3; in grey) the possibility of an alternative cGMP binding site

was exploited. A PBC-like motif was identified in the N-terminal domain, between the structurally defined LRR motif (residues 24-166) and the substrate inhibitor sequence. This PBC-like sequence was aligned and compared to the previously characterized PBC domains, as shown below.

Fig. 4.4. A PBC-like motif in the N-terminal of kinetoplastids PKAR: a multi-alignment of the PKG, the mammalian and an N-terminal PBC-like sequence in kinetoplastids. The same colour scheme was used as in Fig. 4.3. The asterisks denote the phosphorylated residues in TbPKAR as discussed in section 4.1.2.

This motif was identified based on the established general consensus sequence for cyclic nucleotide binding motifs (F-G-E-[LIV]-A-L-[LIMV]-x(3)-[PV]-R-[ANQV]-A, discussed in section 1.7.1. Although this PBC-like motif is not conserved to the latter, it presents key elements worth exploiting.

The ribose-sugar interaction would be ensured by the PBC-conserved Gly and Glu, in blue (Fig. 4.4). The specific phosphate interaction with the PBC-conserved Arg is functionally conserved in *T. brucei* (but not in other kinetoplastids) where a Thr at the same position would fulfill the same role. In place of the Glu, earlier predicted to clash with the phosphate group, are residues with shorter side chains (Val, Pro and leu), in grey (Fig. 4.4). More noteworthy is the conservation of the Thr involved in the cGMP specific interaction (in green; Fig. 4.4), as discussed above.

cGMP binding to this motif appears to be more likely than in the actual PBC domains. Whether binding of cGMP, or any other ligand, uniquely to this motif would be sufficient to induce the conformational changes necessary for activation is also arguable. However, given that TbPKAR's long N-terminal domain is involved in the R/C interface, this PBC-like motif would act as a relay for the conformational changes required for full release of the catalytic subunit.

However speculative this notion might be, what's noteworthy is the fact that 50% of the phosphorylation sites mapped in TbPKAR are found within this PBC-like motif (Fig. 4.2 & 4.4). This enhances the possibility of its involvement in the activation mechanism, amongst other roles.

4.7 Physiological relevance of TbPKA nucleoside activation

Despite the overwhelming evidence in this thesis that TbPKA is much better suited for nucleoside-mediated activation, this mechanism has not been captured in the

physiological setup. The closest analogy to the actual in vivo activation mechanism had been obtained from studying the agonistic and antagonistic effect of adenosine analogues and dipyridamole (S. Kramer, Ph.D. thesis 2006; S. Bachmaier, this lab).

The agonistic effect of adenosine analogues was shown to be by direct interaction with the kinase (see section 3.3.3.1). Some of the analogues tested are naturally occurring antibiotics synthesized by various bacteria species (section 3.3.3.1). The relatively high activation potency of toyocamycin would lead one to postulate that similar biosynthetic pathways would exist in *T. brucei*. However, no homologues of these pathways were found in *T. brucei's* genome (F. Scharf, this lab). Additionally, most of these compounds have in the past been reported to have anti-trypanosomal effects. For example, tubercidin has been shown to inhibit glycolysis through phosphoglycerate kinase (Drew et al., 2003). These analogues would therefore be unsuitable second messengers for *T. brucei*.

In vitro analysis of dipyridamole's agonistic effect showed that this compound does not interact directly with TbPKA (section 3.3.3.3). It had earlier been shown that the in vivo effect is not directly linked to the intracellular increase of cAMP resulting from the inhibition of PDE (section 1.9.2). The pathway engaged by this compound is therefore likely to lead to the availability of the endogenous ligand, resulting in the activation of the kinase. Furthermore, the TbPKAR PBC mutant was no longer responsive to dipyridamole activation (section 3.3.3.3), probably because the mutations affected binding of the natural ligand. The mutations on the PBC also abolished the cold shock mediated activation of the kinase (section 3.3.2.4). The cold shock activation was earlier shown to be inhibited by 8-pCPT-adenosine (S. Bachmaier, this lab). In vitro analysis of this compound showed no direct influence on the kinase's activation (section 3.3.3.2). Understanding the mechanism by which 8-pCPT-adenosine inhibits the cold shock activation is also likely to lead to the identification of the natural ligand.

The activation potency portrayed by purine base nucleosides (especially guanosine and inosine; section 3.4.4.2) and their already established roles as second messengers make them the more probable TbPKA activators. The physiological availability of these nucleosides and their possible involvement in TbPKA activation is hereby discussed.

4.7.1 The possible involvement of the purine salvage pathway in TbPKA activation

Contrary to the mammalian system, protozoa lack a *de novo* purine base biosynthesis mechanism and hence rely on their host for nucleobases and nucleosides (Berens et al., 1995). The uptake is mediated by permeases belonging to the Equilibrative Nucleoside Transporter (ENT) family. Twelve members of this family have been identified in *T. brucei* and named TbNT1-11. The members characterized so far have been shown to transport adenosine, guanosine, inosine and hypoxanthine (in some cases) with different substrate specificity and life cycle expression patterns (de Koning et al., 2005; Landfear et al., 2004; Ortiz et al., 2009). For example, TbNT9 expressed mainly in the BSF short stumpy

and procyclic stages of the life cycle was shown to have an up to 40-fold higher affinity for adenosine than inosine with the difference at position 6 of the purine (amine vs keto group) having a major influence (Al-Salabi et al., 2007). This is the inverse of TbPKA affinity for the two nucleosides, observed in this thesis.

Once taken up, the nucleobases /nucleosides partake numerous pathways involving inter nucleoside/nucleotide conversions as depicted below. Earlier reports on nucleoside uptake in *T. brucei* indicated that adenosine is preferentially taken up in comparison to inosine and guanosine (James and Born, 1980).
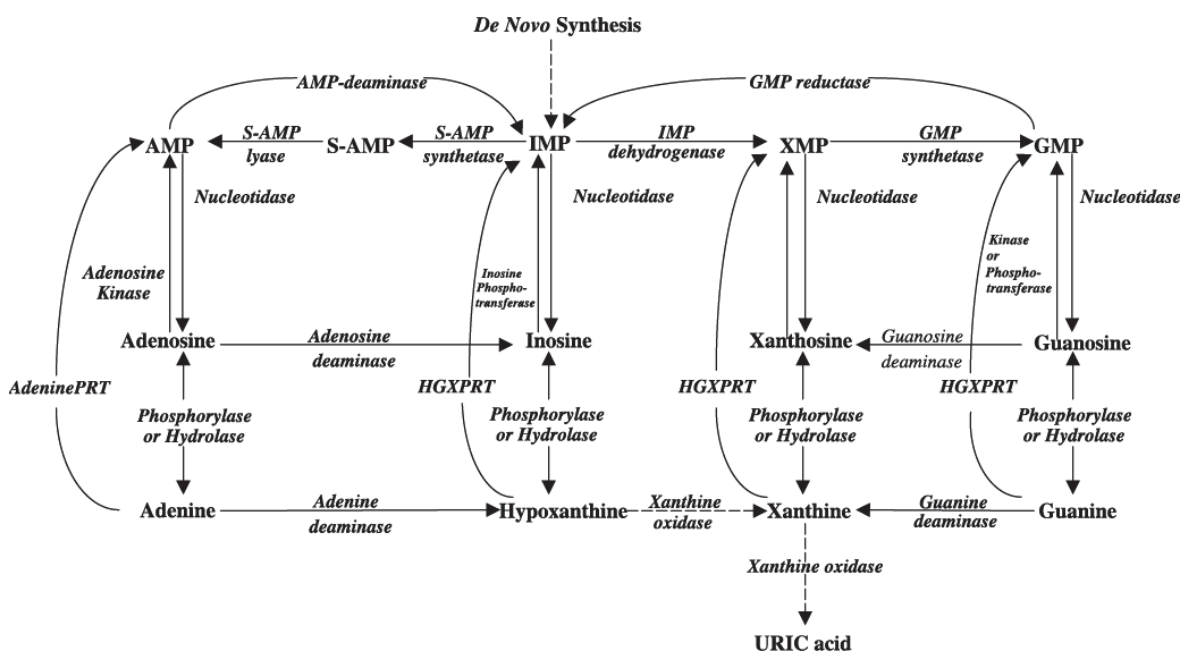

Fig. 4.4. Purine salvage pathways in protozoa, according to El Kouni et al (2003). The dashed lines indicate absent or non-identified reactions

❖ **Does dipyridamole recruit the purine salvage pathway?**

Dipyridamole has been shown to be a highly specific inhibitor of the mammalian ENT family of nucleoside transporters (Hyde et al., 2001). Most protozoan nucleoside transporters have been shown to be insensitive to dipyridamole (el Kouni, 2003). Inhibition of adenosine uptake by dipyridamole has however been reported in *T. brucei*, for two insect form specific nucleoside transporters (TbNT9 and TbNT10) with a K_i of 0.64 µM (Al-Salabi et al., 2007). In blood stream form, earlier reports claimed that at least 100 µM of dipyridamole is required for full inhibition of adenosine uptake (James and Born, 1980). This is probably due to the inhibition of TbAT1, the only nucleoside transporter in BSF known to be specific for adenosine and adenine (Maser et al., 1999). There is to date no evidence that the uptake of any other nucleoside, apart from adenosine, is inhibited by dipyridamole. TbPKA activation by this compound has been shown to be blood stream form specific (S. Bachmaier, this lab) and therefore probably associated with the stage specific expression the nucleoside transporters.

The nucleoside salvage pathway (Fig 4.5) indicates that adenosine is converted to inosine by adenosine deaminase. Dipyridamole has been shown to inhibit this kinase in the mammalian system (Wang et al., 1992). There is however no evidence, to date, that this also applies in *T. brucei.*

The known effects of dipyridamole points to either the inhibition of adenosine uptake or its conversion to inosine. This does not provide any plausible explanation as to how this would translate to TbPKA activation. A better understanding of the purine salvage pathway in kinetoplastids is required. The intracellular targets of dipyridamole can also be identified by pull-down experiments but would necessitate immobilization of dipyridamole to a suitable matrix.

❖ **Does 8-pCPT-adenosine recruit the purine salvage pathway?**

Agarose immobilized 8-pCPT-adenosine was used on a pull-down assay to show that this compound does not bind to TbPKA (section 3.3.3.2). The same approach, coupled to mass spectrometry analysis, was exploited to identify the intracellular target of this compound (E. Polatoglou. this lab). An inosine-guanosine preferring nucleoside hydrolase (Tb427.07.4570) was the best candidate. This enzyme cleaves the N-glycosidic bond in nucleosides, generating ribose and the respective purine base. This feature has been biochemically put to evidence in *T. brucei* (Vandemeulebroucke et al., 2010). The 8-pCPT-adenosine mode of action is still not known. Some adenosine analogues have however been shown to be competitive inhibitors of this enzyme, namely; tubercidin, 3'-deoxyadenosine and 3-deaza-adenosine (Parkin, 1996). It is likely that 8-pCPT-adenosine also inhibits the nucleoside hydrolase, resulting in nucleoside accumulation. This would however not be compatible with the loss of activation upon cold shock, assuming that TbPKA cold shock activation is mediated by nucleosides. If the antagonistic effect of 8-pCPT-adeosine is indeed by inhibiting the nucleoside hydrolase then the hydrolyzed purine bases would be the cold shock activation ligands. There is, so far, no evidence to suggest that purine bases have any activation potency.

The pathway acted upon by this analogue is therefore yet to be discovered. It is however interesting to already deduce that a key enzyme in the purine salvage pathway could be involved in the cold shock mediated activation of the kinase.

4.7.2 The interplay between cold shock and ligand activation

Cold shock activation of TbPKA is not only life cycle stage dependent (only in the BSF) but also isoform specific where only the TbPKAC1 holoenzyme isoform is involved (see section 3.3.1). There is sufficient evidence from this thesis to suggest that this kinase is very likely activated by nucleosides. A key question would therefore be how cold shock specifically activates the TbPKAC1 holoenzyme. Previous sub-localization studies of TbPKA could not reveal any isoform specificity since all the subunits were shown to be predominantly localized in the flagellum (C. Krumbholz, Ph.D. thesis 2006). There is however a life cycle stage expression pattern where for example the TbPKAC1 is not

expressed in the PCF and thereby the absence of the cold shock mechanism in this stage. This is however not sufficient since in the BSF form all the TbPKAC isoforms co-exist, although their relative amounts are yet to be determined. A key feature, analysed earlier, is the very distinct phosphorylation pattern between the catalytic subunits, which is very likely to impose holoenzyme specific features to each complex, such as different R/C affinities. It is therefore possible that the activation would then be dependent on the concentration of the ligand at a given time.

It was postulated in this thesis that cold shock could sensitize the holoenzyme complex for activation, such that a given ligand would have a higher activation potency at lower temperatures. Dose response measurements of adenosine at 20°C and 30°C indicated that the same ligand could indeed gain potency by decreasing temperature (see section 3.5). Although this notion is yet to be investigated further, its appeal is undeniable, as it would mean that cold shock does not activate signaling pathways for production of the activating ligand but rather sensitizes the kinase to the local ligand concentration. This is supported by the fact that more than 90% of the reporter protein in the in vivo kinase assay is phosphorylated within the 1st minute of cold shock induction (J. Pepperl, Diploma thesis 2007).

4.8 Conclusion and perspectives

The in silico approach coupled with in vitro kinase assays has been instrumental in shedding more light on how TbPKA is activated and also creating a clear divergence of this kinase from the rest of the PKA family. The molecular bases of nucleoside activation established in this thesis will be highly useful in the eventual identification of the endogenous ligand. Further exploitation of the isoform difference will deepen the understanding of the interplay between ligand activation and how this is coupled to the environmental cues already shown to influence the kinases activity. Almost as paramount as capturing the in vivo activation mechanism is the structural analysis of this kinase, which should confirm the structure model predictions while making a blue print for any future analysis of PKA in kinetoplastids.

5   References

Acs, G., Reich, E., and Mori, M. (1964). Biological and Biochemical Properties of the Analogue Antibiotic Tubercidin. Proc Natl Acad Sci U S A *52*, 493-501.

Aksoy, S., Gibson, W.C., and Lehane, M.J. (2003). Interactions between tsetse and trypanosomes with implications for the control of trypanosomiasis. Adv Parasitol *53*, 1-83.

Al-Salabi, M.I., Wallace, L.J., Luscher, A., Maser, P., Candlish, D., Rodenko, B., Gould, M.K., Jabeen, I., Ajith, S.N., and de Koning, H.P. (2007). Molecular interactions underlying the unusually high adenosine affinity of a novel Trypanosoma brucei nucleoside transporter. Molecular pharmacology *71*, 921-929.

Alsford, S., Eckert, S., Baker, N., Glover, L., Sanchez-Flores, A., Leung, K.F., Turner, D.J., Field, M.C., Berriman, M., and Horn, D. (2012). High-throughput decoding of antitrypanosomal drug efficacy and resistance. Nature *482*, 232-236.

Alsford, S., Turner, D.J., Obado, S.O., Sanchez-Flores, A., Glover, L., Berriman, M., Hertz-Fowler, C., and Horn, D. (2011). High-throughput phenotyping using parallel sequencing of RNA interference targets in the African trypanosome. Genome Res *21*, 915-924.

Anand, G.S., Hughes, C.A., Jones, J.M., Taylor, S.S., and Komives, E.A. (2002). Amide H/2H exchange reveals communication between the cAMP and catalytic subunit-binding sites in the R(I)alpha subunit of protein kinase A. Journal of molecular biology *323*, 377-386.

Asbroek, A.L., Mol, C.A., Kieft, R., and Borst, P. (1993). Stable transformation of Trypanosoma brucei. Mol Biochem Parasitol *59*, 133-142.

Aslett, M., Aurrecoechea, C., Berriman, M., Brestelli, J., Brunk, B.P., Carrington, M., Depledge, D.P., Fischer, S., Gajria, B., Gao, X.*, et al.* (2010). TriTrypDB: a functional genomic resource for the Trypanosomatidae. Nucleic Acids Res *38*, D457-462.

Banerjee, C., and Sarkar, D. (2001). The cAMP-binding proteins of Leishmania are not the regulatory subunits of cAMP-dependent protein kinase. Comp Biochem Physiol B Biochem Mol Biol *130*, 217-226.

Banky, P., Huang, L.J., and Taylor, S.S. (1998). Dimerization/docking domain of the type I alpha regulatory subunit of cAMP-dependent protein kinase. Requirements for dimerization and docking are distinct but overlapping. J Biol Chem *273*, 35048-35055.

Barquilla, A., Saldivia, M., Diaz, R., Bart, J.M., Vidal, I., Calvo, E., Hall, M.N., and Navarro, M. (2012). Third target of rapamycin complex negatively regulates development of quiescence in Trypanosoma brucei. Proc Natl Acad Sci U S A *109*, 14399-14404.

Barry, J.D., and McCulloch, R. (2001). Antigenic variation in trypanosomes: enhanced phenotypic variation in a eukaryotic parasite. Adv Parasitol *49*, 1-70.

Battaglia, U., Long, J.E., Searle, M.S., and Moody, C.J. (2011). 7-Deazapurine biosynthesis: NMR study of toyocamycin biosynthesis in Streptomyces rimosus using 2-13C-7-15N-adenine. Organic & Biomolecular Chemistry *9*, 2227-2232.

Berman, H.M., Ten Eyck, L.F., Goodsell, D.S., Haste, N.M., Kornev, A., and Taylor, S.S. (2005). The cAMP binding domain: an ancient signaling module. Proc Natl Acad Sci U S A *102*, 45-50.

Berriman, M., Ghedin, E., Hertz-Fowler, C., Blandin, G., Renauld, H., Bartholomeu, D.C., Lennard, N.J., Caler, E., Hamlin, N.E., Haas, B.*, et al.* (2005). The genome of the African trypanosome Trypanosoma brucei. Science *309*, 416-422.

Bhattacharya, A., Biswas, A., and Das, P.K. (2012). Identification of a protein kinase A regulatory subunit from Leishmania having importance in metacyclogenesis through induction of autophagy. Mol Microbiol *83*, 548-564.

Bieger, B., and Essen, L.O. (2001). Structural analysis of adenylate cyclases from Trypanosoma brucei in their monomeric state. Embo J *20*, 433-445.

Biswas, A., Bhattacharya, A., and Das, P.K. (2011). Role of cAMP Signaling in the Survival and Infectivity of the Protozoan Parasite, Leishmania donovani. Molecular biology international *2011*, 782971.

Bos, J.L. (2006). Epac proteins: multi-purpose cAMP targets. Trends in biochemical sciences *31*, 680-686.

Boshart, M., and Mottram, J.C. (1997). Protein phosphorylation and protein kinases in trypanosomatids. In Trypanosomiasis and Leishmaniasis, G. Hide, J.C. Mottram, G.H. Coombs, and P.H. Holmes, eds. (Wallingford, UK: CAB International), pp. 227-244.

Boynton, A.L., and Whitfield, J.F. (1983). The role of cyclic AMP in cell proliferation: a critical assessment of the evidence. Advances in Cyclic Nucleotide Research *15*, 193-294.

Bradford, M.M. (1976). A rapid and sensitive method for the quantitation of microgram quantities of protein utilizing the principle of protein-dye binding. Anal Biochem *72*, 248-254.

Bringaud, F., Barrett, M.P., and Zilberstein, D. (2012). Multiple roles of proline transport and metabolism in trypanosomatids. Frontiers in bioscience *17*, 349-374.

Brown, S.H., Wu, J., Kim, C., Alberto, K., and Taylor, S.S. (2009). Novel isoform-specific interfaces revealed by PKA RIIbeta holoenzyme structures. Journal of molecular biology *393*, 1070-1082.

Brun, R., Jenni, L., Tanner, M., Schonenberger, M., and Schell, K.F. (1979). Cultivation of vertebrate infective forms derived from metacyclic forms of pleomorphic Trypanosoma brucei stocks. Short communication. Acta Trop *36*, 387-390.

Brun, R., and Schonenberger, M. (1981). Stimulating effect of citrate and cis-Aconitate on the transformation of Trypanosoma brucei bloodstream forms to procyclic forms in vitro. Z Parasitenkd *66*, 17-24.

Burkard, G., Fragoso, C.M., and Roditi, I. (2007). Highly efficient stable transformation of bloodstream forms of Trypanosoma brucei. Mol Biochem Parasitol *153*, 220-223.

Butter, F., Bucerius, F., Michel, M., Cicova, Z., Mann, M., and Janzen, C.J. (2013). Comparative proteomics of two life cycle stages of stable isotope-labeled Trypanosoma brucei reveals novel components of the parasite's host adaptation machinery. Mol Cell Proteomics *12*, 172-179.

Cadd, G.G., Uhler, M.D., and McKnight, G.S. (1990). Holoenzymes of cAMP-dependent protein kinase containing the neural form of type I regulatory subunit have an increased sensitivity to cyclic nucleotides. Journal of Biological Chemistry *265*, 19502-19506.

Canaves, J.M., Leon, D.A., and Taylor, S.S. (2000). Consequences of cAMP-binding site mutations on the structural stability of the type I regulatory subunit of cAMP-dependent protein kinase. Biochemistry *39*, 15022-15031.

Canaves, J.M., and Taylor, S.S. (2002). Classification and phylogenetic analysis of the cAMP-dependent protein kinase regulatory subunit family. Journal of molecular evolution *54*, 17-29.

Cantrell, A.R., Tibbs, V.C., Yu, F.H., Murphy, B.J., Sharp, E.M., Qu, Y., Catterall, W.A., and Scheuer, T. (2002). Molecular mechanism of convergent regulation of brain Na(+) channels by protein kinase C and protein kinase A anchored to AKAP-15. Mol Cell Neurosci *21*, 63-80.

Cheng, X., Ma, Y., Moore, M., Hemmings, B.A., and Taylor, S.S. (1998). Phosphorylation and activation of cAMP-dependent protein kinase by phosphoinositide-dependent protein kinase. Proc Natl Acad Sci U S A *95*, 9849-9854.

Chun, M.W., Shin, D.H., Song, S.Y., Lee, Y.H., Lee, C.H., Jeong, L.S., and Lee, S.K. (1999). Synthesis of L-Sangivamycin and Toyocamycin Analogues and Their Inhibitory Activities of SER/THR Protein Kinases. Nucleosides and Nucleotides *18*, 617-618.

Chung, C.T., and Miller, R.H. (1988). A rapid and convenient method for the preparation and storage of competent bacterial cells. Nucleic Acids Res *16*, 3580.

Cole, C., Barber, J.D., and Barton, G.J. (2008). The Jpred 3 secondary structure prediction server. Nucleic Acids Res *36*, W197-201.

Corbin, J.D., Keely, S.L., and Park, C.R. (1975). The distribution and dissociation of cyclic adenosine 3':5'-monophosphate-dependent protein kinases in adipose, cardiac, and other tissues. J Biol Chem *250*, 218-225.

Corbin, J.D., Sugden, P.H., Lincoln, T.M., and Keely, S.L. (1977). Compartmentalization of adenosine 3':5'-monophosphate and adenosine 3':5'-monophosphate-dependent protein kinase in heart tissue. J Biol Chem *252*, 3854-3861.

Cross, e.a. (1975). Defined media for Trypanozoon. Kinetoplastida, 78-88.

Cross, G.A., and Manning, J.C. (1973). Cultivation of Trypanosoma brucei sspp. in semi-defined and defined media. Parasitology *67*, 315-331.

Cummings, D.E., Brandon, E.P., Planas, J.V., Motamed, K., Idzerda, R.L., and McKnight, G.S. (1996). Genetically lean mice result from targeted disruption of the RII beta subunit of protein kinase A. Nature *382*, 622-626.

de Koning, H.P., Bridges, D.J., and Burchmore, R.J. (2005). Purine and pyrimidine transport in pathogenic protozoa: from biology to therapy. FEMS microbiology reviews *29*, 987-1020.

de Koning, H.P., Gould, M.K., Sterk, G.J., Tenor, H., Kunz, S., Luginbuehl, E., and Seebeck, T. (2012). Pharmacological validation of Trypanosoma brucei phosphodiesterases as novel drug targets. The Journal of infectious diseases *206*, 229-237.

Dean, S., Marchetti, R., Kirk, K., and Matthews, K.R. (2009). A surface transporter family conveys the trypanosome differentiation signal. Nature *459*, 213-217.

Delauw, M.F., Pays, E., Steinert, M., Aerts, D., Van Meirvenne, N., and Le Ray, D. (1985). Inactivation and reactivation of a variant-specific antigen gene in cyclically transmitted Trypanosoma brucei. Embo J *4*, 989-993.

Demaille, J.G., Peters, K.A., Strandjord, T.P., and Fischer, E.H. (1978). Isolation and properties of the bovine brain protein inhibitor of adenosine 3':5'-monophosphate-dependent protein kinases. In FEBS letters, pp. 113-116.

Diller, T.C., Madhusudan, Xuong, N.H., and Taylor, S.S. (2001). Molecular basis for regulatory subunit diversity in cAMP-dependent protein kinase: crystal structure of the type II beta regulatory subunit. Structure *9*, 73-82.

Diskar, M., Zenn, H.M., Kaupisch, A., Kaufholz, M., Brockmeyer, S., Sohmen, D., Berrera, M., Zaccolo, M., Boshart, M., Herberg, F.W*., et al.* (2010). Regulation of cAMP-dependent protein kinases: the human protein kinase X (PrKX) reveals the role of the catalytic subunit alphaH-alphaI loop. J Biol Chem *285*, 35910-35918.

Dower, W.J., Miller, J.F., and Ragsdale, C.W. (1988). High efficiency transformation of E. coli by high voltage electroporation. Nucleic Acids Res *16*, 6127-6145.

Drew, M.E., Morris, J.C., Wang, Z., Wells, L., Sanchez, M., Landfear, S.M., and Englund, P.T. (2003). The adenosine analog tubercidin inhibits glycolysis in Trypanosoma brucei as revealed by an RNA interference library. J Biol Chem *278*, 46596-46600.

el Kouni, M.H. (2003). Potential chemotherapeutic targets in the purine metabolism of parasites. Pharmacology & therapeutics *99*, 283-309.

El-Sayed, N.M., Myler, P.J., Bartholomeu, D.C., Nilsson, D., Aggarwal, G., Tran, A.N., Ghedin, E., Worthey, E.A., Delcher, A.L., Blandin, G*., et al.* (2005). The genome sequence of Trypanosoma cruzi, etiologic agent of Chagas disease. Science *309*, 409-415.

Engstler, M., and Boshart, M. (2004). Cold shock and regulation of surface protein trafficking convey sensitization to inducers of stage differentiation in Trypanosoma brucei. Genes Dev *18*, 2798-2811.

Esseltine, J.L., and Scott, J.D. (2013). AKAP signaling complexes: pointing towards the next generation of therapeutic targets? Trends Pharmacol Sci *34*, 648-655.

Eswar, N., Eramian, D., Webb, B., Shen, M.Y., and Sali, A. (2008). Protein structure modeling with MODELLER. Methods Mol Biol *426*, 145-159.

Fenn, K., and Matthews, K.R. (2007). The cell biology of Trypanosoma brucei differentiation. Curr Opin Microbiol *10*, 539-546.

Fiser, A., and Sali, A. (2003). Modeller: generation and refinement of homology-based protein structure models. Methods Enzymol *374*, 461-491.

Fitzgerald, D.J., Berger, P., Schaffitzel, C., Yamada, K., Richmond, T.J., and Berger, I. (2006). Protein complex expression by using multigene baculoviral vectors. Nat Methods *3*, 1021-1032.

Flockhart, D.A., and Corbin, J.D. (1982). Regulatory mechanisms in the control of protein kinases. CRC critical reviews in biochemistry *12*, 133-186.

Gallagher, S.R. (2001). One-Dimensional SDS Gel Electrophoresis of Proteins. In Current Protocols in Molecular Biology (John Wiley & Sons, Inc.).

Gassen, A., Brechtefeld, D., Schandry, N., Arteaga-Salas, J.M., Israel, L., Imhof, A., and Janzen, C.J. (2012). DOT1A-dependent H3K76 methylation is required for replication regulation in Trypanosoma brucei. Nucleic Acids Res *40*, 10302-10311.

Gaud, A., Carrington, M., Deshusses, J., and Schaller, D.R. (1997). Polymerase chain reaction-based gene disruption in Trypanosoma brucei. Mol Biochem Parasitol *87*, 113-115.

Geigy, R., Jenni, L., Kauffmann, M., Onyango, R.J., and Weiss, N. (1975). Identification of T. brucei-subgroup strains isolated from game. Acta Trop *32*, 190-205.

Gelbin, A., Schneider, B., Clowney, L., Hsieh, S.-H., Olson, W.K., and Berman, H.M. (1996). Geometric Parameters in Nucleic Acids: Sugar and Phosphate Constituents. Journal of the American Chemical Society *118*, 519-529.

Gherardini, P.F., Ausiello, G., Russell, R.B., and Helmer-Citterich, M. (2010). Modular architecture of nucleotide-binding pockets. Nucleic Acids Res *38*, 3809-3816.

Glass, D.B., Cheng, H.C., Kemp, B.E., and Walsh, D.A. (1986). Differential and common recognition of the catalytic sites of the cGMP-dependent and cAMP-dependent protein kinases by inhibitory peptides derived from the heat-stable inhibitor protein. J Biol Chem *261*, 12166-12171.

Gould, M.K., Bachmaier, S., Ali, J.A., Alsford, S., Tagoe, D.N., Munday, J.C., Schnaufer, A.C., Horn, D., Boshart, M., and de Koning, H.P. (2013). Cyclic AMP effectors in African trypanosomes revealed by genome-scale RNA interference library screening for resistance to the phosphodiesterase inhibitor CpdA. Antimicrob Agents Chemother *57*, 4882-4893.

Gould, M.K., and de Koning, H.P. (2011). Cyclic-nucleotide signalling in protozoa. FEMS microbiology reviews *35*, 515-541.

Grossman, T.H., Kawasaki, E.S., Punreddy, S.R., and Osburne, M.S. (1998). Spontaneous cAMP-dependent derepression of gene expression in stationary phase plays a role in recombinant expression instability. Gene *209*, 95-103.

Gruszynski, A.E., van Deursen, F.J., Albareda, M.C., Best, A., Chaudhary, K., Cliffe, L.J., del Rio, L., Dunn, J.D., Ellis, L., Evans, K.J.*, et al.* (2006). Regulation of surface coat exchange by differentiating African trypanosomes. Mol Biochem Parasitol *147*, 211-223.

Gunasekera, K., Wuthrich, D., Braga-Lagache, S., Heller, M., and Ochsenreiter, T. (2012). Proteome remodelling during development from blood to insect-form Trypanosoma brucei quantified by SILAC and mass spectrometry. BMC Genomics *13*, 556.

Hammarton, T.C. (2007). Cell cycle regulation in Trypanosoma brucei. Mol Biochem Parasitol *153*, 1-8.

Hanks, S.K., Quinn, A.M., and Hunter, T. (1988). The protein kinase family: conserved features and deduced phylogeny of the catalytic domains. Science *241*, 42-52.

Harbeck, B., Huttelmaier, S., Schluter, K., Jockusch, B.M., and Illenberger, S. (2000). Phosphorylation of the vasodilator-stimulated phosphoprotein regulates its interaction with actin. J Biol Chem *275*, 30817-30825.

Hastie, C.J., McLauchlan, H.J., and Cohen, P. (2006). Assay of protein kinases using radiolabeled ATP: a protocol. Nat Protoc *1*, 968-971.

Haston, W.S. (1972). Development of Trypanosoma brucei in the gut of Glossina morsitans. Trans R Soc Trop Med Hyg *66*, 548.

Hemmings, B.A. (1986). cAMP mediated proteolysis of the catalytic subunit of cAMP-dependent protein kinase. FEBS letters *196*, 126-130.

Herberg, F.W., Taylor, S.S., and Dostmann, W.R. (1996). Active site mutations define the pathway for the cooperative activation of cAMP-dependent protein kinase. Biochemistry *35*, 2934-2942.

Hidaka, H., Inagaki, M., Kawamoto, S., and Sasaki, Y. (1984). Isoquinolinesulfonamides, novel and potent inhibitors of cyclic nucleotide dependent protein kinase and protein kinase C. Biochemistry *23*, 5036-5041.

Hildebrand, A., Remmert, M., Biegert, A., and Soding, J. (2009). Fast and accurate automatic structure prediction with HHpred. Proteins *77 Suppl 9*, 128-132.

Hink, W.F. (1970). Established insect cell line from the cabbage looper, Trichoplusia ni. Nature *226*, 466-467.

Hirumi, H., and Hirumi, K. (1989). Continuous cultivation of Trypanosoma brucei blood stream forms in a medium containing a low concentration of serum protein without feeder cell layers. J Parasitol *75*, 985-989.

Ho, S.N., Hunt, H.D., Horton, R.M., Pullen, J.K., and Pease, L.R. (1989). Site-directed mutagenesis by overlap extension using the polymerase chain reaction. Gene *77*, 51-59.

Hofmann, F., Beavo, J.A., Bechtel, P.J., and Krebs, E.G. (1975). Comparison of adenosine 3':5'-monophosphate-dependent protein kinases from rabbit skeletal and bovine heart muscle. J Biol Chem *250*, 7795-7801.

Huang, H., Weiss, L.M., Nagajyothi, F., Tanowitz, H.B., Wittner, M., Orr, G.A., and Bao, Y. (2006). Molecular cloning and characterization of the protein kinase A regulatory subunit of Trypanosoma cruzi. Mol Biochem Parasitol *149*, 242-245.

Huang, H., Werner, C., Weiss, L.M., Wittner, M., and Orr, G.A. (2002). Molecular cloning and expression of the catalytic subunit of protein kinase A from Trypanosoma cruzi. International journal for parasitology *32*, 1107-1115.

Hyde, R.J., Cass, C.E., Young, J.D., and Baldwin, S.A. (2001). The ENT family of eukaryote nucleoside and nucleobase transporters: recent advances in the investigation of structure/function relationships and the identification of novel isoforms. Molecular membrane biology *18*, 53-63.

Ivens, A.C., Peacock, C.S., Worthey, E.A., Murphy, L., Aggarwal, G., Berriman, M., Sisk, E., Rajandream, M.A., Adlem, E., Aert, R.*, et al.* (2005). The genome of the kinetoplastid parasite, Leishmania major. Science *309*, 436-442.

James, D., and Born, G. (1980). Uptake of purine bases and nucleosides in African trypanosomes. Parasitology.

Jensen, B.C., Sivam, D., Kifer, C.T., Myler, P.J., and Parsons, M. (2009). Widespread variation in transcript abundance within and across developmental stages of Trypanosoma brucei. BMC Genomics *10*, 482.

Jones, N.G., Thomas, E.B., Brown, E., Dickens, N.J., Hammarton, T.C., and Mottram, J.C. (2014). Regulators of Trypanosoma brucei cell cycle progression and differentiation identified using a kinome-wide RNAi screen. PLoS Pathog *10*, e1003886.

Kabani, S., Fenn, K., Ross, A., Ivens, A., Smith, T.K., Ghazal, P., and Matthews, K. (2009). Genome-wide expression profiling of in vivo-derived bloodstream parasite stages and dynamic analysis of mRNA alterations during synchronous differentiation in Trypanosoma brucei. BMC Genomics *10*, 427.

Kajava, A.V. (1998). Structural diversity of leucine-rich repeat proteins. Journal of molecular biology *277*, 519-527.

Kannan, N., Haste, N., Taylor, S.S., and Neuwald, A.F. (2007). The hallmark of AGC kinase functional divergence is its C-terminal tail, a cis-acting regulatory module. Proc Natl Acad Sci U S A *104*, 1272-1277.

Kase, H., Iwahashi, K., Nakanishi, S., Matsuda, Y., Yamada, K., Takahashi, M., Murakata, C., Sato, A., and Kaneko, M. (1987). K-252 compounds, novel and potent inhibitors of protein kinase C and

cyclic nucleotide-dependent protein kinases. Biochemical and biophysical research communications *142*, 436-440.

Kaupp, U.B., and Seifert, R. (2002). Cyclic nucleotide-gated ion channels. Physiological reviews *82*, 769-824.

Kemp, B.E., Benjamini, E., and Krebs, E.G. (1976). Synthetic hexapeptide substrates and inhibitors of 3':5'-cyclic AMP-dependent protein kinase. Proc Natl Acad Sci U S A *73*, 1038-1042.

Kemp, B.E., Bylund, D.B., Huang, T.S., and Krebs, E.G. (1975). Substrate specificity of the cyclic AMP-dependent protein kinase. Proc Natl Acad Sci U S A *72*, 3448-3452.

Kim, C., Cheng, C.Y., Saldanha, S.A., and Taylor, S.S. (2007). PKA-I holoenzyme structure reveals a mechanism for cAMP-dependent activation. Cell *130*, 1032-1043.

Kim, C., Xuong, N.H., and Taylor, S.S. (2005). Crystal structure of a complex between the catalytic and regulatory (RIalpha) subunits of PKA. Science *307*, 690-696.

Kim, J.J., Casteel, D.E., Huang, G., Kwon, T.H., Ren, R.K., Zwart, P., Headd, J.J., Brown, N.G., Chow, D.-C., Palzkill, T.*, et al.* (2011). Co-Crystal Structures of PKG Iβ (92‑227) with cGMP and cAMP Reveal the Molecular Details of Cyclic-Nucleotide Binding. PLoS ONE *6*, e18413.

Knighton, D.R., Bell, S.M., Zheng, J., Ten Eyck, L.F., Xuong, N.H., Taylor, S.S., and Sowadski, J.M. (1993). 2.0 A refined crystal structure of the catalytic subunit of cAMP-dependent protein kinase complexed with a peptide inhibitor and detergent. Acta Crystallogr D Biol Crystallogr *49*, 357-361.

Knighton, D.R., Zheng, J.H., Ten Eyck, L.F., Ashford, V.A., Xuong, N.H., Taylor, S.S., and Sowadski, J.M. (1991a). Crystal structure of the catalytic subunit of cyclic adenosine monophosphate-dependent protein kinase. Science *253*, 407-414.

Knighton, D.R., Zheng, J.H., Ten Eyck, L.F., Xuong, N.H., Taylor, S.S., and Sowadski, J.M. (1991b). Structure of a peptide inhibitor bound to the catalytic subunit of cyclic adenosine monophosphate-dependent protein kinase. Science *253*, 414-420.

Kobe, B., and Kajava, A.V. (2001). The leucine-rich repeat as a protein recognition motif. Current opinion in structural biology *11*, 725-732.

Kohl, L., Sherwin, T., and Gull, K. (1999). Assembly of the paraflagellar rod and the flagellum attachment zone complex during the Trypanosoma brucei cell cycle. J Eukaryot Microbiol *46*, 105-109.

Kramer, S., Klockner, T., Selmayr, M., and Boshart, M. (2007). Interstrain sequence comparison, transcript map and clonal genomic rearrangement of a 28 kb locus on chromosome 9 of Trypanosoma brucei. Mol Biochem Parasitol *151*, 129-132.

Krebs, E.G., and Beavo, J.A. (1979). Phosphorylation-dephosphorylation of enzymes. Annual review of biochemistry *48*, 923-959.

Kunz, S., Kloeckner, T., Essen, L.O., Seebeck, T., and Boshart, M. (2004). TbPDE1, a novel class I phosphodiesterase of Trypanosoma brucei. European journal of biochemistry / FEBS *271*, 637-647.

Kushnir, S., Gase, K., Breitling, R., and Alexandrov, K. (2005). Development of an inducible protein expression system based on the protozoan host Leishmania tarentolae. Protein Expr Purif *42*, 37-46.

Kyhse-Andersen, J. (1984). Electroblotting of multiple gels: a simple apparatus without buffer tank for rapid transfer of proteins from polyacrylamide to nitrocellulose. J Biochem Biophys Methods *10*, 203-209.

Laemmli, U.K. (1970). Cleavage of structural proteins during the assembly of the head of bacteriophage T4. Nature *227*, 680-685.

Landfear, S.M., Ullman, B., Carter, N.S., and Sanchez, M.A. (2004). Nucleoside and nucleobase transporters in parasitic protozoa. Eukaryotic cell *3*, 245-254.

Laxman, S., Riechers, A., Sadilek, M., Schwede, F., and Beavo, J.A. (2006). Hydrolysis products of cAMP analogs cause transformation of Trypanosoma brucei from slender to stumpy-like forms. Proc Natl Acad Sci U S A *103*, 19194-19199.

Leon, D.A., Herberg, F.W., Banky, P., and Taylor, S.S. (1997). A stable alpha-helical domain at the N terminus of the Rlalpha subunits of cAMP-dependent protein kinase is a novel dimerization/docking motif. J Biol Chem *272*, 28431-28437.

Levitzki, A. (1988). From epinephrine to cyclic AMP. Science *241*, 800-806.

Li, M., West, J.W., Numann, R., Murphy, B.J., Scheuer, T., and Catterall, W.A. (1993). Convergent regulation of sodium channels by protein kinase C and cAMP-dependent protein kinase. Science *261*, 1439-1442.

Lincoln, T.M. (1983). cGMP-dependent protein kinase. Methods Enzymol *99*, 62-71.

Liu, A.Y. (1982). Differentiation-specific increase of cAMP-dependent protein kinase in the 3T3-L1 cells. J Biol Chem *257*, 298-306.

Lucast, L.J., Batey, R.T., and Doudna, J.A. (2001). Large-scale purification of a stable form of recombinant tobacco etch virus protease. Biotechniques *30*, 544-546, 548, 550 passim.

Lugnier, C. (2006). Cyclic nucleotide phosphodiesterase (PDE) superfamily: a new target for the development of specific therapeutic agents. Pharmacology & therapeutics *109*, 366-398.

Mancini, P.E., and Patton, C.L. (1981). Cyclic 3',5'-adenosine monophosphate levels during the developmental cycle of Trypanosoma brucei brucei in the rat. Molecular and Biochemical Parasitology *3*, 19-31.

Maser, P., Sutterlin, C., Kralli, A., and Kaminsky, R. (1999). A nucleoside transporter from Trypanosoma brucei involved in drug resistance. Science *285*, 242-244.

Massillon, D., Stalmans, W., van de Werve, G., and Bollen, M. (1994). Identification of the glycogenic compound 5-iodotubercidin as a general protein kinase inhibitor. The Biochemical journal *299 (Pt 1)*, 123-128.

Matthews, K.R., Ellis, J.R., and Paterou, A. (2004). Molecular regulation of the life cycle of African trypanosomes. Trends Parasitol *20*, 40-47.

Matthews, K.R., and Gull, K. (1994). Cycles within cycles: the interplay between differentiation and cell division in Trypanosoma brucei. Parasitol Today *10*, 473-476.

McCulloch, R., Vassella, E., Burton, P., Boshart, M., and Barry, J.D. (2004). Transformation of monomorphic and pleomorphic Trypanosoma brucei. Methods Mol Biol *262*, 53-86.

McKean, P.G. (2003). Coordination of cell cycle and cytokinesis in Trypanosoma brucei. Curr Opin Microbiol *6*, 600-607.

Miroux, B., and Walker, J.E. (1996). Over-production of proteins in Escherichia coli: mutant hosts that allow synthesis of some membrane proteins and globular proteins at high levels. Journal of molecular biology *260*, 289-298.

Montminy, M. (1997). Transcriptional regulation by cyclic AMP. Annual review of biochemistry *66*, 807-822.

Morris, J.C., Wang, Z., Drew, M.E., and Englund, P.T. (2002). Glycolysis modulates trypanosome glycoprotein expression as revealed by an RNAi library. EMBO J *21*, 4429-4438.

Murray, A.J. (2008). Pharmacological PKA inhibition: all may not be what it seems. Science signaling *1*, re4.

Nett, I.R., Martin, D.M., Miranda-Saavedra, D., Lamont, D., Barber, J.D., Mehlert, A., and Ferguson, M.A. (2009). The phosphoproteome of bloodstream form Trypanosoma brucei, causative agent of African sleeping sickness. Mol Cell Proteomics *8*, 1527-1538.

Newlon, M.G., Roy, M., Morikis, D., Hausken, Z.E., Coghlan, V., Scott, J.D., and Jennings, P.A. (1999). The molecular basis for protein kinase A anchoring revealed by solution NMR. Nature Structural Biology *6*, 222-227.

Nishimura, H., Katagiri, K., Sato, K., Mayama, M., and Shimaoka, N. (1956). Toyocamycin, a new anti-candida antibiotics. The Journal of antibiotics *9*, 60-62.

Nobeli, I., Laskowski, R.A., Valdar, W.S., and Thornton, J.M. (2001). On the molecular discrimination between adenine and guanine by proteins. Nucleic Acids Res *29*, 4294-4309.

Oberholzer, M., Marti, G., Baresic, M., Kunz, S., Hemphill, A., and Seebeck, T. (2007). The Trypanosoma brucei cAMP phosphodiesterases TbrPDEB1 and TbrPDEB2: flagellar enzymes that are essential for parasite virulence. FASEB J *21*, 720-731.

Ogreid, D., and Doskeland, S.O. (1981). The kinetics of the interaction between cyclic AMP and the regulatory moiety of protein kinase II. Evidence for interaction between the binding sites for cyclic AMP. FEBS letters *129*, 282-286.

Ogreid, D., and Doskeland, S.O. (1983). Cyclic nucleotides modulate the release of [3H] adenosine cyclic 3',5'-phosphate bound to the regulatory moiety of protein kinase I by the catalytic subunit of the kinase. Biochemistry *22*, 1686-1696.

Olmsted, J.B. (1981). Affinity purification of antibodies from diazotized paper blots of heterogeneous protein samples. J Biol Chem *256*, 11955-11957.

Ortiz, D., Sanchez, M.A., Quecke, P., and Landfear, S.M. (2009). Two novel nucleobase/pentamidine transporters from Trypanosoma brucei. Mol Biochem Parasitol *163*, 67-76.

Paindavoine, P., Rolin, S., Van Assel, S., Geuskens, M., Jauniaux, J.C., Dinsart, C., Huet, G., and Pays, E. (1992). A gene from the variant surface glycoprotein expression site encodes one of several transmembrane adenylate cyclases located on the flagellum of Trypanosoma brucei. Mol Cell Biol *12*, 1218-1225.

Parca, L., Gherardini, P.F., Truglio, M., Mangone, I., Ferre, F., Helmer-Citterich, M., and Ausiello, G. (2012). Identification of nucleotide-binding sites in protein structures: a novel approach based on nucleotide modularity. PLoS One *7*, e50240.

Parkin, D.W. (1996). Purine-specific nucleoside N-ribohydrolase from Trypanosoma brucei brucei. Purification, specificity, and kinetic mechanism. J Biol Chem *271*, 21713-21719.

Parsons, M., Worthey, E.A., Ward, P.N., and Mottram, J.C. (2005). Comparative analysis of the kinomes of three pathogenic trypanosomatids: Leishmania major, Trypanosoma brucei and Trypanosoma cruzi. BMC Genomics *6*, 127.

Pays, E. (2005). Regulation of antigen gene expression in Trypanosoma brucei. Trends Parasitol *21*, 517-520.

Pays, E. (2006). The variant surface glycoprotein as a tool for adaptation in African trypanosomes. Microbes and infection / Institut Pasteur *8*, 930-937.

Portman, N., and Gull, K. (2012). Proteomics and the Trypanosoma brucei cytoskeleton: advances and opportunities. Parasitology *139*, 1168-1177.

Priest, J.W., and Hajduk, S.L. (1994). Developmental regulation of mitochondrial biogenesis in Trypanosoma brucei. J Bioenerg Biomembr *26*, 179-191.

Rangel-Aldao, R., and Rosen, O.M. (1976). Dissociation and reassociation of the phosphorylated and nonphosphorylated forms of adenosine 3':5' -monophosphate-dependent protein kinase from bovine cardiac muscle. J Biol Chem *251*, 3375-3380.

Rao, K.V. (1968). Structure of sangivamycin. Journal of medicinal chemistry *11*, 939-941.

Rehmann, H., Wittinghofer, A., and Bos, J.L. (2007). Capturing cyclic nucleotides in action: snapshots from crystallographic studies. Nature reviews Molecular cell biology *8*, 63-73.

Reuner, B., Vassella, E., Yutzy, B., and Boshart, M. (1997). Cell density triggers slender to stumpy differentiation of Trypanosoma brucei bloodstream forms in culture. Mol Biochem Parasitol *90*, 269-280.

Rico, E., Rojas, F., Mony, B.M., Szoor, B., MacGregor, P., and Matthews, K.R. (2013). Bloodstream form pre-adaptation to the tsetse fly in Trypanosoma brucei. Frontiers in Cellular and Infection Microbiology *3*.

Rinaldi, J., Wu, J., Yang, J., Ralston, C.Y., Sankaran, B., Moreno, S., and Taylor, S.S. (2010). Structure of yeast regulatory subunit: a glimpse into the evolution of PKA signaling. Structure *18*, 1471-1482.

Roditi, I., Schwarz, H., Pearson, T.W., Beecroft, R.P., Liu, M.K., Richardson, J.P., Buhring, H.J., Pleiss, J., Bulow, R., Williams, R.O.*, et al.* (1989). Procyclin gene expression and loss of the variant surface glycoprotein during differentiation of Trypanosoma brucei. J Cell Biol *108*, 737-746.

Rolin, S., Hancocq-Quertier, J., Paturiaux-Hanocq, F., Nolan, D.P., and Pays, E. (1998). Mild acid stress as a differentiation trigger in Trypanosoma brucei. Mol Biochem Parasitol *93*, 251-262.

Rolin, S., Hanocq-Quertier, J., Paturiaux-Hanocq, F., Nolan, D., Salmon, D., Webb, H., Carrington, M., Voorheis, P., and Pays, E. (1996). Simultaneous but independent activation of adenylate cyclase and glycosylphosphatidylinositol-phospholipase C under stress conditions in Trypanosoma brucei. J Biol Chem *271*, 10844-10852.

Sadana, R., and Dessauer, C.W. (2009). Physiological roles for G protein-regulated adenylyl cyclase isoforms: insights from knockout and overexpression studies. Neuro-Signals *17*, 5-22.

Sali, A., and Blundell, T.L. (1993). Comparative protein modelling by satisfaction of spatial restraints. Journal of molecular biology *234*, 779-815.

Sambrook, J., Fritsch, E.F. and Maniatis, T. (1989). Molecular cloning: a laboratory manual. Cold Spring Harbor Laboratory Press, Plainview, NY, USA.

Saran, S., Meima, M.E., Alvarez-Curto, E., Weening, K.E., Rozen, D.E., and Schaap, P. (2002). cAMP signaling in Dictyostelium. Complexity of cAMP synthesis, degradation and detection. J Muscle Res Cell Motil *23*, 793-802.

Saraswat, L.D., Filutowicz, M., and Taylor, S.S. (1986). Expression of the type I regulatory subunit of cAMP-dependent protein kinase in Escherichia coli. J Biol Chem *261*, 11091-11096.

Sbicego, S., Vassella, E., Kurath, U., Blum, B., and Roditi, I. (1999). The use of transgenic Trypanosoma brucei to identify compounds inducing the differentiation of bloodstream forms to procyclic forms. Mol Biochem Parasitol *104*, 311-322.

Schimanski, B., Nguyen, T.N., and Gunzl, A. (2005). Highly efficient tandem affinity purification of trypanosome protein complexes based on a novel epitope combination. Eukaryotic cell *4*, 1942-1950.

Schumann, G., Jutzi, P., and Roditi, I. (2011). Genome-wide RNAi screens in bloodstream form trypanosomes identify drug transporters. Mol Biochem Parasitol *175*, 91-94.

Schwartz, D.A., and Rubin, C.S. (1985). Identification and differential expression of two forms of regulatory subunits (RII) of cAMP-dependent protein kinase II in Friend erythroleukemic cells. Differentiation and 8-bromo-cAMP elicit a large and selective increase in the rate of biosynthesis of only one type of RII. Journal of Biological Chemistry *260*, 6296-6303.

Scott, J.D., and McCartney, S. (1994). Localization of A-kinase through anchoring proteins. Molecular endocrinology *8*, 5-11.

Seebeck, T., Schaub, R., and Johner, A. (2004). cAMP signalling in the kinetoplastid protozoa. Curr Mol Med *4*, 585-599.

Seed, J.R. (1978). Competition among serologically different clones of Trypanosoma brucei gambiense in vivo. J Protozool *25*, 526-529.

Seidler, J., Adal, M., Kubler, D., Bossemeyer, D., and Lehmann, W.D. (2009). Analysis of autophosphorylation sites in the recombinant catalytic subunit alpha of cAMP-dependent kinase by nano-UPLC-ESI-MS/MS. Analytical and bioanalytical chemistry *395*, 1713-1720.

Shabb, J.B., Buzzeo, B.D., Ng, L., and Corbin, J.D. (1991). Mutating protein kinase cAMP-binding sites into cGMP-binding sites. Mechanism of cGMP selectivity. J Biol Chem *266*, 24320-24326.

Shalaby, T., Liniger, M., and Seebeck, T. (2001). The regulatory subunit of a cGMP-regulated protein kinase A of Trypanosoma brucei. European journal of biochemistry / FEBS *268*, 6197-6206.

Sievers, F., Wilm, A., Dineen, D., Gibson, T.J., Karplus, K., Li, W., Lopez, R., McWilliam, H., Remmert, M., Soding, J.*, et al.* (2011). Fast, scalable generation of high-quality protein multiple sequence alignments using Clustal Omega. Mol Syst Biol *7*, 539.

Siman-Tov, M.M., Aly, R., Shapira, M., and Jaffe, C.L. (1996). Cloning from Leishmania major of a developmentally regulated gene, c-lpk2, for the catalytic subunit of the cAMP-dependent protein kinase. Mol Biochem Parasitol *77*, 201-215.

Siman-Tov, M.M., Ivens, A.C., and Jaffe, C.L. (2002). Molecular cloning and characterization of two new isoforms of the protein kinase A catalytic subunit from the human parasite Leishmania. Gene *288*, 65-75.

Simarro, P.P., Cecchi, G., Paone, M., Franco, J.R., Diarra, A., Ruiz, J.A., Fevre, E.M., Courtin, F., Mattioli, R.C., and Jannin, J.G. (2009). The Atlas of human African trypanosomiasis: a contribution to global mapping of neglected tropical diseases. Int J Health Geogr *9*, 57.

Slice, L.W., and Taylor, S.S. (1989). Expression of the catalytic subunit of cAMP-dependent protein kinase in Escherichia coli. J Biol Chem *264*, 20940-20946.

Soberg, K., Jahnsen, T., Rognes, T., Skalhegg, B.S., and Laerdahl, J.K. (2013). Evolutionary paths of the cAMP-dependent protein kinase (PKA) catalytic subunits. PLoS One *8*, e60935.

Soding, J. (2005). Protein homology detection by HMM-HMM comparison. Bioinformatics *21*, 951-960.

Stano, N.M., and Patel, S.S. (2004). T7 lysozyme represses T7 RNA polymerase transcription by destabilizing the open complex during initiation. J Biol Chem *279*, 16136-16143.

Steichen, J.M., Kuchinskas, M., Keshwani, M.M., Yang, J., Adams, J.A., and Taylor, S.S. (2012). Structural basis for the regulation of protein kinase A by activation loop phosphorylation. J Biol Chem *287*, 14672-14680.

Steinberg, R.A., Cauthron, R.D., Symcox, M.M., and Shuntoh, H. (1993). Autoactivation of catalytic (C alpha) subunit of cyclic AMP-dependent protein kinase by phosphorylation of threonine 197. Mol Cell Biol *13*, 2332-2341.

Studier, F.W. (2005). Protein production by auto-induction in high density shaking cultures. Protein Expr Purif *41*, 207-234.

Su, Y., Dostmann, W.R., Herberg, F.W., Durick, K., Xuong, N.H., Ten Eyck, L., Taylor, S.S., and Varughese, K.I. (1995). Regulatory subunit of protein kinase A: structure of deletion mutant with cAMP binding domains. Science *269*, 807-813.

Szoor, B., Ruberto, I., Burchmore, R., and Matthews, K.R. (2010). A novel phosphatase cascade regulates differentiation in Trypanosoma brucei via a glycosomal signaling pathway. Genes Dev *24*, 1306-1316.

Szoor, B., Wilson, J., McElhinney, H., Tabernero, L., and Matthews, K.R. (2006). Protein tyrosine phosphatase TbPTP1: A molecular switch controlling life cycle differentiation in trypanosomes. J Cell Biol *175*, 293-303.

Takio, K., Smith, S.B., Krebs, E.G., Walsh, K.A., and Titani, K. (1984). Amino acid sequence of the regulatory subunit of bovine type II adenosine cyclic 3',5'-phosphate dependent protein kinase. Biochemistry *23*, 4200-4206.

Tash, J.S., and Means, A.R. (1983). Cyclic adenosine 3',5' monophosphate, calcium and protein phosphorylation in flagellar motility. Biol Reprod *28*, 75-104.

Taylor, S.S., Ilouz, R., Zhang, P., and Kornev, A.P. (2012). Assembly of allosteric macromolecular switches: lessons from PKA. Nature reviews Molecular cell biology *13*, 646-658.

Taylor, S.S., Kim, C., Cheng, C.Y., Brown, S.H., Wu, J., and Kannan, N. (2008). Signaling through cAMP and cAMP-dependent protein kinase: diverse strategies for drug design. Biochimica et biophysica acta *1784*, 16-26.

Taylor, S.S., Radzio-Andzelm, E., Knighton, D.R., Ten Eyck, L.F., Sowadski, J.M., Herberg, F.W., Yonemoto, W., and Zheng, J. (1993). Crystal structures of the catalytic subunit of cAMP-dependent protein kinase reveal general features of the protein kinase family. Receptor *3*, 165-172.

Tholey, A., Pipkorn, R., Bossemeyer, D., Kinzel, V., and Reed, J. (2001). Influence of myristoylation, phosphorylation, and deamidation on the structural behavior of the N-terminus of the catalytic subunit of cAMP-dependent protein kinase. Biochemistry *40*, 225-231.

Titani, K., Sasagawa, T., Ericsson, L.H., Kumar, S., Smith, S.B., Krebs, E.G., and Walsh, K.A. (1984). Amino acid sequence of the regulatory subunit of bovine type I adenosine cyclic 3',5'-phosphate dependent protein kinase. Biochemistry *23*, 4193-4199.

Ullu, E., Tschudi, C., and Chakraborty, T. (2004). RNA interference in protozoan parasites. Cell Microbiol *6*, 509-519.

Urbaniak, M.D., Guther, M.L., and Ferguson, M.A. (2012). Comparative SILAC proteomic analysis of Trypanosoma brucei bloodstream and procyclic lifecycle stages. PLoS One *7*, e36619.

Urbaniak, M.D., Martin, D.M., and Ferguson, M.A. (2013). Global quantitative SILAC phosphoproteomics reveals differential phosphorylation is widespread between the procyclic and bloodstream form lifecycle stages of Trypanosoma brucei. J Proteome Res *12*, 2233-2244.

van Weelden, S.W., Fast, B., Vogt, A., van der Meer, P., Saas, J., van Hellemond, J.J., Tielens, A.G., and Boshart, M. (2003). Procyclic Trypanosoma brucei do not use Krebs cycle activity for energy generation. J Biol Chem *278*, 12854-12863.

Vandemeulebroucke, A., Minici, C., Bruno, I., Muzzolini, L., Tornaghi, P., Parkin, D.W., Versees, W., Steyaert, J., and Degano, M. (2010). Structure and mechanism of the 6-oxopurine nucleosidase from Trypanosoma brucei brucei. Biochemistry *49*, 8999-9010.

Vanhollebeke, B., De Muylder, G., Nielsen, M.J., Pays, A., Tebabi, P., Dieu, M., Raes, M., Moestrup, S.K., and Pays, E. (2008). A haptoglobin-hemoglobin receptor conveys innate immunity to Trypanosoma brucei in humans. Science *320*, 677-681.

Vassella, E., and Boshart, M. (1996). High molecular mass agarose matrix supports growth of bloodstream forms of pleomorphic Trypanosoma brucei strains in axenic culture. Mol Biochem Parasitol *82*, 91-105.

Vassella, E., Reuner, B., Yutzy, B., and Boshart, M. (1997a). Differentiation of African trypanosomes is controlled by a density sensing mechanism which signals cell cycle arrest via the cAMP pathway. J Cell Sci *110 (Pt 21)*, 2661-2671.

Vassella, E., Reuner, B., Yutzy, B., and Boshart, M. (1997b). Differentiation of african trypanosomes is controlled by a density sensing mechanism which signals cell-cycle arrest via the camp pathway. Journal of Cell Science *110*, 2661-2671.

Vaughn, J.L., Goodwin, R.H., Tompkins, G.J., and McCawley, P. (1977). The establishment of two cell lines from the insect Spodoptera frugiperda (Lepidoptera; Noctuidae). In vitro *13*, 213-217.

Ventra, C., Porcellini, A., Feliciello, A., Gallo, A., Paolillo, M., Mele, E., Avvedimento, V.E., and Schettini, G. (1996). The differential response of protein kinase A to cyclic AMP in discrete brain areas correlates with the abundance of regulatory subunit II. J Neurochem *66*, 1752-1761.

Vickerman, K. (1965). Polymorphism and mitochondrial activity in sleeping sickness trypanosomes. Nature *208*, 762-766.

Vickerman, K. (1985). Developmental cycles and biology of pathogenic trypanosomes. Br Med Bull *41*, 105-114.

Wagner, S., Klepsch, M.M., Schlegel, S., Appel, A., Draheim, R., Tarry, M., Hogbom, M., van Wijk, K.J., Slotboom, D.J., Persson, J.O*., et al.* (2008). Tuning Escherichia coli for membrane protein overexpression. Proc Natl Acad Sci U S A *105*, 14371-14376.

Walter, R.D. (1978). Adenosine 3´,5´-cyclic monophosphate-binding proteins from Trypanosoma gambiense. Hoppe-Seyler´s Zeitschrift für Physiologische Chemie *359*, 607-612.

Walter, R.D., and Opperdoes, F.R. (1982). Subcellular distribution of adenylate cyclase, cyclic-AMP phosphodiesterase, protein kinases and phosphoprotein phosphatase in Trypanosoma brucei. Molecular and Biochemical Parasitology *6*, 287-295.

Wang, T., Mentzer, R.M., and Van Wylen, D.G. (1992). Interstitial adenosine with dipyridamole: effect of adenosine receptor blockade and adenosine deaminase. American Journal of Physiology - Heart and Circulatory Physiology *263*, H552-H558.

Waterhouse, A.M., Procter, J.B., Martin, D.M., Clamp, M., and Barton, G.J. (2009). Jalview Version 2-- a multiple sequence alignment editor and analysis workbench. Bioinformatics *25*, 1189-1191.

WHO (2013). Control and surveillance of human African trypanosomiasis. World Health Organization technical report series, 1-237.

Witt, J.J., and Roskoski, R., Jr. (1975). Rapid protein kinase assay using phosphocellulose-paper absorption. Anal Biochem *66*, 253-258.

Wu, J., Brown, S.H., von Daake, S., and Taylor, S.S. (2007). PKA type IIalpha holoenzyme reveals a combinatorial strategy for isoform diversity. Science *318*, 274-279.

Yonemoto, W., McGlone, M.L., Grant, B., and Taylor, S.S. (1997). Autophosphorylation of the catalytic subunit of cAMP-dependent protein kinase in Escherichia coli. Protein Eng *10*, 915-925.

Zawadzki, K.M., and Taylor, S.S. (2004). cAMP-dependent protein kinase regulatory subunit type IIbeta: active site mutations define an isoform-specific network for allosteric signaling by cAMP. J Biol Chem *279*, 7029-7036.

Zetterqvist, O., Ragnarsson, U., Humble, E., Berglund, L., and Engstrom, L. (1976). The minimum substrate of cyclic AMP-stimulated protein kinase, as studied by synthetic peptides representing the phosphorylatable site of pyruvate kinase (type L) of rat liver. Biochemical and biophysical research communications *70*, 696-703.

Zhang, P., Smith-Nguyen, E.V., Keshwani, M.M., Deal, M.S., Kornev, A.P., and Taylor, S.S. (2012). Structure and allostery of the PKA RIIbeta tetrameric holoenzyme. Science *335*, 712-716.

7 Acknowledgements

I would first like to express my gratitude to Prof. Michael Boshart for his supervision on this ever-fascinating story and his continual support, both in and out of the lab.

Many thanks to Prof. Martin Parniske for agreeing to be by second examiner, for his interest in this project and always commending our progress along the way.

I am also very grateful to the other members of the thesis committee for accepting to partake in my final steps of this journey.

To all members of the "AG" (past and present), many thanks for the great atmosphere and also for all your support. To those who helped in the proof-reading; Stefan, Matt and Kat (AG Bramkamp).
Special thanks to Markus and Martin; you guys were instrumental to my settling in, both scientifically and socially, and you've been there for me since.

To all the students that I had the honor of supervising and whose work helped to forge the path of this project; Feli, Nada, Marko and Ana David. I salute you.

Many thanks to collaboration partners and friends:
Andreas Anger (Gene center, Munich) for helping me to literally add a 3rd dimension to the PKA story, which allowed us to uncover more hidden treasures.
Prof. F. Herberg (Kassel) and his "AG" for the great time during my stay over there and for elevating my biochemistry know-how.

To Mae and Pae, i couldn't have done this without you. Many thanks for all your love and support. Muinto obrigado.